HOLOCENE RELATIVE SEA-LEVEL CHANGES IN SOUTH HINNØYA, ARCTIC NORWAY

by

ROBERT L. BARNETT

A thesis submitted to Plymouth University in partial fulfilment for the degree of

DOCTOR OF PHILOSOPHY

School of Geography, Earth and Environmental Sciences

Faculty of Science and Technology

Plymouth University

October 2013

This copy of the thesis has been supplied on condition that anyone who consults it is understood to recognise that its copyright rests with its author and that no quotation from the thesis and no information derived from it may be published with the author's prior consent.

ABSTRACT

Holocene relative sea-level changes in south Hinnøya, Arctic Norway

Robert. L. Barnett

This study develops techniques for the preparation and counting of testate amoebae for Holocene sea-level reconstructions. In addition, this study provides a ~3000 year relative sea-level reconstruction for south Hinnøya in the Vesterålen islands off mainland Norway, adding new data to a poorly defined period of the Holocene sea-level history of north-western Norway. This is important to quantify rates of glacial-isostatic adjustment (GIA), to refine GIA models, and to establish baseline (pre-industrial) rates of relative sea-level change. Surface sediments from two salt marshes (Storosen and Svinøyosen) in south Hinnøya are used to assess the effects of using different preparation procedures and count totals when analysing for testate amoebae. Analytical efficiency can be improved upon by using a mild alkali, chemical disaggregant (5 % KOH) to break up fibrous salt-marsh sediment and concentrate tests prior to counting. A count total of 100 individuals, rather than 150, can be used to make time gains with little or no effects on assemblages. Training sets of salt-marsh surface testate amoebae, foraminifera and elevational data are established for the two field sites. For testate amoebae, species – elevation relationships are constructed using regression modelling and applied to downcore fossil samples using a transfer function to derive estimates of sea level for the past ~100 years. The greater water depths reconstructed between ~3000 and ~100 years ago are not covered by modern foraminiferal training sets and are therefore estimated qualitatively from the fossil foraminiferal assemblages supplemented by information derived from fossil molluscs. Chronology is based on a combination of AMS^{14}C, ^{210}Pb, ^{137}Cs and a suite of geochemical markers. At south Hinnøya, sea level has been falling at a rate of ~0.5 mm yr^{-1} over the last 3000 years.

CONTENTS

LIST OF FIGURES

LIST OF TABLES

ACKNOWLEDGEMENTS

the Greenland Ice Sheet" (NE/H000860/1, 2009-2012), NERC allocation numbers 1530.0311 and 1577.0911.

AUTHORS DECLARATION

At no time during the registration for the degree of Doctor of Philosophy has the author been registered for any other university award without prior agreement of the Graduate Committee.

During the course of study, relevant scientific seminars, conferences and workshops were attended, at which work was often presented. External institutions were visited for consultation purposes. One article has been published, and several more are in the preparation stages.

Publications:

Barnett, R.L., Charman, D.J., Gehrels, W.R., Saher, M.H. and Marshall, W.A. (2013) Testate amoebae as sea-level indicators in north-western Norway: developments in sample preparation and analysis. *Acta Protozoologica,* 52. pp 115-128.

Conference presentations:

Barnett, R.L., Gehrels, W.R., Marshall, W.A., Charman, D.J. and Saher, M.H. (2012) Late Holocene relative sea-level changes in south Hinnøya, Arctic Norway. *The 3rd Joint IGCP588 / INQUA1001 conference,* Christian-Albrechts University, Kiel, Germany

Barnett, R.L., Gehrels, W.R., Marshall, W.A., Charman, D.J. and Saher, M.H. (2012) Late Holocene relative sea-level changes in south Hinnøya, Arctic Norway. *Quaternary Research Association Postgraduate Symposium,* University of Aberdeen, UK

Barnett, R.L., Gehrels, W.R., Marshall, W.A., Charman, D.J. and Saher, M.H. (2012) A multi-proxy approach towards reconstructing late Holocene relative sea-level changes in south Hinnøya, Arctic Norway. *Sea Level and Adjustment of the Land, Observations and Models (SLALOM2012).* National University, Athens, Greece

Barnett, R.L., Gehrels, W.R., Marshall, W.A., Charman, D.J. and Saher, M.H. (2010) Recent sea-level change in Arctic Norway, reconstructed from salt-marsh sediments (poster presentation). *Quaternary Research Association Postgraduate Symposium,* University of Exeter, UK

Barnett, R.L., Gehrels, W.R., Marshall, W.A., Charman, D.J. and Saher, M.H. (2010) Recent sea-level change in Arctic Norway, reconstructed from salt-marsh sediments (poster presentation). *Palaeochronology Building Workshop,* San Miguel de Allende, Mexico

Barnett, R.L., Gehrels, W.R., Marshall, W.A., Charman, D.J. and Saher, M.H. (2010, 2011, 2012) A multi-proxy approach towards reconstructing late Holocene relative sea-level changes in south Hinnøya, Arctic Norway. '*PHUNCH' presentations,* Plymouth University, UK

Other conference and workshop attendances:

- Holocene Climate Change (conference) 2013. The Geological Society, London, UK
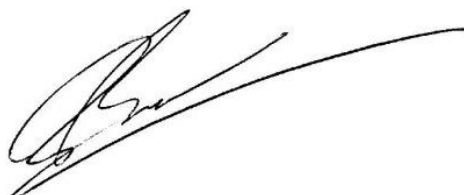
- North East Atlantic Benthic Foraminifers (workshop) 2012. University of St Andrews, UK

- All at Sea? Coastal Environments: a holistic appraisal (conference) 2011 York University, UK

- Palaeochronology Building Workshop (workshop) 2010. San Miguel de Allende, Mexico

- Past and present land-ocean interactions: blueprints for the 21st century? (INQUA field meeting) 2010. Arundel, UK

- Sea-level changes: the science of a changing world. (Quaternary Research Association discussion meeting) 2010. Durham University,UK

Additional funding awards:

- Natural Environment Research Council. Radiocarbon Facility (Environment) 2011. **£6380**

- Quaternary Research Association. New Research Worker's Award 2011. **£600**

- Royal Geographical Society. Dudley Stamp Memorial Award 2011. **£500**

Word count: 55,612 (main body of thesis including captions & references)

Signed:

Date: 13 – 08 – 2013

CHAPTER 1 - Introduction

1.1 Introduction

The topic of sea level features heavily in the fourth assessment report (AR4) of the Intergovernmental Panel on Climate Change (IPCC). Sections are attributed to observed historical sea-level change, total sea-level budgets and predictions of sea-level movement for the 21st century. The direction of sea-level movement, especially as experienced along coastlines, is a major concern for the global population and the topic is to feature again in the next IPCC report (AR5) due in 2014. Recent advancements in technology allow us to monitor accurately current trends in coastal sea level with tide gauges and satellite altimetry. Tide-gauge records, however, do not extend far back in time; a few hundred years at most. They provide little information on long-term sea-level variability and are therefore of limited use as a tool in predicting future changes.

Sea-level trends as derived from proxy information allow for much more lengthy records than those provided from direct measurements. Commonly used proxy sources of sea-level data include coral microatolls, archaeological indicators, and vermetid bioconstructions (Gehrels et al. 2011). Possibly the most widely used in mid latitude sites, however, are proxies derived from salt-marsh sediments which are capable of reconstructing past sea levels with precisions as low as ± 5 cm (Gehrels & Woodworth 2013).

Extensive salt marshes are rare along steep, glaciated Arctic coastlines. The few published high latitude salt-marsh based sea-level studies include work in Greenland by Woodroffe & Long (2009) and Long et al. (2010). This PhD project has identified some presently accreting salt marshes in Arctic Norway suitable for investigations into sea-level history. Arctic Norwegian coastlines are of particular interest to sea-level research as they sit near the limit of ice extent during the Last Glacial Maximum and relative sea-level data derived from these regions is important for constraining models of glacio-isostatic adjustment (Lambeck et al. 1998b). These models are dependent on field studies which contribute to knowledge of ice sheet thickness, extent and timings of retreat. Empirical sea-level data are then used to validate model outputs and refine model parameters. The field sites are located on the south coast of Hinnøya, an island in the Vesterålen archipelago (Figure 1.1). Studies from this area have only found proxy evidence of sea-level change for the early and mid Holocene (Møller 1984, 1986; Vorren & Moe 1986; Balascio et al. 2011). This study, using salt-marsh sediments, will provide insight into recent sea-level change over the last few thousand years. This is important because this period is poorly covered by existing data, yet information on late Holocene sea-level change contributes to: (1) quantification of rates of (ongoing) postglacial isostatic rebound; (2) refinement of models of glacial-isostatic adjustment (GIA); and (3) establishment of a baseline (pre-industrial) rate of relative sea-level change.

Virtually all existing sea-level data originating from salt-marsh sediments make use of either foraminifera or diatoms as sea-level indicating proxies (e.g. Scott & Medioli 1982; Gehrels 1994; Horton & Edwards 2006; Long et al. 2010; Barlow et al. 2012). The type and abundance of species for both organism groups change with elevation across the

marsh. This change can be related to inundation rates and sea level. By establishing a relationship between assemblage composition and elevation relative to sea level using modern surface data fossil assemblages can be analysed and used to infer past sea levels. This concept has been used in sea-level studies for the past three decades yet it is only very recently that a third proxy, testate amoebae, has been used (Charman et al. 2010). These organisms are associated with hydro-terrestrial ecosystems, most commonly peat bogs. Their occurrence on salt marshes is relevant to sea-level studies as with increasing proximity to sea water their habitat becomes more taxing, thereby forcing changes in assemblage composition, as saline tolerant species become more dominant. By establishing and applying the same assemblage - elevation relationship this proxy could potentially become a powerful tool in developing sea-level histories. The vertical distribution of testate amoebae extend above the supra tidal setting, beyond the upper limits of foraminifera. In addition, the proxy shows a stronger vertical distribution across salt marshes than is shown by diatoms and foraminifera (Gehrels et al. 2001; Charman et al. 2010). This study will develop the potential of this new sea-level proxy and evaluate its capability at predicting past changes in sea level against existing tide-gauge data. More established techniques using foraminifera will then be used to develop a late Holocene sea-level record for south Hinnøya.

1.2 Aims, objectives and justification

The purpose of this thesis is to develop a new and unique record of sea-level change for the south coast of Hinnøya in north-western Norway which can be used to test the

hypothesis that, models of GIA can accurately predict past relative sea-level in Arctic Norway during the late Holocene. The reconstruction will rely on extensive training sets of modern testate amoebae and foraminifera from two salt marshes (Storosen and Svinøyosen) which show species zonation attributed to changing elevations. Detailed lithostratigraphy from Svinøyosen will provide insight into past environmental changes and a study of the fossil biostratigraphy will allow the development of a well constrained relative sea-level reconstruction.

An important aim of the thesis is to test rigorously the potential of testate amoebae as sea-level indicators. This project will build on existing working practices and suggest improved preparatory and analytical procedures. A recent sea-level reconstruction shall be developed using a new training set of Norwegian salt-marsh testate amoebae to test their suitability in predicting past sea-level change. The primary goals of this project can be summarised into two main aims, both of which will be achieved through completing a series of specific objectives.

1.2.1 Aim 1

To develop a late Holocene relative sea-level curve for South Hinnøya based on the biostratigraphy of nearshore (salt marsh) and shallow marine deposits which can then be used to test predictions of modelled relative sea-level

Objectives:

- Document modern foraminifera assemblage data against elevation for samples taken from salt marshes, tidal creeks, mudflats and low intertidal environments of Svinøyosen and Storosen, south Hinnøya

- Define the indicative meaning of the assemblage data by surveying their occurrences relative to elevation

- Establish a detailed stratigraphy for the marsh at Svinøyosen using a programme of hand coring

- Interpret the facies using sedimentological analysis (grain size, loss-on-ignition, bulk density) and micropalaeontological evidence.

- Establish water-level depths for the late Holocene sediment based on microfossils, using transfer functions where appropriate.

- Build a chronology for the near shore sediments using radiocarbon dating, stable geochemistry analysis and radionuclide (^{210}Pb, ^{137}Cs, ^{241}Am) dating techniques

1.2.2 Aim 2

To examine the preparatory procedures and methodology involved with salt-marsh testate amoebae and establish their value as sea-level indicators

Objectives:

- Sample the marshes at Svinøyosen and Storosen for testate amoebae whilst accurately recording the elevation of the samples relative to mean sea level

- Using replicate subsamples, prepare testate amoebae for analysis using different methods, adapting the treatments when appropriate

- Statistically compare the results of the preparation techniques and establish the most efficient yet reliable method for the preparation and analysis of salt-marsh testate amoebae for sea-level studies

- Using the most suitable technique, derive a transfer function of modern testate amoebae and elevation suitable for recent (~ 100 year) sea-level reconstruction

- Establish a chronology for the recent reconstruction using ^{210}Pb, ^{137}Cs and ^{241}Am radionuclide dating techniques

- Compare the recent sea-level reconstruction based on testate amoebae analysis with tide-gauge records for the region to validate the reconstruction

1.2.3 Justification

Since the LGM, Norway has had a history of relative sea-level (RSL) fall due to the rapid isostatic land uplift experienced following the retreat of the Fennoscandian Ice Sheet (Svendsen & Mangerud 1987). Despite this history, with the onset of more rapid global sea-level rise (Bindoff et al. 2007) and the slowing down of crustal rebound it has been shown that many locations along the Norwegian coast will see a rise in sea-level in the order of tens of centimetres during the 21st century (Simpson et al. 2012). High end estimates suggest a possible rise of over a metre at specific localities. As many as 110,000 buildings are located less than 1 m above present sea level in Norway (Almås & Hygen 2012) which gives perspective to the threat of sea-level rise over the next 100 years. The municipality of Nordland where the field sites are located has the second highest concentration of buildings situated less than 1 m above sea level in Norway. Under worst case scenarios, this municipality may experience an average sea-level rise of 90 cm along its coastlines (Vasskog et al. 2009). The added threat from increased storm surges (frequency and severity) means this is an important location for sea-level study, and, as previously mentioned, a sound understanding of past sea-level trends is imperative. Considering the lack of relative sea-level data for the last few

thousand years the need for a well constrained late Holocene record is apparent. GIA and ice sheet models must be assessed rigorously against palaeosea-level data in order to provide a reliable tool for future sea-level prediction. Their performance in the late Holocene is hereby of greatest relevance.

1.3 Previous work

1.3.1 Published sea-level records for NW Norway

Long term records of relative sea-level change that extend back into the Holocene (especially the last 2000 years) provide important tools for examining the drivers of sea level variations (Gehrels et al. 2011). Coastal sedimentary sequences are sources of sea-level information which can be used for the collections of a series of sea-level index points. These have an advantage over alternative sea-level indicators such as isolation basins and coastal archaeological evidence as they can provide tightly constrained records from single locations, provided they are well constrained chronologically.

Existing sea-level data from the region are mostly obtained from isolation basins and raised beaches (Mathinussen 1960, 1962; Møller 1982, 1984, 1986; Vorren et al. 1988; Corner & Haugane 1993). Isolation basins are standing bodies of water situated in an isostatically uplifting area which has been cut off from the sea as the land uplifted. This isolation event is recorded in the sedimentary sequence of the basin and if this horizon is dated can provide a sea-level index point (SLIP). Occasionally a single isolation basin

may provide multiple SLIPs as demonstrated by Lloyd (2000). More commonly, however, each basin only provides one SLIP as is the case in Norway. The resolution of sea-level reconstructions is therefore limited by the number of isolation basins available and the distribution of their elevations. Archaeological and raised beach data likewise provide isolated data points and a long record would require many sites located close together providing SLIPs over a range of elevations. In this study salt marshes were targeted as they potentially represent an opportunity to obtain a series of Holocene sea-level index points from a single location within a stratigraphical context that provides additional palaeoenvironmental information about changing sea levels.

A record of past relative sea-level change from this region will be a useful tool for establishing the deglacial history of Fennoscandia. Glacial isostatic adjustment (GIA) modelling has become a key component in predicting future patterns of sea-level change (Simpson et al. 2012). These models must be tested against historical sea-level trends to prove their validity. For Fennoscandia, the most recent GIA models (e.g. Lambeck et al. 2010) are built using an ice sheet retreat model produced by Lambeck et al. (1998b). This model was substantiated using post glacial sea- and lake- level observations from around Fennoscandia including two from northern Andøya, 100 km north of this study's field sites and two from the Lofoten islands, 90 km south east of Hinnøya (Lambeck et al. 1998a). The four mentioned studies fail to account accurately for late Holocene sea-level trends for this part of north western Norway. The Andøya work comprises a single, pre Holocene, isolation basin study (Vorren et al. 1988) and an investigation of early to mid Holocene raised beach deposits. The Lofoten studies comprise a study of submarine peats dated at between 9000 and 10000 calibrated years before present (cal yrs BP;

Vorren & Moe 1986) and another early Holocene study of raised beach deposits (Møller 1984).

1.3.2 Salt-marsh testate amoebae as sea-level indicators

Known and well used sea-level proxies derived from salt-marsh stratigraphies include foraminifera (Scott & Medioli 1978) and diatoms (Palmer & Abbott 1986). These proxies, although widely used, are not always suitable for sea-level studies. Effects of dissolution can alter assemblage characteristics (e.g. Green et al. 1993), or low species diversity may provide large vertical uncertainties during the reconstruction stage. A third group of micro-organisms proffer an opportunity to be used in conjunction with, or in lieu of, other existing proxies. Testate amoebae were first identified as a potential sea-level indicator from UK salt-marshes by Charman et al. (1998) and Gehrels et al. (2001). Since then they have been further identified in salt marshes along the North American east coast (Gehrels et al. 2006a) and in estuarine marshes in Belgium (Ooms et al. 2011, 2012). Beyond these studies little has been done to progress the use of this proxy as a sea-level indicator despite the recurring positive results. As indicated by Charman et al. (2010), the methodological approaches involved with testate amoebae, especially the preparation techniques, require careful attention and improvement. Issues that need addressing include improving the separation technique between tests and organic particles which share a similar size range, avoiding test destruction from overly aggressive chemical pre-treatments, and reducing the count time it takes for each sample, a common issue involved with salt-marsh samples of testate amoebae. Salt-marsh testate amoebae have regularly been prepared using methods derived from fresh-water peat studies (e.g. Roe et al. 2002). Movement away from this is needed and the

development of a 'best practice' preparation technique suitable for salt-marsh samples is required.

1.4 Study area and rationale

Hinnøya is an island belonging to the Vesterålen archipelago which are situated off the coast of north-western Norway at around 68° north, above the Arctic Circle (Figure 1.1). Due to the extensive glaciation of the area the coastlines of the Vesterålen and Lofoten islands are characteristically steep and comprise of many drowned glacial fjords. There is little protection from the northern Atlantic Ocean and weather systems for low energy, intertidal deposits to accrete. Two study sites were found in July 2011 at the landward end of marine inlets on the south coast of Hinnøya (Figure 1.1). Both inlets are flanked by protuberant headlands which have allowed the steady accretion of salt marsh and near shore facies. Storosen (68°20'50 N, 15°41'26 E) is the younger of the two marshes and has only very shallow stratigraphy. Svinøyosen (68°20'15 N, 15°33'06 E) is a much larger marsh, occupying ~0.13 km^2 and the subsurface lithology contains a record of sedimentation for much of the Holocene. Both sites were chosen as good examples of modern, accreting salt marshes showing surface profiles gradually descending from the high-marsh zone, through the mid- and low-marsh zones and into the low-tidal environment (Figure 1.2). Cold region salt-marshes are affected by seasonal gradients which influence their morphodynamics (e.g. Kershaw 1976). Snow and ice cover can protect salt marshes from erosion by winter storms, although sediment supply may not be heavily affected as flooding tidal waters penetrate beneath the ice, depositing sediment on the salt-marsh surface (Bryne & Dionne 2002). Microfossil productivity is

likely to be affected from seasonal changes in temperature demonstrating the importance of analysing both live and dead proxy assemblage crops.

When salt-marsh foraminifera were first being used to study sea-level change it was hypothesised that once the worldwide reliability of the faunal assemblage to elevation relationship was established the information could be universally applied to derive previous sea levels (Scott & Medioli 1978, 1980b). It is now commonly accepted that a localised relationship must first be determined from surface foraminifera which is then applied specifically to fossil assemblages extracted from the same marsh (Gehrels 1994). This relies on faunal assemblages showing a zonation with respect to elevation, often accompanied by a similar zonation in flora. Both Storosen and Svinøyosen marshes demonstrate this characteristic very well and are therefore viable locations for developing a localised training set (or modern analogue) of foraminifera and testate amoebae.
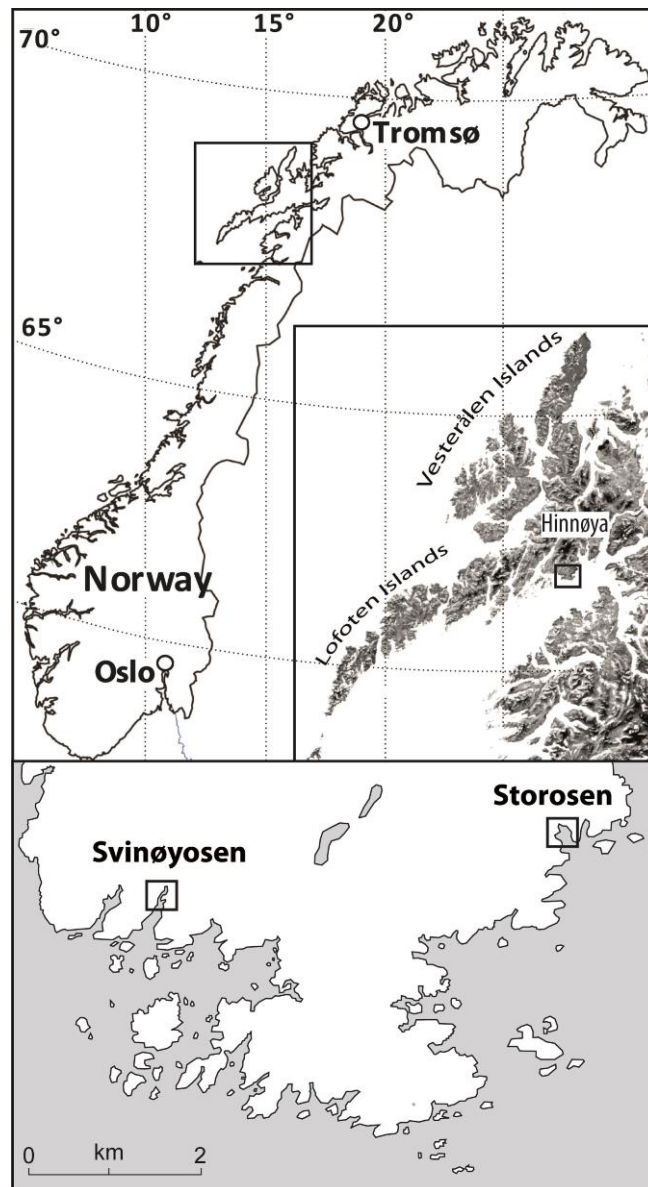
Figure 1.1 Location map of the two field sites, Storosen and Svinøyosen, in south Hinnøya

Salt-marsh based sea-level studies are most commonly performed in temperate mid latitude locations (e.g. east coast USA: Gehrels et al. 2002; Donnelly et al. 2004; Kemp et al. 2009a, b, c, 2011; Spain: Leorri et al. 2008; UK: Horton & Edwards 2005; Massey et al. 2008). The techniques have also been applied to tropical locations (e.g. Horton et al. 2003) where problems arise concerning the poor preservation potential of agglutinated foraminifera in mangrove sediments and the range of different

environments calcareous species represent (Woodroffe 2009). In high Arctic environments salt marshes are much rarer; coastlines are dominated by exposed rock, steep glacial fjords and unconsolidated moraines. Salt marshes are often thin and very small in area, such as those encountered in West Greenland (Woodroffe & Long 2009). Salt-marsh accretion will preferentially occur in locations with a relatively rising sea level where accommodation space is created for the build-up of sediments. High latitude environments, much like the field site in this study, experience substantial rates of land uplift as a result of glacial unloading since the LGM and subsequent isostatic rebound. In this scenario uplift rates can outpace sea-level rise making salt-marsh accretion an unlikely occurrence. Due to the distance of the Vesterålen Islands from the centre of maximum uplift in Fennoscandia (i.e. the Gulf of Bothnia; Ekman 1996) a few salt marshes have been able to accrete in protected inlet areas providing a unique setting for this sea-level study to take place at latitudes that must normally rely on isolation basins for derived proxy sea-level information.

Figure 1.2 a) Salt marsh at Storosen looking seaward (south east), b) Salt marsh at Svinøyosen looking inland (north east)

CHAPTER 2 - Background

2.1 Introduction

The isostatic history associated with Fennoscandia since the LGM has dramatically
influenced Norway's RSL history, and continues to be a dominant component of sea-
level change today. Rates of isostatic uplift have varied throughout the Holocene, and
measuring the current rate of uplift along the Norwegian coast continues to be a
challenge. This chapter will discuss the deglacial history of the Vesterålen – Lofoten
archipelago, introduce attempts made at estimating modern and palaeouplift rates, and
present existing RSL information available for the region. This chapter also introduces
the concept of generating RSL data from groups of salt-marsh microorganisms,
specifically focussing on the use of foraminifera and testate amoebae in sea-level
studies.

2.2 Deglaciation and isostasy in north-western Norway

The Vesterålen and Lofoten islands off north-western Norway were fully glaciated
during the LGM, around 21000 cal yrs BP when the Eurasian ice sheet covered
Fennoscandia, the Barents Sea shelf, the north-western Russian plain and much of the
British Isles and Low Countries of northern Europe (Svendsen et al., 2004). The
northern Vesterålen islands experienced multiple phases of ice melt and readvance

following the LGM but were fully deglaciated during a warming period between 15100 and 13700 cal yrs BP (Vorren et al. 1988; Vorren & Plassen, 2002). The Vestfjorden, representing the southern coast line of the Vesterålen islands, became ice free somewhat later between 13100 and 12700 cal yrs BP (Bergstrøm et al., 2005). The study sites on the south coast of Hinnøya were free from ice during the Younger Dryas (~13000 to 11500 cal yrs BP), yet were positioned extremely close to the ice margin (see Figure 2.1) at this time (Fløistad et al. 2009).
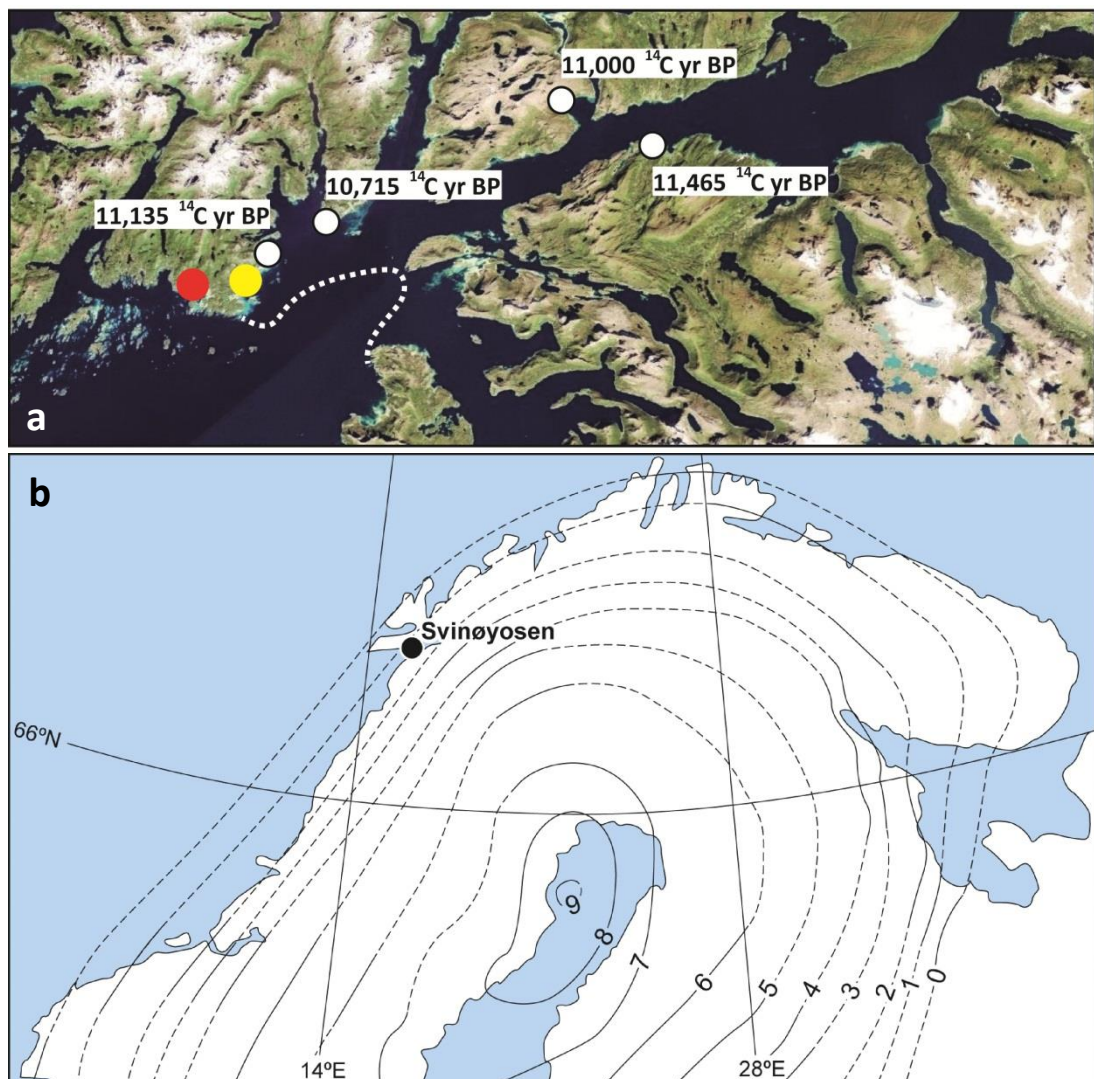
Figure 2.1 a) The Younger Dryas ice position (dashed white line) after Fløistad et al. (2009). Radiocarbon dates are of ice reworked fossils from Bergstrøm et al. (2005). Field sites at Svinøyosen (red) and Storosen (yellow) are also indicated. b) Estimated Fennoscandian uplift rates (mm yr^{-1}) after Ekman (1996)

Following the removal of the ice mass after deglaciation, the depressed elastic lithosphere under Fennoscandia rebounded as mantle material migrated back from the offshore glacial forebulges. The modern centre of uplift is located in the Gulf of Bothnia (Figure 2.1b) and has been recorded using a variety of techniques (GPS - Milne et al. 2004; satellite altimetry - Kuo et al. 2008; satellite gravimetry - Steffen et al. 2008). Modern rates here are around 11 mm yr^{-1}. Well constrained modern day estimates of crustal uplift for much of Fennoscandia are offered by the BIFROST (Baseline Inferences for Fennoscandian Rebound Observations Sea Level and Tectonics) project (Bennet et al. 1996). Continuous daily solutions of GPS recorded land motion exist from 1993 (Scherneck et al. 1998) for individual point sources. Three dimensional crustal velocities modelled from these data provide good constraints on modern day GIA estimates for the areas where the GPS recorders are located (Milne et al. 2001; Johansson et al. 2002; Milne et al. 2004; Lidberg et al. 2007; Lidberg et al. 2010). Vertical uplift rates, however, are site specific and velocity uncertainties rapidly increase when the data are extrapolated. The nearest BIFROST network receiver to the field sites is located 200 km up the coast and is incapable of providing a reasonable estimate of local uplift for the study region.

An alternative satellite based method for estimating Fennoscandian land motion is provided by the GRACE (Gravity Recovery and Climate Experiment) mission. Planetary mass variations are monitored via changes in gravity strength by a twin-satellite system. Solutions can be converted to land uplift velocities via post processing of data (e.g. Wahr et al. 2000). Recent studies have corroborated their results using comparisons with geodynamical models (Steffen et al. 2008), absolute gravimetry measurements (Steffen et al. 2009) and GPS solutions (van de Wal et al. 2011) of

Fennoscandian uplift. GRACE data have the benefit of not being spatially biased therefore having the potential of providing well constrained modern day uplift rates for remote yet critical locations associated with sea-level studies. A recent study by van de Wal et al. (2011) has demonstrated that GRACE solutions, once approximated to uplift rates, can correlate strongly with land motion rates derived from the BIFROST network in Lidberg et al. (2007) with total average uncertainties of 0.57 mm yr^{-1} across Fennoscandia. The study however eliminates GPS and GRACE data which show uplift rates of < 2mm yr^{-1} which ignores much of the Norwegian coastline including this study's field sites which have approximate GIA uplift rates of between 1 and 2 mm yr^{-1} (Ekman 1996). Vestøl (2006) uses a combination of GPS measurement interpolation, levelling and tide-gauge measurements to estimate uplift rates for Kabelvåg (a nearby port) at 2.6 mm yr^{-1}, slightly more than the estimations from Ekman (1996) and van de Wal et al. (2011).

2.3 Modelling GIA histories

GIA models are used to define the elastic response of Earth's lithosphere through time due to changes in continental surface load from global ice-water dynamics. They rely on: (1) sound knowledge of ice-sheet growth and decay histories which are provided by an ice-sheet model constrained by observed geomorphological markers, (2) assumptions made on Earth rheology including mantle viscosities and response type (e.g. Maxwell/Burger) and lithospheric thicknesses, (3) observed relative sea-level data which can be used to constrain and improve the assumptions made in (1) and (2).

A handful of global ice-sheet models exist which reconstruct ice margins and thicknesses for the LGM across the globe (ICE-3G - Tushingham & Peltier 1991; ICE-4G - Peltier 1994, 1996; ICE-5G - Peltier 2004; RSES - Lambeck et al. 2000). A detailed regional model for Fennoscandia has also been constructed (FKBS8), which, when applied alongside rheological assumptions can predict glacial isostatic response for northern Europe since the LGM (Lambeck et al. 1998b). This model uses both recent instrumental sea-level data (Lambeck et al. 1998a) and longer term, proxy based records (Lambeck et al. 2010) to constrain Fennoscandian ice-sheet characteristics and rheological parameters.

Lambeck et al. (1998a, 2010) use a handful of RSL studies from the Vesterålen – Lofoten region to constrain their GIA model. This region is a critical location for model validation as it sits furthest from the centre of uplift meaning uplift isobars are situated close together along a steep gradient running approximately perpendicular to the shoreline. Sea-level histories from the region are therefore different depending on their position on the uplift isobases, yet sea-level data from here are sparse. A single isolation basin provides one sea-level index point (SLIP) on Andøya locating RSL to around 36 m above present day sea level between 18500 and 15500 cal yr BP (Vorren et al. 1988). Early Holocene RSL data is taken from Møller (1984) and Vorren & Moe (1986) of raised shoreline features and submerged peat deposits. Little consideration is given to the large indicative range of the marine and beach deposits. There are no RSL data from after ~5000 cal yrs BP used to constrain the GIA model. Existing GIA models will greatly benefit from more, tightly constrained SLIPs from the Vesterålen Islands throughout the Holocene and, particularly, the late Holocene.

2.4 Holocene sea-level variability in the Vesterålen and Lofoten region

The 'classic' RSL curve for the Vesterålen – Lofoten region is provided by Marthinussen (1962). This sea-level curve was drawn up for the location of Ramså, Andøya, although data were taken from other localities (including Finnmark) to supplement the record. Attempts were made by the author to adjust the data for the effects of variable rates of uplift through northern Norway. Much of the curve is based on datings of peat deposits sitting near modern sea level, raised driftwood deposits and marine shells from exposed stratigraphic sections. The reconstruction demonstrates a typical sea-level curve for a deglaciated, ice marginal coastal zone (Figure 2.2).
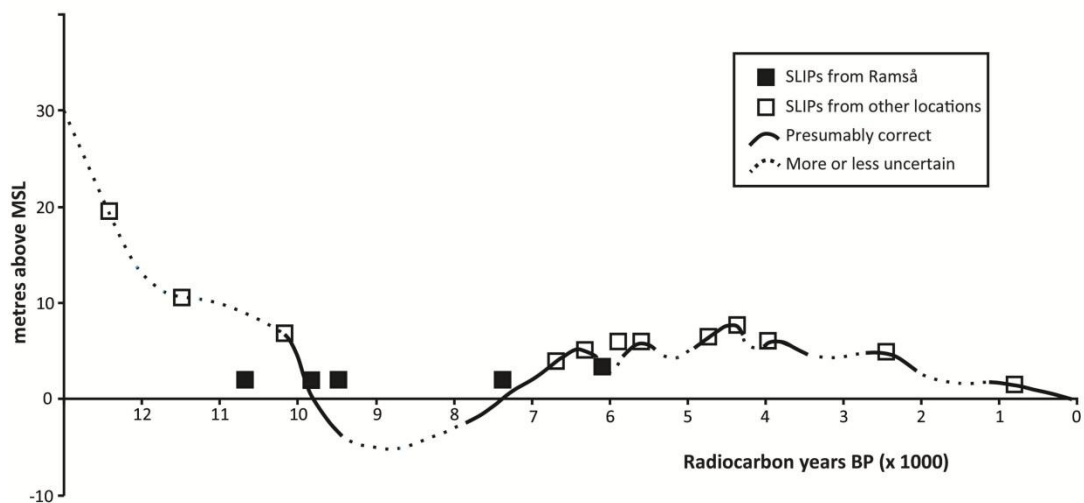
Figure 2.2The shoreline displacement curve for Ramså after Marthinussen (1962). The annotation has been kept the same as the original, as has the x-axis in uncalibrated radiocarbon years before present

Following deglaciation, initial rapid isostatic recovery caused RSL to fall during a shoreline regression to an early Holocene low stand below that of present day. At Ramså, this low stand lasted from around 11000 to 8000 cal yrs BP. A marine transgression, known locally as the Tapes, followed and resulted in a sea-level maximum of 10 to 12 m above mean sea level (MSL) sometime during the mid Holocene. As the marine transgression subsided and rates of uplift once again outpaced the rate of sea-surface elevation rise, a series of regressions caused RSL to fall to modern day levels over a ~5000 year period. Marthinussen (1962) implies that there were up to five oscillations or reversals that brought about land emergence during this regressive period.

At Ramså, Marthinussen's study relies on non-local, interpolated SLIPs from ~6000 cal yrs BP onwards. The only observed proxy data presented for the last 3000 years are two datings of driftwood logs found in Finnmark. Despite these limitations, subsequent late and postglacial RSL studies from the Vesterålen – Lofoten archipelago often use the sea-level reconstruction from Marthinussen (1962) to complete their sea-level histories for the late Holocene (e.g. Møller 1984, 1986; Vorren et al. 1988).

2.4.1 Sea-level high stand isobase diagrams

As Mathinussen (1962) correctly identified, SLIPs from different localities were not always relevant to the same sea-level curve due to the strong gradient of uplift rate that existed perpendicular to Norway's coastline. The different rates of uplift can be represented by marine limits during different stages following ice retreat. Møller (1982)

collated data on raised shoreline features and mapped out the marine limits of the 'main shoreline'. The main shoreline represented the highest vertical limit of sea levels since deglaciation and was dated to between 14000 and 11500 cal yrs BP. The isobases of the main shoreline for the Vesterålen and Lofoten islands from Møller (1982) are presented in Figure 2.3 and show the palaeosea-level depths in relation to present day MSL.
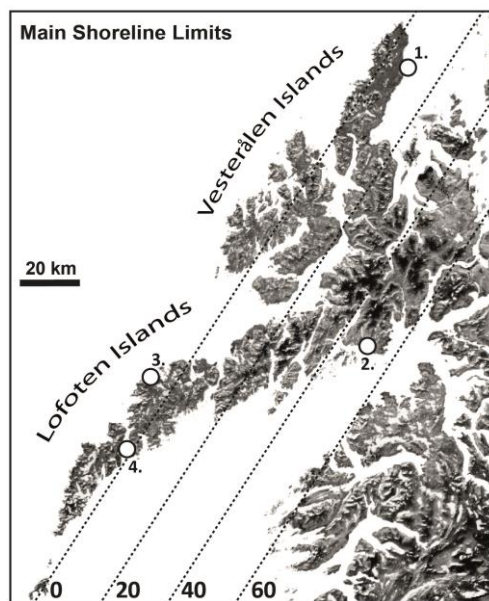
Figure 2.3 Isobases of the Main shoreline limits after Møller (1982) and locations mentioned in the text: 1. Ramså, 2. Svinøyosen, 3. Eggum, 4. Napstraumen

The Tapes high stand, as recorded by Mathinussen (1962), represented another opportunity to derive shoreline isobases. Raised shoreline features associated with the mid Holocene Tapes high stand were collated by Møller (1987) and used to draw up isobases representing the Tapes shoreline limits (Figure 2.4). As can be seen, the classic RSL curve by Mathinussen (1962) is situated on the 9 m Tapes isobase. Careful adjustment of SLIPs that are located beyond this isobase is required if such data are to be incorporated into the sea-level history. However, it is preferable to obtain sea-level

index points from a single locality so that uncertainties introduced by this adjustment can be avoided.
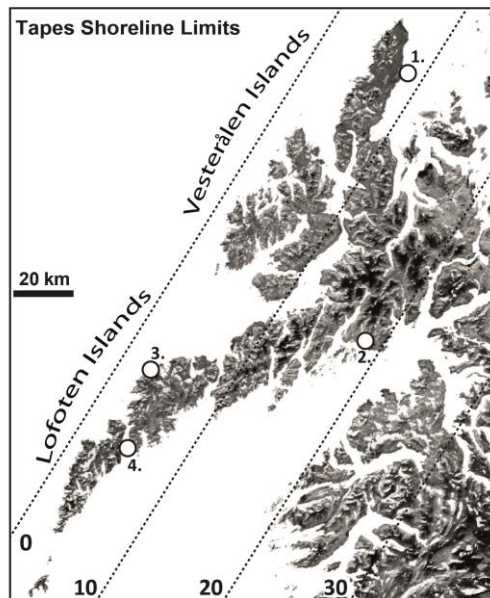
Figure 2.4 Isobases of the Tapes shoreline limit, after Møller (1987) and locations mentioned in the text: 1. Ramså, 2. Svinøyosen, 3. Eggum, 4. Napstraumen

2.4.2 Subsequent relative sea-level studies

Møller (1984) concentrated on a different location to Ramså that was situated on a similar Tapes isobase line. He collected sea-level data from around Napstraumen, in the southern Lofoten islands (Location 4, Figure 2.4). A marine limit of 9 m for the Tapes maximum was identified by mapping raised shoreline features. In addition, submerged peat deposits sitting below present day MSL were used to constrain the early Holocene low stand that had been suggested by Mathinussen (1962). This study failed to provide any data younger than ~4000 cal yrs BP.

The sea-level study site at Ramså was revisited by Møller (1986) in an attempt to constrain better the timing of the Tapes maximum for the region through analysing three exposed stratigraphic sections. The interspersed raised beach and peat deposits were radiocarbon dated and inferred that the Tapes culminated in a maximum at around 7000 cal yrs BP. In the same year, Vorren & Moe (1986) published more RSL data from Ramså, alongside more submerged peat deposits from southern Lofoten. The work further constrained the early Holocene low stand, and the timing of the Tapes transgression. However, both studies still relied heavily on the Marthinussen (1962) curve to provide a full Holocene sea-level reconstruction.

The most recent addition to Vesterålen − Lofoten Holocene sea-level data comes from an isolation basin study by Balascio et al. (2011) near Eggum. The study site is situated in the southern Lofoten islands on the ~ 1 m Tapes isobase (Møller 1987). The threshold of the basin was estimated to be 5 m above present MSL and isolation from the sea took place sometime around 6000 cal yrs B as RSL was falling following the Tapes high stand. The authors identify similar trends between their reconstruction and the Ramså data by Møller (1986), which is associated with the 9 m Tapes isobase. According to the mapped Tapes shoreline limits (Møller 1987), relative sea levels should have only been ~ 1 m above present MSL and the basin used in Balascio et al. (2011) would not have been flooded. The disagreement raises questions about the studies involved. By using only one isolation basin, the study by Balascio et al. (2011) could only infer that after 5000 cal yrs BP sea levels were somewhere lower than 5 m above MSL. There remains a lack of RSL data representing the late Holocene across the region.

2.5 Recent sea-level change

The oldest tide-gauge data from the study region extend as far back as the 1930s. (Figure 2.5). Of the five tide gauges shown in Figure 2.5, two are located in the Vesterålen islands (Andenes and Harstad), one in the Lofoten islands (Kabelvåg) and two on main land Norway (Narvik and Bodø). Narvik represents the longest tide-gauge record, although is situated further inland than the field site, and is situated on a higher isobase of uplift then Svinøyosen. Although Harstad is not the closest tide gauge, it sits on a similar isobase to the field site and therefore probably represents the closest estimation of recent sea-level change at Svinøyosen. The tide gauge at Kabelvåg is also potentially useful for comparison, although the length of the record is limiting. Harstad has a RSL trend of -1 mm yr-1 for the last ~70 years. RSL trends for the shorter length tide gauges are skewed by (1) the short nature of the records and (2) the high MSL value of the first data points (Figure 2.5). These first data points coincide with a timing of high NAO index in 1990 (Hurrel 2003). Data points for 2010 from tide-gauge records show low MSL values corresponding with a low NAO index.
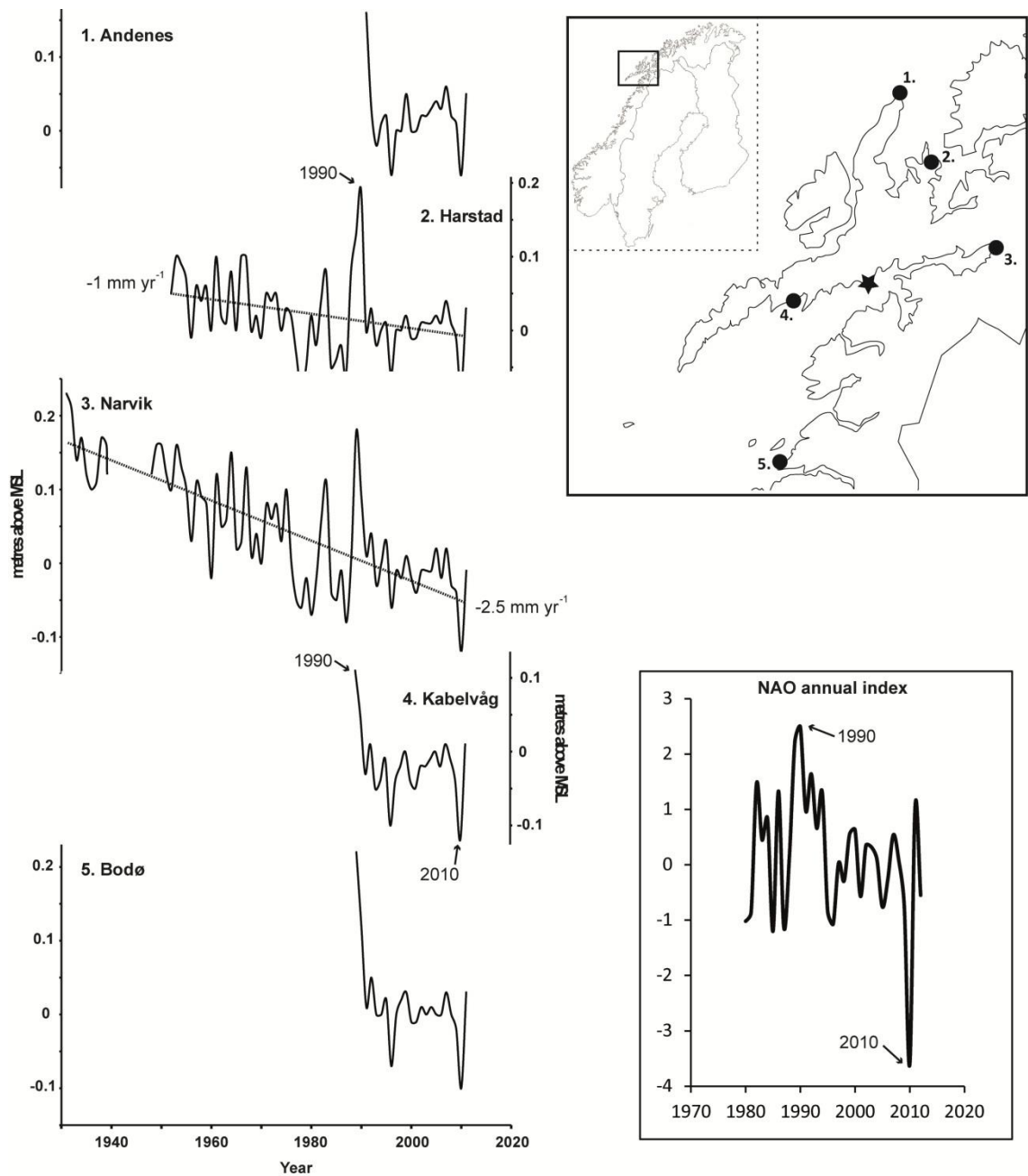
Figure 2.5 Tide gauge-records that are situated less than 125 km from the field site (star) and the NAO index from Hurrel (2003) for 1980 onwards

2.6 Salt marshes and sea-level indicators

Salt marshes occupy the upper reaches of the intertidal zone and are often found fringing estuaries. They are covered by halophytic vegetation and the height of the marsh surface is controlled by sedimentation (plant productivity and suspended sediment deliveries) and tidal inundation rates (Allen 2000). Transgressive and regressive stratigraphic overlaps depend on the rates of sedimentation and water-level change, i.e. if the local water-level rise outpaces sedimentation rates then transgression is seen; if sedimentation rates outpace water-level rise then regression is seen (Gehrels et al. 2005). The water-level change is usually interpreted as a sea-level change. Erosion can be a threat to salt-marsh surfaces. If sea-level rise is too rapid then wave action increases over the drowned surface reducing sedimentation rates and potentially causing net erosion (Mariotti & Fagherazzi 2010). Microorganism groups that readily occur in salt-marsh sediments include diatoms, foraminifera and testate amoebae. This project focuses on the use of foraminifera and testate amoebae as salt-marsh proxies of sea level.

2.6.1 Salt-marsh proxies: foraminifera

Foraminifera are a group of marine unicellular protists (test building organisms) that inhabit salt marshes. Their tests are made up of one or more chambers which are formed from $CaCO_3$ (calcareous foraminifera) or detrital clastic material (agglutinated foraminifera) (Gehrels 2002). Agglutinated forms are most commonly found on the vegetated salt-marsh surface, the calcareous forms generally being restricted to tidal

creeks, mud flats and the deeper environs. The distribution of different species of foraminifera across the surface of a marsh was first recognised by Phleger & Walton (1950). They found that assemblage diversity was being driven by changes in vegetation, organic production, temperature and salinity. This early study speculated that fossil foraminiferal assemblage information taken from a sediment core could be used to reconstruct characteristics of historical salt-marsh surfaces. A key subsequent study was later able to attribute changes in foraminiferal assemblage composition to salinity and elevation specifically and therefore sea level (Scott & Medioli 1980b).

In order to derive sea-level estimates from foraminifera, species, or groups of species, need to be related to a tidal water level. Due to elevation gradients along salt marshes, lower environments are more frequently submerged by tidal inundation. This gives rise to zonation of both vegetation and foraminifera (Scott & Medioli, 1978, 1980b) as different species are more susceptible or hardy towards flooding conditions. The zonation can be quantified through simple plotting of species abundance against elevation, or through the use of regression modelling (Gehrels 2002). Both methods provide a species or group of species with an indicative meaning. An indicative meaning defines the relationship between a proxy and a tidal water level and is composed of a measured reference water level and an indicative range – the vertical extent of a species or assemblage composition (Shennan 2007). This relationship is most commonly quantified through the use of ordination and regression analysis (see Barlow et al. 2013 for a review). Once established, the relationship can be attributed to downcore fossilised assemblages via a transfer function. The transfer function provides estimates of palaeomarsh-surface elevations from fossil assemblages which can then be

used to calculate past positions of mean sea level, assuming that historical tidal regimes have not changed significantly in the past (Gehrels 2000).

Since the early sea-level studies by Scott and Medioli, salt-marsh foraminifera have been used to reconstruct former sea levels for locations around the globe. The more successful studies were able to reconstruct these histories with precisions of $\pm$ 10 cm or better (e.g. Gehrels et al. 2005, 2008; Southall et al. 2006; Kemp et al. 2009a, b).

2.6.2 Salt-marsh proxies: testate amoebae

Testate amoebae are a group of freshwater unicellular protists, most commonly found inhabiting peat bogs. They have been used as palaeoenvironmental indicators in peat and lake sediments for over 100 years (Tolonen 1986). In lakes they have been shown to be sensitive to lake water quality and base status, and in peatlands they have been extensively used as indicators of moisture status and hydrochemistry (Charman 2001, Mitchell et al. 2008). In neo-ecological studies they have also been shown to be responsive to factors such as air pollution (Nguyen-Viet et al. 2004), suggesting they have great potential as bio-indicators in a very wide range of settings. Whilst testate amoebae are abundant in terrestrial and freshwater habitats, they also occur in mildly saline soils such as those found in the higher areas of salt marshes, or enclosed lagoonal systems (Lloyd 2000). This has led to a realisation that fossil testate amoebae could be used as a sea-level indicator in salt-marsh sediments (Charman et al. 1998).

Testate amoebae were first systematically recorded in salt-marsh samples prepared for foraminiferal analysis (e.g. Scott and Martini 1982) and, by the mid-1990s, there was growing evidence that, when combined with foraminiferal data, testate amoebae fitted into a vertical zonation sequence, being indicative of upper marsh conditions (e.g. Scott et al. 1991, 1995). However, preparation of samples for foraminifera analyses was based on sieving only a relatively large size fraction (>63 µm), so that the majority of the tests were being lost. Including smaller size fractions (>15 µm) in counts revealed larger numbers of tests, greater taxon diversity (Charman et al. 1998), and a strong vertical zonation of assemblages across the marsh surfaces at a number of locations in the UK (Charman et al. 1998, 2002; Gehrels et al. 2001) and North America (Gehrels et al. 2006a). Furthermore, the testate amoebae assemblages from North American and British salt marshes were surprisingly similar, suggesting similar environmental controls on taxon distribution and the potential for creating robust regional transfer functions applicable to fossil assemblages from a variety of locations (Charman et al. 2010). Other potential advantages of using testate amoebae as an additional sea-level indicator are that the range of sediments that can yield sea-level information can be extended into supratidal settings (Ooms et al. 2011), and that higher precision estimates of palaeosea level are possible, especially when combined with foraminifera and diatoms (Gehrels et al. 2001).

The only comprehensive salt-marsh surface testate amoebae data come from studies in the UK (Charman et al. 1998, 2002; Gehrels et al. 2001), North America (Gehrels et al. 2006a) and from the Scheldt estuary in Belgium (Ooms et al. 2011, Ooms et al. 2012). To date, the only fossil coastal data sets that have been described are from salt marshes in Maine (USA) and Nova Scotia (Canada; Charman et al. 2010) and a range of short

and fragmentary sediments in the UK (Roe et al. 2002). In order to establish the spatial variability shown by salt-marsh testate amoebae, additional surface data sets from locations across the North Atlantic region are required. In addition to this, largely due to the limited number of studies on salt-marsh testate amoebae, preparatory and analytical techniques vary for this proxy. The time consuming nature of testate amoebae data collection and variable preparation techniques available often causes problems in generating large data sets from both modern and fossil samples (Roe et al. 2002, Charman et al. 2010). The establishment of a standardised preparation technique will help future studies to become more comparable, and potentially make significant time gains during the preparatory and analytical stages.

CHAPTER 3 - Methods

3.1 Introduction

This chapter presents the methodology used throughout the project. It largely comprises three main sections. Firstly, an account of the field sites and the field techniques used for sampling and surveying is presented. This includes how vegetation and stratigraphies were mapped in the field and how surface samples and fossil materials were collected. Secondly, details are provided of the laboratory methods. Particular attention is paid to the preparation of testate amoebae, as this provides a novel aspect of research to the thesis. The sampling of material for dating is also covered in this section. Finally, a description of the methods used during data analysis is provided. Details of modelling, computer mapping and statistical analysis are given in this third and final section.

3.2 Study area: South Hinnøya

The study area is located on the south coast of Hinnøya, an island in the Vesterålen archipelago off north-western Norway (Figure 3.1). There are two field sites in this study: Storosen and Svinøyosen. Both are coastal inlets containing salt marshes on South Hinnøya near the peninsula of Offersøy (Figure 3.2a).
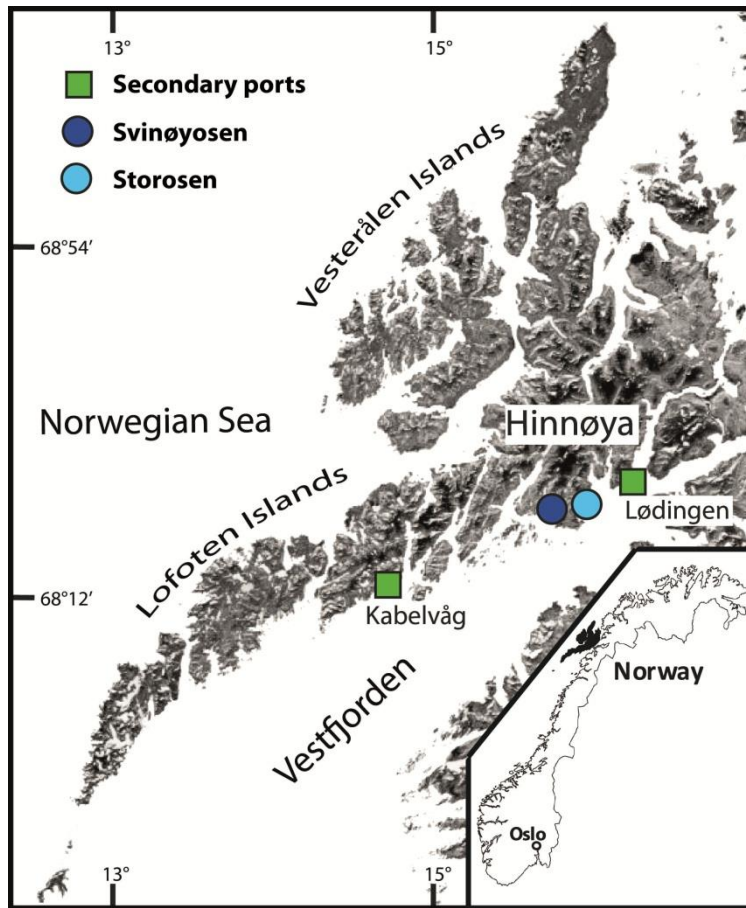
Figure 3.1 Location map of the two study sites in South Hinnøya off the north-west coast of Norway

3.2.1 Local climate

Hinnøya's south coast has a temperate climate. Weather and climate data for the field site are sourced from the Norwegian Meteorological Institute (www.sharki.oslo.dnmi.no ; accessed 09-01-2013). Monthly temperatures range from -2.0 °C in December to 13.0 °C in July (as calculated from mean monthly normals for the period 1964 to 1990). Highest precipitation occurs during the autumn and winter months (117 to 166 mm month^{-1}). Spring and summer monthly averages range from 57 to 87 mm month^{-1}. Records of the last six years show maximum snow cover occurs over January to February. The area is snow free for the months May to November. Despite

being located at 68° North this region enjoys a relatively mild climate due to its oceanographic setting.

3.2.2 Coastal oceanograpgy and tides

The Lofoten and Vesterålen islands, like many coastal areas of western Europe, are influenced by the Gulf Stream and the North Atlantic Current. Warm (~5 to 10 °C; Hansen & Østerhus 2000) North Atlantic waters are transported up the coastline of Norway via the Norwegian Current. This current reaches the southern coastlines of the Lofoten islands and Hinnøya via Vestfjorden (Figure 3.1), located between Lofoten and Vesterålen islands to the west and coastal mainland Norway to the east. The narrowing of the fjord causes tidal amplitudes to increase by 24 cm from the entrance to the head of the fjord (Moe et al. 2002). It was therefore necessary to calculate tidal heights for the field sites which are located part way up this gradient (Table 3.1).

Narvik represents the standard port for the Vestfjorden area and tide levels are calculated and published yearly. Tidal information for nearby secondary ports is calculated by applying time and height differences to the predictions given for Narvik, and is available from the Admiralty Tide Tables (Admiralty Charts and Publications, vol. 2). Chart datum for the area is fixed at the level of lowest astronomical tide (LAT) for this port. Narvik is a port with semi-diurnal tides so predictions for secondary ports are given as mean spring levels and mean neap levels. Two secondary ports exist near to the field area: Lødingen to the north-east, and Kabelvåg to the south-west (Figure 3.1), and offer the best available means for calculating tidal ranges for the field sites. Tidal

characteristics for these two ports are provided in Table 3.1. Tidal information for the field sites was extrapolated between the predictions of these two secondary ports whilst taking into consideration the approximate geographical positions of the ports and the study location. These results are also presented in Table 3.1. Both sites in the study area have a mean tidal range during spring tides of 2.55 m and during neap tides of 1.2 m.

	MLWS	MLWN	MSL	MHWN	MHWS	HAT
Lodingen	0.50	1.10	1.69	2.30	3.10	3.80
Kabelvag	0.50	1.10	1.71	2.30	3.00	3.50
Study site	0.50	1.10	1.70	2.30	3.05	3.65

Table 3.1 Tidal information calculated from the standard port of Narvik. Levels are given in metres above chart datum (LAT for Narvik). MLWS/N – mean low water spring/neap tides, MHWS/N mean high water spring/neap tides, MSL – mean sea level, HAT – highest astronomical tide

3.2.3 Local geology

The geology of the Lofoten and Vesterålen islands mainly comprises a Precambrian basement complex of Archaean gneisses and pluton intrusions of Caledonian age (Koistinen et al. 2001, Nordgulen et al. 2006). Granitic plutons make up approximately 50% of the islands (Malm & Ormaasen 1978) and are dated to between 1790 and 1800 Ma BP (Corfu 2004).

3.2.4 Storosen

The field site at Storosen predominantly contains a large expanse of unvegetated intertidal mud flats. A thin strip of salt marsh, 3500 m^2 in area, is established in the north-west corner between a small tidal stream and a copse of trees (Figure 3.2b). Approximately 500 m of mud flats and shallow tidal channels separate the salt marsh and the open sea during low tides. The low marsh is vegetated with *Plantago maritima* and *Juncus ranarius.* Higher up the marsh *Juncus gerardii* dominates the vegetation. The sediments of the salt marsh here are thin. Only a few tens of centimetres of salt-marsh sediments overlay the Caledonian basement geology.
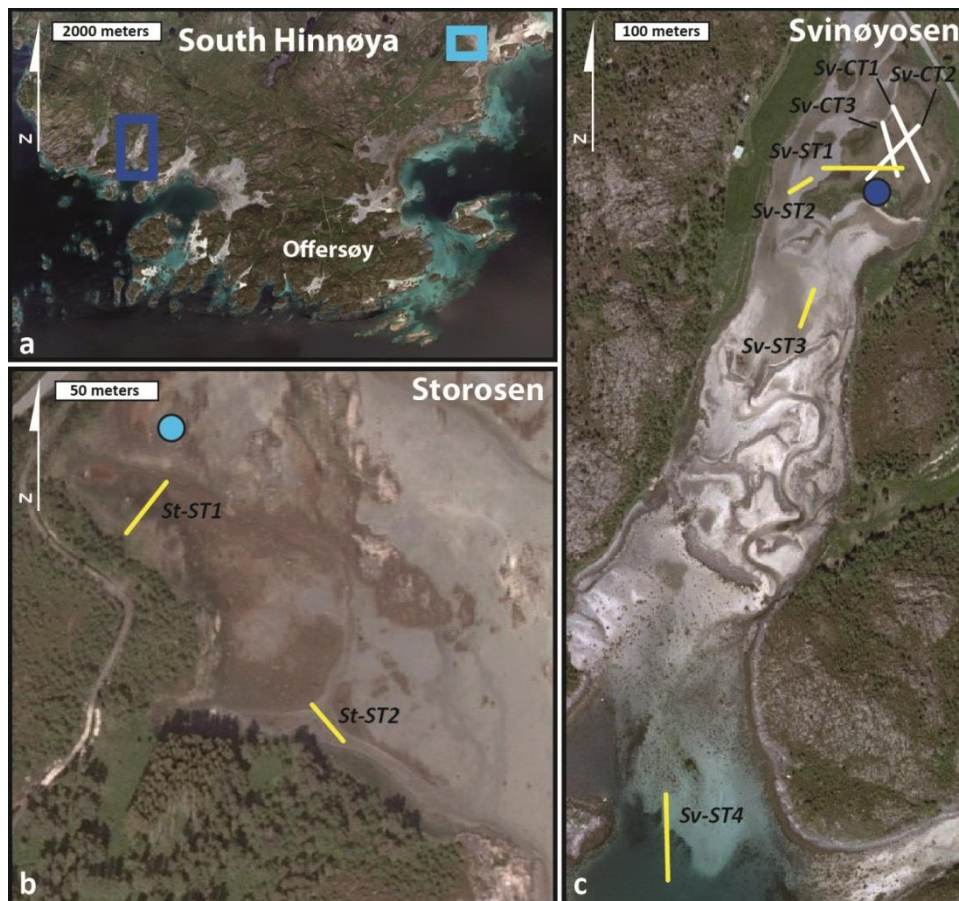
Figure 3.2 Satellite imagery of the study area and location of the two field sites (a), the salt marsh at Storosen (b) and Svinøyosen (c) and associated surface transects (yellow lines), coring transects (white lines) and ground peg locations (blue circles)

3.2.5 Svinøyosen

The field site at Svinøyosen is a coastal inlet, 1 km long and 100 m wide situated between two protruding headlands (Figure 3.2c). Sinusoidal tidal channels, flanked by mudflats, dominate the inlet and ridges of coarse beach-like material dissect the inlet. At the landward end of the inlet a salt marsh, 12000 m^2 in area, larger than that found at Storosen, occupies the north-east corner. A fresh water channel feeds into the inlet along the western banks of the salt marsh from the north-west corner. The vegetation cover of the salt marsh is similar to that of Storosen. The low marsh is dominated by *Plantago maritima* and *Juncus ranarius* and the high marsh is dominated by *Juncus gerardii*. Unlike Storosen, the salt marsh at Svinøyosen contains a thick (up to 2.5 m) sequence of Holocene nearshore sediments overlying a base of stiff, grey, glaciomarine clay.

3.3 Fieldwork

The fieldwork was carried out over two seasons during 2010 and 2011. A total of five weeks of fieldwork was undertaken during July and August 2010 and a further three weeks of fieldwork took place during July 2011. The major objectives of the fieldwork were to: collect surface vegetation information and relate this to tidal elevations, collect surface sediment samples to be analysed for contemporary microorganism assemblages, establish a detailed stratigraphy of the field site, and collect fossil sediments suitable for palaeoenvironmental analysis and for establishing a well-dated sea-level history. The methods employed in the field are presented below.

3.3.1 Vegetation mapping

Vegetation characteristics of the salt marshes at Storosen and Svinøyosen were recorded during the field season of 2010. Vegetation cover was identified along surface transects using local floras (Berg & Anthon 1980; Nilsson 1992) where possible down to species level. Major changes in species composition were identified thereby categorising the surface transects into different vegetation zones. The percentage cover of the vegetation in each zone was determined using the quadrat method (Gleason 1920) and the identified boundary of each zone was surveyed along the transect to provide a measure of elevation (Section 3.3.5).

Vegetation zone borders were mapped using a Trimble differential global positioning system (DGPS) Rover and Base Station system (Figure 3.3). Individual data points recording northing, easting and elevation were collected outlining vegetation zones and major topographical features. A swath pattern was followed to ensure suitable coverage of both marsh surfaces. Data points were imported into the ArcMAP program of the ArcGIS (ESRI; v. 10.0) software suite and were used to: 1) develop height contours for the two marsh surfaces, 2) illustrate vegetation zone boundaries, 3) locate the surface and coring transects and 4) highlight specific features of the two marshes such as raised ridges and tidal creeks. The coverage of data points for both Storosen and Svinøyosen are presented in Figure 3.4.

Figure 3.3 Foreground: Trimble DGPS RTK base station and antenna; background:

Trimble Rover GPS

3.3.2 Surface sampling

Surface sediment samples were collected from both Storosen and Svinøyosen salt marshes for foraminifera and testate amoebae analysis. All samples were collected along straight transects at regular vertical changes in elevation. Surface transects extended from the high marsh, through different vegetation zones, and into regions of low marsh and mudflats. The specifics for each salt marsh are provided below.
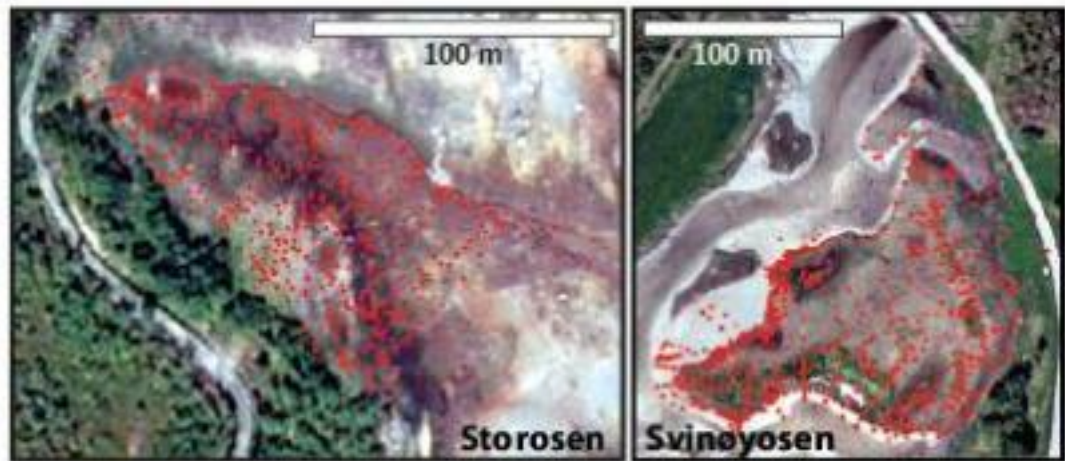
Figure 3.4 Data points from the rover survey for Storosen and Svinøyosen

Storosen

Two surface transects were established for the salt marsh at Storosen, one in 2010 (surface transect 1; *St-ST1*) and one in 2011 (surface transect 2; *St-ST2*). The first transect, *St-ST1*, is 36 m long and extended from the tree line to the tidal creek edge (Figure 3.2b). The second transect, *St-ST2*, is 20 m long and stretched from the low marsh into tidal mudflats in a seaward direction (Figure 3.2b). Elevation measurements were recorded every metre along each transect using a Zeiss total station and prism producing a topographic profile of the transects (Figure 3.5). Twenty-three surface samples (80 mm ø, 30 mm thick) were collected along *St-ST1* at regular elevation intervals (averaging changes of 4 cm). Nine samples were collected along *St-ST2* at average vertical elevation changes of 5 cm (Figure 3.5). Surface samples were collected using a hand held turf cutter (Figure 3.6) and stored in air tight containers. Upon return to Plymouth University samples were kept in refrigeration at 4°C.
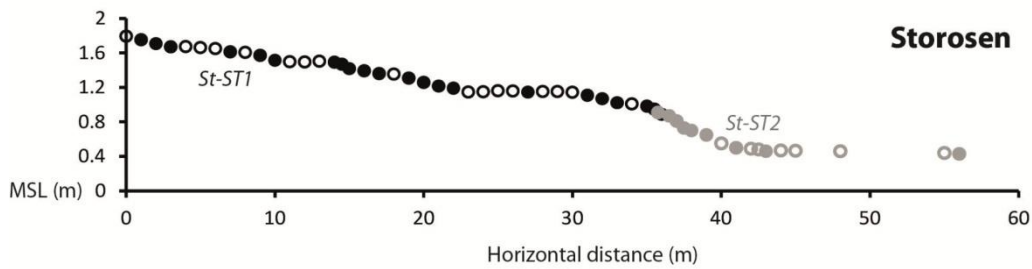
Figure 3.5 Surface topography for the two transects at Storosen. In-filled circles represent elevations that were sampled for microorganism analyses. The horizontal scale is arbitrary

Figure 3.6 Turf cutter and surface sampling tools

Svinøyosen

During the 2010 field season, three surface transects were established at the Svinøyosen field site. Surface transect 1 (*Sv-ST1*) extended from the high marsh, through different vegetation zones and terminated in an area of bare mudflat. Surface transect 2 (*Sv-ST2*) ran from the end of *Sv-ST1*, across mudflats, and descended lower into the intertidal realm. Surface transect 3 (*Sv-ST3*) ran through a more seaward location, originating in

an area of mudflat and extending into the tidal channel (Figure 3.2c). A total station was

used to survey topographic profiles (Figure 3.7). A total of 19 samples were collected

along *Sv-ST1* at average vertical elevation intervals of 5 cm. A further eight samples

were collected along *Sv-ST2* with average vertical elevation intervals of 6 cm and eight

samples were collected along *Sv-ST3* with average vertical elevation intervals of 4 cm

(Figure 3.7).
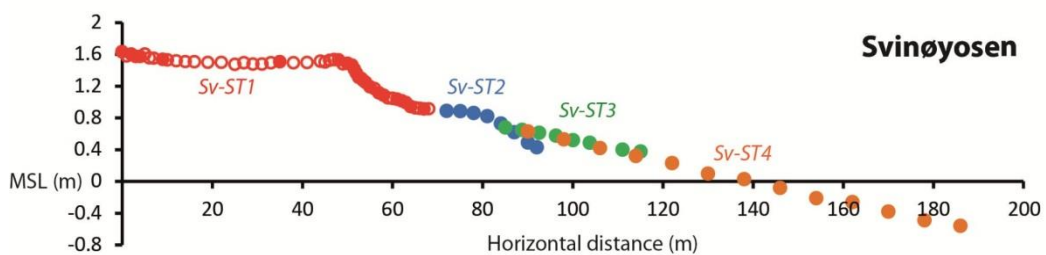
Figure 3.7 Surface topography for the four surface transects at Svinøyosen. In-filled

circles represent elevations that were sampled for microorganism analyses. The

horizontal scale is arbitrary

A fourth transect (*Sv-ST4*) was added in 2011 in order to gather surface samples from

deeper environments. During low tide on 11th July 2011 thirteen samples were collected

from below the water level at average elevation intervals of 10 cm. Their elevations

were recorded using a theodolite and staff. Table 3.2 shows start and end elevations for

all transects mentioned relative to MSL for the region.

Elevation:	Highest	Lowest
Storosen		
ST1	1.85	0.94
Svinøyosen		
ST1	1.63	0.91
ST2	0.89	0.43
ST3	0.68	0.38
ST4	0.63	-0.56

Table 3.2 Elevations of highest and lowest surface samples from each sampling transect relative to MSL

3.3.3 Lithostratigraphy

A detailed programme of coring was performed on the salt marsh at Svinøyosen. The marsh at Storosen was not cored as here the salt-marsh sediments were very thin. Three coring transects were laid out across the marsh at Svinøyosen. Coring transect 1 (*Sv-CT1*) ran for 80 m from north-west to south-east extending from a high marsh zone to a tidal channel edge. Transect 2 (*Sv-CT2*) ran perpendicular to *Sv-CT1* and ran for 70 m between two raised ridges on the marsh. Transect 3 (*Sv-CT3*) ran in a similar orientation to *Sv-CT1* and ran for 50 m between the tidal creek and a raised ridge (Figure 3.2c). Cores were taken at the start and end points along the transects and at regular intervals of 5 or 10 m.

A 20 mm diameter Eijkelkamp gouge auger was used to recover cores in 1 m sections. Each site was cored until there was refusal on an impenetrable substrate. A total of nine cores were recovered from *Sv-CT1*, eight from *Sv-CT2,* and eight from *Sv-CT3*. Each core was examined in the field; different lithofacies were identified and described using

an adaptation of the Troels-Smith (1955) system designed for coastal stratigraphies by Long et al. (1999). The notation used is summarised in Table 3.3. Common facies were identified and extrapolated in order to construct stratigraphic profiles for each coring transect.

Abbreviation	Name	Description	Symbology
Ag	*Argilla granosa*	Silt (0.002-0.06 mm)	
As	*Argilla steatodes*	Clay (<0.002 mm)	
Ga	*Grana arenosa*	Fine and medium sand (0.06-0.6 mm)	
Gs	*Grana suburralia*	Coarse sand (0.6-2mm)	
part. test.	*Particulae testarum*	Shell fragments	
Sh	*Substantia humosa*	Humified organics beyond identification	
test.	*Testae*	Whole mollusc shells	
Th	*Turfa herbacea*	Roots, stems and rhizomes of herbaceous plants	

Table 3.3 Notation used for describing salt-marsh and coastal sedimentary facies according to Long et al. (1999)

3.3.4 Palaeoenvironmental analyses

Subsurface sediments were sampled from Svinøyosen in order to provide material for palaeoenvironmental analyses. The recovered material was subsampled for micropalaeontological analyses (foraminifera and testate amoebae), establishing a chronology, and for investigating environmental variables (grain size and organic content). Fossil sediments were sampled from the marsh using monolith tins and cores.

Site		Elevation	a	b	c
Sv-CT1-0m	M(ex)	1.442	0 - 59	38 - 97	-
Sv-CT1-10m	C	1.469	0 - 91	-	-
Sv-CT1-30m	C	1.454	0 - 68	-	-
Sv-CT1-50m	C	1.514	0 - 86	71 - 118	-
Sv-CT1-80m	M(p)	1.611	0 - 60	36 - 84	-
Sv-CT2-0m	M(p)	1.681	0 - 60	30 - 90	62 - 120
Sv-CT2-70m	M(p)	1.455	0 - 60	33 - 93	
Sv-CT3-0m	M(ex)	1.272	0 - 60	44 - 104	62 - 122
Sv-CT3-0m*	C	1.272	0 - 22	-	-
Sv-CT3-10m	C	1.332	0 - 100	-	-
Sv-CT3-15m*	C	1.465	0 - 38	-	-
Sv-CT3-35m	C	1.486	0 - 100	87 - 155	-

Table 3.4 List of cores (C) and monoliths (M) collected in 2010 and 2011(*). Monoliths from dug pits (p) and cut exposures (ex) are differentiated, as are the separately collected lengths of core or monolith (a, b, c). Core top elevations are presented in m above MSL

A total of twelve monoliths from five sites were recovered, details of which are presented in Table 3.4. Monoliths were retrieved through one of two methods: either by cutting back an exposed section of a creek edge to reveal a clean, unadulterated face (e.g. *Sv-CT1-0m*), or by digging a pit into the marsh surface and sampling a cleaned, vertical face (e.g. *Sv-CT1-80m*). Stainless steel monolith tins (60 x 10 x 8 cm) were aligned vertically and hammered into the sedimentary faces and dug out with a spade, minimising disruption to the sampled material. If multiple tins were used at a single site then the ends of the monoliths were overlapped in order to retain a continuous, undisturbed sequence of stratigraphy (e.g. Figure 3.8).

Figure 3.8 Example of monolith tins being used to collect fossil sediments from a dug pit

In addition to the monoliths, seven cores from four sites were sampled at Svinøyosen (Table 3.4). A 60 mm diameter Eijkelkamp gouge auger was used to retrieve 1 m lengths of cores. Where cores extended beyond 1 m depth two boreholes were used and the ends of the cores were overlapped to ensure the collection of continuous stratigraphy. Sediment cores were wrapped in clingfilm and stored in guttering for protection. Monolith material was kept in the monolith tins, and all retrieved material was kept in refrigeration at the Plymouth University laboratories.

3.3.5 Surveying

Data collected for the purpose of vegetation mapping, surface samples and tops of cores all required accurate positioning horizontally, and most importantly, vertically. Permanent ground pegs were put in place at both Storosen and Svinøyosen above the level of HAT. The top of the pegs were located accurately in terms of X, Y and Z coordinates and all surveyed data was levelled back to this height.

For each field site ground peg coordinates were located precisely using a Trimble DGPS Real-Time Kinematic (RTK) base station (Figure 3.3). Northing and easting solutions refer to the coordinate system group of Norway (NGO48) and vertical references are to the geoid model of Norway Geoid 2008. Predicted levels of MSL from the Admiralty Tide Tables (Admiralty Charts and Publications, vol. 2) for the standard port of Narvik have not changed since 2008. Therefore, field measurements of elevations relative to MSL based on the Norway Geoid Model 2008 and references to predicted MSL and associated modern tide levels are directly compatible. The top of the ground peg in the marsh at Storosen marsh is 1.706 m above MSL and is located to 68°20'50.58746" North and 15°41'26.05039" East. The top of the ground peg in Svinøyosen marsh is 68°20'15.82274" North, 15°33'06.15975" East and 1.905 m above MSL. Vertical errors associated with the DGPS methods used are less than or equal to 1.3 cm (Network Adjustment Reports, Trimble Business Centre).

At Storosen, *St-ST1* was surveyed at 1 m intervals using a Trimble 5600 total station and prism. Surface samples were always recorded with a corresponding elevation. The surface transect collected in 2011, *St-ST2,* was levelled at the same resolution by using a

theodolite and staff and a back-sight to the ground peg via a single, temporary ground peg. Vertical errors associated with this survey totalled ± 1 cm.

The three surface transects and three coring transects established in 2010 at Svinøyosen were all surveyed using a Trimble 5600 total station and prism. Their proximity to the ground peg meant vertical survey errors were ± 0.24 cm (assuming a machine error of 5", and a maximum horizontal distance of 100 m between the total station and prism; Trimble 5600 total station datasheet, trl.trimble.com; accessed 23-01-2013). The lowest surface transect, *Sv-ST4*, was located some distance from the ground peg and a series of five temporary ground pegs was used in order to survey the surface sample elevations relative to MSL. A theodolite and staff were used to survey the temporary ground pegs and sample elevations; low winds and a fine day meant human sighting survey errors were estimated at ± 0.5 cm per survey.

3.4 Laboratory work

Analyses in the Plymouth University laboratories took place between September 2010 and September 2012. Contemporary and fossil sediments were subsampled for two groups of microorganisms; foraminifera and testate amoebae, as well as for environmental indicators. Fossil sediments were also used to provide material for dating. The specifics of the analyses are provided below.

3.4.1 Foraminifera sampling

All surface samples taken in the field were subsampled for foraminifera. A total of 31 samples were analysed from Storosen and 48 from Svinøyosen. Each subsample was prepared using the methods detailed in Gehrels (2002). These methods are based on the original preparation procedures of Scott and Medioli (1980b).

A subsample of 5 cm^3 was taken from the top 0.5 cm of the surface sample and stained using rose Bengal solution. Rose Bengal stains organic proteins pink and helps the identifier to differentiate between live (stained) foraminifera and dead (unstained) foraminifera (Walton 1952; Murray and Bowser 2000). Subsamples were wet sieved, retaining the 63 to 500 μm fraction, and split into eighths using a wet splitter. Individual aliquots were counted for foraminifera until a statistically robust figure was achieved.

Counts were taken of both live and dead foraminifera tests on subsamples from Storosen. Live populations are subject to seasonal variations in standing crops (e.g. Horton and Murray 2007) and therefore a bias may occur determined by the time of sampling. Assemblages of dead individuals represent a time-averaged crop and are immune from the effects of seasonality. Dead assemblages are therefore believed to more closely resemble fossil assemblages and so are the favoured assemblages for establishing a training set of surface data (Murray 1976, 1982, 2000). Each surface subsample from Storosen and Svinøyosen was counted until a minimum of 100 tests from the dead assemblage was reached. A total count of 100 foraminifera tests suitably represents the population of a given sample from a low diversity environment (Fatela and Taborda 2002). Aliquots were counted to their entirety so that the concentration of

tests per unit volume could be calculated (Equation 1). Average counts of unstained tests per sample for Storosen and Svinøyosen were 120 and 350 respectively.

Equation 1

$$C = \frac{\left(\dfrac{n_{tests}}{n_{aliquots}}\right) \times 8}{n_{cc}}$$

C – concentration of tests per cm^3
n_{tests} – number of tests counted
$n_{aliquots}$ – number of aliquots counted
n_{cc} – number of cubic centimetres subsampled

Identification of individuals was done using light microscopy under 40 to 100 x magnification. Where possible, individuals were identified down to species level. Taxonomy of foraminifera was based on Murray (1971), Murray (1979) and Loeblich and Tappan (1988). A taxonomic list of every type of foraminifera encountered, alongside sources of the original descriptions is presented in Appendix I. The British Museum was visited so that archived type specimens could be considered against picked Norwegian material.

Fossil material from Svinøyosen was sampled for foraminifera. The monolith *Sv-CT3-0m* was selected as a master core to provide a high resolution study as it appeared to contain a near continuous sequence of Holocene age sediments. The monolith was subsampled contiguously at 0.5 cm intervals for the topmost 10 cm, then every 1 to 3 cm for the interval 10 to 60 cm and then every 5 cm beyond. Samples were prepared

and counted in the same way to the surface samples. A total of 54 subsamples from this sequence were taken and analysed. On occasion, where the abundance of foraminifera was low the counting target of 100 tests was not met.

3.4.2 Testate amoebae sampling

A major aim of this thesis was to further develop the working practices involved with salt-marsh testate amoebae. Past studies have commonly made use of preparation procedures designed for peatland testate amoebae (e.g. Ooms et al. 2011) or for foraminifera analysis (Riveiros et al. 2007). Charman et al. (2010) modified a peatland preparation technique to study testate amoebae from North American salt marshes in an attempt to increase the concentration of tests on microscope slides for ease of counting. Further investigation designed to establish a preparation technique specific to salt-marsh testate amoebae may help future studies of this group of microorganisms.

A selection of samples was taken from *St-ST1* of Storosen in order to assess the effects of different count totals on the representativeness of salt-marsh testate amoebae populations. Samples from elevations between HAT and MHWS were selected to ensure diverse populations of testate amoebae were recovered. The eleven samples were prepared using a basic soaking preparation technique (preparation A; Table 3.5), similar to that outlined by Charman et al. (2000). For each sample two (dead) assemblage counts were produced, of 100 individuals and 150 individuals. A desired count total of 150 has often been prescribed by researchers (Warner 1990, Gehrels et al. 2006a), yet there is evidence to suggest a lower count total is sufficient (Payne and Mitchell 2009).

The assemblages produced using the different count totals were statistically analysed (see Section 3.6.2) using Bray-Curtis Indices tests (Bray and Curtis 1957).

Previous techniques used in preparing testate amoebae have involved a chemical pretreatment with a weak alkali to help disaggregate the sample to varying degrees of success (Hendon and Charman 1997, Charman et al. 2010). Preparation B (Table 3.5) is largely based on the techniques employed by Charman et al. (2010), and preparation C (Table 3.5) is a further development of this method. Both employ a weak alkali treatment of 5% KOH. The key differences between methods B and C are, i) the stage at which the material is sieved through a 15 μm mesh sieve and ii) a reduction in the size of the larger sieve mesh. A selection of six surface samples from *St-ST1* was used to investigate the effects of applying the three different preparation techniques to populations of salt-marsh testate amoebae. Each was subsampled and prepared three times using preparations A, B and C. Individual subsamples from each surface sample were homogenised before being split into 2 cm^3 portions in order to avoid sampling bias. Following preparation, counts of 100 individuals were used to produce three different assemblages for each sample. These assemblages were statistically analysed (see Section 3.6.2) using Bray-Curtis Indices tests (Bray and Curtis 1957) and Chao's Sørensen abundance based similarity estimator (Chao et al. 2005).

Preparation method		
A	B	C
Take 2 cm^3 of sediment from the top 0.5 cm of a surface sample; stain and store in Rose Bengal for a minimum of 48 hours		
In a 250 ml glass beaker add two *Lycopodium clavatum* L. tabs (Stockmarr 1971) and dissolve in 10 ml of [10 %] HCl; add the stained sample and dilute immediately with 150 ml deionised (DI) H$_2$O		
Warm beaker on a hot plate at 80 °C for 1 hour, stirring every 15 minutes to aid disaggregation of material. Turn off hot plate and leave the sample to cool slowly for a minimum of 12 hours		
Sieve the sample and retain the fraction 15 < µm < 300		Wash the sample through a 15 µm sieve, retaining the >15 fraction
-	Transfer the sample back into the beaker using 25 ml DI H$_2$O; add 4 ml [5 %] KOH and heat immediately on a hot plate at 80 °C for precisely 2 minutes	
-	Dilute the sample with DI H$_2$O and wash through a 15 µm sieve, retaining the >15 fraction	Dilute the sample with DI H$_2$O and sieve, retaining the 15 < µm < 212 fraction
Transfer the sample into a 30 ml Sterilin tube and centrifuge at 3000 RPM for 5 minutes		
Remove the supernatant and mount onto a glass microscope slide; use DI H2O if counting straight away or glycerol jelly if the slides are to be stored		

Table 3.5 Preparation methods used throughout the testate amoebae analyses

To provide a full training set of contemporary salt-marsh testate amoebae, 19 surface samples from *Sv-ST1* were used. These samples were subsampled for testate amoebae using preparation method C and count totals of 100 unstained individuals were used. In order to examine the validity of testate amoebae as sea-level indicators, core *Sv-CT3-15m* was selected for analysis as it had a thick layer of salt-marsh peat (~10 cm). In this layer testate amoebae were expected to be at their most abundant. The clay and silt rich

layers beneath, indicative of lower environments, were more likely to be devoid of testate amoebae. The core was sampled at 1 cm intervals from the top down until testate amoebae were no longer present in the sediments. Method C was used to prepare the samples and, where possible, a count total of 100 individuals was applied.

The concentration of tests per unit volume for each sample was calculated by using *Lycopdium clavatum* L. tabs to provide an exotic marker (Stockmarr 1971). Identifications were performed using light microscopy at 400 x magnification. Taxonomy follows that of by Charman et al. (2000). Keys used to identify testate amoebae down to species level were Charman et al. (2000) and Booth and Sullivan (2007). Descriptions of certain taxa not found in the keys, yet common in salt marshes, have been published in the last decade and were also used (Gehrels et al. 2001; Charman et al. 2002; Gehrels et al. 2006a).

3.4.3 Environmental variables

The sedimentology of salt marsh, coastal and near shore sediments has often been used to infer palaeoenvironmental changes and sea-level direction (e.g. Devoy et al. 1996; Goff and Chague-Goff 1999; Cundy et al. 2006; Panagiotaras et al. 2012). Grain-size analysis, loss on ignition and bulk density measurements were performed on cores *Sv-CT3-0m* and *Sv-CT3-15m* to aid interpretations of past environmental conditions.

Grain size

Particle-size analyses were performed along the entire length of monolith *Sv-CT3-0m* to accurately quantify changes in grain size. The monolith was subsampled at the following resolutions: 0 to 20 cm at 0.5 cm resolution, 20 to 40 cm at 1 cm resolution, 40 to 70 cm at 2 cm resolution, and 70 to 120 cm at 2.5 cm resolution. For each subsample 5 to 10 grams of material was taken, oven dried at 40 °C, and gently disaggregated using a rubber pestle and mortar. The sample was weighed, sieved using 1 mm mesh size, and then weighed again to acquire the percentage of the sample > 1 mm. The < 1 mm fractions were used to determine the relative abundances of clays, silts and sands, providing particle distributions for each sample. Three subsamples of approximately 0.5 cm^3 were taken from each sample (< 1 mm fraction), placed into 10 ml vials and combined with approximately 2 ml of 3% H_2O_2. This addition of hydrogen peroxide is designed to remove detrital organic material from the samples which would otherwise skew the particle size distribution data sets. Samples were left overnight and then warmed "au bain marie" for two hours. A further 2 ml of 6% H_2O_2 was added to each sample which was then warmed again after 12 hours.

A Malvern Mastersizer 2000 and autosampler were used to analyse each sample for particle size distributions at half phi scale resolutions. Each subsample was run five times thereby producing a total of fifteen solutions for each depth sampled. Data quality was determined using coefficients of variance (standard deviation over mean) across the fifteen solutions. If the coefficients of variance exceeded 15% for a given depth then the results were scrutinised, outliers identified and possibly removed. Particle size distributions were calculated using the remaining data.

Loss on ignition

Loss on ignition was used to determine the variability of organic carbon (OC) and CaCO$_3$ throughout *Sv-CT3-0m* and *Sv-CT3-15m*. OC can be removed from sediments through burning at 500°C while CaCO$_3$ oxidises (thus losing carbon via CO$_2$) at 770°C (Rowell 1994). Estimates of OC and CaCO$_3$ can therefore be acquired from dry weighing of material before and after combustion at different temperatures.

Methods used to establish OC and CaCO$_3$ content follow those described by Ball (1964) and Rabenhorst (1988) respectively. Subsamples of sediment were taken from monolith *Sv-CT3-0m* at the following resolutions: 0 to 20 cm at 0.5 cm resolution, 20 to 40 cm at 1 cm resolution, 40 to 70 cm at 2 cm resolution, and 70 to 120 cm at 2.5 cm resolution. Core *Sv-CT3-0m* was subsampled at a resolution of 0.5 cm for the top 20 cm. For each subsample, 1 to 5 grams (dry weight) of material was taken, placed in a crucible, and oven dried at 40 °C. To remove OC, samples were burned in a furnace at 550 °C for 4 hours. To remove CaCO$_3$ samples were burned at 1100 °C for 2 hours. Samples were weighed to 4 decimal places prior to and post each combustion.

Bulk density

Sedimentary density calculations are important for accurately delivering age-depth chronologies based on ^{210}Pb radioisotope analysis (Appleby 2001; Section 3.5.2). Measurements of bulk density can also be a useful tool in determining effects of autocompaction on salt-marsh sediment cores (Tovey and Paul 2002; Brain et al. 2011). The compaction of sediment cores has potentially significant impacts on sea-level reconstructions (Long et al. 2006; Brain et al. 2012). With these implications in mind,

bulk density measurements were done on both monolith *Sv-CT3-0m* and core *Sv-CT3-15m*.

The top 20 cm of each sequence was contiguously sampled at 0.5 cm intervals. This topmost layer of salt-marsh sediment contained the only peaty horizon and, although shallow, was more at risk of compaction than the more minerogenic layers beneath. The surface area of each 0.5 cm thick sediment slice was recorded and samples were oven dried at 50 °C before being weighed. Bulk density was calculated using Equation 2 below.

Equation 2

$$\rho = \frac{A \times d}{m}$$

ρ – bulk density in grams per cm^3
A – area of sediment slice in cm^2
d – thickness of sediment slice in cm
m – mass of sediment slice in grams

3.5 Geochronology

A chronology for the sediments cores from Svinøyosen was constructed using a combination of techniques. Sediments spanning the last ~100 years were dated using

^{210}Pb analysis. The chronologies produced from this technique were scrutinised using ^{137}Cs and ^{241}Am analysis. Radiocarbon dating was used for the dating of older sediments. Geochemical techniques were also applied to core *Sv-CT3-0m* in order to help date horizons which remained otherwise undated. The combined methods were used to provide age constraints on SLIPs from monolith *Sv-CT3-0m* and core *Sv-CT3-15m*.

3.5.1 Radiocarbon dating

Combining radiocarbon dates with biostratigraphic data from coastal sediments is a common way of producing SLIPs and constructing sea-level histories. It is necessary to ensure, however, that the material selected for dating appropriately represents the sedimentary horizon that it is found in. Plant fragments should be horizontally bedded and detrital in nature. Small and fragile fragments are preferred as it is assumed these are likely to have been buried rapidly. Segments of roots should be avoided to minimise the chance of assigning a spuriously young age to a horizon. Marine molluscs should be used with care. Pristine and unbroken shells are preferable to damaged or detrital shell fragments which may indicate excessive pre-burial mobilisation. Bivalve shells should be found in their life positions and be of a non-burrowing nature. This project made use of both terrestrially derived (e.g. Betula fragments) and marine derived (e.g. marine gastropod shells) material for radiocarbon dating.

A number of specific horizons were targeted for ^{14}C dateable material and the following provides the rationale behind the radiocarbon dating strategy. The bottommost

lithological unit was targeted to provide a basal date for the sequence. Changes in lithofacies were identified and these boundaries were also targeted for dateable material. Cores and monoliths from all three coring transects were targeted in order to produce a suite of dates encompassing the palaeosurfaces of the entire marsh. The master core *Sv-CT3-0m* was targeted for a multitude of dates in order to produce a high resolution chronology from a single location.

The accelerator mass spectrometry (AMS) method for analysing ^{14}C was used for radiocarbon dates and allowed the use of small (~0.015 g) samples. Targeted areas were dissected 0.5 cm at a time using stainless steel scalpels and tweezers. Surfaces that were in contact with packaging materials during storage were scraped clean parallel to the surfaces to remove potential contamination. Suitable terrestrial material needed to show evidence of: 1) being sourced from above ground, 2) being surficially deposited, 3) laying horizontally in the lithology, and 4) originating from the surrounding environment. Thus, roots were not selected and material that was selected had not been transported long distances. This approach ensured that dated material accurately reflected the ages of the layer it was discovered in. Occasionally marine material was selected for dating. Bivalves and gastropods were identified down to species level to ascertain that they were benthic dwellers and non-burrowers. Shells were inspected using light microscopy for evidence of abrasion and transport before being prepared for analysis.

All selected material was gently rinsed using deionised H_2O and a fine paint brush in order to remove any attached clastics or unassociated organic material. Cleaned samples

were oven dried at 40 °C before being weighed. All radiocarbon samples associated with this project were sent for AMS ^{14}C analysis to the NERC Radiocarbon Facility (Environment) in East Kilbride, Scotland. High precision analysis was performed on two samples, which returned multiple dates for each. Results from the facility provided ages in conventional radiocarbon years BP with a ± 1 sigma error range. Ages from terrestrial material were calibrated using the IntCal09 curve (Reimer et al. 2009) into years before present (present = 1950 AD). Dates from marine material were calibrated using both accepted reservoir correction methods for comparison. Firstly, dates were calibrated using IntCal09 and a reservoir correction of -440 years was applied (Mangerud and Gulliksen 1975). Secondly, the raw radiocarbon ages were calibrated using the Marine09 curve (Reimer et al. 2009) with a ΔR value of 65 ± 37 (CALIB 6.0; Stuiver and Reimer 1986, 1993).

A total of 22 radiocarbon dates have been sourced and used in this thesis. A separate NERC funded project, "Sea-level changes in the North Atlantic Ocean: implications for the melting history of the Greenland Ice Sheet" (NE/H000860/1, 2009-2012) by Dr William Marshall is responsible for sourcing 14 radiocarbon dates on sediments from Svinøyosen (allocation numbers 1530.0311 and 1577.0911). The remaining eleven radiocarbon dates were awarded to an application made to the NERC Radiocarbon Facility (Environment) on behalf of this project in 2012.

3.5.2 Short lived radionuclide dating

The chronostratigraphic technique of using the fallout radionuclide ^{210}Pb is routinely used in salt-marsh based sea-level studies (e.g. Gehrels et al. 2002; Gehrels et al. 2005; Gehrels et al. 2006b; Kemp et al. 2011; Gehrels et al. 2012). Decay rate profiles of the radioactive isotope ^{120}Pb are able to provide a chronology for sediments of up to the last 150 years (Appleby 2001). An accurate age-depth model for recent sediments from Svinøyosen is necessary in order to compare sea-level reconstructions with historical, time constrained data such as tide-gauge records. These techniques also fill a gap (post 1950s) where conventional ^{14}C dating is incapable of providing a chronology.

Profiles of ^{210}Pb were measured for both the master core *Sv-CT3-0m* and the short core *Sv-CT3-15m*. Methods used follow that outlined by Appleby (2001). Contiguous slices of 0.5 cm were taken from the core tops down to 30 cm (*Sv-CT3-0m*) and 20 cm (*Sv-CT3-15m*). The bulk density of each slice was calculated before each sample was diced, ground up and homogenised into a fine matrix using scissors and a pestle and mortar. The disaggregated material was packed into 4 ml vials (Figure 3.9), and the mass of the packed sample recorded. The vials were sealed, labelled appropriately and left for a minimum of 21 days so that ^{214}Pb was allowed to reach equilibrium with ^{226}Ra. Analyses were run at the Plymouth University Consolidated Radioisotope Facility (CoRIF) using the EG&G Ortec well (GWL-170-15-S) HPGe Gamma spectrometry system. The instrument was calibrated as directed in the GWL-170-15-S Record Manual using soil spiked with a traceable, certified mixed radioactive standard. Samples were counted for a minimum of 24 hours (maximum 48 hours) for activity concentrations of ^{210}Pb, ^{214}Pb, ^{137}Cs and ^{241}Am. Counts were provided for all samples

until a depth in the core was reached where ^{210}Pb activity concentrations dropped below minimum detectable limit (MDA). All counts were recorded in Becquerels per kg.

Figure 3.9 Tools used to prepare samples for radionuclide dating and a packed vial

In order to calculate an age-depth profile, activity measurements of ^{214}Pb were taken so the depth at which unsupported ^{210}Pb reached levels of supported ^{210}Pb could be realised. The modelling approach used (constant rate of supply model; CRS; Appleby 2001) is based on a logarithmic function of total supported and unsupported ^{210}Pb at a given depth and the ^{210}Pb radioactive decay constant. It assumes a constant rate of unsupported ^{210}Pb deposition from the atmosphere through time, however remains robust when sediment deposition rates are variable, and is thus a suitable model for use in salt-marsh chronologies. Sediment ages were calculated using equation 18 from Appleby (2001).

Activity profiles of the radionuclides ^{137}Cs and ^{241}Am were used to provide independent chronological markers during the last 100 years. Peaks in ^{137}Cs can be attributed to nuclear weapons testing, the climax often represented by a peak around 1963 (Cambray

et al.1989), and from the Chernobyl accident in 1986 (Cambray et al. 1987). ^{241}Am is only detected during the period of nuclear weapons testing in the 1950s and the early 1960s (Cambray et al. 1989). The radionuclide signatures of these historical events were used to constrain the modelled ^{210}Pb age-depth profiles for both cores.

3.5.3 Geochemical markers

Metal analyses of salt-marsh sediments have been used to provide chronological markers in western Iceland (Gehrels et al. 2006b, Marshall et al. 2009), New Zealand (Gehrels et al. 2008) and Tasmania (Gehrels et al. 2012). Atmospheric fallout of lead and other metals results from periods of increased mining activity during our historical past. Lead and mercury pollution from far field locations has been recorded in Greenlandic lakes (Bindler et al. 2001), demonstrating the long range transport these airborne pollutants are capable of. Concentrations of lead (Pb) and mercury (Hg) were measured through core *Sv-CT3-0m* to identify atmospheric signatures of mining pollution and concentrations of nickel (Ni), copper (Cu) and zinc (Zn) were measured to define localised metallurgical pollution related to nearby industries.

Contiguous 0.5 cm sediment samples were taken from 0 to 53 cm in core *Sv-CT3-0m*. Subsamples (0.1 g) were digested in a MARS 5 (Environment Canada) microwave open using 3 ml of 5.6% HNO_3 and 16.7% HCl following Hassan et al. (2007). Element analysis was performed using a Thermo Fisher Scientific X-Series II ICP-MS which was calibrated using synthetic standards (Inorganic Ventures Inc, Virgina, USA).

Isotopic ratios of Pb ([206]Pb, [207]Pb and [208]Pb) were collected to aid in determining periods of Pb pollution (e.g. Gehrels et al. 2005, 2006b, 2008, 2012). Procedures followed Ishizuka et al. (2007) using a Thermo Fisher Scientific Neptune multi-collector ICP-MS. Blanks were used throughout the analyses to provide quality control.

The amount of pollution Pb through core *Sv-CT3-0m* was calculated using Equation 3. This method assumes two sources of Pb: natural and anthropogenic pollution Pb, and requires knowledge of the [206]Pb and [207]Pb ratios for each (Renberg et al. 2002). The assumed isotope ratios of pollution Pb are taken from Renberg et al. (2002) for both the pre-industrial era (1.17) and post-industrial era (1.15). The natural isotope ratio was calculated as the mean value of samples below 39 cm depth which represented sediments older than ~2100 cal yrs BP (1.37).

Equation 3

$$Pb_{poll} = \left(\frac{Ratio_{sample} - Ratio_{natural}}{Ratio_{pollution} - Ratio_{natural}} \right) \times Pb_{total}$$

Pb_{poll} – pollution Pb in parts per million
$Ratio_{sample}$ – Pb 206/207 ratio of sample
$Ratio_{pollution}$ – Pb 206/207 ratio of pollution Pb
$Ratio_{natural}$ – natural Pb 206/207 ratio
Pb_{total} – total Pb (i.e. [208]Pb) in parts per million

Changes in Hg, Ni, Cu, and Zn accumulation were calculated as enrichment factors following Klaminder et al. (2003). These pollutants were normalised against the

conservative element scandium (Sc) so that peaks in enrichment could be attributed to pollution rather than sediment accumulation rates or bulk densities. Sc has been used to successfully normalise metal concentrations in the past (Shotyk et al. 1998, Klaminder et al. 2003, Monna et al. 2004).

3.6 Data analysis

A variety of software packages were used to illustrate, model and analyse the primary data. GIS was used to display vegetation and topographic information of the salt marshes at Storosen and Svinøyosen. Replicate surface data of testate amoebae were compared using similarity determination statistics. Training sets of contemporary microfossils were zoned using cluster analysis and environmental gradients of the same data were determined using detrended canonical correspondence analysis. Numerical techniques used to build transfer functions (e.g. ordination and regression) are described in Chapter 6.0.

3.6.1 GIS modelling

GPS data from the Trimble Rover system provided easting, nothing and elevation (X, Y, Z) information for both marshes. These data points were imported into ArcMap (version 10.0) and displayed on their relevant coordinate system (WGS84; UTM zone 33).

Satellite imagery in raster format was obtained from the Norwegian Mapping Authority (Statens Kartverket) and was georeferenced to the data points. Elevation information between the data points was projected onto the entire surface of each marsh using a Delaunay based triangular irregular network (TIN) interpolation in ArcMap. This TIN was converted to raster using natural neighbour interpolation, and allowed the generation of elevation contours for the marsh surfaces. Features such as vegetation zone limits, streams and ponds had been mapped in the field with the Rover GPS and were imaged as layers in ArcMap by creating polygonal shapefiles constrained by the mapped data points.

3.6.2 Similarity determination

The testate amoebae experimental work contained two main aims: (1) to determine how many tests were required to provide a statistically robust count per sample; and (2) to identify the best preparation method which minimised count time per sample but kept the integrity of each sample. The surface testate amoebae data were subjected to statistical comparisons to check rigorously whether by changing the minimum count figure or preparatory procedure the recorded assemblages deviated from one another. Two tests were used to perform the comparisons: 1) the Bray-Curtis index (BCI) of dissimilarity and 2) Chao's Sørensen abundance based similarity estimator (Ch). The specifics of each test, where they were used and the rationales behind using each test are given below.

Bray-Curtis index (Bray & Curtis 1957)

This test is capable of comparing data sets with multiple variables. In addition, the BCI incorporates the relative proportion size of the variables too. When used to compare the pairs of assemblages with different count totals both type *and* abundance of species were taken into consideration. The BCI combines the sum of differences between common species at each site and makes this a function of the combined sum of all species. Hence the result is a measure of dissimilarity bounded between 0 and 1. A ratio of 0 represents perfect similarity and 1 denotes samples are perfectly different. The ratio (*BCI*) is expressed as:

Equation 5

$$BCI_{jk} = \sum \frac{\left| S_{ij} - S_{ik} \right|}{\left(S_{ij} + S_{ik} \right)}$$

j – sample being compared with sample k
k – sample being compared with sample j
S_{ij} – abundance of ith species in the jth sample
S_{ik} – abundance of the ith species in the kth sample

Chao's Sørensen abundance based estimator (Chao et al. 2005)

The BCI is suitable for comparing directly related pairs of assemblages as described above. However, compared assemblage data that do not contain full ecological populations may appear erroneously (dis)similar. The effects of unseen species can skew comparisons and must therefore be accounted for. The surface testate amoebae data representing different preparation techniques were compared using the Ch

86

estimator which makes an adjustment for rare, unseen species, which may occur in the ecological population. The estimate is bound between 0 (perfectly dissimilar) and 1 (perfectly similar) and may be expressed as:

Equation 6

$$Ch_{est} = \frac{2U_{est}V_{est}}{U_{est} + V_{est}}$$

U – total relative abundance of individuals in assemblage 1 of the shared species
V – total relative abundance of individuals in assemblage 2 of the shared species
est – estimate of unseen shared species in assemblage x based on observed shared
species from random sample of individuals

3.6.3 Cluster analysis and environmental gradients

Cluster analysis was used to group assemblages of similar compositions from surface data sets relative to a tidal level. This zonation helps to assign indicative ranges to species and assemblages. The program CONISS (Grim 1987) which produces constrained cluster analyses by the method of incremental sum of squares was applied to surface assemblages. This method kept adjacent samples next to each other during the zonation process. The software program Tilia (version 1.7.16) was used to apply CONISS to the data sets (Grim 1992).

Environmental gradient lengths are used to determine whether collective species within a surface data set respond linearly or unimodally to an environmental variable. This information is important for deciding what type of regression model to use when

applying a transfer function of modern assemblage data to fossil assemblages (Birks 1995, 2010). Environmental gradient lengths can be calculated in terms of standard deviation units of biological turnover. Gradient lengths greater than 2 standard deviations imply species response to the environmental variable is unimodal. Lengths less than 2 indicate a linear response (ter Braak and Prentice 1988). Detrended canonical correspondence analysis (DCCA; ter Braak 1985) was used to define species variation and environmental gradients lengths in terms of standard deviation units. CANOCO for Windows (version 4.56; Jongman et al. 1995) was used to run DCCA analysis.

3.6.4 Synthesis of errors

An approximation of the total errors associated with the sea level reconstructions was performed following Preuss (1979). Total error is equal to the square root of the sum of all individual errors squared (Equation 7).

Equation 7

$$E_t = \sqrt{e^2{}_{tide} + e^2{}_{peg} + e^2{}_{surv} + e^2{}_{smpl} + e^2{}_{func}}$$

E_t – total error
$e^2{}_{tide}$ – tidal extrapolaton error
$e^2{}_{peg}$ – ground peg positioning error
$e^2{}_{surv}$ – core top survey error
$e^2{}_{smpl}$ – sampling error
$e^2{}_{func}$ – transfer function error

The tidal regime of Svinøyosen was calculated via extrapolation using the two secondary ports that flank the field site (Lødingen and Kabelvåg). The difference in

MSL elevations and MHWS elevations of the two ports is 2 and 10 cm respectively. Therefore, using the difference in MHWS as the potential for extrapolation error (it is this tidal elevation that is most associated with salt-marsh foraminifera), the assumed vertical error of tidal range extrapolation was ± 5 cm. The vertical error associated with the DGPS positioning of the ground peg at Svinøyosen was ± 1.3 cm, and the core top survey error was ± 2.4 cm. Fossil samples were collected in 0.5 cm increments, therefore the conservative sampling error associated with this was 0.25 cm. Errors associated with the transfer functions are sample specific and are discussed further in Chapter 6. These composite error estimations were used to provide vertical uncertainties on the final plotted RSL reconstructions. Total errors are presented and discussed further in Section 7.3.

3.7 Summary

The two field sites, Storosen and Svinøyosen, have been described in terms of climate, oceanographic setting, and geology. Fieldwork carried out at the two sites included vegetation mapping, surface sample collection for microorganism analyses, coring to establish lithostratigraphies and sampling of fossil sediments for palaeoenvironmental analyses. All sampling transects and core locations were surveyed relative to common bench marks that were established using DGPS. Laboratory analyses included modern and fossil foraminifera sampling using established methods and a development on the analytical procedures associated with salt-marsh testate amoebae sampling and counting. Sedimentary changes through two cores were quantified using LOI, grain size and bulk

density measurements. The top sediments from both cores were constrained chronologically using short lived radionuclide techniques (^{210}Pb, ^{137}Cs, ^{241}Am); core *Sv-CT3-0m* was further analysed for radiocarbon samples and geochemical marker horizons in order to provide a chronology throughout the Holocene. The following chapter presents results from the modern environments at both Svinøyosen and Storosen.

CHAPTER 4 – Results: modern environments

4.1 Introduction

This chapter presents results from the modern environments found at Storosen and Svinøyosen. Descriptions of topography and surface vegetation are given for the salt marshes and near shore sediments at the two field sites. These descriptions are used to establish zones and demarcate 'high marsh' and 'low marsh' environments, determined by the surface floral composition.

Surface transects were established and surveyed at the two sites to provide elevation specific samples representative of the modern environments. These samples provided material for foraminifera and testate amoebae analyses, the results of which are presented in this chapter. Original counts for all samples are provided in electronic form, located in the back cover of the thesis. Vegetation zonation was also related to elevation so the flora – fauna relationship could be compared with tidal elevations.

A key feature of this research is to investigate the preparatory and analytical procedures involved with salt-marsh testate amoebae analyses. Studies were done on the use of different sample preparation techniques and the influence these have on stain retention and population characteristics, as well as the effects of using different count totals when counting samples. The results of these investigations are presented in this chapter and conclusions regarding the most suitable count totals and preparation techniques are made.

4.2 Storosen: modern environments

This section describes the modern environment of the salt marsh and near shore sediments at Storosen. Two surface transects were established at Storosen, and topographic descriptions and surface vegetation cover are presented relative to these. Vegetation across the salt marsh was identified and related to tidal elevation. Surface samples were collected along the transects for foraminifera and testate amoebae analyses. Assemblages of dead foraminifera were compiled against elevation and grouped into zones of similar samples. Investigations into the preparation and analytical procedures of salt-marsh testate amoebae were performed on these surface samples from Storosen and provide a novel aspect to this thesis.

4.2.1 Topography

The field site at Storosen has a flat topography consisting of expanses of mud flats and thin vegetation (Figure 4.1a). The area is littered with pebbles and boulders up to approximately 2 m^3 in volume. Outcrops of basement rock are also visible (Figure 4.1a). An example of the field site being flooded during high tide is presented in Figure 4.1b. An established strip of salt marsh runs down a gradient from the tree line to a thin tidal stream (Figure 4.1c). Surface transect 1 (*St-ST1*) runs from the treeline at 1.8 m above MSL, down this gradient (approximately 5°), and ends at the tidal stream 0.7 m above MSL (Figure 4.1c). Surface transect 2 (*St-ST2*) can be seen in Figure 4.1d. Here the transect runs from an area of low salt marsh (0.9 m above MSL), into a stretch of tidal mud flats (0.4 m above MSL).
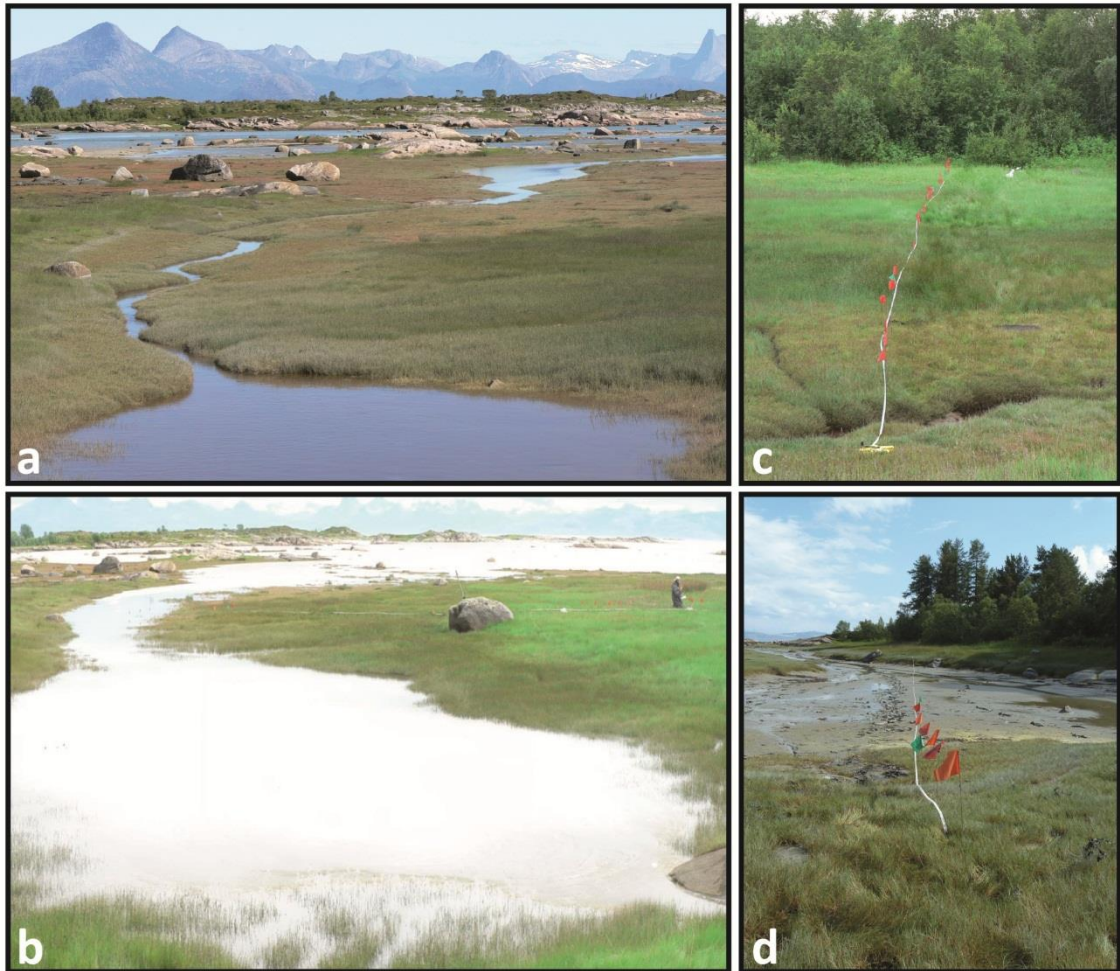
Figure 4.1 a) Storosen salt-marsh, b) Storosen at high tide, c) Transect St-ST1, d) Transect St-ST2

4.2.2 Vegetation cover

Through identifying changes in floral species and percentage cover along *St-ST1*, the vegetation at Storosen could be classified into four zones. Zone 1 characterises the lowest marsh environments and has the lowest floral diversity of all the zones. This zone extends from the tidal stream at 0.89 m above MSL up to 1.11 m above MSL and contains just two species of vegetation: *Plantago maritima* and *Juncus ranarius*. Zone 2 also contains *Plantago maritima*, but is dominated and characterised by the sedge

species *Blysmus rufus*. This zone extends from 1.11 m above MSL to 1.31 m above MSL where it meets zone 3. The 'low marsh' environment is characterised by vegetation zones 1 and 2. Zone 3 can be subdivided into two subgroups: 3a and 3b. Both are dominated by *Juncus gerardii,* but zone 3a is less diverse and contains only two other species: *Plantago maritima* and *Agrostis stolonifera*. Zone 3b includes species of flowering plants (*Glaux maritima*, *Geranium* sp.), grass (*Festuca rubra*), and sedge (*Carex* sp.). Zone 3 defines the 'high marsh' environment and extends from 1.31 m above MSL to 1.51 m above MSL on *St-ST1* where the final zone starts. Zone 4 is the most diverse of the zones and no longer contains halophytic sedges or rushes like the other zones. Here, the majority of the vegetation cover consists of grasses (*Leymus arenarius* and *Arrhenatherum elatius*) and flowering plants (e.g. *Potentilla egedii*, *Trientalis europaea*). This final zone is largely terrestrial and is only influenced by the highest astronomical tides. The species of flora encountered in each zone and their relative abundances are presented in Figure 4.2.

Vegetation zone boundaries were mapped using the Trimble DGPS Rover system. Longitude, latitude and elevation were recorded allowing the zonation to be illustrated two dimensionally against elevation contour data in ArcGIS (Figure 4.3). Transitions between vegetation zones occur at consistent elevation intervals. Zone1, comprising mudflat colonising species *Plantago maritima* and *Juncus ranarius,* is consistently located proximal to a tidal water source and is common at elevations between 0.7 and 1.1 m above MSL. Below this lower limit bare mud flats dominate the environment. Above zone 1 where tidal inundation is less frequent, vegetation zones 2 and 3a occur. The upper limit of zone 3a is consistently found around 1.25 m above MSL. Only above this elevation are flowering plants such as *Glaux maritima* and species of *Geranium* found in zone 3b. The final transition from zone 3b into the terrestrial zone 4 occurs at

elevations between 1.5 and 1.6 m above MSL. The elevations of the zone boundaries recorded linearly along the surface transect correlate strongly with the two dimensional vegetation transitions shown in Figure 4.4 from the DGPS data. There is a strong relationship between elevation, and hence tidal inundation, and floral composition.
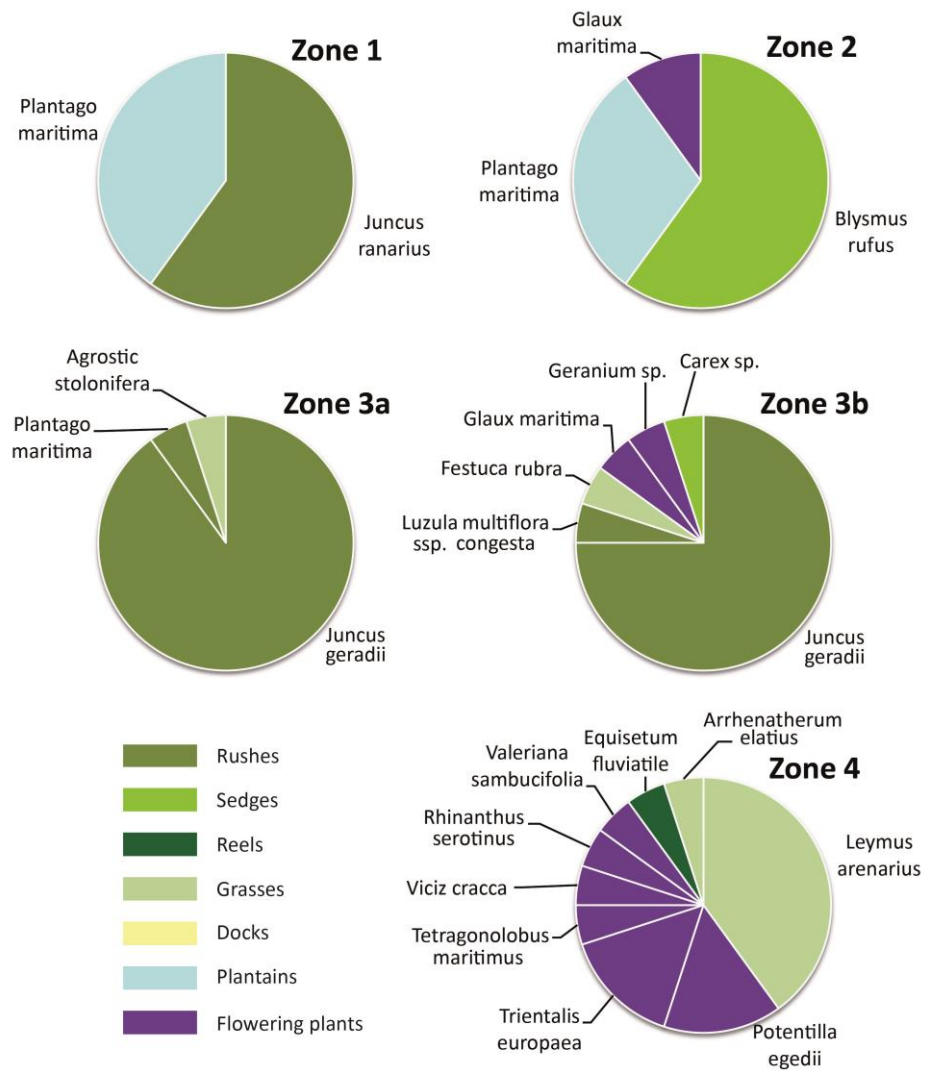
Figure 4.2 Vegetation zones and their characterising flora at Storosen
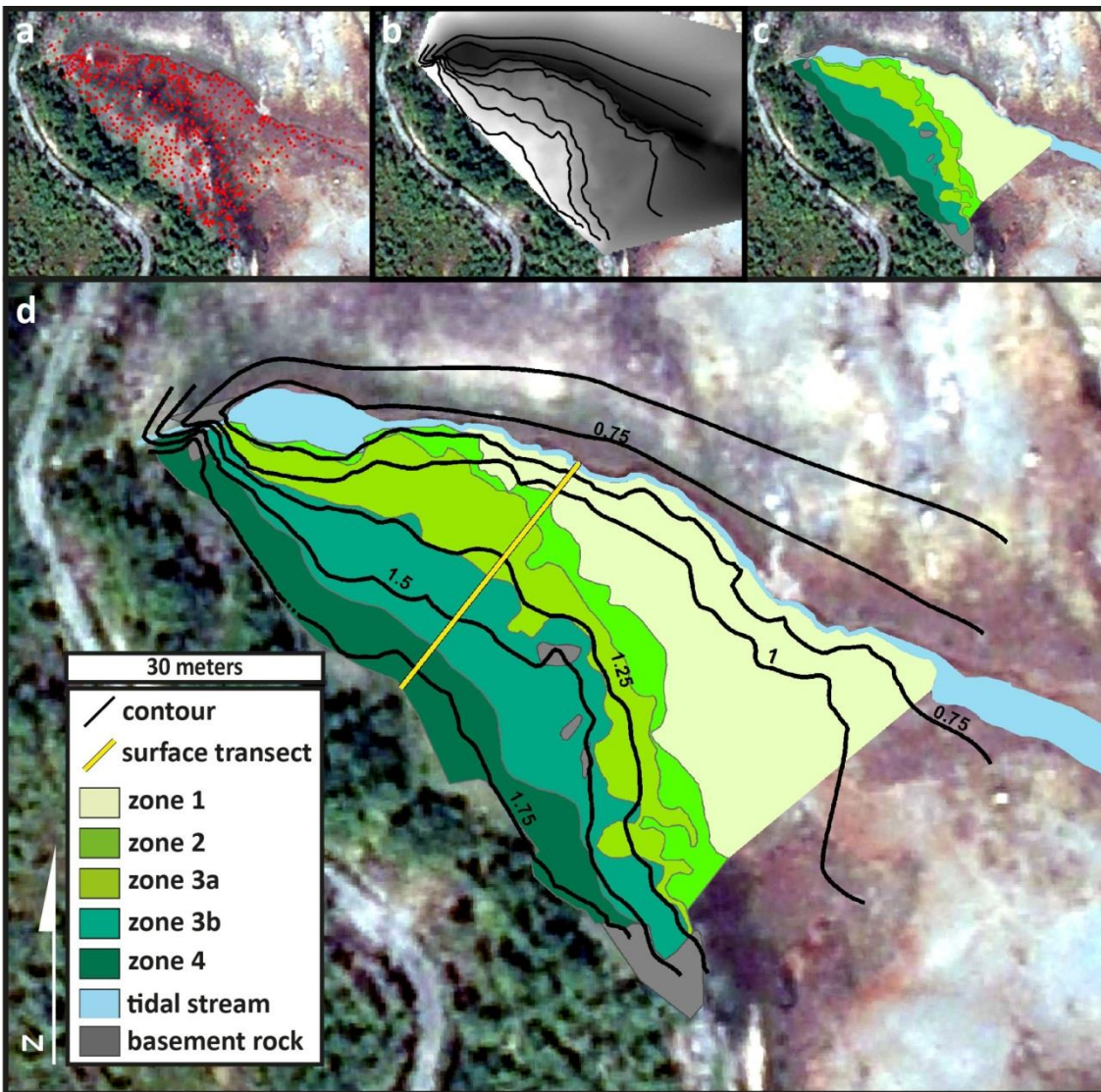
Figure 4.3 Vegetation zonation and elevation contour data (relative to MSL) for the salt marsh at Storosen, a) data points recorded with the DGPS Rover System, b) height contours using surface elevation information, dark shading identifies lower elevations, c) field mapped vegetation zone boundaries, d) combined GIS data and surface features

4.2.3 Modern foraminifera assemblages

Surface samples taken from *St-ST1* and *St-ST2* were inspected for foraminifera and assemblages were plotted as percentages (Figures 4.4 and 4.5). Assemblages of both

live (stained) and dead (unstained) individuals were compiled for the two transects. This allowed the contemporary, and possibly seasonally biased, standing crop to be compared with a time averaged population of surface foraminifera. Dead assemblage data ought to be used for training sets (Murray 1976, 1982, 2000) so these assemblages were first compared with the live assemblages to ensure that fossilised foraminifera appropriately reflected the modern environment. A proportion of species occurred in very low numbers. Where this was the case, species consistently representing less than 2% of the entire assemblage were combined into a subclass of 'rare species'.

Surface transect St-ST1

At Storosen, *St-ST1* produced a total of 23 samples; 15 of these contained assemblages of live foraminifera and 16 samples contained assemblages of dead foraminifera. Samples above 1.5 m above MSL were barren. Figure 4.4 presents the live and dead foraminifera populations along *St-ST1*. Only two different species of foraminifera were encountered along this surface transect, namely *Jadammina macrescens* and *Miliammina fusca*. Both are agglutinated forms and common salt-marsh species. Of the samples containing live foraminifera from *St-ST1*, all except one had populations of both species. Only the highest sample (1.47 m above MSL) contained an assemblage populated by just *J. macrescens*. Of the samples containing dead assemblages, the six highest samples (above 1.26 m above MSL) only contain *J. macrescens*. *Jadammina macrescens* was typically the most abundant species throughout both datasets and rarely occurred in percentages less than 90%. The crop of dead foraminifera closely resembles the standing crop of live foraminifera suggesting that fossilised assemblages accurately represent their pre-burial environment.
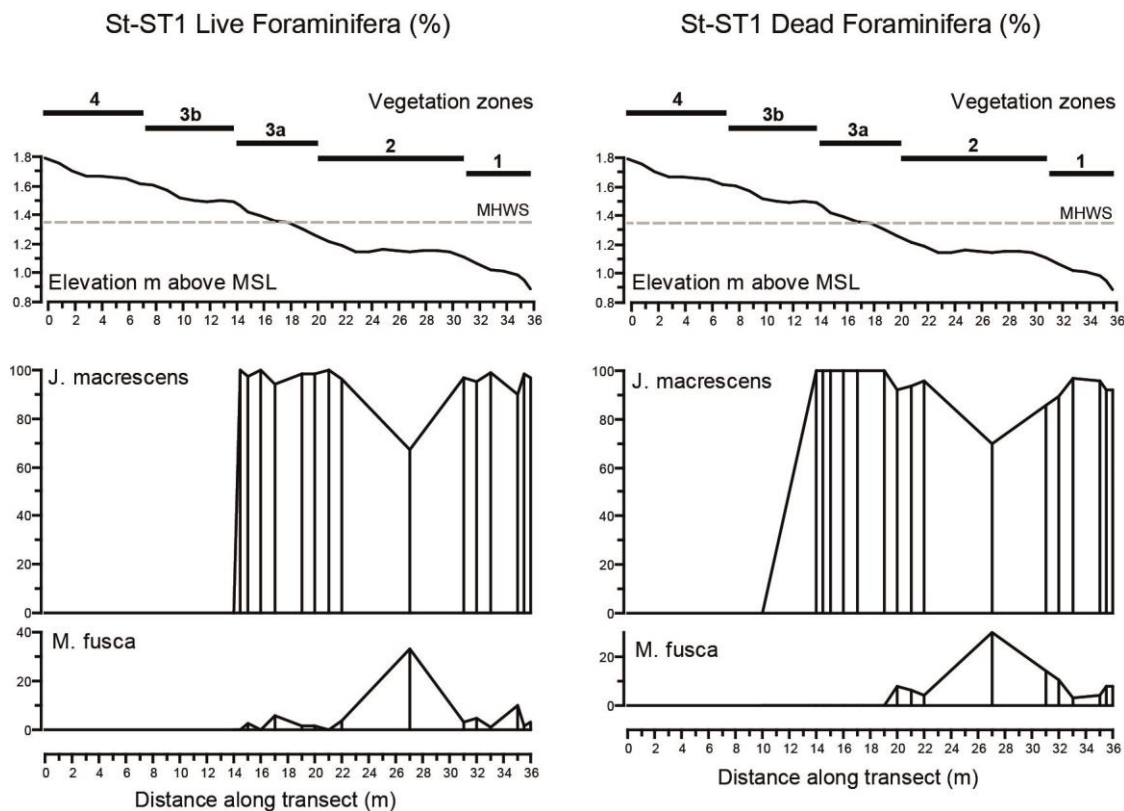
Figure 4.4 Assemblages of live and dead foraminifera from transect St-ST1 shown in relation to surface topography and vegetation zone changes

Surface transect St-ST2

The lower surface transect, *St-ST2,* comprises of nine samples, all of which contained assemblages of both live and dead foraminifera (Figure 4.5). Samples from this transect extended from 0.91 m above MSL down to 0.43 m above MSL and contained a wider variety of live and dead foraminifera in comparison to *St-ST1*. The two agglutinated species *J. macrescens* and *M. fusca* occur in all samples in both assemblages. However, the relative abundance of *J. macrescens* decreases with decreasing elevation. *Miliammina fusca* typically occurs in greater percentages throughout *St-ST2* in comparison to *St-ST1*, potentially as a function of elevation. Calcareous species tended to dominate the samples from *St-ST2*. *Cibicides lobatulus, Elphidium* spp., and, to a lesser extent, *Haynesina germanica,* occurred in significant percentages throughout the

transect in both data sets. Total foraminifera diversity increases with decreasing elevation and there is a significant presence of rare species (those making up < 2 % of the populations) in both the live and dead assemblages. As was the case in *St-ST1*, the crop of dead foraminifera closely resembles that of the live, further suggesting that the fossilised assemblages appropriately reflect the modern environment. Due to the similarities of the two assemblage crops, and due to the importance of using the dead assemblage data in training sets (Murray 1976, 1982, 2000), only data of dead foraminifera were collected for the surface transects at Svinøyosen (Section 4.3).
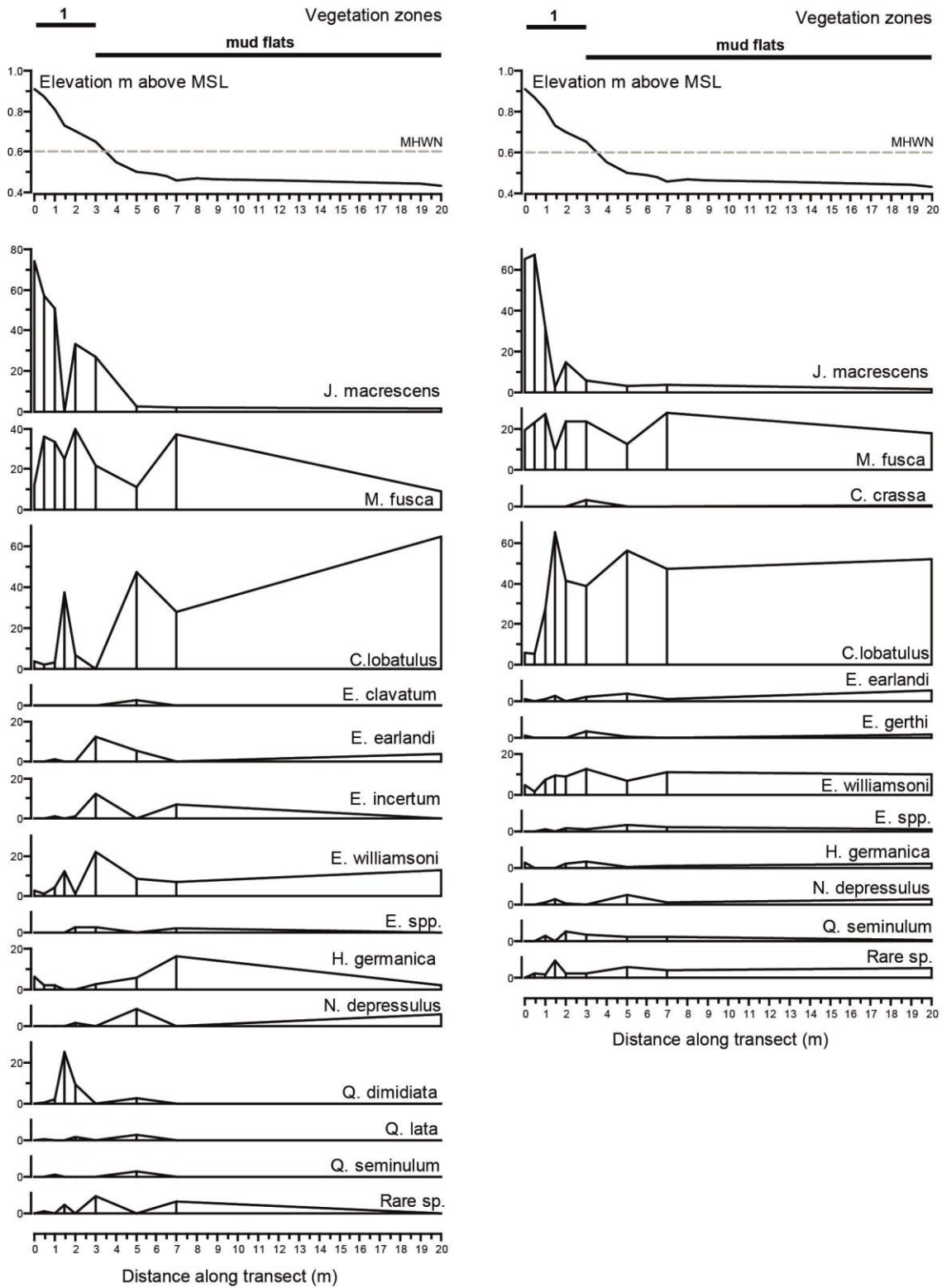
Figure 4.5 Assemblages of live and dead foraminifera from transect St-ST2 shown in relation to surface topography and vegetation zone changes

100

4.2.4 Modern testate amoebae assemblages

As no standardised procedures exist for the preparation of salt-marsh testate amoebae, samples from *St-ST1* were used to investigate the impacts that different preparatory and analytical techniques have on testate amoebae population characteristics. The effects of using two different count totals (100 and 150 individuals per sample) were analysed using eleven samples from Storosen and the effects from using three different preparation techniques (A, B and C; see Table 3.5) were analysed using six samples from this transect. In all cases, investigative statistics were used to analyse the impacts of using different count totals and preparation techniques on population characteristics. The counting of testate amoebae from salt-marsh samples can be time-consuming (Charman et al. 2010) and can be the limiting factor in palaeoenvironmental studies. With this in mind, the success of different preparation techniques was also considered in terms of time taken to count samples as well as in terms of assemblage characteristics. Finally, populations of live and dead testate amoebae were compared along *St-ST1*. These results were used to analyse the effects different preparation techniques had on the retention of Rose Bengal stain to live protoplasm.

Effects of count totals

The eleven pairs of assemblages produced from Storosen using different count totals (100 and 150) are presented in Figure 4.6. These samples were all prepared using preparation method A (Table 3.5). Dominant taxa (such as *Centropyxis cassis* type and *Cyclopyxis arcelloides* type) are consistently represented in similar percentages by the two count totals. Figure 4.6 demonstrates that the percentage counts produced using different count totals are very similar. Assemblage differences are mainly driven by taxa which are encountered in very low numbers. These observations are supported by the

similarity determination statistics. Table 4.1 presents some quantitative characteristics of these assemblages and includes the results from the BCI comparative statistics. On average, by continuing the count total to 150 individuals, rather than stopping at 100, only a single additional taxon was encountered at low abundance. By dividing the assemblages into rare (those making up 2 % or less of the assemblage) and non-rare (> 2 %) taxa it is evident that the total number of non-rare taxa remains more or less consistent. Variations in the total number of taxa are largely driven by the presence of rare taxa, which can often be represented by a single occurrence in a sample.

Elevation m above MSL	Count total	Total taxa	No. taxa >2 % / rare taxa	No. tests per cm^3 (x10^2)	BCI
1.753	100	14	7 / 7	251	
	150	15	7 / 8	245	0.07
1.707	100	21	10 / 11	282	
	150	22	9 / 13	228	0.09
1.67	100	15	11 / 4	211	
	150	17	10 / 7	202	0.06
1.612	100	14	10 / 4	211	
	150	15	10 / 5	221	0.09
1.571	100	11	6 / 5	1689	
	150	11	7 / 4	1394	0.04
1.514	100	12	8 / 4	216	
	150	12	8 / 4	251	0.04
1.492	100	11	6 / 5	282	
	150	12	7 / 5	300	0.04
1.468	100	14	7 / 7	96	
	150	15	7 / 8	107	0.05
1.418	100	8	5 / 3	286	
	150	8	5 / 3	320	0.07
1.392	100	11	6 / 5	86	
	150	14	7 / 7	36	0.06
1.36	100	10	7 / 3	24	
	150	11	7 / 4	25	0.08

Table 4.1 Assemblage characteristics for the count total analyses
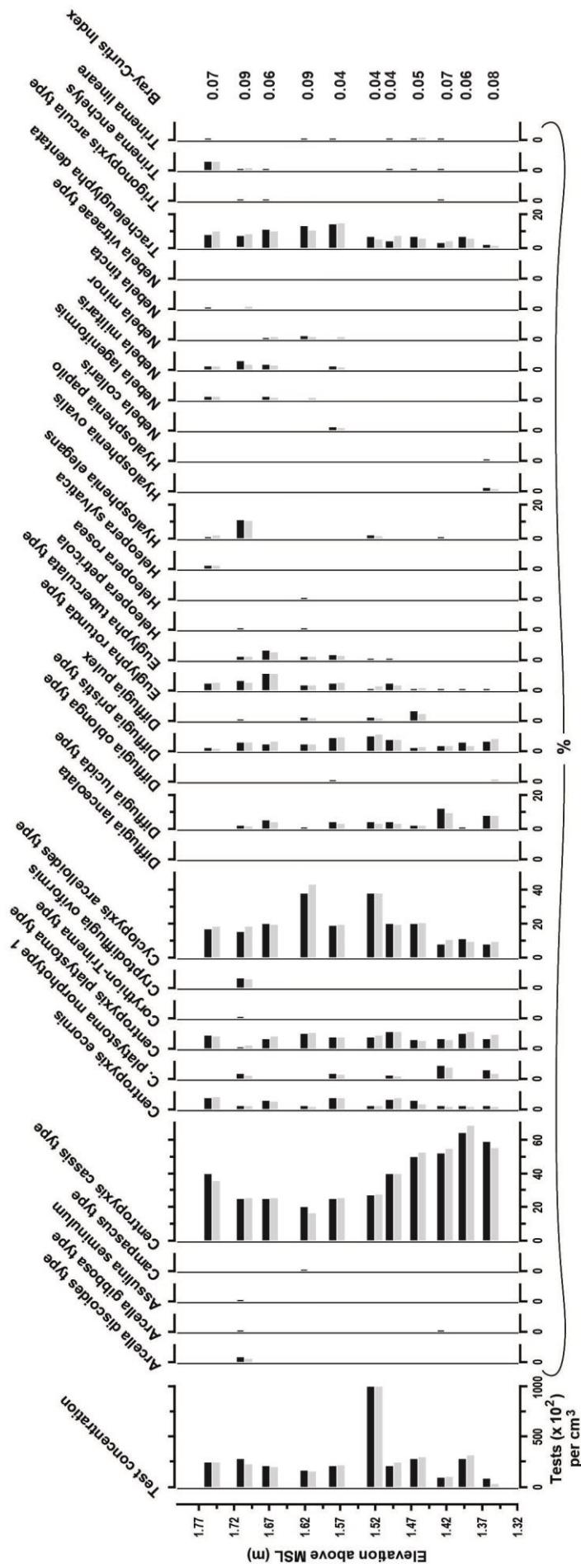
Figure 4.6 Testate amoebae assemblage data from eleven samples after applying a count total of 100 (black) and 150 (grey). Dissimilarity between compared samples are shown in terms of BCI scores

There is a clear tendency for a reduction in the taxon diversity with decreasing elevation. The lower samples typically contain between 8 and 12 taxa, regardless of count totals, whereas the higher elevation samples contain between 11 and 22 taxa. The lowest concentration of tests is found in the lowest sample at 1.36 m above MSL where there are approximately 2,400 to 2,500 tests cm^{-3}. The samples from higher elevations most commonly contain between 20,000 and 30,000 tests cm^{-3}, although numbers are sometimes much higher and highly variable.

A high BCI score, close to 1, indicates that pairs of assemblages are almost entirely different in terms of the taxa present and their relative abundances within the assemblages (e.g. Magurran 2004). All eleven pairs of assemblages have a BCI score of less than 0.1 suggesting that assemblage compositions are nearly identical, regardless of whether count totals of 100 or 150 are used. Again, minor dissimilarities seen between the assemblages are driven by the presence or absence of rare species.

Effects of preparation technique

Assemblage compositions and a summary of assemblage characteristics from the six samples where three different treatments were used are presented in Figure 4.7 and Table 4.2 respectively. Preparation method A, which contained no chemical disaggregation procedures, yielded the highest number of taxa per sample. On average, method A produced 2 and 2.33 more species per sample compared to preparations B

and C respectively. On two occasions preparation B yielded the highest number of taxa, and only once did method C produce the highest number of taxa. As a rule, the different preparation techniques produced similar ratios of non-rare taxa to rare taxa, with very few exceptions. The lowest elevation (1.39 m above MSL) is again associated with the lowest number of taxa encountered. The largest number of taxa is found in the highest elevation sample. In terms of test concentrations, method C produced the highest number of tests per cm^3 of sediment in three out of the six cases. In three cases method A yielded the lowest concentrations of tests. As replicate samples should in theory contain a similar concentration of tests per unit volume, regardless of preparation technique, a low concentration may indicate that some individuals are being 'missed' during the counting process, either by being hidden in debris on the slide, lost during sieving or damaged and dissolved by the treatment.
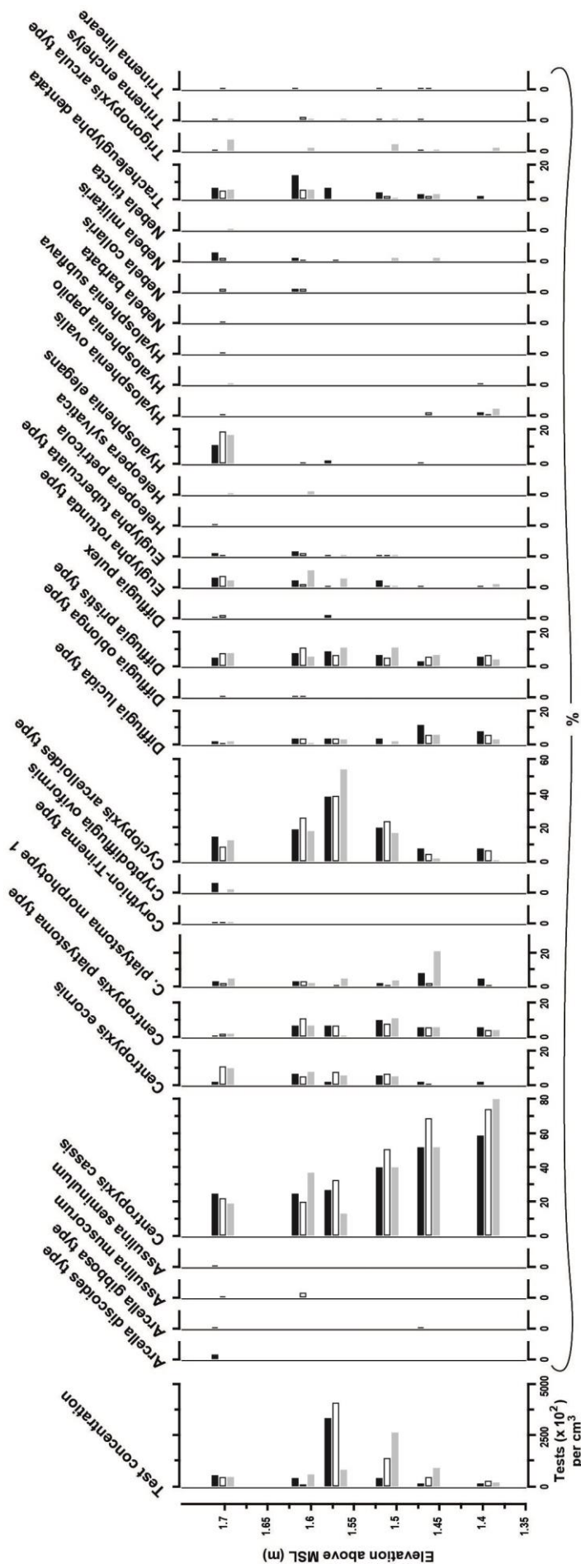
Figure 4.7 Testate amoebae assemblage data from six samples following preparation methods A (black), B (white) and C (grey)

As was seen earlier, the presence or absence of rare species can influence the characteristics of an assemblage significantly. Incomplete inventories may ignore species with low abundances (e.g. Longino et al. 2002; Pfeiffer and Mezger 2012) resulting in a catalogue of unseen species, which remain unaccounted for. When comparing two assemblages with sub-maximal count totals, such as in this case, it is important to adjust for these unseen species. Chao's Sørensen abundance-based similarity estimator makes a probability based estimate of the rare species that are shared, yet not necessarily seen, in both assemblages (Chao et al. 2005). The similarity index is then applied following this correction and ranges between 0 (perfectly dissimilar) and 1 (perfectly similar). All except one of the comparisons show an index score of greater than 0.9 and thirteen of the total eighteen comparisons show an index score of greater than 0.95. When unseen species are accounted for it is therefore apparent that the assemblages produced from the different preparation techniques are very similar. BCI comparison statistics were also performed for all pairs of samples (Table 4.2; for comparison purposes, BCI values have been converted into a similarity matrix where 1.0 represents perfect similarity, as opposed to perfect dissimilarity). The BCI statistics demonstrate the importance of rare species when comparing assemblage populations. As Figure 4.7 shows, proportions of the 'main' species are broadly similar; this is supported by the Chao's estimate also. Similarities between the compared samples are still high (68 to 87 % similarity) when using the BCI scores, which fail to account for unseen rare species.

Elevation m above MSL	Preparation method	Total taxa	No. taxa > 2% / rare taxa	No. tests per cm^3 (x10^2)	Chao's estimate	95% confidence intervals	BCI
1.707	A	21	10/ 11	282	A : B = 0.91	± 0.10	0.69
	B	21	7 / 14	238	B : C = 0.88	± 0.15	0.71
	C	17	9 / 8	235	A : C = 0.93	±0.12	0.78
1.612	A	14	10 / 4	211	A : B = 0.97	± 0.05	0.8
	B	16	9 / 7	60	B : C = 0.94	±0.09	0.76
	C	12	7 / 5	300	A : C = 0.96	±0.10	0.68
1.571	A	11	6 / 5	1689	A : B = 0.92	±0.27	0.85
	B	8	6 / 2	2064	B : C = 0.98	± 0.11	0.68
	C	10	7 / 3	422	A : C = 0.98	± 0.15	0.7
1.514	A	12	8 / 4	216	A : B = 1.00	± 0.05	0.84
	B	9	5 / 4	714	B : C = 1.00	± 0.10	0.87
	C	13	7 / 6	1327	A : C = 0.98	± 0.09	0.79
1.468	A	14	7 / 7	96	A : B = 0.96	±0.08	0.78
	B	10	5 / 5	241	B : C = 0.97	±0.10	0.81
	C	9	6 / 3	464	A : C = 0.96	± 0.12	0.76
1.392	A	11	6 / 5	86	A : B = 1.00	± 0.06	0.84
	B	7	5 / 2	159	B : C = 0.99	± 0.10	0.74
	C	8	5 / 3	104	A : C = 0.96	± 0.18	0.87

Table 4.2 Assemblage characteristics for the preparation analyses

The purpose of the investigation was to identify a procedure that was capable of disaggregating organic rich samples without destroying tests. If a high level of disaggregation was not achieved, then the microscope slides used for counting would be cluttered with organic particles and detritus making identification and counting of testate amoebae a lengthy process. With this in mind, the time taken for samples to be counted was noted (Figure 4.8). Samples produced using preparation A, which involved no chemical disaggregation, proved to take the longest to count. On average a minimum of twelve hours was required to count a full population of 100 tests. This time varied according to the location of the sample on the marsh and the concentration of testate amoebae found in the sediments. The longest time spent counting one sample to gain a

population of 100 tests was 22 hours. Samples produced using method B or C took significantly less time to count and slides appeared less cluttered (Figure 4.9). When a chemical disaggregant was used, samples generally took less than 10 hours to reach a full count. The shortest time taken to count a single sample of 100 tests was 15 minutes. There are clear time gains to be made from using a chemical disaggregant. Considering the high Chao's Sørensen abundance-based similarity estimate scores it is apparent these improvements are not associated with loss of assemblage information.
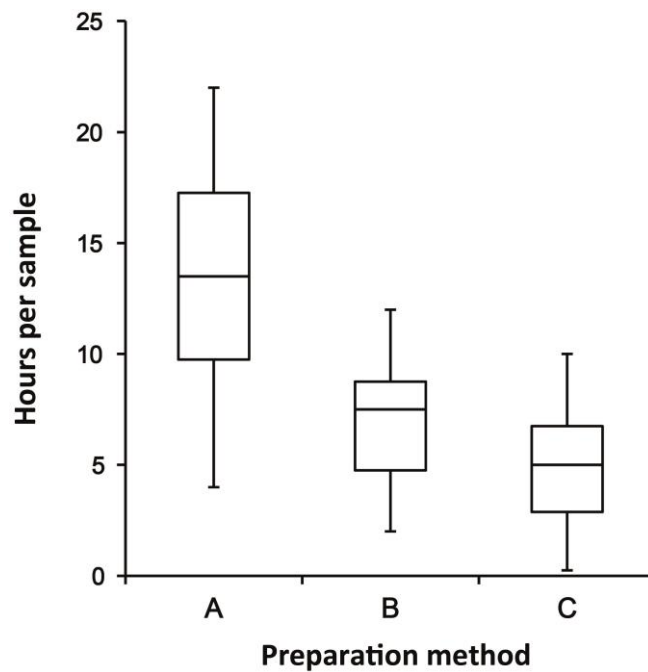
Figure 4.8 Box and whisker plots showing time taken (min, median, max, interquartile range) to count assemblages of 100 individuals following different preparation procedures
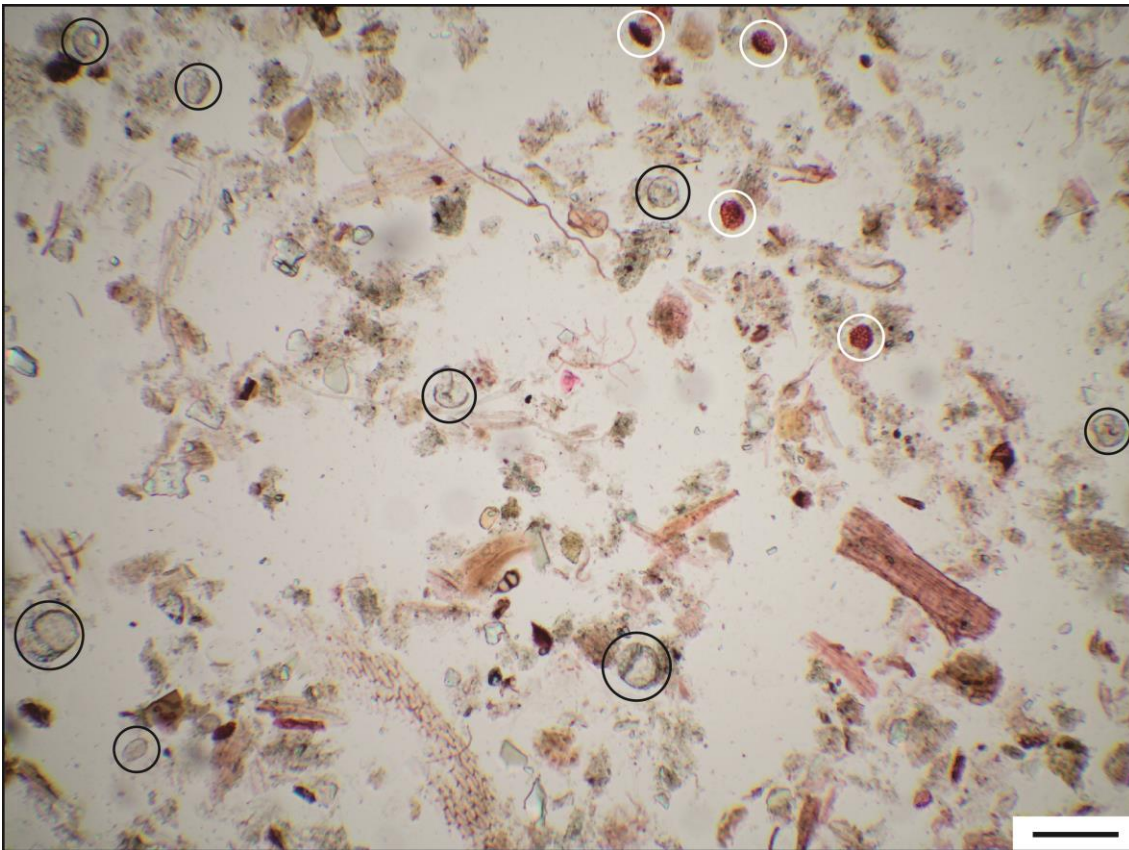
Figure 4.9 Micrograph of an example microscope slide following preparation C.

Testate amoebae (black circles) and lycopodium spores (white circles) are highlighted.

Scale bar represents 100 μm

Living versus dead populations

Contemporary testate amoebae populations, like foraminifera, are subject to seasonal variation. Factors controlling growth patterns include moisture, food and oxygen availability, soil chemistry, temperature, and light variability (Charman and Warner 1992; Charman et al. 2000). All of these are capable of changing throughout the year. It is therefore important to account for both live and dead individuals when compiling representative surface assemblages. Testate amoebae samples were stained with rose Bengal so that dead (unstained) specimens could be identified from the live (stained).

The eleven samples used for comparing the effects of count totals were prepared using preparation method A. Comparisons of live and dead testate amoebae counts are presented below. Figure 4.10 shows the number of live individuals encountered in each sample of 100 dead individuals. This figure also shows live versus dead results from the six samples from Storosen prepared using methods B and C. Here counts of live individuals are also given as per 100 dead individuals.
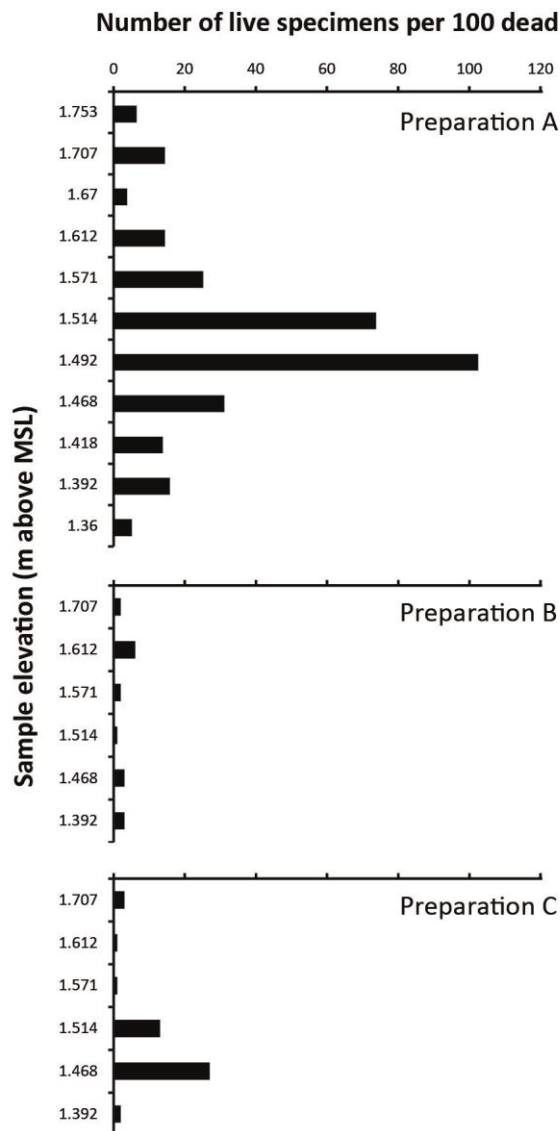
Figure 4.10 Counts of live testate amoebae for each sample of 100 dead tests showing the effects of preparation techniques on rose Bengal stain retention

Samples prepared via method A contained between 5 and 155 live individuals per 100 dead. This shows significant variation in the numbers of live testate amoebae encountered across the marsh surface. The maximum number of live specimens occurs around 1.5 m above MSL. Preparation methods B and C both used a chemical disaggregant to break up the samples. In both cases, the numbers of stained tests encountered in samples prepared this way were significantly lower than their counterpart samples prepared using method A (Figure 4.10). Microscale natural variability of live versus dead forms is unlikely to have caused this ratio change. It is highly plausible that the alkali used in methods B and C may have detrimental effects on the retention of rose Bengal solution used to stain live protoplasm. It is likely that the chemical treatment bleached the rose Bengal, or alternatively, destroyed the live protoplasm. In this case, it is possible that live specimens were included within the dead assemblage count and that either an adaptation of the preparation technique is required, or it may be prudent to include both live and dead crops within the assemblages used for palaeoreconstruction purposes. Due to the inconsistencies of live specimen availability, and to avoid seasonal bias (Murray 2000), only catalogues of dead individuals have been used to construct environmentally representative assemblages.

4.2.5 Summary

Presented in the first half of this chapter are results from an investigation into the modern environment at Storosen salt marsh. Vegetation zones were identified, mapped and related to elevation changes. There proved to be clear zonation of vegetation groups in relation to elevation. Assemblages of surface foraminifera were characterised along transects, crossing the marsh and extending into tidal channels. Assemblages of dead

foraminifera closely resembled assemblages of live foraminifera, both in terms of species present and abundance of shared species. Dead assemblages from Storosen are later incorporated with foraminifera assemblages from Svinøyosen in order to construct a training set of modern foraminifera related to elevation (Section 4.3.3)

An investigation into the preparation procedures and counting styles of surface salt-marsh testate amoebae was also carried out. When evaluating surface populations of testate amoebae, there proved little statistical difference between using a count total of 100 and 150. When preparing the samples in three alternative ways the outcomes showed that:

- Preparation A took the least time to prepare, saving approximately 10 minutes per sample. Slides produced using preparation A however took the longest to count. This method on average produced a higher number of total taxa than the other two procedures, approximately 2 taxa more per sample than preparation B and 2.5 taxa per sample than preparation C.

- Preparation B took slightly longer to prepare than C due to sieving the samples twice. This procedure regularly produced the lowest diversity of taxa that made up more than 2% of the populations. Typically the taxa that were present were recorded in relatively greater abundances in comparison to the other two preparation methods leading to the assemblage data favouring the dominant taxa.

- Preparation C used a more efficient sieving method which reduced the likelihood of losing specimens during the preparation procedures. The technique also used a smaller mesh size for the upper sieve which helped concentrate

testate amoebae on the microscope slides. The method produced the 'cleanest' slides which led to the quickest counting times overall. Comparisons between the assemblages using the Chao's Sørensen abundance-based similarity estimator showed that gains made using methods B or C did not necessarily lead onto a loss of assemblage information.

In addition, it became evident that preparation methods B and C caused live testate amoebae to lose their stain of rose Bengal, possibly as a result from the chemical procedures. The results suggest that the stain should be applied following a chemical treatment, or that the total crop of live and dead forms ought to be included within the sample assemblages. Time saved during the counting process imply that preparation C is a most suitable method for preparing salt-marsh testate amoebae. However, this is dependent on the nature of the individual samples. Method C had a longer preparation time than then standard method (A) and it is possible that not all salt-marsh surface samples require a chemical disaggregant for ease of counting (Tom Newton 2013. pers comms).

The results from this section provide empirically based evidence for the justification of the methods used in the second half of this chapter. The modern assemblages of surface foraminifera and testate amoebae from Svinøyosen are presented below. Samples used for testate amoebae analysis were prepared using procedure C and assemblages were formed based on count totals of 100 tests.

4.3 Svinøyosen: modern environments

This section describes the modern environment of the salt marsh and near-shore sediments at Svinøyosen. Vegetation was studied on the salt-marsh surface. Zones of similar floral compositions were identified and mapped relative to elevation data. A total of four surface transects were established at Svinøyosen and surveyed relative to MSL. Samples from all four transects were analysed for foraminifera. Dead assemblages were used to construct foraminiferal populations relative to elevation and constrained cluster analysis was used to group samples of similar compositions. Samples from the salt-marsh transect *Sv-ST1* were analysed for testate amoebae and populations of dead forms were created and likewise zoned and related to elevation. No testate amoebae were present in the remaining three surface transects.

4.3.1 Topography

The salt marsh at Svinøyosen has a predominantly flat topography which slopes gently down a gradient into mud flats in the south-west corner. Isolated ridges of higher ground are seen across the surface of the marsh and run in various orientations. The tidal channel that flows along the westward edge of the salt marsh is eroding the north-west corner of the marsh, resulting in a micro-cliff (approximately 1 m in size). Small pools of standing water occupy hollows across the marsh surface. In comparison to the field site at Storosen, there is a notable lack of boulder litter on the surface of the salt marsh. Surface transect 1 (*Sv-ST1*) runs east to west from a bank of raised ground at 1.6 m above MSL, across the salt marsh and into tidal mud flats at 0.9 m above MSL (Figure 4.11a). Surface transect 2 (*Sv-ST2*) starts near the end of *Sv-ST1* and extends from the mud flats at 0.9 m above MSL, and into the tidal channel at 0.4 m above MSL.

The remaining two transects are located further seaward, at lower elevations (Figure 3.2c).
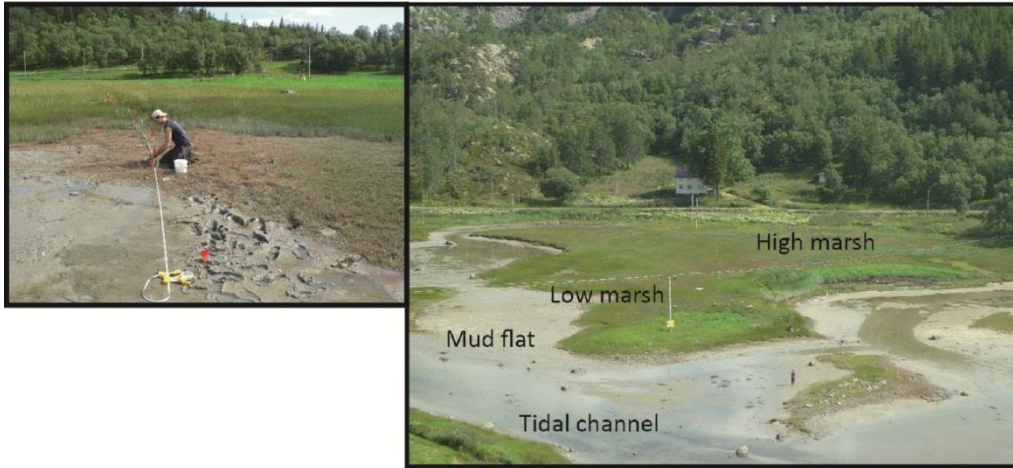
Figure 4.11a) Surface transect Sv-ST1 at Svinøyosen, b) salt-marsh zonation at Svinøyosen

The narrow inlet at Svinøyosen contains ridges of higher ground (Figure 4.12a,b) comprised of coarse grained sands, gravels, pebbles and small boulders. The material occupying the tidal channel is finer and contains living gastropods and bivalves (Figure 4.12c) as well as an abundance of detrital shell material (Figure 4.12d). Surface transect 3 (*Sv-ST3*) runs parallel to the inlet from an area of raised ground (0.7 m above MSL), and further into the channel (0.35 m above MSL). The final transect, *Sv-ST4*, is located at the seaward end of the inlet and encompasses the lowest elevations of the study (Figure 3.2c). This transect extends from 0.6 m above MSL to -0.55 m above MSL. Here, sediments were finer than those encountered in the tidal inlet. Clays, silts and fine sands dominate.

Figure 4.12a) The tidal inlet at Svinøyosen showing the salt marsh (far left) and coarse grained ridges shaping the tidal channel, b) raised ridges, c) living gastropods and bivalves, d) detrital shell material within the tidal channel**

* Photographs taken by Dr. Margot Saher

4.3.2 Vegetation cover

The salt-marsh vegetation cover at Svinøyosen can be separated into four zones. Zone 1, in a similar fashion to Storosen, has the fewest species of plants. This zone is characterised by *Plantago maritima* and *Juncus ranarius*. Zone 2 also contains *Juncus ranarius* but includes *Triglochin maritima*. The equivalent zone at Storosen contains the species *Blysmus rufus*; however, this is not present at Svinøyosen. These two zones characterise the 'low marsh' at Svinøyosen (Figure 4.11b). Zone 3 is subdivided into two subgroups, both dominated by *Juncus gerardii*. Zone 3a includes the species *Luzula multiflora* spp. *congesta* and *Glaux maritima*. Zone 3b includes two species of grass, *Phragmites australis* and *Festuca rubra*. The two subgroups of zone 3, combined, represent the 'high marsh' at Svinøyosen. Zone 4 is the most diverse of the vegetation

zones and contains numerous species of mixed, herbaceous plants as well as grasses.

Figure 4.13 presents floral compositions for the vegetation zones at Svinøyosen.
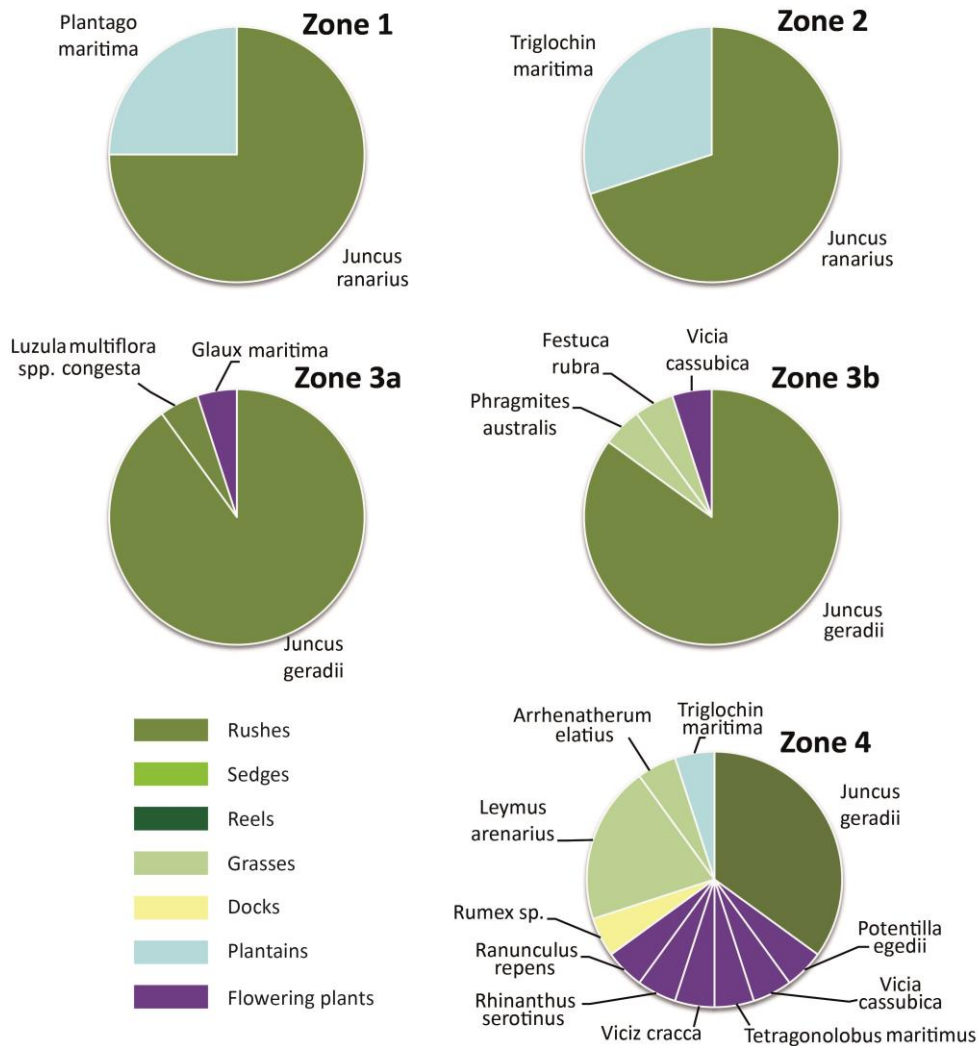
Figure 4.13. Vegetation zones and their characterising flora at Svinøyosen

Changes in vegetation zonation were identified along *Sv-ST1* which ran from vegetation

zone 4, through the high and low marsh and into unvegetated, tidal mud flats. Zone 1

starts at 0.94 m above MSL, near the end of the transect, and terminates at 1.07 m above

MSL where zone 2 begins. Zone 2 ends at 1.19 m above MSL where zone 3 begins. The

upper boundary of zone 3 is at 1.59 m above MSL, and beyond this zone 4 dominates the transect. Figure 4.14 presents images of the different vegetation zones at Svinøyosen.

Figure 4.14 a) Juncus ranarius in vegetation zone 1, b) zone 2 showing both Juncus ranarius and Triglochin maritima, c) Juncus gerardii dominating the vegetation in zone 3a, d) zone 3b sees the appearance of grass species (Festuca rubra and Phragmites australis), e) vegetation zone 4, the purple flowering plants are species of Vicia

Vegetation zone boundaries were mapped in the same fashion as for Storosen. Vegetation cover for the whole marsh and elevation contour data are presented in Figure 4.15. Boundary elevations of the vegetation zones from the DGPS mapping tie in closely with the elevations recorded along *Sv-ST1*. Zone 1 consistently occurs in a narrow band below 1.25 m above MSL. Zones 2 and 3a occupy elevations between 1.25 and 1.50 m above MSL. Only above 1.50 m above MSL does zone 3b (and thus flowering plants) occur. The upper boundary of zone 3b is consistently found around 1.75 m above MSL or slightly above. In comparison to Storosen, there is less low marsh vegetation cover at Svinoyøsen. Only small bands of vegetation zone 1 occur along the peripheries of the salt marsh. Unlike Storosen, there is no treeline abutting vegetation zone 4. Instead this zone occupies areas of higher ground across the marsh surface. These ridge-like mounds are a key feature to the topography of the salt marsh. The existence of the creek cliff edge to the north-west, and the front ridge running east to west along Svinøyosen, limit tidal access to the marsh. During flooding, sea water enters from the south-west corner where the clearest vegetation zonation can be seen.
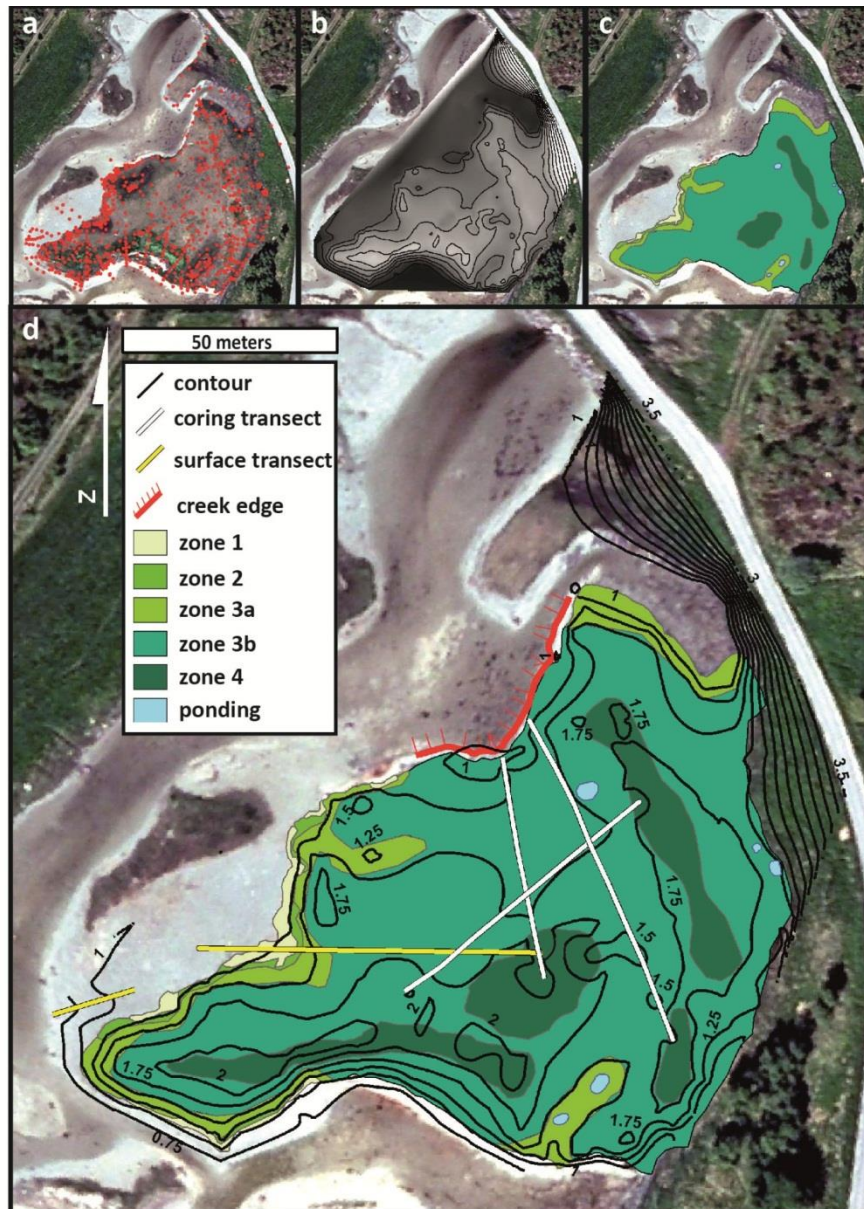
Figure 4.15 Vegetation zonation and elevation contour data for the salt marsh at Svinøyosen, a) data points recorded with the DGPS Rover System, b) height contours using surface elevation information, c) field mapped vegetation zone boundaries, d) combined GIS data and surface features.

4.3.3 Modern foraminifera assemblages

Svinøyosen surface transects

Foraminifera counts of dead individuals were performed along all four surface transects at Svinøyosen. Assemblage data for transects *Sv-ST1* and *Sv-ST2* are presented in Figure 4.16, and assemblage data for transects *Sv-ST3* and *Sv-ST4* are presented in Figure 4.17. Counts are provided as percentages alongside transect topographies and vegetation zonation. Taxa which occur in percentages always less than 2% have been summed and presented as 'rare species'.

Of the 19 samples from *Sv-ST1,* the 13 lowest contained assemblages of dead foraminifera (Figure 4.16). The six highest samples were barren. Two species dominate *Sv-ST1*, *J. macrescens* and *M. fusca*. Above 0.99 m above MSL these are the only two species encountered. *Jadammina macrescens* makes up between 75 and 95% of these populations. Below 0.99 m above MSL the relative abundance of *M. fusca* increases to represent approximately 50% of the assemblages. The three lowest samples (0.99, 0.94 and 0.91 m above MSL) contain low percentages of additional calcareous taxa, significantly, *Ammonia beccarii* var. *batavus, C. lobatulus, Elphidium earlandi, E. williamsoni* and *H.germanica*.
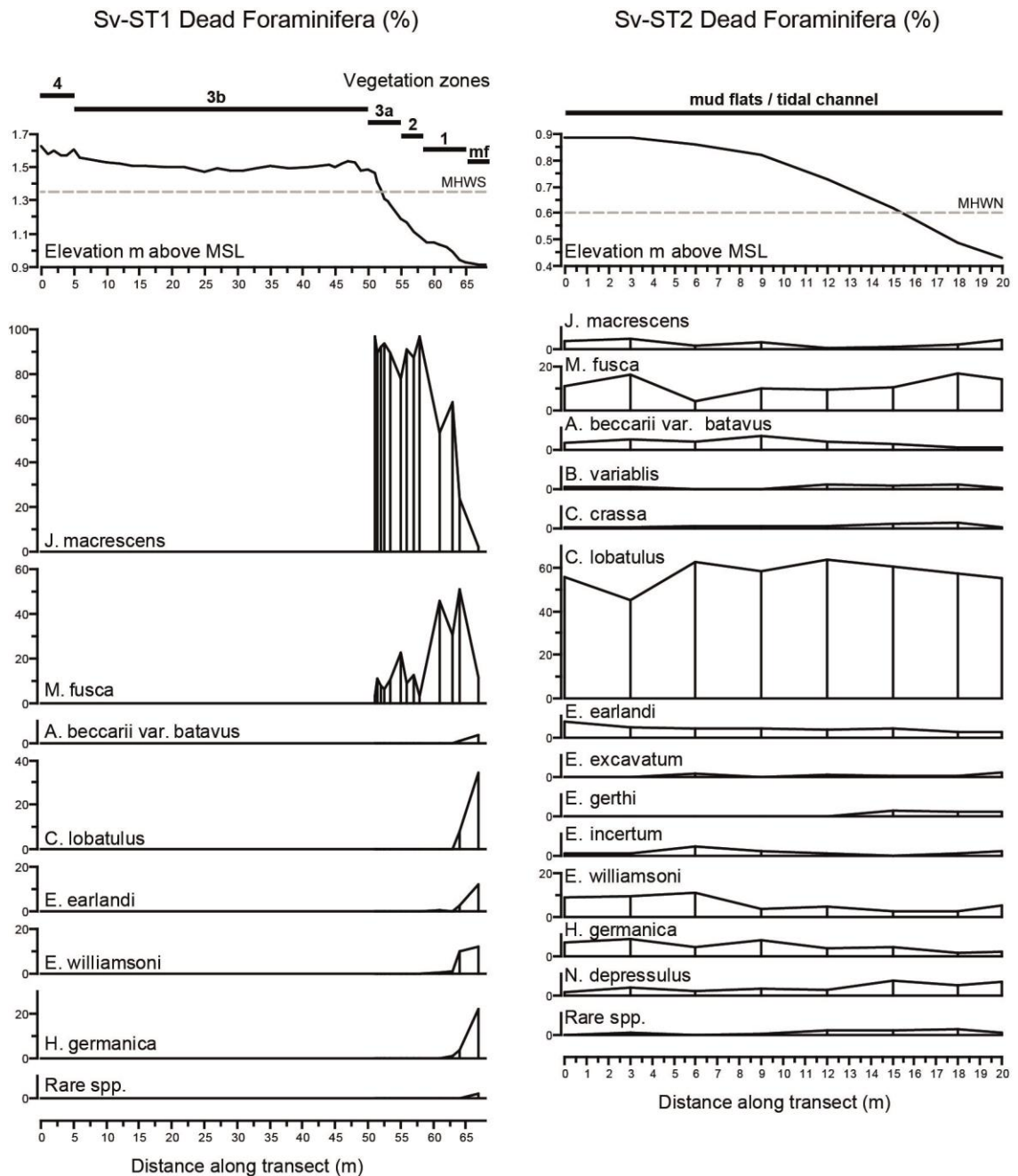
Figure 4.16 Surface foraminifera assemblage data for surface transects Sv-ST1 and Sv-ST2 from Svinøyosen

Surface transect *Sv-ST2* occupies an elevation range of between 0.89 and 0.43 m above MSL (Figure 4.16). The eight samples associated with this transect all contain populations of dead foraminifera. Assemblages throughout *Sv-ST2* share similar characteristics: *C. lobatulus* dominates and occurs in percentages around 55% and *M.*

123

fusca is consistently present at around 10 to 15% abundance. In comparison to *Sv-ST1*, *Jadammina macrescens* is still present, although in much lower numbers and there is an increase in the number of calcareous species throughout *Sv-ST2*.
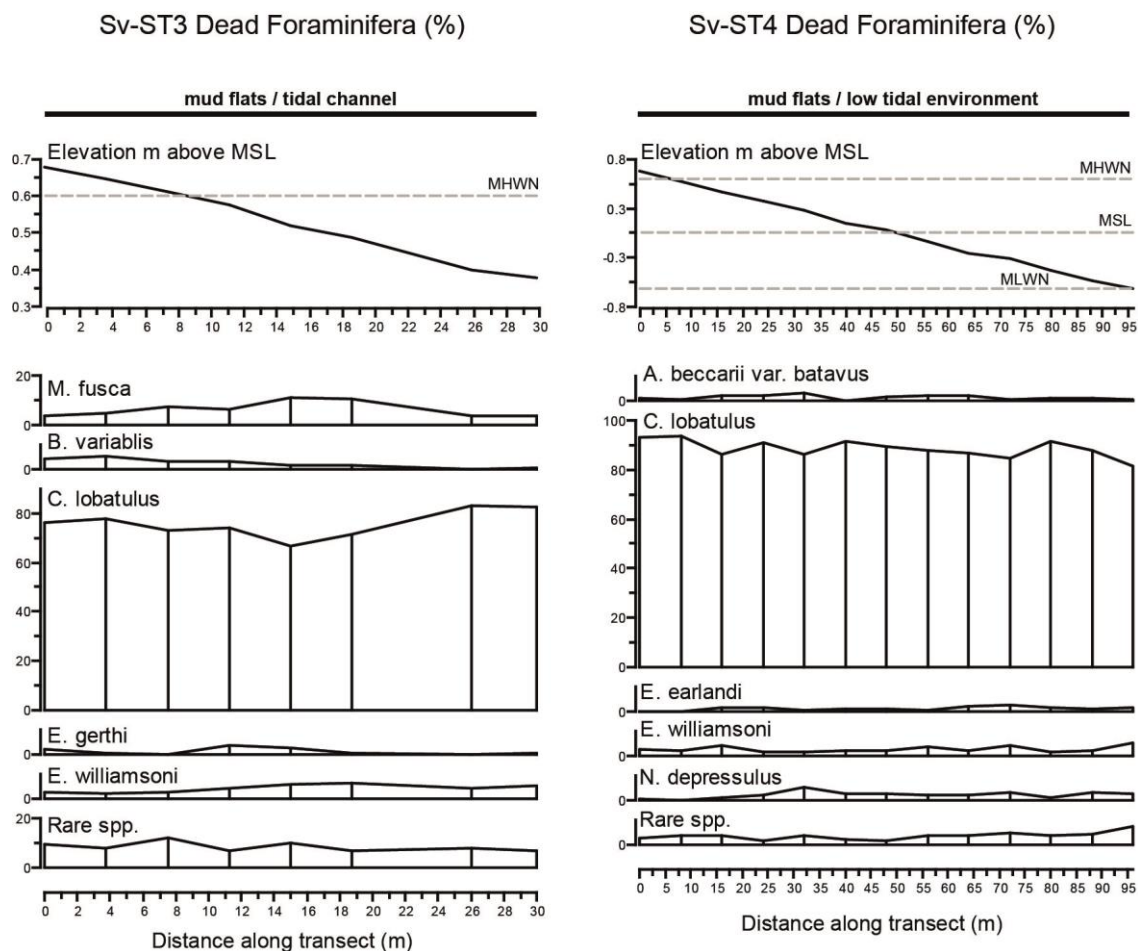
Figure 4.17 Surface foraminifera assemblage data for surface transects Sv-ST3 and Sv-ST4 from Svinøyosen

Samples from transect *Sv-ST3* had similar foraminiferal compositions to *Sv-ST2* (Figure 4.17). The eight samples associated with *Sv-ST3* covered an elevation range from 0.68 to 0.34 m above MSL. Throughout the transect *C. lobatulus* dominated and in greater percentages in comparison to *Sv-ST2*. Of the agglutinated species, *M. fusca* was still present throughout, although in low numbers (~8%), and *J. macrescens* only occurred

as a rare species. The number of calcareous species was high (~10 to 12 species per sample) throughout the transect, as represented by the higher percentages of rare species.

Surface transect 4 spanned a range in elevation of 0.63 to -0.56 m above MSL (Figure 4.17). Despite incorporating the greater range in elevation, the transect showed minimal variation of assemblage composition between samples. *Cibicides lobatulus* was consistently the dominant taxa, occurring at percentages between 80 and 90%. *Ammonia beccarii* var. *batavus, E. earlandi, E. williamsoni* and *N. depressulus* were the only forms to consistently occur in each sample but never at percentages greater than 5%. Minor species making up less than 2% of the population occurred on occasion (*M. fusca, B. variablis, C. crassa, E. gerthi, E. incertum* and *H. germanica*).

Surface foraminifera from Storosen and Svinøyosen

Assemblage data of dead foraminifera from the two surface transects from Storosen and the four surface transects from Svinøyosen were collated to form a training set of contemporary foraminifera, relative to sample elevations (Figure 4.18). Trends in foraminiferal distribution against elevation gradient are clear and data from the two sites complement each other. Constrained cluster analysis (CONISS; Grim 1987) was performed on the dead assemblages in order to help define groups of samples with similar faunal compositions. From the analysis, four zones were identified across the entire elevation gradient sampled (1.5 to -0.6 m above MSL). Assemblage characteristics defining the zones and zone elevation boundaries are presented below:

ZONE 1:   The highest zone is located between 1.49 and 0.95 m above MSL. Only two species of foraminifera are associated with this zone, *J. macrescens* and *M. fusca*. By considering the ratio between these two species, it is possible to subdivide this zone into two subzones, 1a and 1b. Subzone 1a (1.49 to 1.3 m above MSL) is characterised by very low concentrations of tests (< 50 tests per cm^3 of sediment), and assemblages heavily dominated by *J. macrescens* (Storosen: 100 %; Svinøyosen: 90+ %). Subzone 1b (1.3 to 0.95 m above MSL) is characterised by slightly higher concentrations of tests (50 to 250 tests cm^{-3}) and higher abundance of *M. fusca* (5 to 45%).

ZONE 2:   This second zone occupies a narrow elevational niche between 0.95 and 0.87 m above MSL. Test concentrations are similar to that of zone 1b (100 to 300 tests cm^{-3}). *Jadammina macrescens* is still the dominant taxa in these assemblages (50+ %), and *M. fusca* occurs in significant abundance (25 to 50 %). Importantly, assemblages from this zone include a low number of calcareous species such as *C. lobatulus*, *Elphidium* spp. and *H. germanica* in low abundance. The absence of *N. depressulus* is potentially a key indicator for this zone.

ZONE 3:   This zone extends from 0.87 to 0.42 m above MSL. The taxa *J. macrescens* and *M. fusca* are still present, albeit in lower abundance than the previous zone (~5% and 15 to 25% respectively). The species *C. lobatulus* dominates the assemblages from this zone, occurring in high abundance (50 to 90%). Numerous other calcareous species are common in zone 3, typically, many species of *Elphidium*, *B. variablis, C. crassa, H. germanica* and *N. depressulus* occur in low (< 10%) abundance, as do other rare species of calcareous foraminifera. Test concentrations are variable in the samples from zone 3, from 200 to 1300 tests cm^{-3} of sediment.

ZONE 4:   The final zone represents the lowest elevational reaches of the training set and extends from 0.42 to -0.56 m above MSL. The zone is characterised by consistently high percentage of *C. lobatulus* (80 to 95%), the notable exclusion of the two agglutinated species *J. macrescens* and *M. fusca,* and numerous calcareous species in low abundance ($< 5\%$).
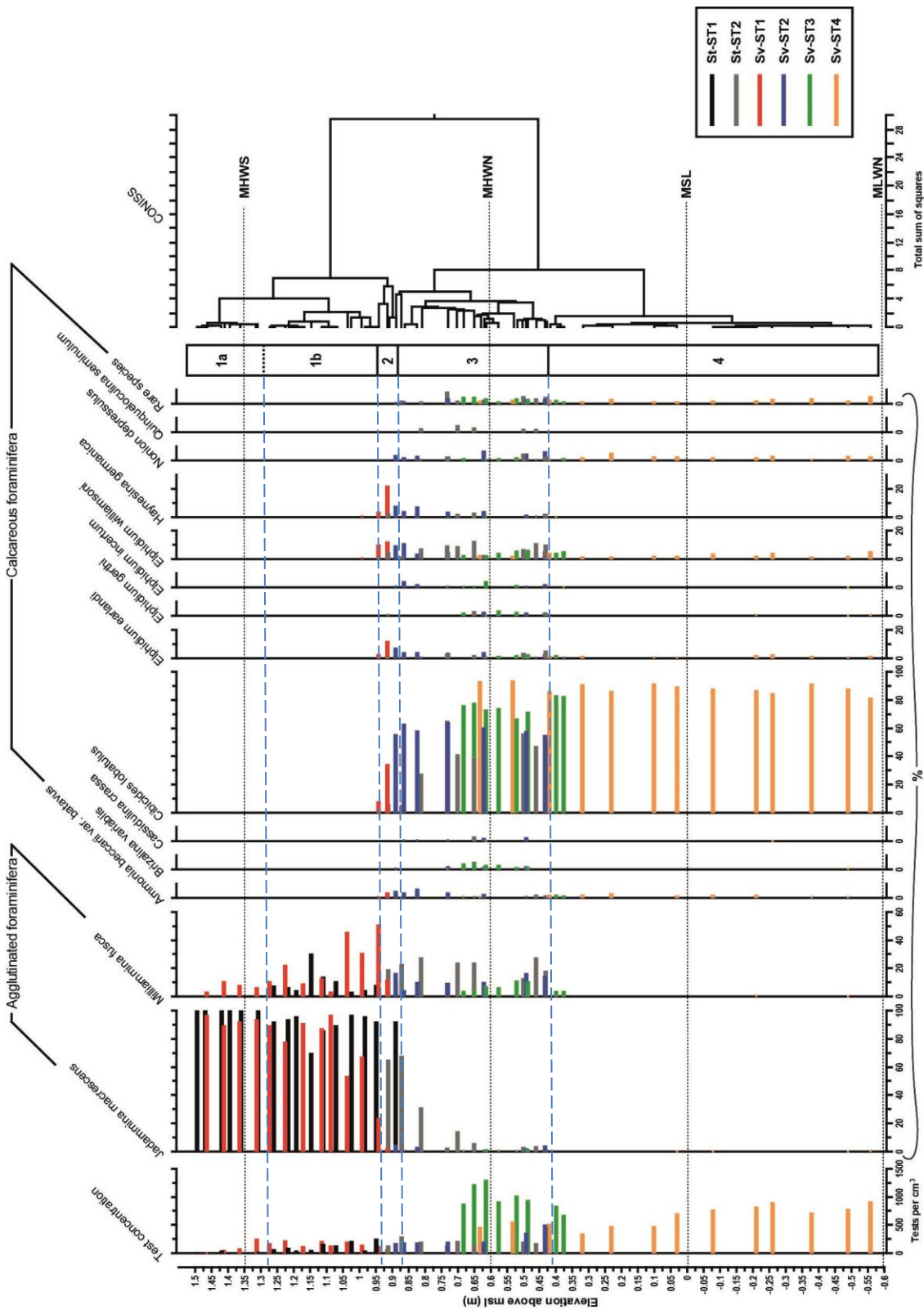
Figure 4.18 Surface foraminifera assemblage data for surface transects from Storosen (black and grey) and Svinøyosen (red, blue, green and orange). Constrained cluster analysis is used to identify assemblage zone relative to elevation which are distinguished by blue dashed lines

Due to *C. lobatulus* dominating the counts of the samples across *Sv-ST4* and throughout assemblage zone 4, potentially valuable information in the form of presence or absence data of rare species may be missed. With this in mind, Figure 4.19 was constructed which shows assemblage data for the four surface transects from Svinøyosen with the counts of *C. lobatulus* removed. It is evident that there is an increasing diversity of rare, calcareous species present in the surface samples with decreasing elevation which can be seen in Figure 4.19 with the removal of *C. lobatulus*. The onset of *N. depressulus* is noted at around 0.9 m above MSL, and the onset of species including *Quinqueloculina* spp. and *E. williamsoni* at around 0.7 m above MSL. The presence or absence of these rare species are potentially useful indicators of water depth and should be noted.
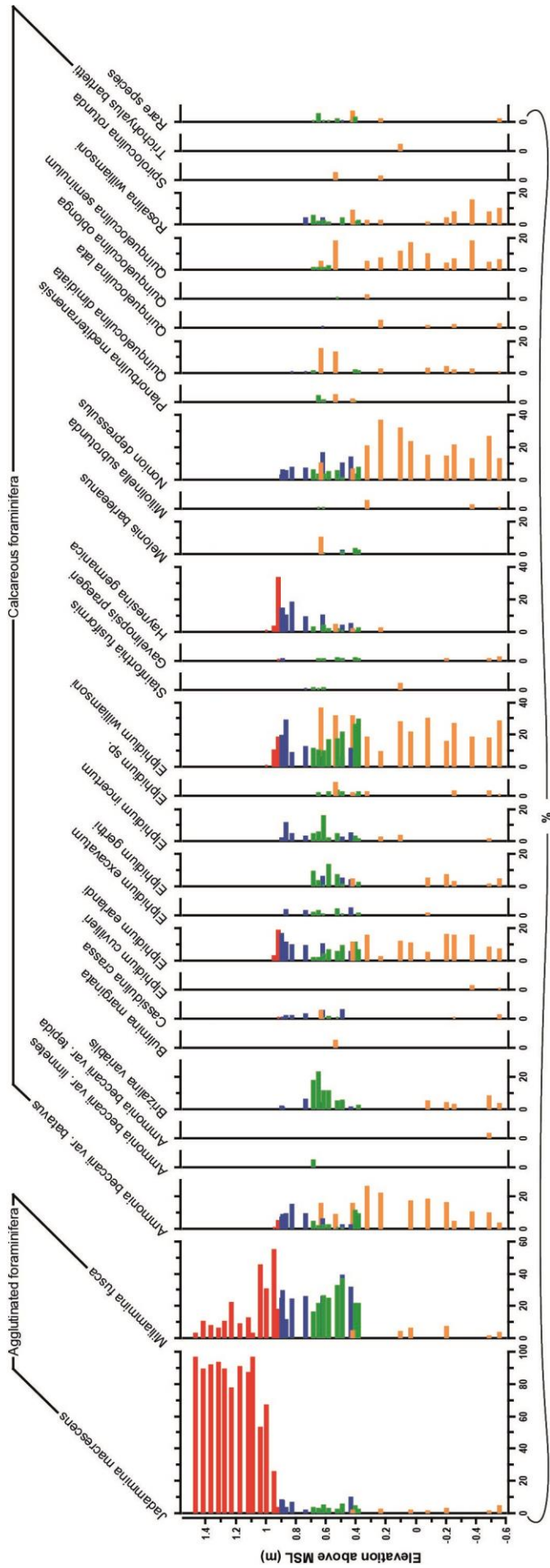
Figure 4.19 Surface foraminifera data for Svinøyosen following the removal of Cibicides lobatulus from the data sets. Red – Sv-ST1, blue – Sv-ST2, green – Sv-ST3, orange – Sv-ST4

4.3.4 Modern testate amoebae assemblages

Contemporary testate amoebae distributions across the salt marsh at Svinøyosen were investigated using transect *Sv-ST1*. All 18 samples from the transect were prepared for analyses using preparation method C and a count total of 100 tests. Samples below 1.36 m above MSL were sparse in testate amoebae and where a count total of 100 was not feasible a reduced count total of 50 was applied. Count totals for the two lowest samples (0.94 and 0.91 m above MSL) only reached 37 and 7 respectively due to scarcity of testate amoebae in the samples.

Surface assemblage data are presented in Figure 4.20 alongside the transect topographic profile and vegetation zonation. A total of seventeen taxa were identified throughout *Sv-ST1*. The most diverse assemblages were encountered in the upper seven samples above 1.47 m above MSL. Samples with fewest taxa were located at the lowest elevations and the lowest sample only contained one taxon of testate amoebae, *Centropyxis platystoma* morphotype 1. Assemblages from samples located above the level of MHWS are dominated by *C. cassis* type which generally makes up > 50% of the populations. This species is most abundant at around 1.45 m above MSL. Above this elevation a number of other taxa occur in numbers greater than 5%, including *C. ecornis*, *C. platystoma* type, *T. dentata, Difflugia* spp., and *Euglypha* spp. Below this elevation the diversity of species decreases, as does the proportion of *C. cassis* type in the assemblages. In the

middle of the transect, *Hyalosphenia ovalis* is often present in numbers greater than 5%. This taxon shows a unimodal distribution, has a maximum abundance at around 1.3 m above MSL, and decreases gradually with changing elevation. *Difflugia pristis* type shows a unique distribution across the marsh. It is found at either ends of the transect but not in the middle. At the lowest end of the transect *C. platystoma* morphotype 1 is most abundant and dominates the assemblages.
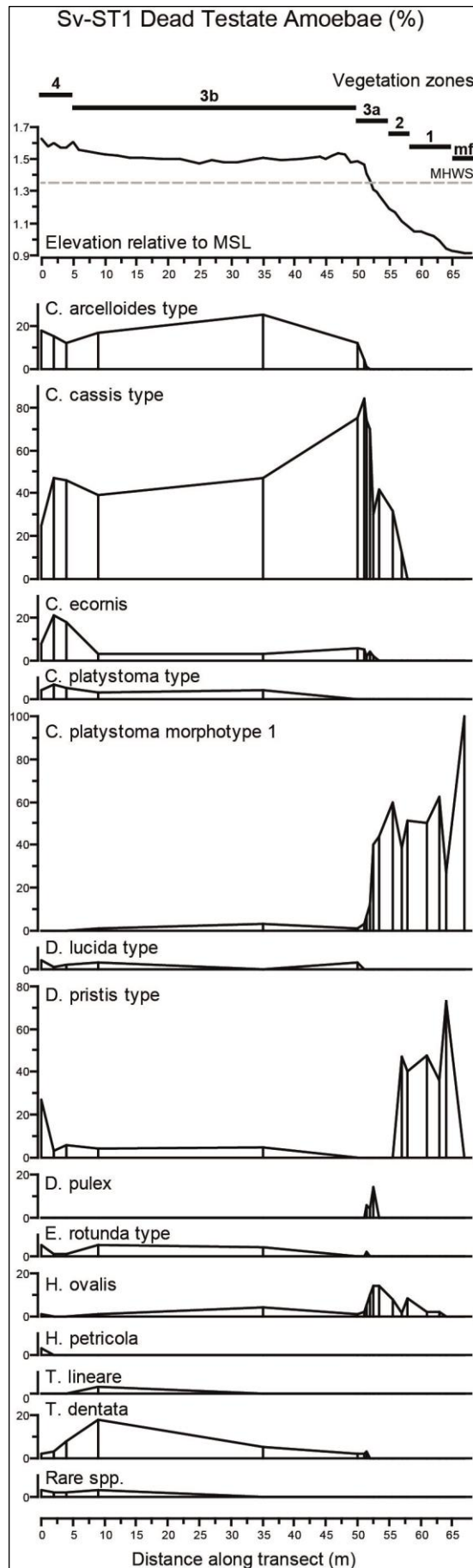
Figure 4.20 Surface testate amoebae assemblage data for transect Sv-ST1 from Svinøyosen

To construct a training set of contemporary testate amoebae in relation to elevation, surface assemblage data from transect *Sv-ST1* at Svinøyosen was combined with the eleven samples used in the count total analyses from Storosen (Figure 4.21). CONISS was again used to define zones of samples with similar assemblage compositions. The constrained cluster analysis identified three main zones of assemblages:

ZONE 1:　　The highest zone is found between 1.5 and 1.75 m above MSL and is characterised by a high diversity of taxa (up to 22) and a high concentration of tests (> 20,000 cm^{-3}). *Centropyxis cassis* type occurs as a dominant taxon and typically makes up half of the assemblages. *Centropyxis ecornis, Centropyxis platystoma* type*, Cyclopyxis arcelloides* type and *Tracheleuglypha dentata* are also characteristic taxa and are all present in percentages greater than 10%. Numerous other taxa occur in lower numbers including *Euglypha* spp., *Nebela* spp. and *Trinema* spp.

ZONE 2:　　The second zone extends from 1.5 to 1.15 m above MSL. Here, *Centropyxis cassis* type makes up a higher percentage of the assemblages than before (~75%). There are fewer rare species such as *Euglypha* spp., *Nebela* spp. and *Trinema* spp. although *Hyalosphenia ovalis* often occurs in this group. *Tracheleuglypha dentata* is still present in the higher samples of zone 2 but is less abundant. The proportion of *Centropyxis platystoma* morphotype 1 increases with the lower samples of the group at the expense of other *Cyclopyxis* and *Centropyxis* taxa.

ZONE 3:　　The lowest zone is composed of samples typically containing few taxa (one to three). *Centropyxis cassis* type is no longer present and two taxa dominate the assemblages, *Centropyxis platystoma* morphotype 1 and *Difflugia pristis* type.
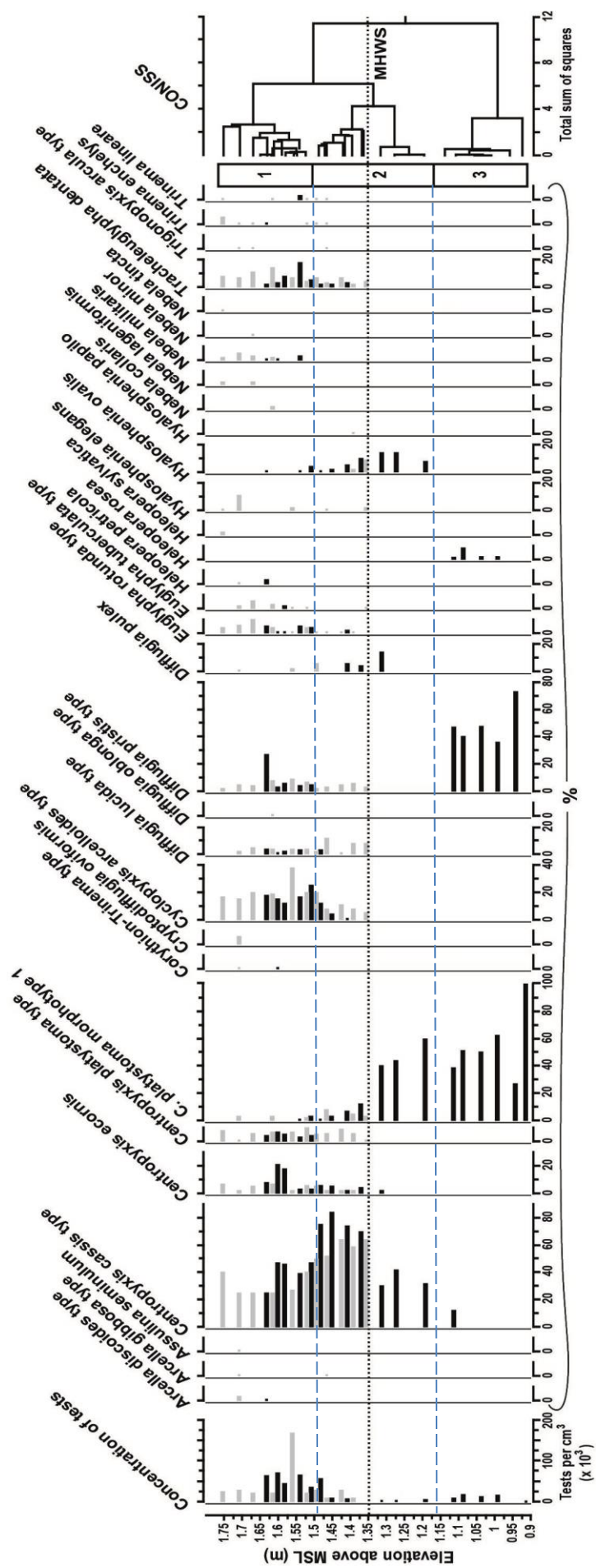
Figure 4.21 Surface testate amoebae assemblage data for transect Sv-ST1 from Svinøyosen (black) and for eleven samples from transect St-ST1 from Storosen (grey). Constrained cluster analysis is used to identify assemblage zone relative to elevation and is distinguished by dashed blue lines

4.3.5 Summary

Investigations into the modern environment at Svinøyosen have revealed a strong relationship between vegetation zonation and elevation. Like Storosen, four floral zones were identified and mapped across the entire salt-marsh surface. The vegetation zone boundaries were found to consistently occur within narrow elevational niches.

Surface foraminifera distributions were studied along four surface transects. Changes in assemblage composition appeared also to be driven by elevation. Constrained cluster analysis highlighted significant changes in foraminifera populations and related these to elevations. Four zones or groups were identified between 1.50 and -0.60 m above MSL. The importance of rare foraminifera species in identifying changes in assemblage patterns was also demonstrated.

Testate amoebae populations were produced for *Sv-ST1* using the most suitable preparatory and analytical methods as identified in the first half of this chapter. The lower extent of their habitat was identified at around 0.90 m above MSL. Above this elevation testate amoebae diversity and abundance increased. Constrained cluster

analysis identified three assemblage zones for surface testate amoebae data. Changes in species occurrence and abundance seemed strongly related to elevation.

Transfer functions based on the modern training sets are derived in Chapter 7. But first, the following chapter presents results from the palaeoenvironment at Svinøyosen. Subsurface litho- and biostratigraphy is investigated alongside environmental parameters. Results from radiocarbon and short-lived radionuclide dating techniques are also presented in the following chapter.

CHAPTER 5 – Results: palaeoenvironments

5.1 Introduction

This chapter describes the results of the palaeoenvironmental analyses. Lithological descriptions of the subsurface sediments are presented and a master core, representative of approximately the last 8,000 years, is identified and described in detail. Loss on ignition, grain-size and bulk-density analyses were performed on this core (*Sv-CT3-0m*). These analyses were used to interpret changes in environmental conditions. Biostratigraphic analyses were also performed on this core. Foraminifera were used as a proxy for water depth. Where appropriate the ecological information provided by molluscs was used to supplement the foraminifera-derived water depths. A chronologic framework for *Sv-CT3-0m* was derived from radiocarbon (^{14}C), geochemical (Pb, Hg, Ni, Cu, Zn) and short lived radionuclide (^{210}Pb, ^{137}Cs, ^{241}Am) dating techniques. Qualitative interpretations of the palaeoenvironments at Svinøyosen are made based on the above descriptions and analyses, prior to the application of quantitative techniques in the following chapter.

In addition to the master core, a secondary core (*Sv-CT3-15m*) was used for testate amoebae analyses. This core, from the high marsh at Svinøyosen, was used to provide assemblages of fossil testate amoebae representing the last ~100 years. This core was described in detail and also analysed using LOI, grain size and bulk density. An age-depth chronology was provided from ^{210}Pb, ^{137}Cs and ^{241}Am activity profiles. The fossil testate amoebae will be used to produce a sea-level reconstruction in Chapter 6.

5.2 Lithostratigraphy

This section describes the physical characteristics of the subsurface sediments at Svinøyosen. Distinct stratigraphic units were defined based on lithological properties as described in the field and in the laboratory.

5.2.1 Coring transect profiles

Three coring transects were used to document the lithostratigraphy at Svinøyosen (Figure 3.2). The longest transect, *CT1*, consists of nine cores over 80 m and runs in a north-west to south-east direction. Coring transect 2 is perpendicular to *CT1* in a north-east to south-west direction and includes eight cores over a distance of 70 m. Finally, *CT3,* parallel to *CT1,* consists of eight cores over 50 m. A total of seven distinct lithostratigraphic units were identified:

Unit 1: basal unit; stiff and impenetrable, battleship blue-grey clay

Unit 2: beige shelly sands; unconsolidated and unstratified hash of shells, shell fragments and sand

Unit 3: grey silts containing some fine sand and clay with abundant shell fragments

Unit 4: grey silts containing some fine sand and clay devoid of shell fragments

Unit 5: organic rich sands, brown to grey in colour

Unit 6: brown organic silts with some fine sand

Unit 7: brown organic clay with identifiable and unidentifiable plant material (salt-marsh sediments)

Coring Transect CT1

This 80 m long coring transect is located between an eroding micro-cliff in the north-west corner of the marsh and a raised ridge in the central part of the marsh (Figure 3.2). A total of nine cores were used to describe the lithological profile (Figure 5.1). A lithological key is presented in Table 3.3.

The basal blue-grey clay (unit 1) was sampled in three cores (*CT1-0m, -10m, and -60m*). The contact of this unit with the overlying shelly sands is unconformable and variable in height (Figure 5.1). The upper contact of the overlying unit of shelly sand (unit 2) is consistently lower at the north-west end of the transect, compared to the south-east end. This contact was also unconformable. Core *CT1-60m* contains the thickest (1.02 m) shelly sand sequence. Frequently, fine to coarse pebbles were encountered at the shell hash – grey silt contact. Contact elevations of the grey silts (units 3 and 4) and of the overlying organic rich sands (unit 5) are consistent throughout the transect (except for core *CT1-80m*). All contacts above the grey silt with shell fragments unit (unit 3) are conformable. Unit 5 is identified throughout the coring transect. However, the organic brown silts (unit 6) are occasionally indistinguishable from the overlying salt-marsh sediments (i.e. cores *CT1-0m, -10m, -70m, -80m*). The top unit of salt-marsh sediments (unit 7) varies in thickness from 0.07 to 0.12 m. Modern roots extend to depths of 0.5 to 0.75 m below the surface.
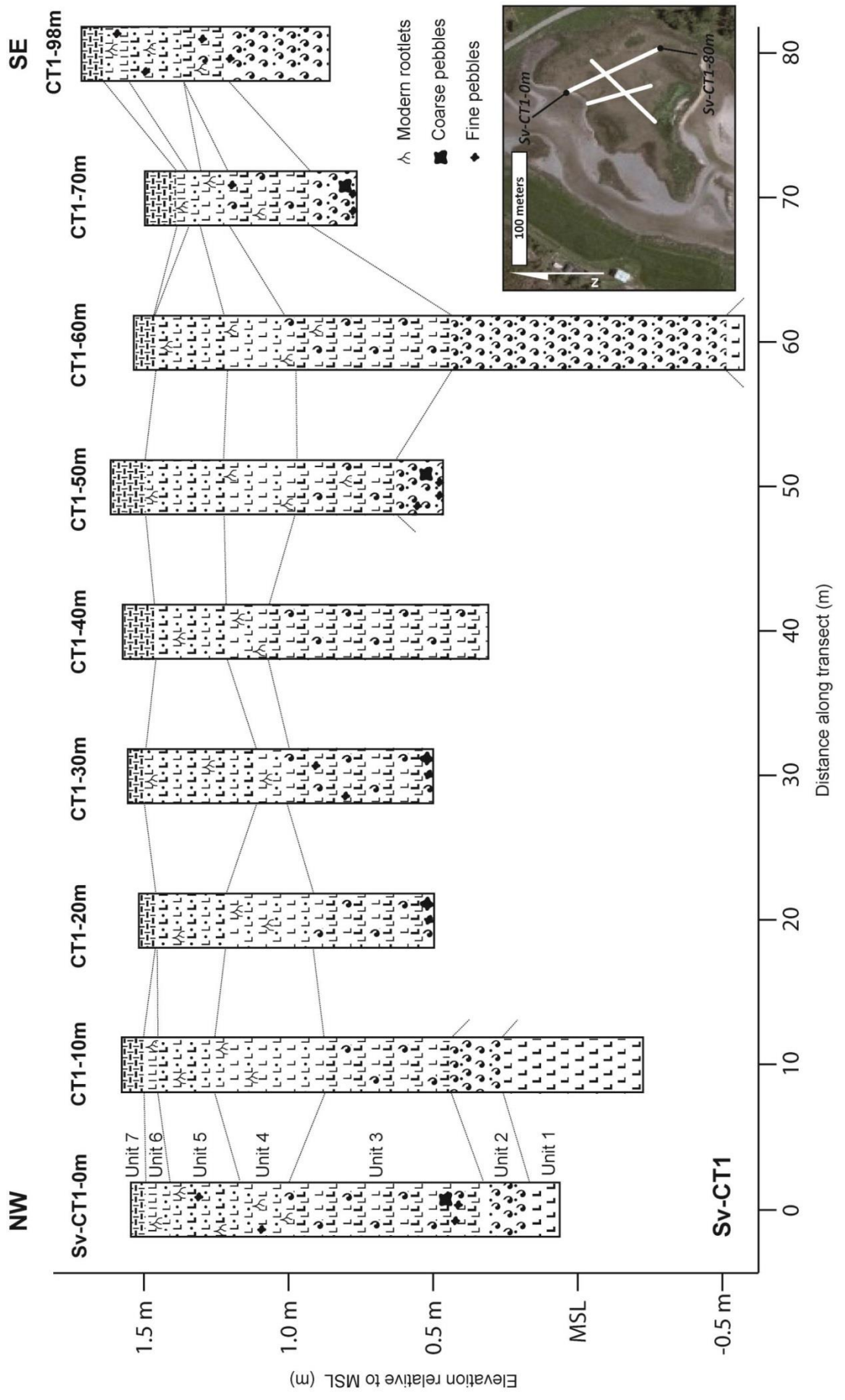
Figure 5.1 Lithological profile of coring transect CT1 showing the seven units identified and described in the text

Coring Transect CT2

Transect *CT2* is located between two raised ridges on the marsh surface. The lithostratigraphy of this transect is presented in Figure 5.2.

As was seen in *CT1*, the elevation of the upper contact of basal unit 1 is quite variable across the transect (by ~1 m) and the contact is erosive in nature. The unconformable upper contact of the shelly sand (unit 2) is fairly level. The thickness of the shelly sand varies from 0.4 to 1.0 m, and appears to be thickest towards the centre of the transect. The overlaying grey silts containing mollusc shells (unit 3) are thickest (~0.5 m) at the ends of the transect. The grey silts without mollusc shells (unit 4) vary in thickness between 0.1 and 0.5 m. The organic rich sands (unit 5) are thickest (~0.4 m) towards the middle of the transect at *CT2-30m*. The two uppermost units are both uniform in thickness, the salt-marsh sediments (unit 1) consistently being approximately 0.12 m thick. The lithological contacts in *CT2* are consistently higher at the two ends of the transect compared to the middle. Fine roots extend as far down to ~0.75 m below the surface.
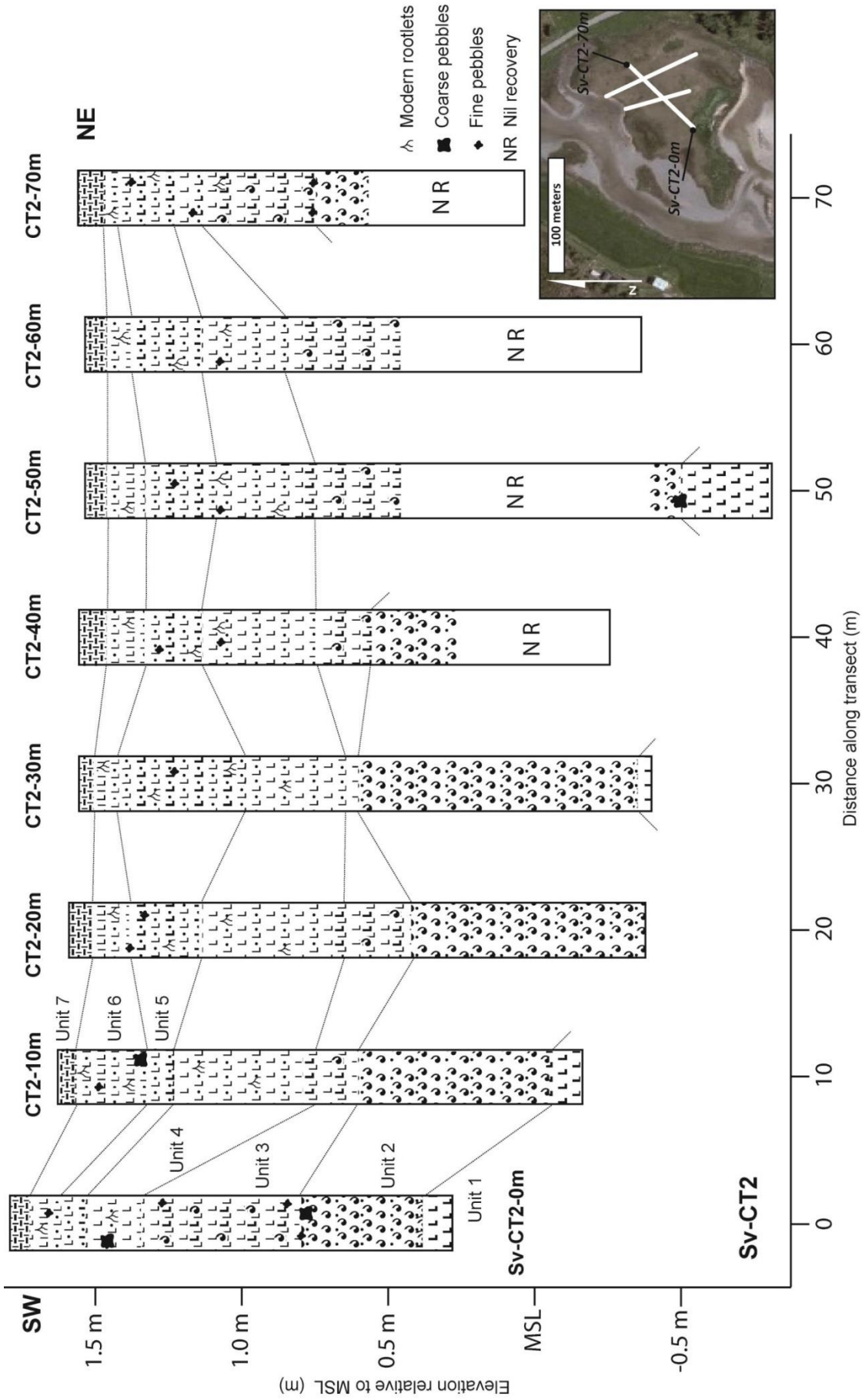
Figure 5.2 Lithological profile of coring transect CT2 showing the seven units identified and described in the text

Coring Transect CT3

This transect extends from an eroding micro-cliff and terminates on a ridge of raised ground on the marsh surface. Core top elevations generally increase with distance into the marsh. Figure 5.3 presents the lithostratigraphy for this transect.

The blue-grey basal clay (unit 1) was only encountered close to the micro-cliff edge (cores *CT3-0m, -10m, -20m*). Like the previous two transects, the elevation of the upper contact of this unit is undulating, reflecting its unconformable nature. The shelly sand (unit 2) is only encountered in half of the cores (*CT3-0m, -10m, -20m, -40m*), in consistent thicknesses (~0.2 to ~0.5 m). The overlying grey silts with mollusc shells (unit 3) vary in thickness from ~0.3 to ~0.55 m and are found at fairly uniform depths. The contact between the two grey silts (units 3 and 4) is conformable, as are all contacts above this. The grey silts devoid of mollusc shells (unit 4), and overlying organic sands (unit 5), are both uniform in thickness across the profile (approximately 0.45 and 0.3 m respectively). The two topmost units are also of uniform thickness. Elevations of all units are higher at core *CT3-50m* in comparison to the rest of the profile.
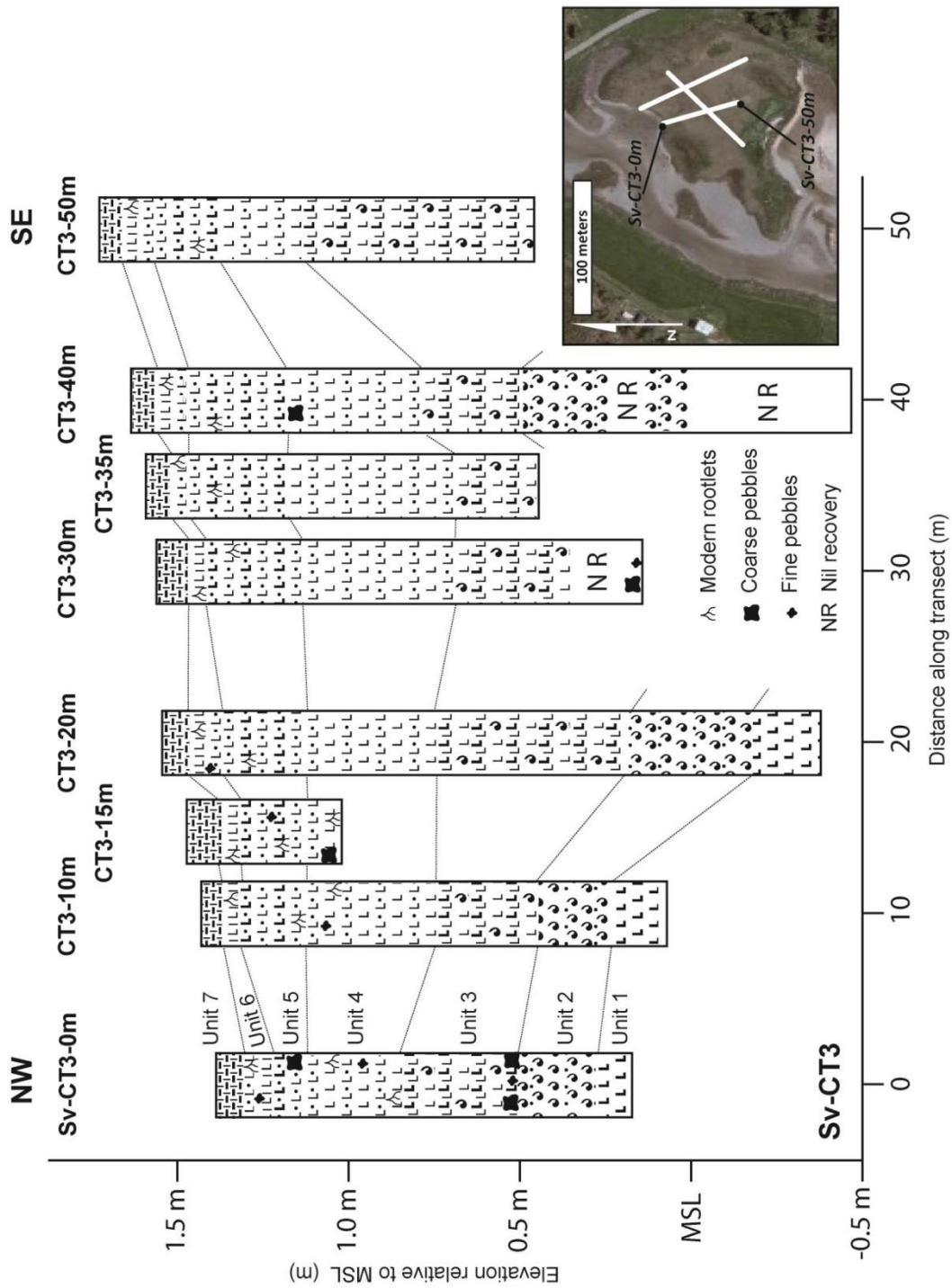
Figure 5.3 Lithological profile of coring transect CT3 showing the seven units identified and described in the text

5.2.2 Core: Sv-CT3-0m

The master core (*Sv-CT3-0m*) selected for high resolution palaeoenvironmental study was extracted from the most westward end of *CT3*, 0 m along the transect. This core provided a seemingly uninterrupted sequence of sediments, covering most of the Holocene, and represented a model core containing all the units described above. The core was cut from the face of an eroding bank, collected using monolith tins, and provided 1.22 m of sediments. The monolith top was surveyed to 1.37 ± 0.015 m above MSL.

Lithostratigraphy

Figure 5.4 presents a lithostratigraphic description of the monolith showing sample depths for foraminiferal and sedimentological analyses. The seven lithological units identified throughout the profiles are all represented within core *Sv-CT3-0m*.

Unit 1

The basal clay unit extended from 1.12 to 1.22 m in core *Sv-CT3-0m*. Nothing was recovered below 1.22 m. The unit has an erosive and unconformable contact (Figure 5.5) with the overlying shelly sands.

Unit 2

At this location the shelly sands are 0.20 m thick and extend from 0.92 to 1.12 m through the core. Whole shells vary in size from 2 mm to 30 mm and include species of gastropods (*Lunatia montagui, Cingula trifasciata, Pusillina inconspicua* and *Gibbula cineria*) and bivalves (*Thracia villosiuscula*, *Dosinia exoleta* and *Spisula subtruncata*)

Unit	Facies components	Nigor	Stratificatio	Siccitas	Elasticitas	Limes superior	Munsell colour	Physical description
7	Th2, Sh2, As+	3	0	2	1	-	7.5R 3/1	Dark brown organic rich salt-marsh peat
6	Ag2, Th1, Ga1, As+	2	0	2	0	0	7.5R 3/2	Mid brown organic rich sandy silt with some fine clay. Occasional medium to coarse pebbles
5	Ga2, Ag1, As1, Th+	2	0	2	0	0	2.5Y 4/1	Mid brown to grey clayey silty sand with some organics. Occasional medium to coarse pebbles
4	Ag3, Ga1, As+, Th+	2	0	2	0	0	5Y 3/1	Dull grey sandy silt with some clay and rare organics. Occasional modern rootlets present
3	Ag3, As1, Ga+, part. test.+	2	0	2	0	0	5Y 4/1	Dull grey clayey silt with some sand and occasional marine shell fragments increasing in abundance with depth
	Ag3, As1, Ga+, part. test.‡							90 cm - coarse pebbles (40 mm) at the gradational contact
2	part. test.2, Ga1, test.1, Gs+	1-	0	1	0	0	2.5Y 6/3	Light beige wet and unconsolidated sandy shell hash containing abundant marine shell fragments and whole shells
1	As4	2	0	3	0	2	Gley1 5/10Y	Battleship blue - grey stiff clay with an unconformable upper contact

Column headers: Foraminifera, LOI / Grain size, Troels - Smith symbology, Facies components, Nigor, Stratificatio, Siccitas, Elasticitas, Limes superior, Munsell colour, Physical description

Figure 5.4 Detailed description of core Sv-CT3-0m. Red and blue dots show sampling depths for foraminifera and sedimentary analyses respectively

as shown in Figure 5.6. The matrix predominantly comprises of mixed beige sands (fine to coarse), but becomes more clay rich closer to the lower contact with the basal unit. The upper contact is gradational, takes place over approximately 0.05 m and shows signs of reworking (Figure 5.7) suggesting that this upper contact is unconformable.

Figure 5.5 Photograph showing the unconformable contact between the basal clay (unit 1) and the overlying shelly sands (unit 2)

Unit 3

The grey silts with abundant mollusc shells and shell fragments extend from 0.45 to 0.92 m depth. At the contact between this unit and the shelly sand (unit 2) are numerous subangular to subrounded coarse (16 to 32 mm) pebbles (Figure 5.7). Above this contact, the abundance of shelly detritus decreases with decreasing depth. Small black flecks of decomposed organic material are present throughout this unit.
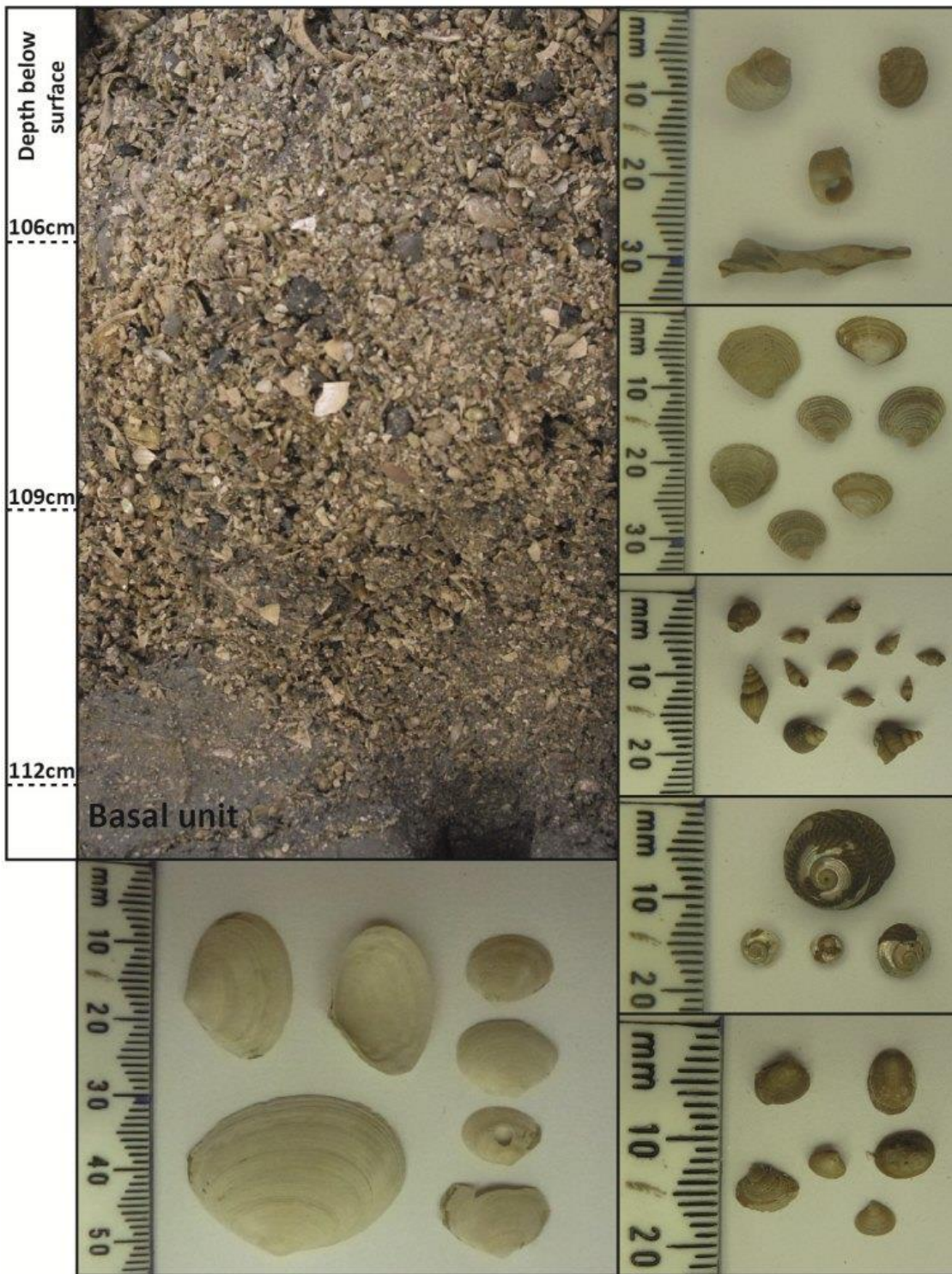
Figure 5.6 Photograph showing the shelly sand (unit 2) and examples of molluscs found through the unit. Identifications are provided within the text
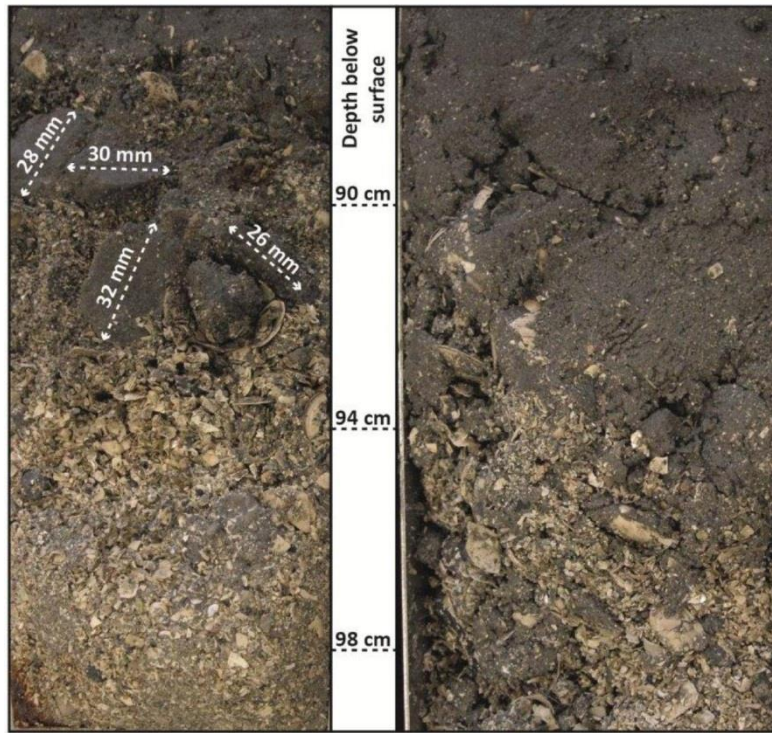
Figure 5.7 Uunconformable contact between the shelly sands (unit 2) and the overlying grey silts containing mollusc shells (unit 3). Note the fine to coarse pebbles occupying the contact and the erosional surface

Unit 4

The upper grey silts are devoid of the detrital mollusc material described above. This unit extends from 0.26 to 0.45 m depth. Detrital organic material is rare, but modern organic roots and rootlets are abundant. Both the upper and lower contacts of this unit are diffuse and conformable. A small amount of sand and clay is present throughout both grey silt units.

Unit 5

Brown to grey sands overlay the grey silt units and are rich in organic (decomposing and modern) material. These sands extend from 0.15 to 0.26 m depth and have a

conformable and diffuse upper contact. Both clay and silt is present in small amounts throughout this unit. Gravel and small pebbles are also present and large pebbles occur occasionally.

Unit 6

This unit extends from 0.06 to 0.15 m down the core and consists of a brown silt unit containing some fine sand and clay and abundant herbaceous material. Larger grained material, similar to that found in unit 5, is found throughout this unit.
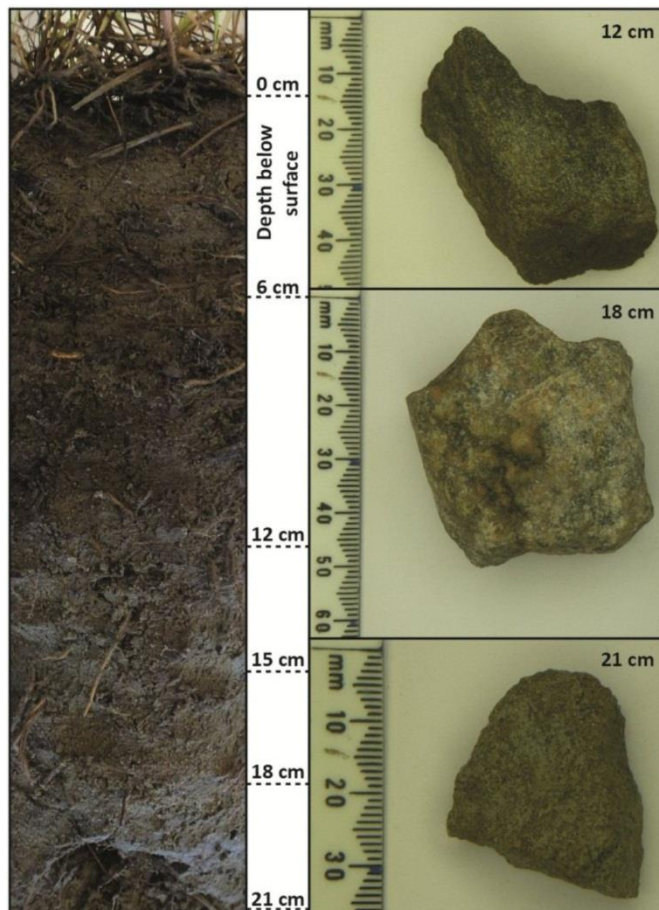
Figure 5.8 Photograph showing the top three units from Sv-CT3-0m and some of the subangular pebbles found in these units.

Unit 7

Sitting topmost is a 0.06 m thick salt-marsh peat, rich in identifiable and humified organics. Here, and throughout the top three units, are occasional, isolated fine to very coarse (8 to 64 mm) pebbles of mixed mineralogy (Figure 5.8).

Sedimentology

Changes in organic carbon and $CaCO_3$ content were estimated using LOI throughout core *Sv-CT3-0m*. A total of 93 samples were analysed and the results are presented in Figure 5.9. Analyses on grain size were also conducted on 85 samples. No grain size information is available for the top 0.05 m of *Sv-CT3-0m*. The components of each sample were categorised into percentages of clay, silt, sand and grains > 1 mm (Figure 5.9). Bulk density measurements were taken for the top 0.20 m because they are needed for modelling ^{210}Pb age-depth profiles and are a useful tool for assessing the effects of sediment compaction within cores (e.g. Brain et al. 2012).

LOI – organic carbon

From 1.20 to 0.15 m through the core (units 1 through 5 inclusive) organic carbon was low at around 2 to 3%. In Unit 6 (0.15 to 0.06 m) the amount of organic carbon increased up to a maximum of around 25%. Organic carbon was highest at ~45% in unit 1, near the surface.
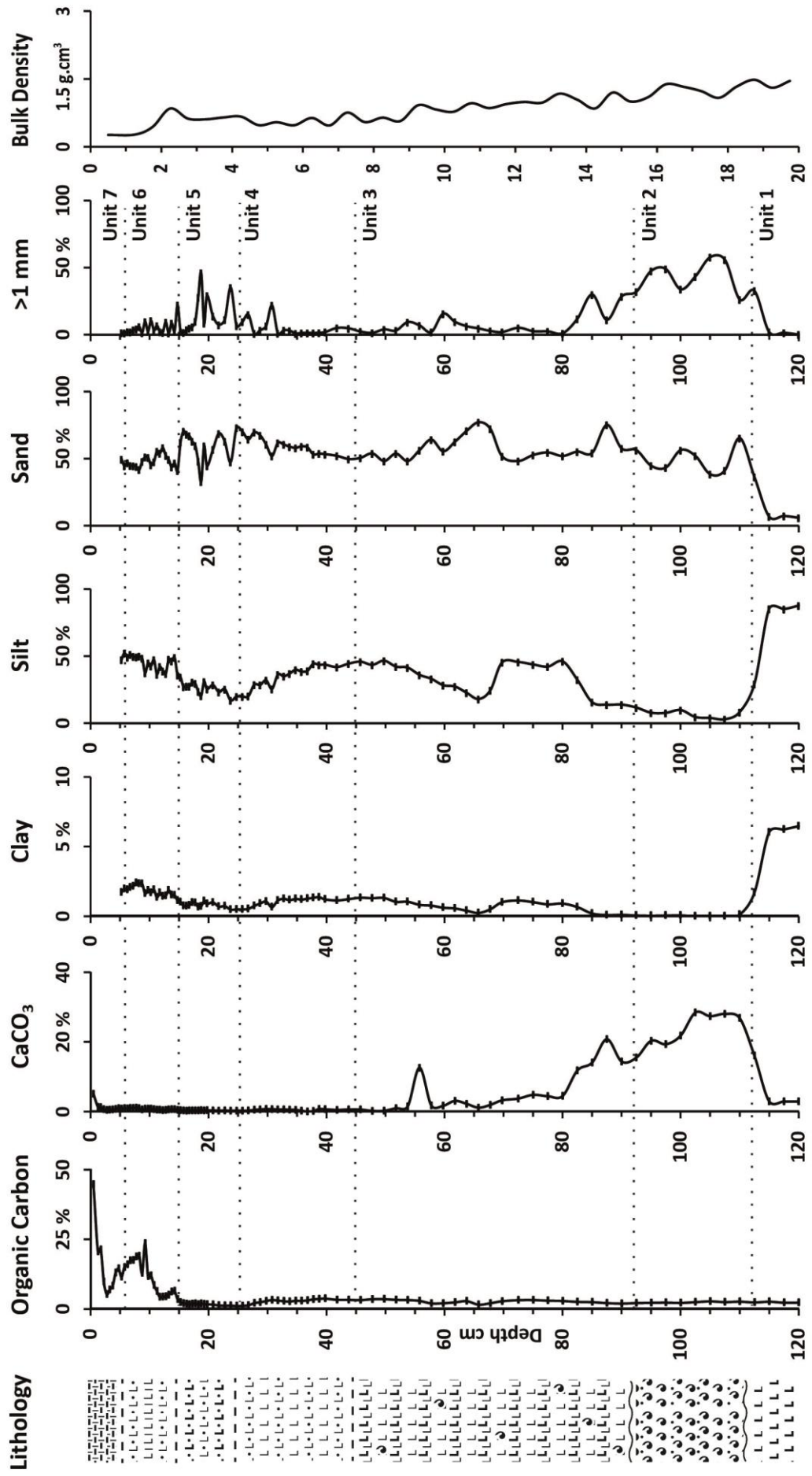
Figure 5.9 Sedimentological characteristics for core Sv-CT3-0m showing results from loss on ignition analyses (organic carbon and CaCO$_3$ content), grain size analyses and bulk density measurements. Notice change in axes on the final graph

LOI – CaCO$_3$

The percentage of CaCO$_3$ is low (~3%) at the bottom of the core, coinciding with the basal clay (unit 1). CaCO$_3$ peaks at 30% in unit 2 between 0.92 and 1.12 m. There is a reduction in CaCO$_3$ content across the unit 2 – unit 3 unconformable contact which continues throughout unit 3. Between 0.45 m depth and the surface (units 4 through 7 inclusive), CaCO$_3$ remains below 1%, although there is a small rise in the top sample to 5 %.

Grain size

The bulk of unit 1 is composed of silt (85%). Here, clay is most abundant (~5%) in comparison to anywhere else in the core, there are almost no large (> 1 mm) grains and very little sand. There is a sharp change in all grain size categories across the unit 1 – unit 2 unconformable contact. Unit 2 predominantly consists of sand and large grains in approximately equal quantities (~45%). Clay is virtually imperceptible in this unit. Gradational changes in grain size are seen across the unit 2 – unit 3 unconformable contact. Here, the amount of sand and silt increases at the expense of larger grains. There is a small increase in the amount of clay through unit 3 where sand dominates the lithology (~50%). Unit 4 is categorised by almost equal quantities of sand and silt, and very few larger grains. There is an increase in the amount of larger grains in unit 5 at the expense of silt. Above this unit the amount of larger grains decreases to less than 2%,

there is also a decline in the amount of sand. Unit 6 is categorised by a small increase in the amount of clay, although silt and sand dominate the lithology of the unit.

Bulk density

Bulk density measurements are provided in grams per cubic centimetre. For core *Sv-CT3-0m* bulk density was greatest (approximately 2 g cm^{-3}) at around 0.20 m depth. Bulk density decreases gradually with decreasing depth. The topmost sample has the lowest bulk density of approximately 0.1 g cm^{-3}.

The master core *Sv-CT3-0m* has been described in terms of the seven distinct lithological units identified at Svinøyosen salt-marsh. The sedimentary analyses have provided some quantification of the components present within the units. The results of these analyses will be used alongside biostratigraphic data to help with environmental interpretation. Grain size is a useful tool for inferring the energy of tidal and near shore environments in terms of flow velocity (Hjulström 1935), and the presence of different forms of carbon can indicate towards the nature of a depositional environment.

5.2.3 Core: Sv-CT3-15m

The short core (*Sv-CT3-15m*) selected for testate amoebae analysis came from 15 m along coring transect *CT3* at Svinøyosen. The core was taken from a cleaned face of a shallow pit near the middle of the marsh with small (40 x 6 x 3 cm) monolith tins. The top of the core was surveyed to 1.47 m ± 0.018 m above MSL.

Lithostratigraphy

Figure 5.10 presents a lithostratigraphic description of the short (0.38 m) core. Of the seven lithological units encountered throughout the marsh, only the topmost three were sampled in *Sv-CT3-15m* and are described below. Unit 6 has been subdivided into two separate units (6a and 6b) for the core description.
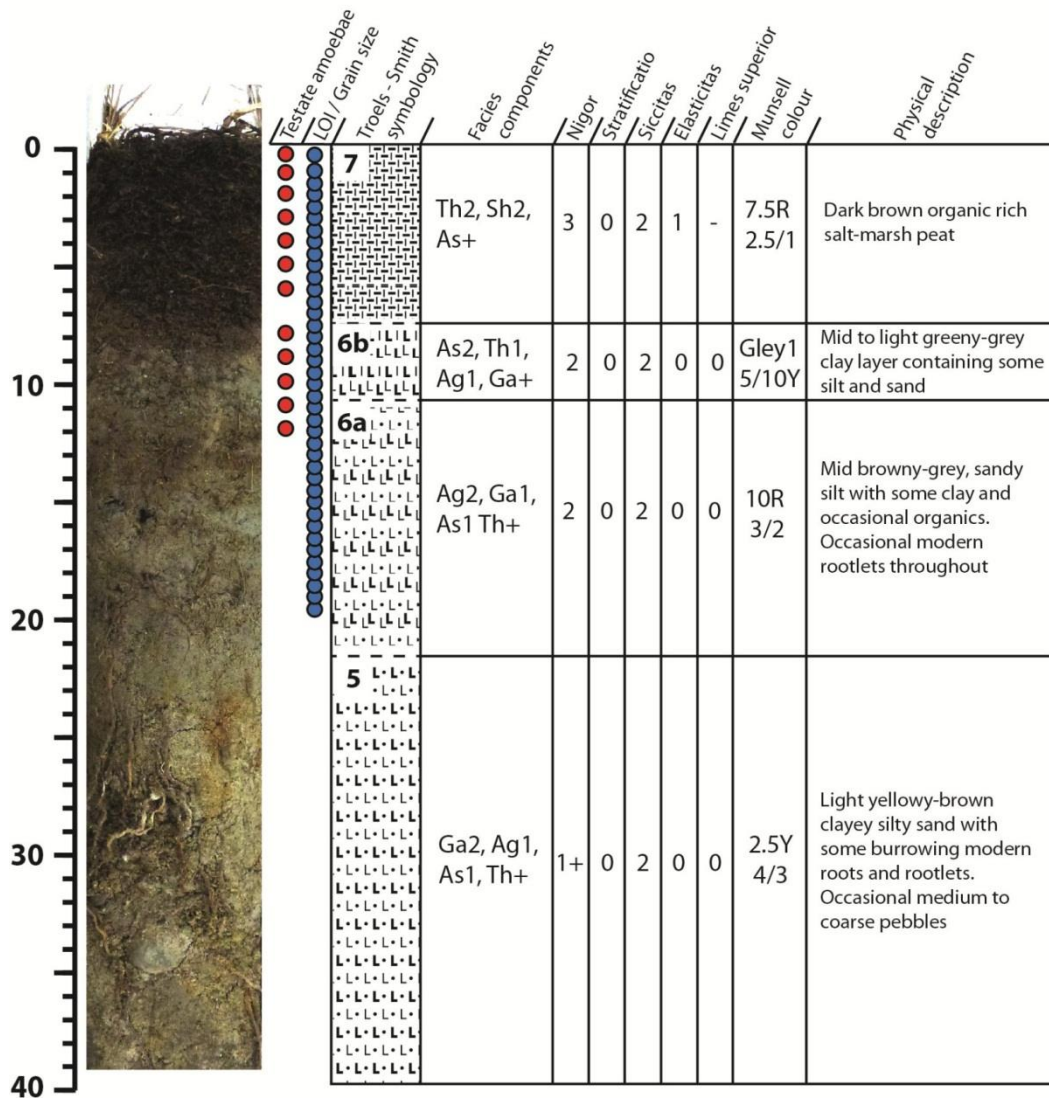
Figure 5.10 Detailed description of core Sv-CT3-15m. Red and blue dots show samples for foraminifera and sedimentary analyses respectively. Note that unit 6 has been divided into two subunits as described in the text

Unit 5

From 0.23 m to the bottom of the core is a silt and clay rich, yellowy brown sand unit. Thin (< 1 mm) to thick (1 to 3 mm) roots dissect this unit throughout and fine to coarse pebbles are common (Figure 5.11). Iron oxide staining of the sediments provides a yellow tint to the unit which is unstratified and has a gradational upper contact.

Figure 5.11 Photograph showing the abundant roots and pebbles present throughout unit 5 from Sv-CT3-15m

Unit 6a

Above the sand unit, from 0.12 to 0.23 m, is a mid-brown to grey silt unit containing some fine sand and clay, as well as abundant organic material. This unit is synonymous to the organic silt unit in *Sv-CT3-0m*. Iron oxide staining is present in a band at 0.19 to

0.22 m of the short core (Figure 5.12). Occasional fine to coarse pebbles are also common throughout.

Figure 5.12 Photograph showing the iron oxide band present in unit 6a from Sv-CT3-15m, also note the pebbles within the unit

Unit 6b

From 0.08 to 0.12 m is a thin unit of green-grey clay containing some silt, fine sand and abundant organic material. This band is not present in core *Sv-CT3-0m.* Upper and lower contacts of the unit are gradational.

Unit 7

Topping the monolith is 0.08 m of salt-marsh sediments which also caps the organic units in *Sv-CT3-0m.* At this location the unit is thick and is why core *Sv-CT3-15m* was selected for testate amoebae analysis. Cores from the higher reaches of salt marshes are more likely to provide abundant and diverse populations of testate amoebae than cores taken from the mid or low marsh (Charman et al. 2010). With this in mind, the area

where the salt-marsh sediment unit was thick was presumed to have the longest records of preserved testate amoebae and was therefore targeted when sampling.

Sedimentology

Grain size and LOI analyses were performed on 39 samples from the short testate amoebae core, *Sv-CT3-15m* (Figure 5.13). In addition, bulk density measurements were taken for the top 0.20 m. Results are given for contiguous, 0.5 cm thick, samples. The top two samples (from 0 to 1 cm) were combined together as these were low in density and contained little material.

LOI – organic carbon

The amount of organic carbon in the core increases gradually from 1% at 20 cm to 70% at the surface. Unit 6a typically contains the lowest amount of organic carbon ($< 2\%$). Unit 6b demonstrates an increasing trend from ~4 to ~15%, which continues throughout unit 7 (Figure 5.13).

LOI – CaCO$_3$

In *Sv-CT3-15m,* below 0.05 m the amount of CaCO$_3$ fluctuates between 0.1 and 1.3%. This profile is very similar to that seen in *Sv-CT3-0m*. Above this depth there is more variation, although never more than 2.5% of CaCO$_3$ is encountered.

159
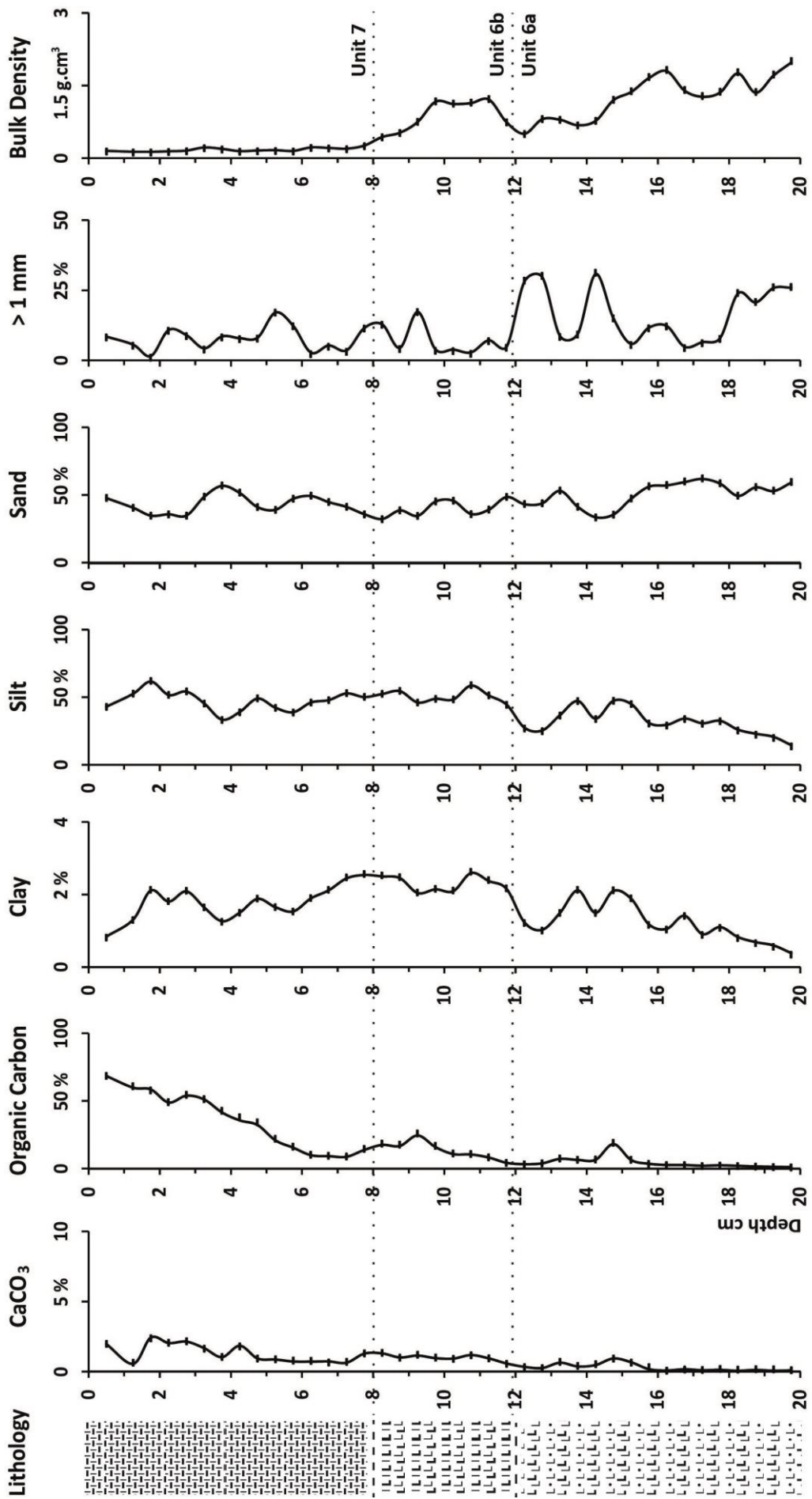
Figure 5.13 Sedimentological characteristics for core Sv-CT3-15m showing results from loss on ignition analyses (organic carbon and CaCO₃ content), grain size analyses and bulk density measurements

Grain size

Unit 6a is predominantly composed of sand (~ 50%), although there is a slight increasing trend in the amount of clay throughout this unit (from ~1 to 2%). Larger grains are common in the samples from this unit, although the abundance of them is variable. In unit 6b there are fewer larger grains (~2 to ~10%), and a slight decline in the amount of sand is seen through the unit. Here, clay is at its highest abundance. Unit 7 is characterised by similar quantities of silt and sand (~45%) and low amounts of larger grains and clay.

Bulk density

For core *Sv-CT3-15m*, bulk density showed a similar profile as core *Sv-CT3-0m*. Greatest bulk density was found at 0.20 m depth (approximately 1.5 g cm^{-3}) and this figure decreased in value with decreasing depth.

The sedimentary descriptions and biostratigraphic data (Section 5.4) of core *Sv-CT3-15m* were used to infer past water depths at Svinøyosen for the last ~100 years. The reconstruction for this core was chronologically constrained using techniques outlined in Section 5.3.

5.3 Chronostratigraphy

Three techniques have been used to provide a chronology for the sediments at Svinøyosen. Radiocarbon dating provided the means of generating dates from approximately 7700 to 2000 cal yrs BP. No older dates were obtained beyond 7700 cal yrs BP. A combination of ^{210}Pb, ^{137}Cs and ^{241}Am radiometric techniques was used to date the topmost sediments in the two cores described above. This provided a chronology for the last ~100 years at Svinøyosen. Because of the lack of radiocarbon samples, it was necessary to use geochemical marker horizons to fill the chronology from ~2000 cal yrs BP to the 20th century. Metal accumulation profiles for lead, mercury, nickel, copper and zinc were constructed through core *Sv-CT3-0m* and trends in accumulation were identified. These trends were related to historical events of mining and industrial activity in order to identify recorded periods of metal pollution and thereby infer approximate ages for the sediments at Svinøyosen since the Roman era approximately 2000 year ago.

5.3.1 Radiocarbon dates

A total of 22 radiocarbon dates from three NERC allocations have been used in this thesis (see Acknowledgements). A summary of the dates is presented in Table 5.1 and includes the core and depth they originated from under the sample identifier. Radiocarbon ages are given with 1 sigma error ranges for all samples. Calibrated ages are presented with 2 sigma error ranges.

161

Allocation #	Publication code	Sample Identifier	Depth to MSL (m)	Material	^{14}C Years BP ± 1 sigma	intcal09 Years BP	Reservoir corrected (440 years)	marine09 (ΔR 65, ±37)
Transect 1								
1530.0311	SUERC-34678	T1_0_95a	0.59	bivalve (*Thracia villosiuscula*)	3436 ± 37		3150 - 3388	3079 - 3363
1530.0311	SUERC-34685	T1_0_95b	0.59	wood piece	3713 ± 37	3928 - 4212		
1606.0312	SUERC-41141	T1_30_64	0.91	bark fragments	2282 ± 37	2158 - 2352		
1606.0312	SUERC-41142	T1_50_109	0.52	plant & stem fragments	3314 ± 35	3461 - 3635		
Transect 2								
1606.0312	SUERC-41149	T2_0_64	1.14	gastropod (*Lunatia montagui*)	2209 ± 37		1700 - 1893	1590 - 1866
1530.0311	SUERC-34683	T2_0_86	0.92	bivalve (*Thracia villosiuscula*)	2690 ± 35		2310 - 2413	2149 2449
1530.0311	SUERC-34682	T2_0_110	0.68	bivalve (*Dosinia exoleta*)	7189 ± 39		7498 - 7714	7488 - 7700
1606.0312	SUERC-41150	T2_0_111	0.67	gastropod (*Cingula trifasciata*)	7126 ± 37		7427 - 7574	7443 - 7642
1530.0311	SUERC-34681	T2_70_39	1.17	gastropod (*Littorina saxatilis*)	1122 ± 37		499 - 728	529 - 707
1606.0312	SUERC-41143	T2_70_81	0.75	bark fragments	3229 ± 37	3377 - 3556		
Transect 3								
1577.0911	SUERC-39977	T3_0_37.25	1.00	betula bark	2140 ± 37	2000 - 2304		
1577.0911	SUERC-39983	T3_0_38.5	0.99	wood piece*	4303 ± 37*	4829 - 4964*		
					4273 ± 38*	4658 - 4960*		
1577.0911	SUERC-39980	T3_0_39.00	0.98	wood piece	2279 ± 35	2158 - 2351		
1577.0911	SUERC-39981	T3_0_46.75	0.90	charcoal	2634 ± 35	2718 - 2843		
1530.0311	SUERC-34686	T3_0_49.5	0.87	betula fragments	2437 ± 37	2354 - 2702		
1577.0911	SUERC-39987	T3_0_53.5	0.84	gastropod (*Littorina saxatilis*)*	2862 ± 37*		2427 - 2698*	2362 - 2690*
					2817 ± 37*		2359 - 2621*	2334 - 2659*
					2777 ± 36*		2345 - 2516*	2299 - 2642*
1606.0312	SUERC-41146	T3_0_85	0.52	plant fragments & bark pieces	3020 ± 35	3080 - 3341		
1606.0312	SUERC-41151	T3_0_95	0.42	9 gastropods (*Pusillina inconspicua*)	6939 ± 35		7242 - 7406	7278 - 7484
1606.0312	SUERC-41152	T3_0_110	0.27	gastropod (*Lunatia montagui*)	5395 ± 35		5583 - 5848	5584 - 5837
1606.0312	SUERC-41156	T3_0_112	0.25	foraminifera (*C. lobatulus, A. beccarii*)	6233 ± 35		6576 - 6814	6469 - 6732
1606.0312	SUERC-41147	T3_35_71	0.89	wood piece & plant fragments	2212 ± 37	2144 - 2334		
1606.0312	SUERC-41148	T3_35_82	0.78	plant fragments & bark pieces	2518 ± 35	2473 - 2742		

Table 5.1 A summary of the radiocarbon dates used in this thesis. High precision dates where multiple analyses were performed on the same piece of material have been denoted*

The 22 dates were distributed across all three coring transects, and the material originated from all lithostratigraphical units, except the top two units. This was to ensure a holistic understanding of past chronological events was gained. A total of four dates came from *Sv-CT1*, six from *Sv-CT2* and 12 from *Sv-CT3*. Ten dates were associated with the master core, *Sv-CT3-0m*, as a detailed chronology was required at this location to accompany the palaeoenvironmental analyses. In terms of a rationale, a basal date was sourced to provide an oldest chronological context and dates either side of unit boundaries were targeted to help identify timings of environmental changes. In order to present the dates in context, the calibrated ages have been presented alongside their associated lithological profiles (Figure 5.14). Marine dates in Figure 5.14 are given from the set of Marine09, ΔR 65 calibrations.

Figure 5.14 The distribution of calibrated radiocarbon dates (cal yrs BP) across the lithological profiles at Svinøyosen

A single date was sourced from the basal unit of stiff clay. Two species of foraminifera, *Cibicides lobatulus* and *Ammonia beccarii* var. *batavus*, provided the material for dating. Between 1,500 and 2,000 tests were acquired for a dry weight of 0.0127 g. The unit was dated at 6469-6732 cal yrs BP. A total of four dates came from the overlying unit of shelly sand. The lowest date from this unit came from *Sv-CT3-0m*, just above the contact with the basal clay and provided an age of 5584-5837 cal yrs BP. The remaining three dates from this unit all provided ages of between 7278 and 7700 cal yrs BP. A total of ten dates came from the grey silt unit containing mollusc shells. Three dates representative of the lower contact of this unit all provided ages between 3080 and 3635 cal yrs BP. The upper contact of this unit was dated in two locations at 2473-2742 and 2354-2702 cal yrs BP. Three dates originated from the lower contact of the overlying grey silts devoid of mollusc shells. In this case all ages were between 2158 and 2843 cal yrs BP. From relatively higher in the unit and from within *Sv-CT3-0m* one date at 0.385 m provided an age of 4829-4960 cal yrs BP, and another at 0.39 m provided an age of 2158-2351 cal yrs BP. The youngest radiocarbon date originates from unit 4 (grey silts devoid of shell material) and provides an age of 529-707 cal yrs BP.

A number of age reversals can be seen in Figure 5.14. A total of four dates are located within unit 5 (shelly sand), three of which date the unit to between approximately 7200 and 7700 cal yrs BP, notably older than the basal date of 6469-6732 cal yrs BP. The basal data may be spuriously young, although it is taken from a unit representing a low energy environment which is likely not reworked, and it is hard to explain the presence

of young carbon in the form of foraminifera tests. It is more likely that the older overlying sediments have been reworked and deposited on top of unit 1. This hypothesis is supported by the fact that the lower contact of unit 2 is erosional and unconformable, the upper contact is unconformable with the overlying silts of unit 3, and that unit 2 contains shelly debris and sand, indicative of a high energy environment or event. Another date from *Sv-CT3-0m* provides an age of 4829-4960 cal yrs BP from a high precision sample at 0.385 m depth. This date does not conform to a neighbouring date from the same core at a depth of 0.39 m (2158-2351 cal yrs BP). Nor does the older date conform to equivalent dates from this unit from coring transects 2 and 3, or the sequence of dates in *Sv-CT3-0m*. The relatively older date stems from a piece of wood (0.2 g) which may have been reworked and not representative of the environment it was deposited in. For these reasons this date is also considered with caution.

The 22 radiocarbon dates from Svinøyosen provide a chronology from ~7700 until ~500 cal yrs BP. Only two dates were sourced younger than 2000 cal yrs BP, yet neither occurs in the master core *Sv-CT3-0m*. The use of stable geochemical markers was required in order to construct a reasonable chronology for the depths between 0.05 and 0.30 m in this core, spanning the last ~2000 years. From the radiocarbon evidence there appears to be two hiatuses within core *Sv-CT3-0m*. The earliest occurs prior to ~7500 cal yrs BP, and the second occurs prior to ~4000 cal yrs BP. Both hiatus depths correspond with the unconformable contacts described in the lithostratigraphy. The radiocarbon dates infer some loss of sediments from Svinøyosen at these hiatus locations.

5.3.2 Geochemical markers

Concentrations of lead (Pb), mercury (Hg), nickel (Ni), copper (Cu) and zinc (Zn) were measured through core *Sv-CT3-0m*. The analyses were performed on the top 53 cm of the core, and therefore extend back to approximately 2500 cal yrs BP. Changes in metal accumulation were tentatively related to historical events which have been referred to in terms of calendar years here, in order to concur with the literature. Figure 5.15 illustrates the locations of different records of metal pollution that have been referred to in the text. Included are some locations of the major mining and industrial sources of Pb, Hg, Ni, Cu and Zn pollution over the last ~2000 years.

Stable lead

Changes in atmospheric Pb deposition through the last ~2000 years were recorded using three isotopes of stable lead. ^{206}Pb and ^{207}Pb were used firstly as a ratio to identify source changes in Pb delivery, and secondly used in conjunction with total Pb (here defined as ^{208}Pb) to calculate and quantify the amount of pollution Pb in the sediments (Renberg et al. 2002). Periods of lead exploitation were identified through negative shifts in the ^{206}Pb / ^{207}Pb ratio. Natural background ^{206}Pb / ^{207}Pb ratios for Fennoscandia are high at around 1.3 to 1.6 (Chow 1965, Renberg et al. 2002), whereas European lead ore bodies have a lower ratio of around 1.17(Rossman et al. 1997), and petrol lead has a ratio lower still (Keinonen 1992). Examples of depositional environments which have recorded historical events in the last ~2000 years through ^{206}Pb / ^{207}Pb ratios include lake environments in Sweden (Renberg et al. 1994, 2002) and Finland (Meriläinen et al. 2011), Baltic Sea sediments (Zillén et al. 2012), Swedish sphagnum peat bogs (Klaminder et al. 2003) and salt-marsh deposits in Iceland (Marshall et al. 2009). These studies, along with Renberg et al. (2001) and Bindler et al. (2008) have been used to

infer ages from peaks in Pb pollution, and shifts in ^{206}Pb / ^{207}Pb experienced at Svinøyosen (Figure 5.16).

The onset of airborne lead pollution began around 5500 cal yrs BP (Bindler et al. 2008), although the first significant peak of lead mining and exploitation was during the Roman period. This peak has been dated to last from approximately 0 to 400 AD (Renberg et al. 2002; Meriläinen et al. 2011), although there is evidence of an earlier onset at around 100 BC (Renberg et al. 2001; Klaminder et al. 2003; Marshall et al. 2009). In core *Sv-CT3-0m,* the first significant shift in ^{206}Pb / ^{207}Pb coupled with a peak in pollution lead is seen at around 29 to 26 cm. The onset of this event occurs approximately 10 and 7 cm higher in core *Sv-CT3-0m* than two radiocarbon dates which have provided ages of 304 ± 98 BC and 202 ± 152 BC respectively. The evidence from the radiocarbon dates supports the hypothesis that the first significant evidence of lead exploitation seen in core *Sv-CT3-0m* represents the Roman era of around 0 to 400 AD.
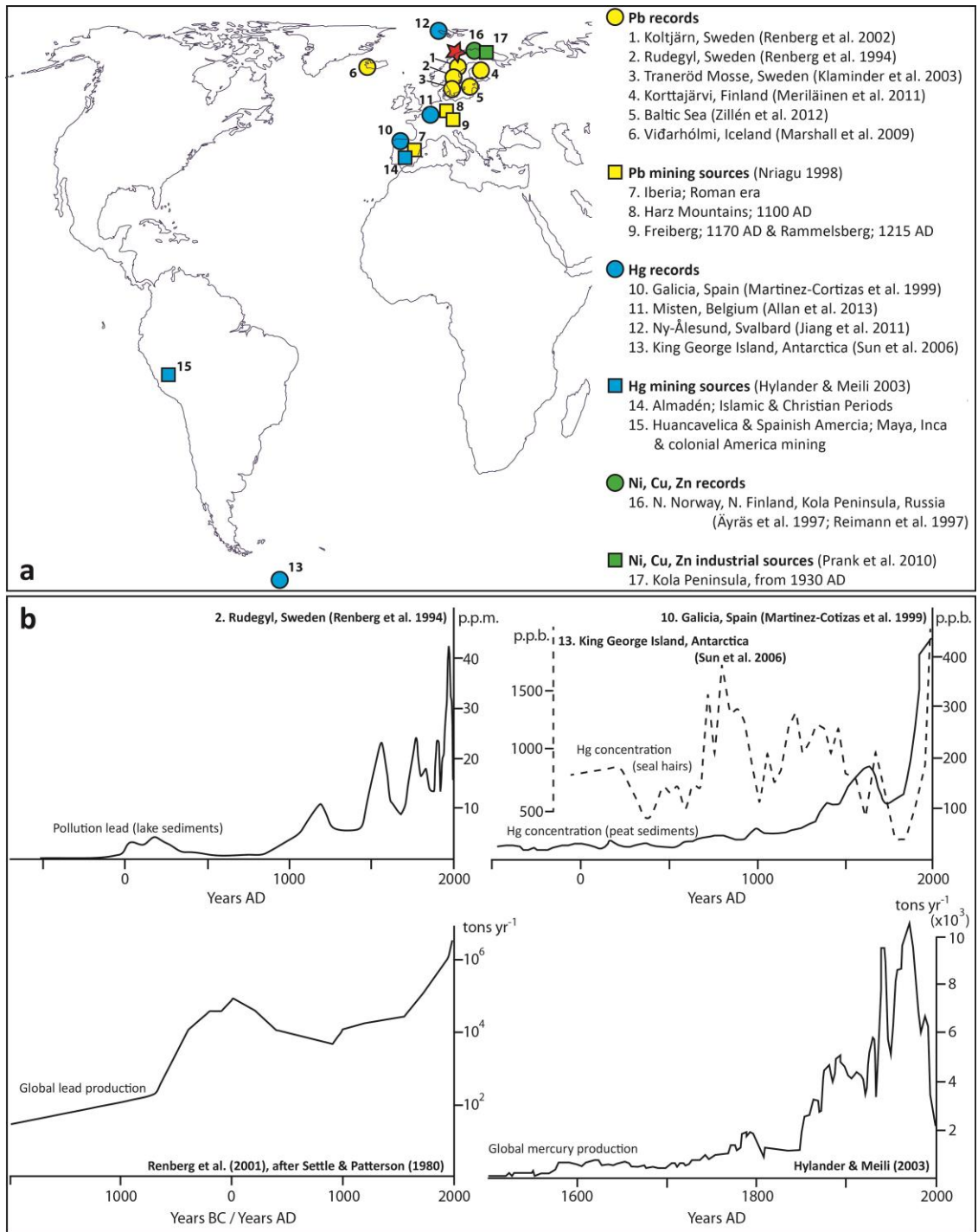
Figure 5.15 (a) Locations of the published pollution records that have been used to describe changes in Pb, Hg, Ni, Cu and Zn through core Sv-CT3-0m (coloured circles); some locations of major sources of metal pollution (coloured squares); field site location (red star). (b) Example records of lead and mercury pollution, and estimates of global lead and mercury production. Note scale changes on axes

The collapse of the Roman Empire is recognised in a positive shift of the ^{206}Pb / ^{207}Pb ratio and a decrease in Pb pollution. The next expansion of European mining started with the Medieval period from around 1000 AD, or just before (e.g. Renberg et al. 2002). Numerous sources recognise this onset, along with a peak at around 1200 AD (Renberg et al. 1994, 2001; Meriläinen et al. 2011; Zillén et al. 2012). In *Sv-CT3-0m,* following the initial event at 26 to 29 cm in the core, the subsequent rise in pollution Pb begins at around 24 cm, and peaks a little higher, possibly representing the Medieval maximum. Preceding this peak is a steady increase in pollution Pb and steady decline in the ^{206}Pb / ^{207}Pb ratio. Between the Medieval period and the Industrial Revolution some minor peaks in pollution Pb have been recorded by Renberg et al. (2002). However such deviations are hard to detect in the salt-marsh data from Svinøyosen.

The Industrial Revolution characterises European lead pollution profiles clearly. Abrupt increases in pollution Pb are seen at around 1800 AD (e.g. Renberg et al. 2002; Klaminder et al. 2003; Marshall et al. 2009) and start an increasing trend which continues through war time Europe and peaks in the 1970s, due to petrol lead pollution. Following policy based emission controls through Europe, pollution Pb declines through the 1980s. In core *Sv-CT3-0m* there is an inflexion from the rising trend of pollution Pb at 16 cm which may identify the start of the Industrial Revolution. The 1970s peak in pollution Pb is clearly visible at 9 cm. Both these events conform chronologically with the tail end of the ^{210}Pb data as presented in Figure 5.16.
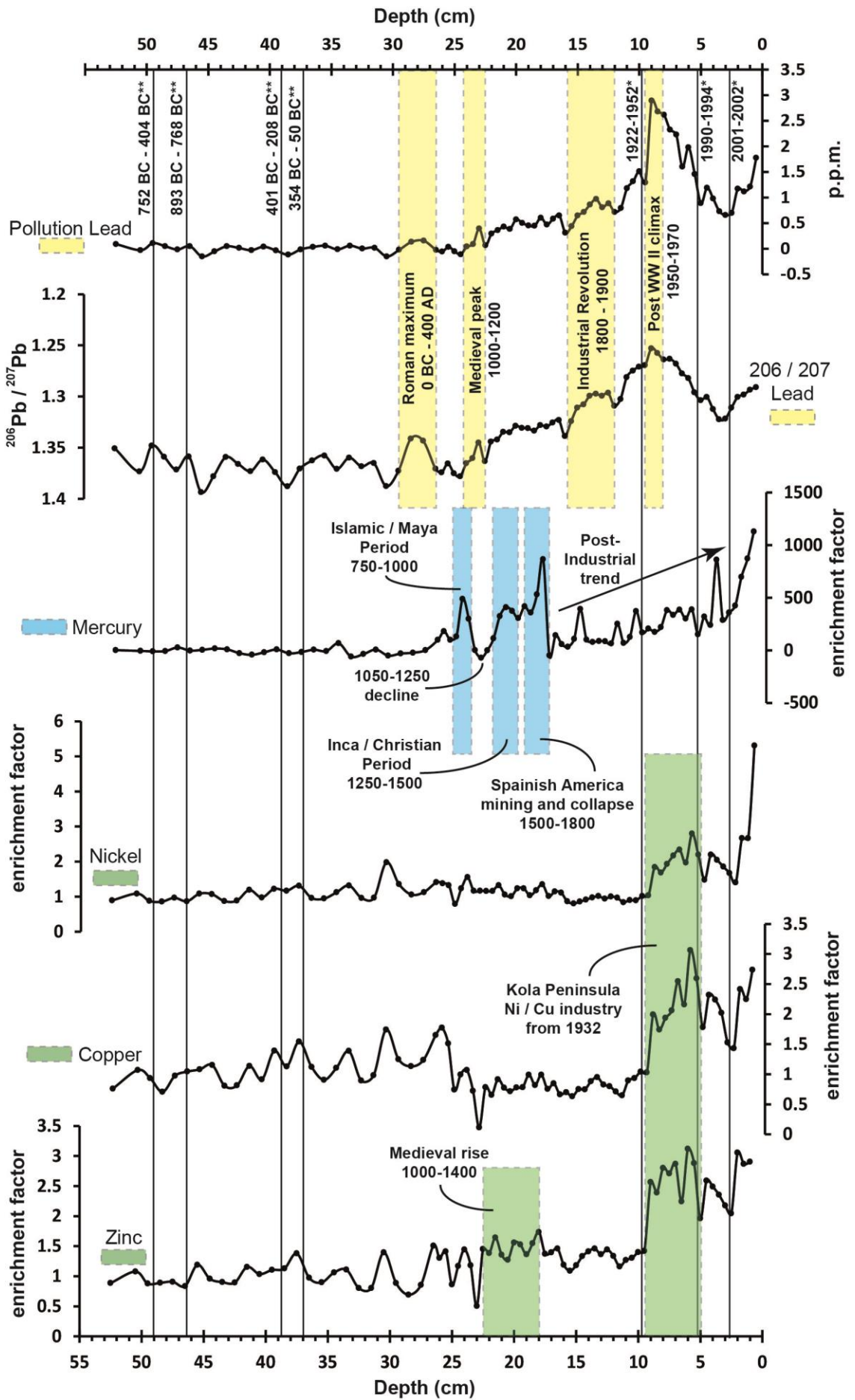
Figure 5.16 Profiles of lead through the top 53 cm of core Sv-CT3-0m are shown in ppm and as ^{206}Pb / ^{207}Pb ratios. Profiles of mercury, nickel, copper and zinc are shown as enrichment factors, normalised against scandium to account for natural metal accumulation changes in the sediments. Inferred historical events have been suggested based on the metal accumulation profiles. ^{210}Pb dates* and radiocarbon dates** are shown alongside

Mercury

Sources for anthropogenic mercury over the last ~2000 years include large scale mining and associated metallurgy emissions. The mining histories of the Almadén region in Spain and of southern and central America are largely responsible for shifts in the Hg enrichment factor seen at numerous sites around the globe. The first influx of pollution Hg is associated with Celtic mining in Spain around 400 BC, followed by continued mining of the Almadén region by the Romans (Martinez-Cortizas et al. 1999). These initial exploitations might be indicated by small peaks in the Hg enrichment record from Svinøyosen at around 35 and 31 cm. The clearest increase in Hg is first seen at around 25 cm. Following the fall of the Roman Empire, a subsequent Hg mining revolution in Europe occurred during the Islamic period (Martinez-Cortizas et al. 1999). This influx coincided with the timing of the Maya civilisation in Central America which has been identified as a source period of pollution Hg (Biester et al. 2002). A mercury record from Antarctica dates this rise associated with the Islamic and Maya periods to 750 AD (Sun et al. 2006). A subsequent decrease in global Hg production is associated with Islamic and Christian conflict in Europe and the decline of the Maya civilisation after 1000 AD.

The establishment of the Inca civilisation, coupled with the reconquest of Almadén by the Christians at around 1200 AD, caused an increase in the mining and exploitation of Hg (Martinez-Cortizas et al. 1999; Sun et al. 2006) which may be represented in core *Sv-CT3-0m* at around 22 cm. There is a subsequent increase in the production of pollution Hg commencing around 1500 AD associated with the destruction of the Inca civilisation and the resultant silver mining of Spanish America (Bindler 2003; Hylander and Meili 2003; Allan et al. 2013). This expansion culminated in a peak around 1800, prior to the collapse of New World Spanish mining (Hylander and Meili 2003; Sun et al. 2006; Allan et al. 2013). These events are potentially recorded in the core between the depths of 20 and 17 cm. Before the Industrial Revolution, Hg accumulation in various deposits has followed a rising trend (Bindler 2003; Allan et al. 2013) due to further mining activities and coal burning. Numerous records demonstrate a decline in pollution Hg around the 1970s following mitigation policies (Hylander and Meili. 2003; Jiang et al. 2009; Allan et al. 2013).

The preindustrial trends described in the literature are potentially recorded in the coastal sediments found at Svinøyosen. Indeed, the enrichment factors seen through core *Sv-CT3-0m* are larger than the terrestrial counterparts (e.g. from peat bogs or lake sediments). This may be associated with the global transport pathways of Hg (Mason and Sheu 2002), potentially providing coastal sediments with a more detailed history of Hg accumulation than terrestrial deposits (Reimann et al. 1997a). The hypothesised ages generated through the Hg enrichment history conform to the existing radiocarbon and ^{210}Pb chronologies, as well as the hypothesised stable Pb chronology described above.

Nickel, copper, zinc

Atmospheric transport of Ni and Cu pollution is less widespread than that of Hg or Pb for example. However anthropogenic Ni and Cu accumulation in terrestrial deposits is evident proximal to industrial smelters through southern Norway, Finland and north-western Russia (Äyräs et al. 1997; Nieminen et al. 2000; Rognerud and Fjeld 2001). Industry associated within the Kola Peninsula, Russia is largely nickel and copper based and commenced circa 1932 with the establishment of the Soviet Union. Numerous studies have demonstrated the large amount of airborne pollution associated with the industries, and often present a sharp rise in Ni and Cu pollution around the early 1930s (Äyräs et al. 1997; Reimann et al. 1997b, Langedal & Ottensen 1998; Rigina 1998; Meriläinen et al. 2010). There is evidence that pollutant emissions from the Kola Peninsula were still being produced through the 2000s (Prank et al. 2010).

The preindustrial Ni and Cu record from Svinøyosen shows a noisy background trend. However, both pollutants show a sharp rise followed by a positive trend at ~10 cm. This depth coincides with an age of 1937 AD ± 15 years generated from the ^{210}Pb data. It is possible that pollutant Ni and Cu originating from the Kola Peninsula is being detected at Svinøyosen. The sharp decline in Ni and Cu pollutants at ~5 cm in core *Sv-CT3-0m* coincides with a ^{210}Pb age of 1992 AD ± 2 years, coincidentally during the time of the Soviet Union dissolution in 1991.

As an airborne pollutant, zinc has greater potential than Ni or Cu to be transported long distances (Boutron et al. 1995; Rognerud & Fjeld 2001) and therefore the Zn enrichment record may identify periods of pollution beyond the Kola Peninsula and Scandinavian industries. However, variation in zinc accumulation due to natural sources

is high compared to that of Pb and Hg (Nriagu 1989) and anthropogenic trends can be hard to discern (Hong et al. 1997). Despite this, the first consistently high enrichment factors for Zn occur from around 22 cm and may identify the onset of the Medieval period and higher levels of mining and metallurgy (Pontevedra-Pombal et al. 2013). Minor peaks in Cu and Zn enrichment coincide at 13 cm down the core. The absence of an equivalent Ni peak suggests the source may not emanate from Russian industry. No evidence from the literature has identified comparable peaks at around 1900 AD from European or Arctic locations. The major enrichment in Zn occurs at ~10 cm, corresponding in timing and size with the Ni and Cu rises and is potentially also associated with the Kola Peninsula smelting industries.

Trends in metal accumulation through core *Sv-CT3-0m* were tentatively associated with historical events and used to infer ages for sedimentary horizons. Table 5.2 provides a summary of the inferred dates obtained through the stable geochemistry analyses. These dates were used to provide a chronology for the last ~2000 years, where radiocarbon and ^{210}Pb ages were unavailable. The ages based on geochemical analyses are inferred only, and do not necessarily reflect a robust or empirically tested chronology. They are therefore treated with caution when used to describe palaeoenvironmental changes below (Section 5.5).

Depth (cm)	Event mid-point (calendar years)	Age range (calendar years)	Source	Inferred calendar age and error	Inferred cal yrs BP age and error	Comments
29-26	27.5	0 - 400	Renberg et al. (2002), Meriläinen et al. (2011)	200 ± 200	1750 ± 200	Pb; broad peak during Roman Maximum
25-24	24.5	750 - 1000	Martinez-Cortizas et al. (1999), Biester et al. (2002), Sun et al. (2006)	875 ± 125	1075 ± 125	Hg, sharp peak but broad event during Islamic and Maya periods
23.5-22.5	23	1200	Renberg et al. (1994, 2001), Zillén et al. (2012)	1200 ± 100	750 ± 100	Pb; peak at 1200 AD, coinciding with Hg decline at 1150 AD ± 100
22-20	21	1250 - 1500	Martinez-Cortizas et al. (1999), Sun et al. (2006)	1375 ± 125	575 ± 125	Hg; rising trend during Inca and Christian periods
20-17	18.5	1500 - 1800	Bindler (2003), Hylander & Meili (2003), Allan et al. (2013)	1650 ± 150	300 ± 150	Hg; sharply rising trend during mining of Spanish America
17-16	16.5	1800	Renberg et al. (2002), Hylander & Meili (2003), Klaminder et al. (2003), Marshall et al. (2009)	1800 ± 50	150 ± 50	Pb; onset of Industrial Revolution, coinciding with collapse of American mining
10	10	1932-1936	Langedal & Ottensen (1998)	1934 ± 5	16 ± 5	Ni, Cu, Zn; onset of Kola Peninsula industries
9-8	8.5	1970-1980	Renberg et al. (2001)	1975 ± 5	-25 ± 5	Pb; 1970s peak from petrol lead

Table 5.2 Inferred dates derived from the metal accumulation analyses. Dates are given in both calendar years and calibrated years BP

5.3.3 Short lived radionuclide chronologies

The most recent sediments from the two cores, *Sv-CT3-0m* and *Sv-CT3-15m*, were dated using ^{210}Pb techniques as described by Appleby (2001). The depths at which supported and unsupported ^{210}Pb reached equilibrium in the cores were determined using graph A of Figure 5.17 and 5.19. The surface age of core *Sv-CT3-0m* was fixed at 2010, and the surface age of core *Sv-CT3-15m* was fixed at 2011. Activity measurements of ^{137}Cs and ^{241}Am were used to validate independently the ^{210}Pb age profiles. Measurements of these two radionuclides were taken and plotted alongside the chronologies derived from the CRS modelling of the ^{210}Pb data.

Core: Sv-CT3-0m

^{210}Pb activity measurements are presented below. Figure 5.17 shows total, supported and unsupported ^{210}Pb through core *Sv-CT3-0m.* Supported and unsupported measurements reached equilibrium in this core at 11.25 cm depth. Data below this depth has been truncated from the figures as it is not useable in the CRS dating model. Activity of unsupported ^{210}Pb is given as total Becquerel counts and not as unit mass values. Hence, the decline in activity at 2 to 3 cm seen in Figure 5.17 is associated with changes in bulk density and grain size, and does not represent sedimentary disturbance. Adherence of ^{210}Pb to particulates is influenced by particle size and the modelling approach used takes this into account prior to calculating sediment ages from decay rates.
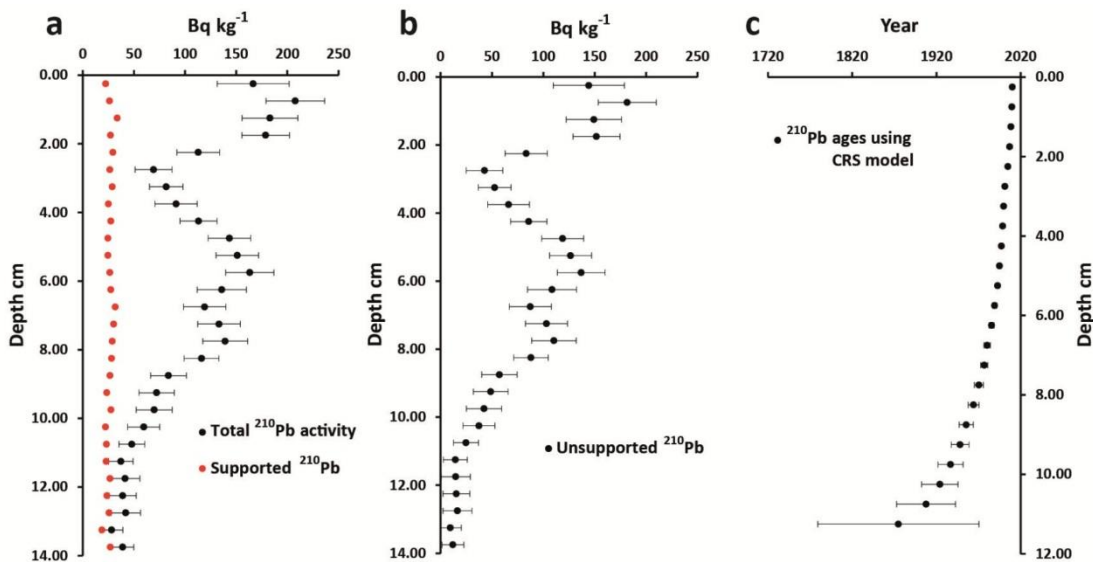
Figure 5.17 ^{210}Pb activity through core Sv-CT3-0m. a) total and supported ^{210}Pb activity, b) unsupported ^{210}Pb activity, c) ^{210}Pb chronology for the core based on the CRS model

Ages are produced for the top 11.5 cm of core *Sv-CT3-0m.* Sediments at 11.25 cm were dated to 1875 (calendar years; AD), however have an error range of ± 96 yrs. Above this depth, errors improve. The ^{210}Pb chronology places the year 1986 AD at 5.75 cm, and 1963 AD at 7.75 cm. Figure 5.17a shows activity measurements of ^{137}Cs and ^{241}Am. Peaks can be seen in the ^{137}Cs curve at 6.25 and 8.25 cm. If it is assumed that these peaks represent 1986 and 1963 respectively, there is very good agreement between the ^{137}Cs chronological markers and the ^{210}Pb age curve (Figure 5.17b). The presence of ^{241}Am at depths between 6.25 and 9.75 cm, (Figure 5.17a) suggest that it is highly likely that the lower peak in ^{137}Cs may represent 1963 AD, and the weapons testing throughout the 1950s and early 1960s.
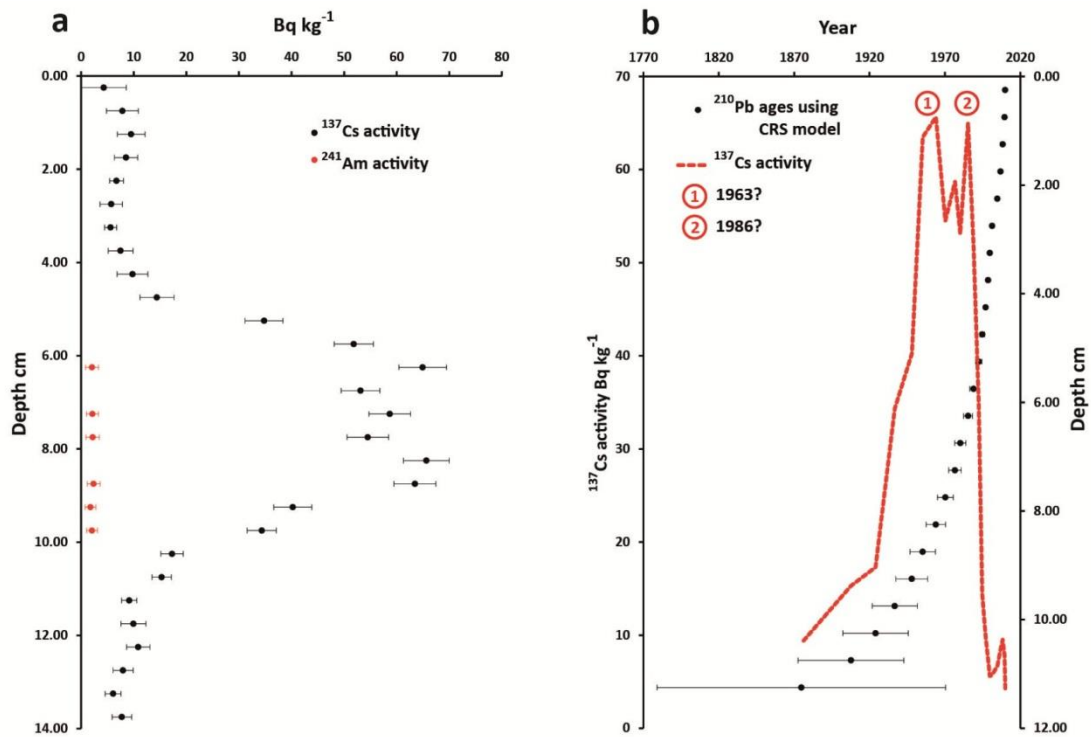
Figure 5.18 ^{137}CS and ^{241}Am activity through core Sv-CT3-0m (a) and peaks in ^{137}Cs activity compared to the ^{210}Pb chronology (b)

Core: Sv-CT3-15m

Activity of unsupported and supported ^{210}Pb reach equilibrium in core *Sv-CT3-15m* at 9.25 cm (Figure 5.19a), a shallower depth than the core above. A decline in unsupported ^{210}Pb is seen in this core at ~3.5 cm which is associated with changes in bulk density and grain size. The oldest age produced from the CRS model is 1877 AD $\pm$ 86 yrs, at 9.25 cm (Figure 5.19c). This model places the year 1986 AD at 3.25 cm depth, and the year 1963 AD at 5.75 cm.
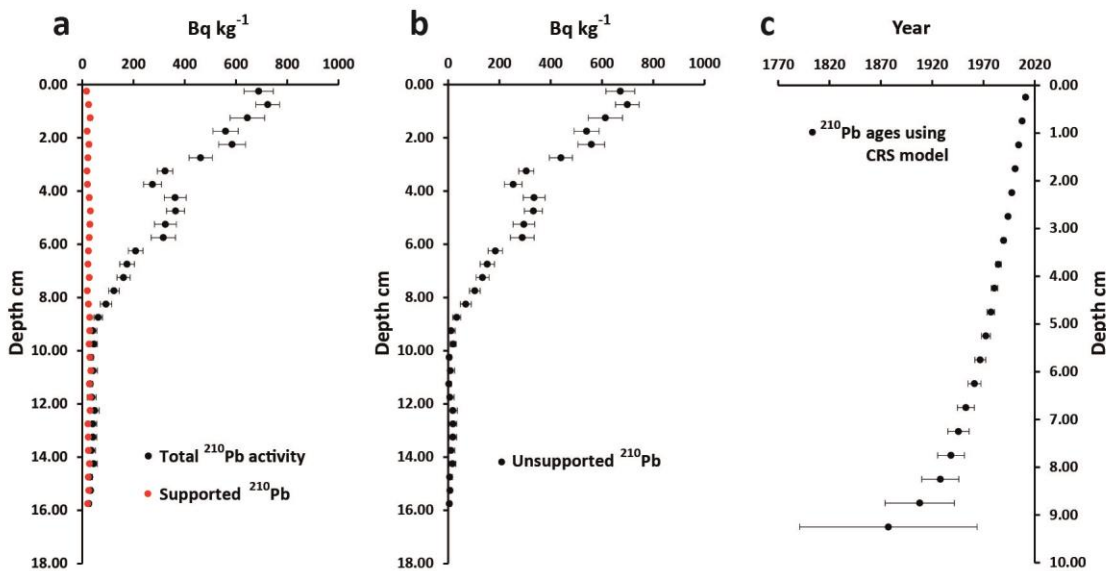
Figure 5.19 ^{210}Pb activity through core Sv-CT3-15m. a) shows total and supported ^{210}Pb activity, b)unsupported ^{210}Pb activity, c) ^{210}Pb chronology for the core based on the CRS model

Profiles of ^{137}Cs activity show a significant peak at 6.75 cm depth (Figure 5.20a). Combined with the activity of ^{241}Am between 5.75 and 7.75 cm, this likely represents the 1963 AD weapons testing peak. There is a smaller peak in ^{137}Cs at 3.25 cm, and although less noticeable, may represent the 1986 AD Chernobyl peak. If this assumption is made, then the peaks in ^{137}Cs correspond well with the ^{210}Pb CRS dating model (Figure 5.20b).

Two chronologies spanning the 20th century have been constructed using ^{210}Pb, ^{137}CS and ^{241}Am data from cores *Sv-CT3-0m* and *Sv-CT3-15m.* Older dates have been acquired through radiocarbon and stable geochemistry dating techniques.
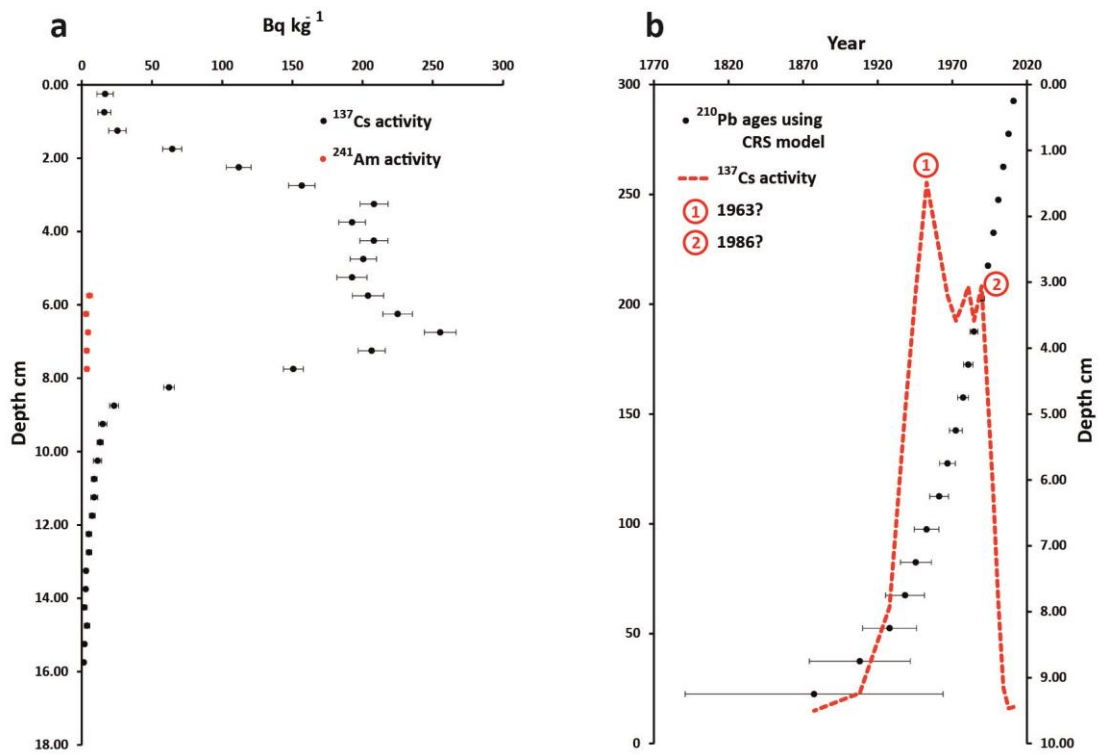
Figure 5.20 ^{137}CS and ^{241}Am activity through core Sv-CT3-0m (a) and peaks in ^{137}Cs activity compared to the ^{210}Pb chronology (b)

5.4 Biostratigraphy

Foraminiferal analyses on core *Sv-CT3-0m* were used to investigate palaeoenvironmental changes that occurred through the last ~7000 years of the Holocene. This core contained the most complete set of Holocene sediments encountered across the entire marsh with well-preserved foraminifera. The top of *Sv-CT3-0m* was situated relatively low in the salt-marsh environment and therefore did not present a suitable opportunity for studying fossil assemblages of testate amoebae. With this in mind, the short core *Sv-CT3-15m* was collected and used to produce these assemblages. Testate amoebae were encountered down to a depth of 0.08 m in this core.

5.4.1 Core: Sv-CT3-0m

From the master core 54 samples were analysed for foraminifera. Results from these analyses are presented in Figure 5.21. Counts of foraminifera species which consistently form less than 2% of the populations were summed together and presented as 'rare species' in the figure. Likewise, counts of different *Elphidium* species have been summed also, although *Elphidium subarcticum* which was only found in the basal clay was kept separate. The sampling interval was increased towards the top of the core in an attempt to provide high-resolution information for recent palaeoenvironmental interpretation. Where possible, a minimum of 100 tests were counted for each sample to provide an indicative assemblage. On average, 160 tests were counted per sample. Occasionally, when test concentrations were low (i.e. between 0.20 and 0.50 m depth below surface) this target was not met.

In all, 35 different taxa of foraminifera are encountered throughout the core. In the top 0.25 m only two species of foraminifera are found. Foraminifera diversity increases gradually with depth down the core. Between 0.25 and 0.70 m, taxa numbers increase from two to 18. Between 0.70 and 1.10 m, taxa numbers are at their greatest (between 19 and 22). Agglutinated foraminifera are most abundant in the top 0.50 m of the core. With increasing depth, the numbers of agglutinated foraminifera decline, and the relative abundance of calcareous species increase.

The lowermost sample contains a distinct assemblage of foraminifera in comparison to the rest of the core. This sample, representing the basal clay, is the only sample to be dominated by the species *E. subarcticum* and is devoid in other *Elphidium* taxa, *H. germanica* or any agglutinated taxa. The presence of *E. subarcticum* decreases across

the unit 1 – unit 2 contact and the species does not occur above 1.05 m in the core. Unit 2 contains a high proportion of *C. lobatulus*, *A. beccarii* var. *batavus*, *N. depressulus* and *Elphidium* species. The abundance of *N. depressulus* increases across the unit 2 – unit 3 contact, whereas the opposite occurs for *C. lobatulus*. Throughout unit 3, the amount *N. depressulus* decreases with decreasing depth, and the amount of *H. germanica* increases with decreasing depth. Numbers of *Elphidium* species remain fairly consistent at ~20% between 1.10 and 0.45 m. At ~0.45 m the presence of any calcareous foraminifera terminates abruptly. Test concentrations between 0.45 and 0.20 m are very low (< 50 tests cm^{-3}). Both *E. scaber* and *T. adaperta* type occur through unit 4, but neither was encountered in the modern assemblages. From 0.45 m up, the abundance of *J. macrescens* increases with decreasing depth. This species makes up nearly 100% of the assemblages from 0.30 m to the surface. The salt-marsh species *M. fusca* is present at around 10% from 0.15 m to the surface. Differences between groups of samples were further distinguished using constrained cluster analysis. The analyses identified three main zones of samples, which could be further divided into subzones.

ZONE 1: The lowest of the three zones can be separated into three subzones. All subzones are virtually devoid of agglutinated taxa, although *E. scaber* does occur in 1b and 1c in very low ($< 3\%$) percentages. Subzone 1a is composed of just one sample and is predominantly characterised by the significant presence of *E. subarcticum.* Subzone 1b is characterised by high numbers of *C. lobatulus* and the absence of *H. germanica* Characteristics of 1c include high percentages ($> 40\%$) of *N. depressulus*, the presence of *H. germanica,* albeit in low numbers, and the regular occurrence of *Elphidium* spp. (around 25%).

ZONE 2: This zone can be separated into two subzones, both of which contain a dominance of *H. germanica* and relatively high numbers of *Elphidium* spp. The main distinguishing factor between the two subzones is the greater number of calcareous species that occur in 2a in comparison with 2b.

ZONE 3: Samples from zone 3 comprise of agglutinated species of foraminifera with the exception of the two lowest samples. The zone extends from 0 to 0.48 m depth and can be split into three subzones. Subzone 1a is distinguished by the presence of *E. scaber* and *T. adaperta* type. Subzone 1b contains assemblages virtually entirely composed of *J. macrescens* and subzone 1c is characterised by a majority of *J. macrescens* coupled with 10 to 20% of *M. fusca*.

There is clear succession from calcareous rich assemblages at the base of the core which contain a high diversity of species, through assemblages dominated by different key species, towards agglutinated dominated assemblages at the top of the core. Indicative ranges of salt-marsh foraminifera can be narrow, making these species good potential sea-level indicators (Gehrels 1994). Chapter 6 develops transfer functions using the modern assemblages and applies these to the fossil assemblages presented here to imply past sea-level heights.
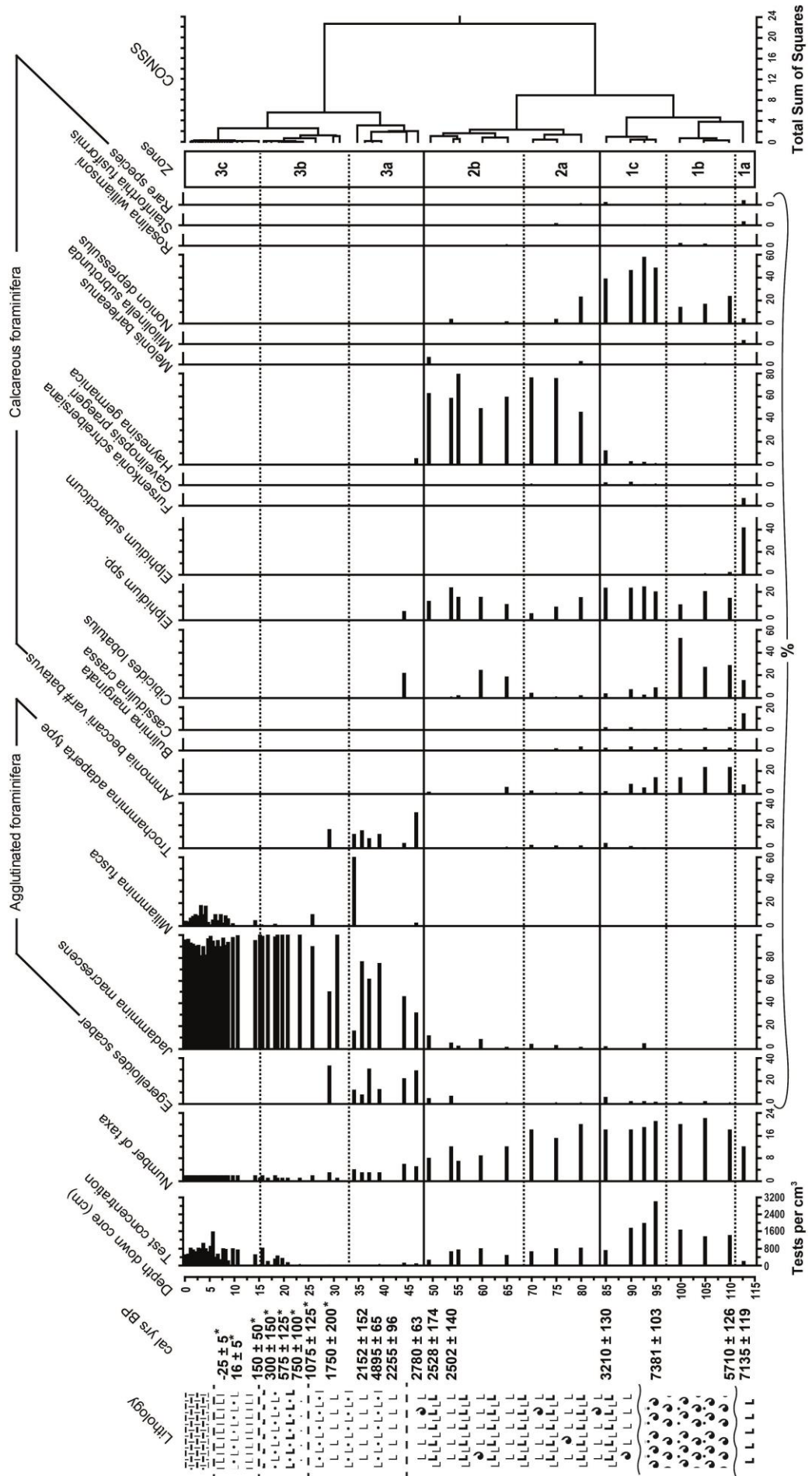
Figure 5.21 Diagram showing fossil foraminifera data through core Sv-CT3-0m. CONISS is used to identify zones of samples with similar assemblage compositions. Dates from the radiocarbon and geochemical* chronologies are included within the figure and are calibrated ages

5.4.2 Core Sv-CT3-15m

The top of this core is located at 1.47 ± 0.018 m above MSL, 0.10 m higher than *Sv-CT3-0m*. Core *Sv-CT3-15m* provided suitable material to test the validity of salt-marsh testate amoebae as sea-level indicators. Analyses were performed on the core from the top down and eight samples provided assemblages of preserved testate amoebae. No testate amoebae were encountered below 0.08 m. A minimum of 100 tests per sample although in two cases (at 5.75 and 7.75 cm depth), where concentrations of tests were very low (< 5000 tests cm^{-3}), only a count of 50 individuals was reached. Figure 5.22 presents the testate amoebae assemblage information for core *Sv-CT3-15m*.

The deepest assemblages contain a low diversity of taxa and are predominantly composed of *C. cassis* type and *C. platystoma* morphotype 1. From 0.06 m up, the number of taxa in each sample increases, but *C. cassis* type remains the dominant taxa. In addition to diversity increasing, the concentration of tests in each samples increases with decreasing depth. Numbers of *C. platystoma* morphotype 1 decreases up the core, and this taxon is replaced by increasing numbers of *T. dentata*, *H. ovalis* and *Difflugia* and *Euglypha* taxa. The topmost sample contains higher numbers of *C. ecornis* and *C. arcelloides* type than any other samples. The clear occurrence and disappearance of specific taxa suggests these testate amoebae assemblages may well be responding to changes in the palaeoenvironment.
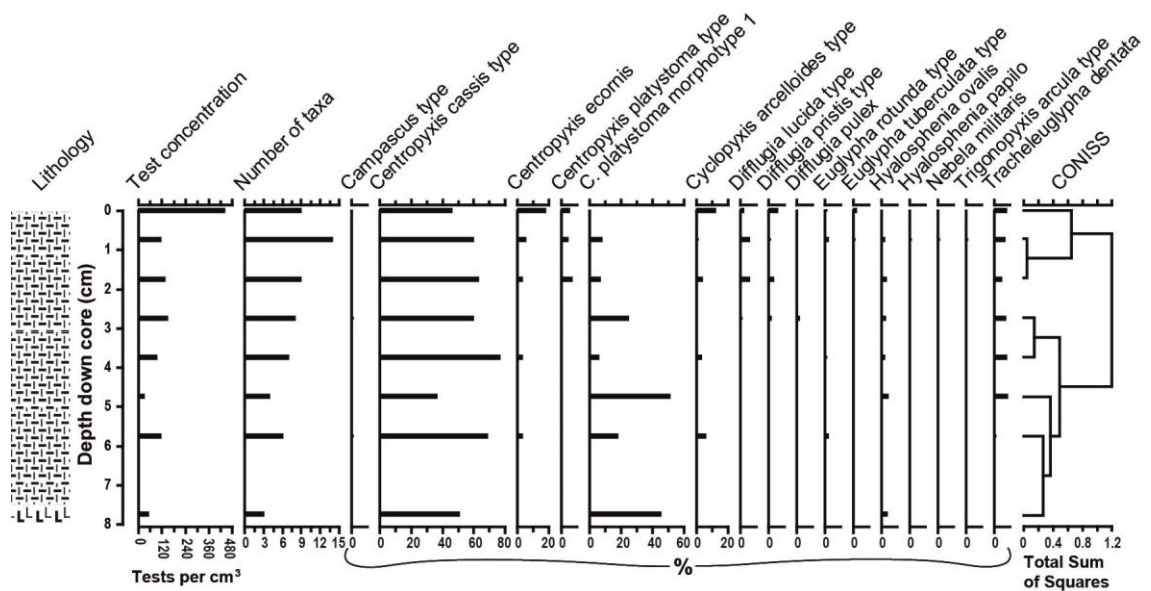
Figure 5.22 Diagram showing fossil testate amoebae data through core Sv-CT3-0m. CONISS is used to identify zones of samples with similar assemblage compositions.

Constrained cluster analysis was again used to identify changes in assemblages (Figure 5.22). It is important to note that, in comparison to the foraminifera assemblages from *Sv-CT3-0m,* the relative degree of difference between the testate amoebae assemblages from *Sv-CT3-0m* is much less, as shown by the total sum of squares. Despite this, CONISS is still able to highlight where slight changes in assemblage types occurred. The greatest difference seen between the assemblages was at 2 cm down the core. Samples above this depth contained more taxa, and relatively higher percentages of the less common taxa. Below this depth the assemblages were broadly similar, although relative changes can be noted at 4 cm, and again at 7 cm.

Despite testate amoebae only occurring to a depth of 8 cm, these fossil assemblages are useful for providing a sea-level reconstruction for the past ~100 years. Testate amoebae based transfer functions are constructed in the following chapter using the combined

Svinøyosen and Storosen surface assemblage data and tested using the fossil assemblages presented here.

5.5 Qualitative palaeoenvironmental interpretation

Descriptions of the lithostratigraphy, sedimentology and biostratigraphy at Svinøyosen were combined with the chronology data presented above to aid interpretations of palaeoenvironments since deglaciation of the region. Particular reference is made to the inferred water depth and tidal regime at Svinøyosen throughout much of the Holocene.

Unit 1: Arctic marine

The basal clay of unit 1 is interpreted as an Arctic marine deposit. The fine silts and clays indicate a low energy, offshore and subtidal environmental. The foraminifera from zone 1a (Figure 5.21) are not encountered in the modern environment at Svinøyosen, although *Elphidium subarcticum* is found in marginal marine and shelf environments as far south as southern Scandinavian fjords (Murray 2006).

The field site on south Hinnøya was deglaciated following the termination of the Younger Dryas 11500 cal yrs BP when the Vestfjorden palaeoice stream finally retreated (Fløistad et al. 2009). Glacial marine conditions would have prevailed following the ice retreat with a maximum water depth of around 50 to 60 m (Møller 1982; Møller 1984). The single date from the basal unit in *Sv-CT3-0m* (6469 to 6732 cal yrs BP) implies that subtidal, Arctic marine conditions persisted into the mid Holocene.

Three of the dates from within unit 2 (shelly sand unit), which overlies the basal clay, predate the age for this unit and imply that reworking of older sediments into Svinøyosen occurred sometime between ~6500 and ~4000 cal yrs BP. Figure 5.9 demonstrates that unit 2 fines upwards across the two unconformable boundaries, possibly suggesting that the reworking of the shelly sands maybe have been caused by a single high energy event. The time window of the reworked sediments correspond with a large submarine landslide that occurred immediately prior to 4000 cal yrs BP called the Traenadjupet Slide (Labeg & Vorren 2000; Laberg et al. 2002a, b; Haflidason et al. 2007). Beyond the fining up sequence of unit 2, and the timing of the event, there is little evidence available to test this hypothesis. There is little evidence for the Traenadjupet Slide along the Norwegian coastline, despite search attempts (Bondevik et al. 2005), although Mills et al. (2009) suggest that shifts in percent carbon and nitrogen, and grain size changes in a lacustrine core from Indrepollen, Vestvågoy, may represent marine minerogrenic influx from a tsunami dated around 4000 cal yrs BP.

Unit 2: high energy, reworked deposition

The lithological descriptions and sedimentary analyses from unit 2 identify this unit as a calcareous rich, mixed sand unit containing very little clay or silt. The grain size analyses imply this unit originates from a high energy environment or event. The presence of *C. lobatulus* in this unit (zone 1b in Figure 5.21) supports this interpretation. This foraminifera is found in high energy, subtidal environments, attached to sandy and gravelly substrates (Murray1991, Murray 2006). *C. lobatulus* represents a high proportion of the modern intertidal samples which are taken from channel deposits at Svinøyosen. The sample elevations correspond to the elevation of unit 2 and it is possible that some of these specimens are being reworked out of the unit, into the modern environment. Radiocarbon dating of the modern specimens would help test this

hypothesis. As discussed, the dates and grain size analyses from unit 2 imply that the shelly sands were reworked into the site, rather than deposited in situ. The diverse calcareous foraminifera assemblages from the unit, which include *Ammonia, C. lobatulus, C. reniforme, B. marginata* and occasionally *M. barleeanus,* suggest that the reworked material originated from offshore (Polyak et al. 2002; Murray 2006).

Unit 3: shallow subtidal to intertidal muds

The grey silts overlying the ~4000 cal yrs BP unconformity have a lower mean grain size in comparison to the underlying shelly sand unit and contain occasional calcareous shell material which decreases in abundance up the unit. The shell and foraminifera identifications indicate a shallowing environment. The gastropod species *Litorrina saxatilis* is found in this unit, and unlike the mollusc species found in unit 2, is commonly found in subtidal, but also intertidal, regions. The decreasing presence of *N. depressulus* across the boundary between zone 1c and 2a (Figure 5.21) and the increasing portion of *H. germanica* in zones 2a and 2b indicate that the environment is developing from near marine, subtidal towards intertidal (Murray 2006). The foraminifera *H. germanica,* is most frequently found in the intertidal realm, and at Svinøyosen, it is found most abundant in the upper intertidal zone (near MHWN). Despite this, the species also extends to shallow subtidal realms (Alve & Murray 1999).

The appearance of *J. macrescens* in the upper parts of unit 3 (zone 2b, Figure 5.21) further indicates shallowing. This shallow marine to intertidal environment persisted from ~4000 cal yrs BP to at least around 2500 cal yrs BP. Dates from *Sv-CT2-0m* suggest the upper sections of this unit may be as young as 1728 ± 138 cal yrs BP. The lithological contact between units 3 and 4 is gradual and diffuse. The onset of the deposition of unit 4 is dated in three places at around 2100 and 2400 cal yrs BP.

Unit 4: intertidal muddy sandflat

The lithology of unit 4 is distinguished from unit 3 by the absence of calcareous mollusc material. There is a gradual reduction in the quantity of silt in the unit and increasing amounts of sand. These gradual changes in grain size are mirrored by changes in the biostratigraphy. At the contact between units 3 and 4 there is a sharp decrease in the quantity of calcareous foraminifera coupled with a fall in test concentrations. The total absence of calcareous material, calcareous foraminifera, very low (minimum 10 tests cm^{-3}) test concentrations, and the presence of the shelf species *Eggerelloides scaber* indicate that changes in foraminifera assemblages may not be controlled by water depth alone. Despite numerous agglutinated species occurring, there is no evidence of salt-marsh accumulation from the organic carbon or grain size analyses. Indeed, salt-marsh samples from Svinøyosen and Storosen containing agglutinated foraminifera have much higher test concentrations than those seen in unit 4. It is therefore possible that carbonate dissolution has occurred. This may be caused by proximity of the unit to an organic rich environment generating acidic pore waters. This unit is interpreted as a shallowing low intertidal environment due to the low numbers of agglutinated foraminifera, the increasing quantity of *J. macrescens* and the silt – sand dominated matrix coupled with low quantities of organic carbon. From the chronology based on geochemical analyses, this environment persisted to around 1075 ± 125 cal yrs BP.

Unit 5: high intertidal sandflat

Unit 5 represents a thin (~10 cm) sedimentary horizon containing more sand and larger grains in comparison to the underlying grey silts. Foraminifera assemblages remain exclusively agglutinated. However, the concentration of tests begins to increase again in

this unit at around 20 cm depth (~600 cal yrs BP). It is likely that the environment is shallowing and becoming more preferable to species such as *J. macrescens*. Although the foraminifera assemblages (zone 3b) imply an upper salt-marsh environment, the high amount of sand in the unit, coupled with minimal organic carbon content, the absence of *M. fusca* and the continued possibility of dissolution effects suggest that a salt-marsh environment is still yet to become established. This unit is therefore interpreted as a high intertidal environment. The ages for this environment are again based on stable geochemistry which dates the top of the unit to approximately 150 ± 50 cal yrs BP.

Unit 6: salt marsh

The onset of unit 6 is distinguished by increasing quantities of clay and silt and a rising trend in the percentage of organic carbon within the sediments. These changes coincide with the establishment of *M. fusca* as a regular species (~ 5 to 20%) within the foraminifera assemblages which occurs in these percentages in the modern environment between the elevations of MHWN and MHWS. The presence of this species, coupled with the already established presence of *J. macrescens* and rising test concentrations suggests that a salt-marsh environment is becoming established for the first time at Svinøyosen. The onset of this establishment occurs at 15 cm, after around 150 cal yrs BP.

Unit 7: high salt marsh

There is little change seen between unit 6 and unit 7. The foraminifera biostratigraphy implies the salt-marsh environment continues to exist through to the present day based on comparisons with the modern environment. Changes in lithology are confined to an

increasing amount of decaying organic material. The testate amoebae biostratigraphy from Svinøyosen suggests the environment may have been evolving from a low marsh, towards a high-marsh environment in the last few decades. This regressive sequence may be picked up by the foraminifera from *Sv-CT3-0m* through an increasing ratio of *J. macrescens* to *M. fusca* in the top 2 cm.

5.6 Summary

The palaeoenvironments at Svinøyosen have been described in terms of lithology, sedimentology and biostratigraphy. Changes in these characteristics have been constrained chronologically using a suite of radiocarbon dates, short lived radiometric techniques (^{210}Pb, ^{137}Cs, ^{241}Am) and stable geochemistry analyses (lead, mercury, nickel, copper and zinc profiles). These descriptions have facilitated the interpretation of past environments since deglaciation of the region following the Younger Dryas. There is evidence of mid Holocene Arctic marine sediments at the base of the sequences from Svinøyosen. There is good evidence suggesting that the environment at Svinøyosen has been subtidal throughout the mid-Holocene, and only became intertidal in the last ~2000 yrs. There is evidence of an erosional event occurring just prior to 4000 cal yrs BP which overtopped the mid Holocene sediments with older, early Holocene sediments.

A detailed history of environmental change since ~2000 cal yrs BP has been provided through the analysis of foraminifera in core *Sv-CT3-0m*. The biostratigraphy suggests a

steadily shallowing sequence of events from ~2000 to present culminating in the present-day salt marsh.

In order to quantify the direction of sea-level fluctuations that have been demonstrated in this chapter, transfer functions have been constructed and are presented in the following chapter. They are based on modern analogues using the contemporary foraminifera and testate amoebae data from both Svinøyosen and Storosen salt marshes, which are then used to infer palaeomarsh surfaces and sea-level heights. The resultant sea-level reconstructions are constrained chronologically using dates presented in this chapter.

CHAPTER 6 – Sea-level reconstructions

6.1 Introduction

This chapter presents the transfer functions based on modern salt-marsh testate amoebae and foraminifera that are used to reconstruct relative sea-level changes. Training sets of modern foraminifera and testate amoebae were compiled to quantify the relationship between assemblages and elevation. These relationships were applied to fossil assemblages to derive palaeomarsh-elevation estimates. Relative sea-level curves were created from the reconstructed palaeomarsh-elevations and validated using similarity measures of the fossil and modern assemblages and comparisons with local tide-gauge data.

6.2 Testate amoebae transfer function

There are no empirically derived requisites for the number of samples in a modern training set of salt-marsh testate amoebae. As a general rule, larger datasets are preferred for transfer functions of this kind, although published sample numbers vary greatly. For example, Birks (1995) dictates that "a large high-quality training set of modern surface samples" is a basic requirement for quantitative palaeoenvironmental reconstruction. In the most recent development of a salt-marsh testate amoebae based transfer function, Ooms et al. (2012) used a training set of 37 samples, which was, in

their opinion, "rather low" on numbers. With this in mind, the training set used in this testate amoebae transfer function was composed of every modern sample available (18 from Svinøyosen, 11 from Storosen). It is necessary for a training set to represent adequately full species variety across the entire environmental range (Reavie & Juggins 2011). Due to the regular and high resolution surface sampling (every 4 to 5 cm change in vertical distance) across both salt marshes, it is assumed that the training set of 29 samples sufficiently represents the modern environment, despite containing relatively few samples.

This dataset underwent ordination analysis to investigate species turnover along the environmental gradient and to analyse species response to changes in elevation. Different regression models were then used to determine the most suitable transfer function applicable to the training set. The most appropriate model was selected and applied to fossil assemblages from core *Sv-CT3-0m* to reconstruct palaeomarsh-surface elevations (PMSEs) and thereby past sea-levels.

6.2.1 Ordination

Selection of the appropriate ordination method is vital to producing robust relationship models. Comprehensive reviews of the different techniques are available in Birks (1995, 2010). For the testate amoebae surface dataset, detrended canonical correspondence analysis (DCCA) was selected. DCCA is an example of constrained ordination, (i.e. direct gradient analysis), which is most appropriate when multiple response variables (in this case, testate amoebae taxa) are known, and an explanatory variable (in this case, elevation) is available and known (Lepš and Šmilauer 2003). Detrending is required to

linearize the compositional gradient prior to its length estimation. In this case detrending by segments (Hill and Gauch 1980) was used, as is appropriate for constrained ordination using only one environmental variable.

DCCA is a quantitative approach towards investigating the relationship between taxa and their environment. Taxon response to environmental variables can be either linear or unimodal. It is important to determine which of these underlying responses is the most appropriate assumption, prior to attempts at modelling the assemblage – environment relationship. This response can be defined by the gradient length of the environmental variable in a constrained ordination. A relatively short gradient length indicates a linear underlying response and a long gradient length usually indicates a unimodal response. Ordination (DCCA) is used here to determine the nature of the taxon – environmental variable relationship, and to quantify statistically the strength of this relationship.

Results from the DCCA analysis on the testate amoebae training set are presented in Table 6.1. The environmental variable gradient length is given in standard deviation (SD) units. The gradient length is > 2 SD units. It is therefore assumed that taxa are responding unimodally to the environmental variable and a unimodal transfer function model is appropriate (ter Braak and Prentice 1988). Gradient lengths of < 2 SD units represent a linear taxa response to the environmental variable, and an alternative type of transfer function would be required. Eigenvalues are presented and represent the amount of assemblage variability attributed to different environmental variables. In this case, only one variable (elevation) is known, thus only the first axis is canonical and represents this variable. Other axes have been included to demonstrate the proportion of

assemblage variability explained by other, unrecorded variables. It is important to acknowledge the influence of other variables, although determining the exact environmental source is not a necessity for sea-level reconstructions based on palaeoelevation estimates.

	Axis 1	Axis 2	Axis 3	Axis 4
Gradient Length	3.066	2.26	1.416	1.069
Eigenvalue	0.589	0.163	0.095	0.04

No samples	29
No taxa	32
Significance (*P value)*	0.002

Table 6.1 Results from the DCCA analysis performed on the testate amoebae dataset showing taxa response to changing elevation (gradient length, axis 1) and the taxa variation explained by elevation (eigenvalue, axis 1)

The long environmental gradient length (3.066 SD units) demonstrated by the training set data indicate that a unimodal type regression model should be used in the transfer function. Suitable models that were considered and applied in Section 6.2.2 include weighted averaging (WA), weighted averaging partial-least squares (WAPLS) and maximum likelihood (ML). Two additional models were available, the modern analogue technique (MAT) and correspondence analysis (CA). However, these were discounted from further analysis. CA was not used as it is an example of indirect ordination where no known environmental variable is required and was therefore not suited to the dataset (Birks 1995). MAT was also discarded as this technique is potentially sensitive to the effects of autocorrelation (Telford and Birks 2005, 2009).

Autocorrelation is the tendency of geographically nearby sites to show more of a resemblance to each other in comparison to isolated or separated sites (Legendre and Fortin 1989). Cross-validation of autocorrelated datasets tend to underestimate prediction errors and steps must be taken to avoid such overly ambitious predictions (e.g. Telford and Birks 2011b). Recently, WA has been demonstrated to be more robust to the effects of autocorrelation in comparison to MAT (Telford and Birks 2005) and was therefore considered a more suitable option.

The DCCA analysis (Table 6.1) also quantifies how much of the taxa variability is explained by changes in elevation. Axis 1 (elevation) explains over 58% of the variation in testate amoebae populations. The significance of the ordination was analysed using Monte Carlo Permutation testing with 499 permutations. The statistical test held significant value with P values of 0.002.

Figure 6.1 shows the ordination bi-plot of the taxa – elevation relationship for the testate amoebae training set. The horizontal axis represents taxa variation explained by elevation, the secondary, vertical axis represents a portion of the residual variation not explained by changes in elevation. Taxa occurring in similar samples tend to group. Those taxa more commonly found at lower elevations are situated high on axis 1. Higher elevation taxa tend to occur low on axis 1. The strong relationship shown between taxon variation and elevation implies a suitable transfer function based on unimodal regression is likely to produce robust predictions of elevation, based on taxa assemblages.
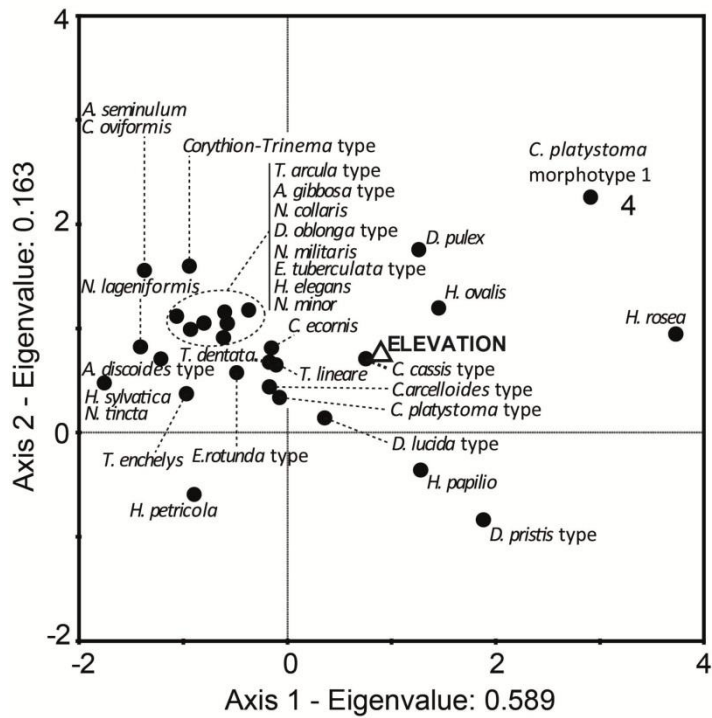
Figure 6.1 Ordination bi-plot showing the relationship between taxa (annotated circles) and elevation (axis 1)

6.2.2 Model development

Modelling using WA and WAPLS has been widely used in salt-marsh foraminifera based transfer functions (e.g. WA: Gehrels et al. 2005, 2006b; Southall et al. 2006 and WAPLS: Massey et al. 2006; Callard et al. 2011; Kemp et al. 2012) and both are used and compared here. ML calibration is a probabilistic based approach which infers unknown values of a variable from assemblage information. This method employs similar aims to WA and is capable of outperforming both this and WAPLS models (Birks 2010), although has been used less in palaeoenvironmental reconstructions. The

training set was run using five models based on one of the three approaches described above.

Two different WA models were used. A form of deshrinking is required with WA modelling to prevent inferred values of elevation clustering towards the mean of observed values (Birks 1995). Inverse deshrinking can cause underestimation at the highest elevations and overestimation at the lowest elevations (ter Braak and Juggins 1993). Because of this, classical deshrinking was used in both WA models to provide the greatest accuracy at the transect ends, where taxanomic representation of elevation is most sensitive and valuable. Tolerance downweighting of taxa is an acceptable approach to reducing standard errors in modelling. Taxa with narrow tolerance ranges are more valuable as sea-level indicators than taxa with wide ecological niches. With this in mind, one WA model was run with tolerance downweighting of species, and another without. The third and fourth models were based on WAPLS approaches. WAPLS with 1 component (i.e. one environmental axis) was not used as this essentially represents a WA model. A maximum of 3 components was applied, as by increasing the number of components further may have led to erroneous over-fitting of the data (Birks 1998). The fifth and final model used was based on the ML approach. In all cases cross-validation was performed using bootstrapping (1000 cycles) to provide error estimates and no data transformations were required as samples were from an even distribution. Performance characteristics of the five models on the dataset are presented in Table 6.2.

Dataset	Model	RMSEP	% change (RMSEP)	r^2(boot)	Av_Bias (boot)	Max_Bias (boot)
Testate amoebae	WA	0.091	N/A	0.87	-0.002	0.096
	WA_Tol	0.094	N/A	0.87	-0.006	0.111
env. range = 0.84	WAPLS(2)	0.085	8.68	0.89	0.005	0.102
env. grad. length = 3.066	WAPLS(3)	0.083	2.31	0.90	0.005	0.077
	ML	0.092	N/A	0.92	-0.001	0.074

Table 6.2 Performance statistics of the five models run on the testate amoebae training set. The vertical distance represented by the dataset (env.range) and the gradient length of the dataset in SD units (env.grad.length)is presented

6.2.3 Model comparisons

A combination of four performance statistics was used to analyse the predictive power of each model. The square root of the mean squared residuals (differences between observed and predicted values) was provided for the cross-validated data (RMSEP). The sampling techniques ensured even vertical distributions which promotes confidence in an unbiased RMSEP (Telford and Birks 2011b) The coefficient of determination ($r^2_{(boot)}$) was also provided to measure correlation between observed and predicted variable values following bootstrap cross-validation. Over- and underestimations of the environmental variable were also calculated and presented as average biases and maximum biases. Percentage changes in RMSEP are also shown in Table 6.2 to help determine the most appropriate number of components to use in WAPLS models (Birks 1998). Finally, environmental ranges are also provided for comparisons with RMSEP

values. Models where RMSEP values are close to or above the value of the environmental range should be dismissed (Telford and Birks 2011a).

According to the performance statistics, WAPLS with 2 components is the best performing model overall. WAPLS(3) has a lower RMSEP for the dataset, although the small gains in percentage change of RMSEP suggest that the additional (third) component may be artificially improving the predictions. Modelling using ML provides the strongest correlation between observed versus predicted sample elevations, although this model contains higher uncertainties in comparison to WAPLS(2). Average biases of elevation estimations (5 cm) using WAPLS(2) are within the stated error range of this model (8.5 cm) and the RMSEP value is virtually 10% of the entire environmental range, which suggests this transfer function is fairly robust and reliable. A scatter plot of observed versus predicted values, residual values and sample specific standard errors is presented in Figure 6.2.

Figure 6.2a illustrates the good fit between the observed sample elevations and the predicted sample elevations produced by the transfer function. It is evident from the correlation and residual plots that the transfer function is less able to predict elevations at the lower end of the transect. This may be unsurprising as there are far fewer species in these samples. This uncertainty is encompassed within the greater standard errors for these samples as shown in Figure 6.2c.
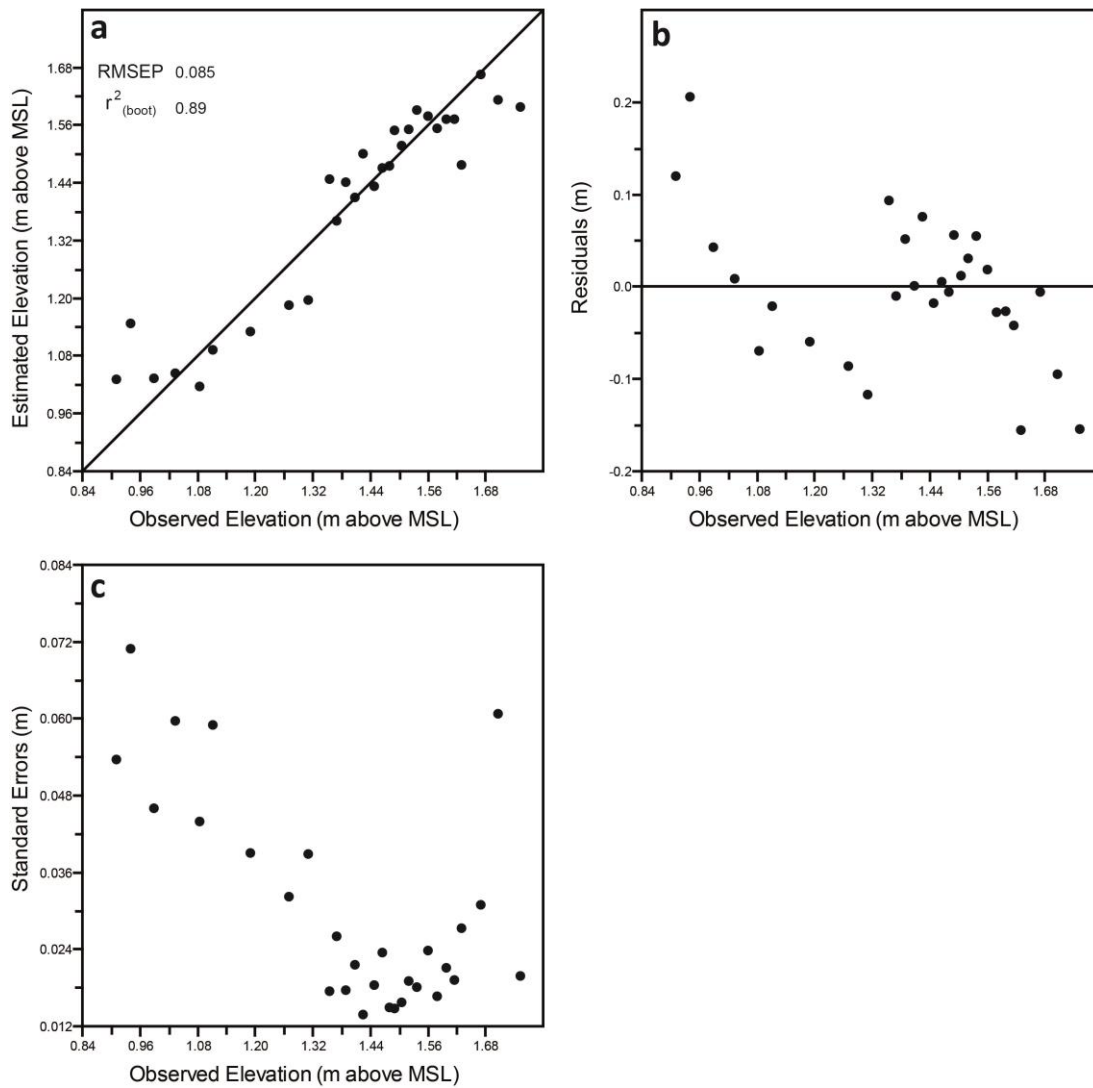
Figure 6.2 a) Measured sample elevations shown against predicted sample elevations using the WAPLS(2) model. The sample specific residuals and standard errors are also shown (b and c respectively)

In summary, the testate amoebae assemblage counts from Svinøyosen and Storosen were combined to construct a dataset for transfer function purposes. The training set demonstrated a long (> 2 SD units) environmental gradient length on the first axis implying a unimodal taxon response to change in elevation. Elevation (axis 1) explained more than 58% of taxa variability, suggesting a strong relationship between assemblage composition and height above sea level. The predictive power of the dataset was

analysed using five different regression models. The WAPLS(2) model stood out in terms of performance statistics and predicted marsh surface elevations to within ± 8.5 cm based on the testate amoebae dataset. Therefore, the model, weighted averaging partial least squares with species tolerance downweighting, classical deshrinking and no data transformation was used to estimate PMSEs from the fossil testate amoebae assemblages in core *Sv-CT3-15m*. These results were used to calculate past sea levels and validated using a number of techniques to finally assess the suitability of testate amoebae as sea-level indicators.

6.2.4 Model application and validation

The transfer function model selected above was used to generate PMSE estimates from the fossil testate amoebae data in core *Sv-CT3-15m* and bootstrapping cross-validation was used to calculate sample specific RSMEP values (Table 6.3). A total of eight fossil samples were available for the analysis and extended down to 8 cm depth in the core. No testate amoebae were present below this depth. An age-depth chronology for the near surface sediments of the core was provided by the ^{210}Pb, ^{137}Cs and ^{241}Am dating techniques and extended from 2011 AD at the surface, to 1938 ± 13 AD at 8cm. The first validation technique applied to the reconstruction was used to determine the similarity between fossil samples and the modern analogues. The modern analogue technique (MAT) was therefore used to assess the similarity between fossil and modern samples using a squared chord distance dissimilarity measure to produce a minimum dissimilarity coefficient (minDC) for each fossil sample (Birks 1995; Barlow et al. 2013). Higher minDC values indicate greater dissimilarity between the fossil sample and the closest modern analogue (Jackson and Williams 2004). Threshold values were

used to determine whether fossil samples had good, close or poor modern analogues following Simpson (2007), Watcham et al. (2013) and Barlow et al. (2013). The 5th and 20th percentiles of the modern sample dissimilarity coefficients were used to determine these thresholds (Table 6.3).

Depth down core (m)	Age (210Pb)	WAPLS(2) PMSE (m)	RMSEP (m)	minDC	Modern analogue fit
0.0025	2011 ± 1	1.553	0.079	9.000	Good
0.0075	2008 ± 1	1.448	0.079	18.549	Close
0.0175	2001 ± 1	1.429	0.079	8.576	Good
0.0275	1994 ± 1	1.317	0.079	27.290	Close
0.0375	1985 ± 3	1.432	0.079	10.297	Good
0.0475	1977 ± 4	1.209	0.081	15.237	Good
0.0575	1967 ± 5	1.376	0.078	24.168	Close
0.0775	1938 ± 13	1.211	0.080	14.299	Good

Table 6.3 Palaeomarsh-surface elevations generated by applying the WAPLS(2) transfer function model to the fossil assemblages in core Sv-CT3-15m. Ages are derived from the ^{210}Pb chronology, RMSEP provides sample specific error ranges and the similarity between fossil assemblages and their closest modern analogue are quantified using the modern analogue technique

Of the eight fossil samples used, five had 'good' modern analogues, and the remainder had 'close' modern analogues. The lack of any poor modern analogues suggest that environmental conditions influencing testate amoebae populations may not have changed much in the last 100 years or so. The good to close modern analogue fit provides reassurance on the reliability of the estimated PMSEs. Sample specific error

terms are less than 10% of the measured environmental range (0.84 m of vertical distance) adding to the credibility of the reconstruction.

A secondary validation technique is to compare the predicted PMSEs of the top sample (1.55 ± 0.079 m) with the measured elevation of the core top (1.47 ± 0.018 m). The reconstructed marsh surface is 8 cm higher than the measured core top elevation. However, when the combined errors are taken into account (9.7 cm) it is evident that the testate amoebae transfer function model is capable of accurately reconstructing PMSEs to within quoted uncertainties.

In order to compare the model results with historical data, in this case tide gauge measurements, the estimated PMSEs were calculated relative to MSL using Equation 8 following Gehrels (1999). It is important to consider the effects of sediment compaction when generating sea-level reconstructions (Brain et al. 2012). In this instance, the reconstruction is based on the top 8 cm of a light, semi-elastic, salt-marsh peat, representing a regressive sequence with a uniformly low bulk density down to 8 cm (Figure 5.13) implying that the effects of compaction are negligible. TheSLIPs were plotted against time, as opposed to depth, using the ^{210}Pb chronology for the core (Figure 6.3). A nearby tide-gauge record of yearly MSL was plotted alongside the reconstruction for comparison. The record from Harstad provided the most comparable record to the reconstruction as Sinvøyosen and Harstad are situated on similar palaeoisobase lines (Møller 1982; Møller 1987). The tide-gauge record from Harstad is the second longest record available and extends back to 1952.

Equation 8

$$S = H - I + C$$

S – former sea level
H – sample height relative to MSL
I – indicative meaning (palaeomarsh surface elevation)
C – compaction

Of the seven samples that overlap with the tide-gauge data, five of them reconstruct sea-level elevations accurately (Figure 6.3). The deepest sample extends the sea-level reconstruction (SLR) just beyond the length of the tide gauge. The linear sea-level trend recorded by the tide gauge suggests a falling RSL of -1 mm yr^{-1}. The SLR infers a linear sea-level trend of -2.7 mm yr^{-1} which overestimates the rate of sea-level fall. This offset can be largely explained by the outlier in the reconstruction at ~1977 and the oldest data point at ~1938. When these outliers are removed the trend is -1.5 mm yr^{-1}.
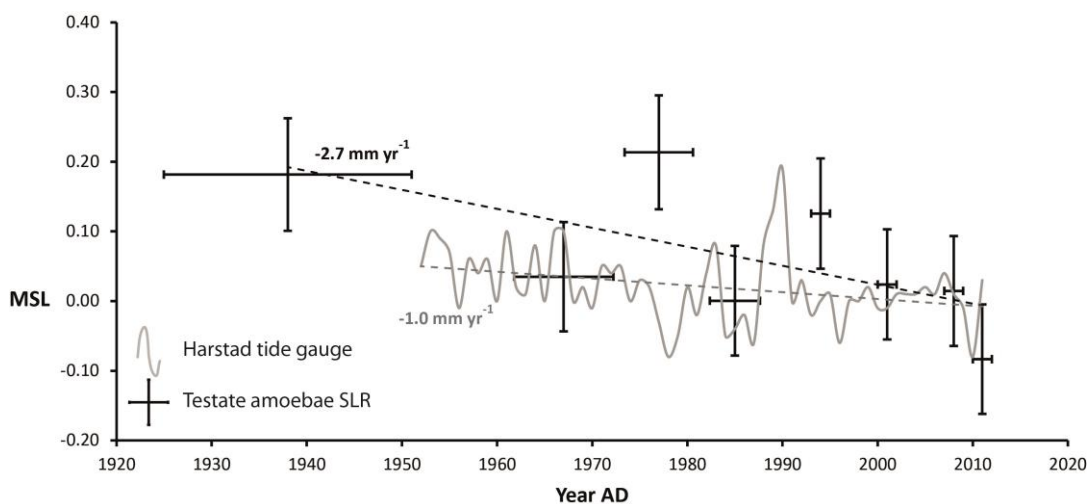
Figure 6.3 The testate amoebae based sea-level reconstruction (crosses) compared against tide gauge data from Harstad (grey line). The solid lines represent linear trendlines for the reconstruction and tide gauge

208

The result in Figure 6.3 demonstrates that by compiling a dataset of modern salt-marsh testate amoebae and by establishing a relationship with elevation, a transfer function can be applied to fossil assemblages to produce accurate reconstructions of sea level. The only existing studies that compare salt-marsh testate amoebae sea-level reconstructions to tide-gauge data also report similar success, with comparable errors of ± 5cm (Charman et al. 2010). For the first time, this thesis has successfully applied such methods to a region of falling sea level.

6.3 Foraminifera based reconstructions

Foraminifera from core *Sv-CT3-0m* were used to reconstruct past sea levels at Svinøyosen as they were present throughout the entire sequence. Two methods were applied to the reconstruction. Firstly, a quantitative technique is performed based on ordination and regression modelling, similar to the methods used in the testate amoebae reconstruction. Secondly, qualitative methods are used to extend the sea-level reconstruction back beyond depths where fossil foraminifera samples have no close modern analogue and are thus unsuitable for qualitative transfer function methods. This is in part similar to the visual assessment method that was applied by Long et al. (2010) to interpret key changes in fossil diatom taxa using contemporary microorganism data, but also stratigraphy trends and changes in LOI and grain size. Shennan (2007) provides a review of these techniques where SLIPs are derived from the indicative meanings of microfossil assemblages.

Contemporary surface samples from Storosen and Svinøyosen were combined to provide a modern training set of 66 samples, representing an elevation range from 1.46 to -0.56 m above MSL. Rare species (< 2%) that only occurred in one sample were removed from the dataset as their relationship with elevation was poorly defined, thus would lead to increased uncertainties in the transfer function.

6.3.1 Ordination

The same ordination techniques were used as in Section 6.2.1. In order to determine environmental gradient lengths and quantify the relationship between species variation and elevation, direct gradient analysis (DCCA) was again used. Table 6.4 presents the results from the DCCA on the three foraminifera training set.

	Axis 1	Axis 2	Axis 3	Axis 4
Gradient Length	2.826	2.599	1.260	1.387
Eigenvalue	0.582	0.163	0.066	0.049

No samples	66
No taxa	27
Significance (*P value*)	0.002

Table 6.4 Results from the DCCA analysis performed on the foraminifera dataset showing taxa response to changing elevation (gradient length, axis 1) and the taxa variation explained by elevation (eigenvalue, axis 1)

Axis 1 of the environmental gradient lengths represents species response to changes in elevation, measured in SD units. The dataset demonstrates a long gradient length on axis 1 (i.e. >2 SD units) and therefore a unimodal species distribution (ter Braak and Prentice 1988). Axis 1 of the eigenvalues demonstrates the amount of species variation explained by changes in elevation. Elevation can explain over 58% of species variation in the combined Svinøyosen – Storosen training set. The remaining axes of eigenvalues represent species variation explained by alternative variables. In all cases, it is clear that species response is predominantly attributed to changes in elevation.

6.3.2 Model development and comparisons

The same five regression models were used on the foraminifera datasets, as for the testate amoebae datasets, and the same comparative statistics were used to test the performance of each model (Table 6.5). WAPLS at 2 components is the best performing model for the training set. Although WAPLS(3) has a similar RMSEP, and slighty better correlation, the percentage change in RMSEP (-0.18 %) suggests that the model is over-predicting accurate surface elevations by including the extra component. WA_Tol would be a suitable choice as there is reasonable correlation between observed and predicted surface elevations (0.72), however this model has greater vertical uncertainties in comparison to WAPLS(2).

Dataset	Model	RMSEP	% change (RMSEP)	r2(boot)	Av_Bias (boot)	Max_Bias (boot)
Foraminifera	WA	0.347	N/A	0.67	-0.004	0.623
	WA_Tol	0.309	N/A	0.72	-0.007	0.569
env. range = 2.02	WAPLS(2)	0.268	7.91	0.73	-0.001	0.653
env. grad. length = 2.826	WAPLS(3)	0.268	-0.18	0.74	-0.002	0.609
	ML	2.827	N/A	0.33	-0.579	3.710

Table 6.5 Performance statistics of the five models run on each of the foraminifera

datasets including the vertical distance represented by the dataset (env.range) and the

gradient length in SD units (env.grad.length)

Scatterplots showing sample specific elevation predictions, residuals and standard errors were constructed for the WAPLS(2) regression modelling of the surface samples (Figure 6.4). There is poor correlation between observed and predicted elevations at either end of the surface data. At the higher end, there are only two salt-marsh species which show little variation in abundance, and at the lower end, a single species dominates the assemblages. This poor correlation is accounted for by large residuals and standard errors at the extremes of the surface data. Many residuals and standard error values are greater than 10% of the total environmental range (2.02 m), calling into question the reliability of the transfer function. Where the transfer function model performs poorly, the visual assessment method may represent the most suitable choice for reconstructing sea levels.
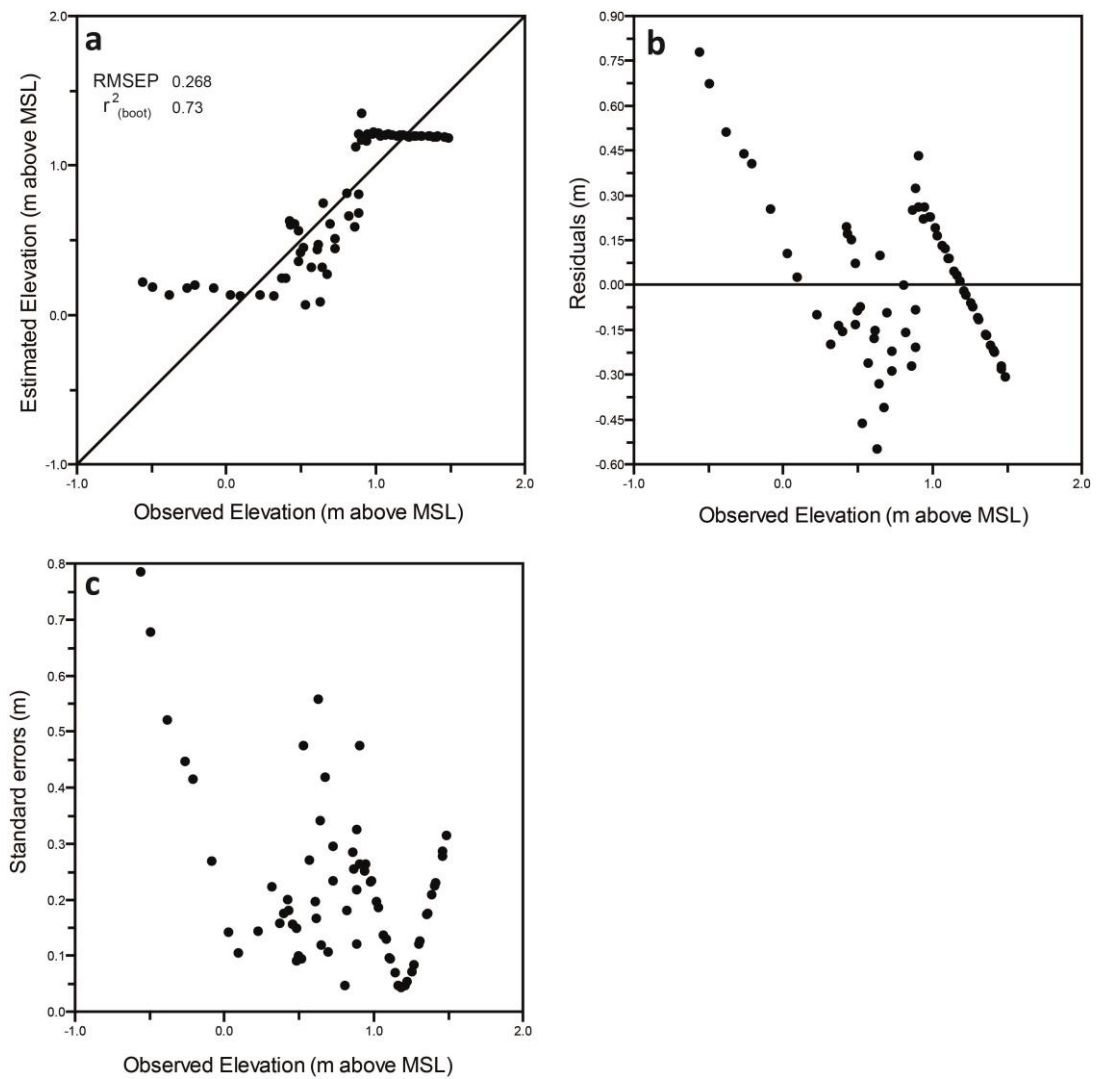
Figure 6.4 Plots showing the observed versus predicted sample elevations of the transfer function model (a), alongside sample elevation residuals (b) and standard errors (c)

In summary, foraminifera surface assemblages were used to construct a training set for transfer function purposes. The species – elevation relationship was quantified using ordination (DCCA). The best performing transfer function model was weighted averaging partial least squares with two components, classical deshrinking and no data transformation, WAPLS(2). This model was capable of predicting elevation values to within ± 27 cm, based on foraminifera alone.

6.3.3 Transfer function application

The transfer function was applied to fossil foraminifera assemblages from core *Sv-CT3-0m*. The results produced PMSE estimates for the fossil samples as shown in Table 6.6. The modern analogue technique was again used to quantify similarities between fossil assemblages and their closest modern sample. The same threshold boundaries as those used in the testate amoebae reconstruction applied (5th and 20th percentiles). Fossil samples with 'good' analogues had a minDC of < 2.037, and those with 'close' analogues had a minDC of < 14.263. Those with a minDC of > 14.263 had 'poor' modern analogues. Relative sea-level predictions were calculated using Equation 8 and are presented in Table 6.6. Fossil samples with poor modern analogues were not used to calculate sea-level estimates.

The transfer function results produced PMSE estimates for the top 20 samples from core *Sv-CT3-0m*. Below 11 cm no fossil samples had close or good modern analogues. As all 20 sample horizons have been dated directly using ^{210}Pb techniques, all represented suitable SLIPs. These were plotted to show a recent (~100 year) RSL reconstruction for Svinøyosen with the Harstad tide gauge data for comparison. Figure 6.5 shows the foraminifera based transfer function reconstruction implies RSL rise over the last 100 years. This pattern is an artefact of the wide vertical ranges and low diversity of modern salt-marsh foraminifera at Svinøyosen and the process of salt-marsh accretion. The RSL trend shown by the tide-gauge data sits well within the error margins of the reconstruction which is limited by wide PMSE estimations.

Depth down core (m)	Age (cal yrs BP)	Age Error (± yrs)	WAPLS(2) PMSE (m above MSL)	RMSEP (± m)	minDC	Modern analogue fit	RSL (m above MSL)
0.0025*	-60	1	1.200	0.262	0.250	Good	0.168
0.0075*	-59	1	1.200	0.262	0.754	Good	0.162
0.0125*	-58	1	1.199	0.261	1.256	Good	0.159
0.0175*	-57	1	1.198	0.261	1.752	Good	0.155
0.0225*	-55	1	1.197	0.261	2.282	Close	0.150
0.0275*	-51	1	1.197	0.261	2.751	Close	0.145
0.0325*	-50	1	1.193	0.261	3.827	Close	0.145
0.0375*	-49	1	1.197	0.261	3.768	Close	0.136
0.0425*	-47	1	1.193	0.261	4.69242	Close	0.134
0.0475*	-45	2	1.200	0.262	4.75006	Close	0.122
0.0525*	-42	2	1.201	0.263	6.13228	Close	0.116
0.0575*	-39	2	1.199	0.262	5.85577	Close	0.113
0.0625*	-35	3	1.197	0.261	6.258	Close	0.111
0.0675*	-30	4	1.200	0.262	6.76722	Close	0.103
0.0725*	-27	4	1.197	0.261	7.25893	Close	0.101
0.0775*	-20	5	1.201	0.262	7.78285	Close	0.092
0.0825*	-14	6	1.198	0.261	8.25309	Close	0.090
0.0875*	-5	8	1.199	0.262	8.75006	Close	0.084
0.0975*	13	15	1.201	0.262	9.99162	Close	0.072
0.1075*	42	35	1.202	0.263	11.1641	Close	0.061
0.1425			1.200	0.262	14.3025	Poor	-
0.1525			1.202	0.263	15.25	Poor	-
0.1575			1.201	0.263	16.6299	Poor	-
0.1675^	150	50	1.202	0.263	16.75	Poor	-
0.1825			1.201	0.263	18.8874	Poor	-
0.1875			1.202	0.263	18.75	Poor	-
0.1975			1.202	0.263	19.75	Poor	-
0.2075^	575	125	1.202	0.263	20.75	Poor	-
0.2325^	750	100	1.202	0.263	23.25	Poor	-
0.2575^	1075	125	1.197	0.261	25.768	Poor	-
0.2925			1.253	0.412	95.9167	Poor	-
0.3075			1.202	0.263	30.75	Poor	-
0.3425			1.196	0.361	81.0061	Poor	-
0.3575			1.236	0.336	61.837	Poor	-
0.3725‡	2152	152	1.227	0.302	85.5259	Poor	-
0.3925‡	2254	97	1.231	0.317	67.8214	Poor	-
0.4425			0.978	0.275	114.537	Poor	-
0.4675‡	2780	63	1.421	0.647	144.789	Poor	-
0.4925‡	2528	174	2.523	0.561	161.14	Poor	-
0.5375‡	2502	140	2.482	0.568	156.556	Poor	-
0.5525			2.697	0.607	165.862	Poor	-

0.5975			1.933	0.456	127.386	Poor	-
0.6500			2.047	0.462	116.905	Poor	-
0.7000			2.537	0.552	162.12	Poor	-
0.7500			2.525	0.559	185.163	Poor	-
0.8000			1.803	0.441	190.916	Poor	-
0.8500‡	3210	131	1.031	0.359	197.69	Poor	-
0.9000			0.775	0.348	198.771	Poor	-
0.9275			0.694	0.355	212.596	Poor	-
0.9500‡	7381	103	0.647	0.343	208.386	Poor	-
1.0000			0.396	0.281	139.376	Poor	-
1.0500			0.690	0.306	175.513	Poor	-
1.1000‡	5710	127	0.630	0.310	181.344	Poor	-
1.1275‡	6600	132	0.912	0.351	231.591	Poor	-

Table 6.6 Palaeomarsh-surface elevation estimates from fossil foraminifera samples using the WAPLS(2) transfer function and the calculated RSL predictions. Ages derived from ^{210}Pb(*), geochemical markers(^), and radiocarbon dating(‡), are distinguished
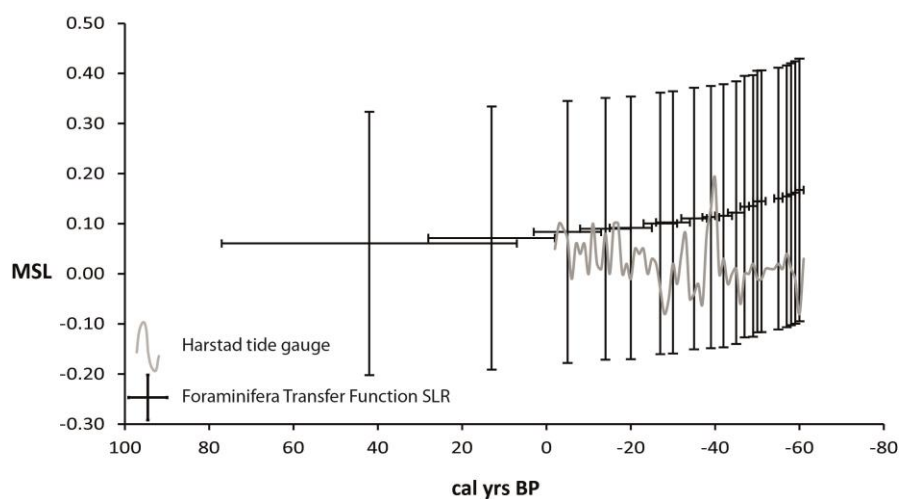
Figure 6.5 The foraminifera transfer function based RSL reconstruction for Svinøyosen with RMSEP transfer function errors (vertical lines) and chronological uncertainties (horizontal lines)

6.3.4 Qualitative assessment

The secondary reconstruction method was developed as a comparison and validation tool for the statistical based modelling described in Section 6.3.3. It is well known that transfer functions developed using foraminifera from lower tidal environments, such as mud flat or estuarine species contain greater uncertainties then those based on salt-marsh species alone and that statistical modelling may underestimate prediction errors (Allen 1990; Horton et al. 2007; Woodroffe 2009; Barlow et al. 2013). In addition, the regressive sequence demonstrated through core *Sv-CT3-0m* contains foraminifera that are indicative of deeper environments than what is covered by the modern training set. For this reason, a qualitative assessment method was also used to reconstruct past sea levels for fossil samples deeper than 11 cm which could not be used with the transfer function approach.

The techniques used in the visual assessment approach largely follow those described by Shennan (2007) and applied by Long et al. (2010). The modern vertical ranges of key foraminifera species (notably *J. macrescens* and *M. fusca*) were used to constrain PMSE estimations of fossil samples. This was done by assigning an indicative meaning (i.e. an elevational range) to different modern foraminifera assemblages (Shennan 2007) and applying these to downcore fossil assemblages. In addition, as per Long et al. (2010), trends in species abundance, test concentration, stratigraphy, LOI and grain size through the core were also considered and used to infer indicative meanings of elevation. For example, the modern distributions of foraminifera fauna, specifically the salt-marsh species *J. macrescens* and *M. fusca*, and the key indicator species *H. germanica*, provide indicative meanings of 1.25 ± 0.2 m above MSL and 0.55 ± 0.35 m above MSL respectively. Table 6.7 shows the indicative meanings assigned to each fossil

assemblage, alongside the chronological constraint for the samples from core *Sv-CT3-0m*.

Depth down core (m)	Sample elevation (m above MSL)	Age cal yrs BP	Age Error (± yrs)	Indicative range (m above MSL)	Reconstructed MSL range (m above MSL)
0.0025	1.3675	-60	1	1.05 - 1.45	0.1175 ± 0.2
0.0075	1.3625	-59	1	1.05 - 1.45	0.1125 ± 0.2
0.0125	1.3575	-58	1	1.05 - 1.45	0.1075 ± 0.2
0.0175	1.3525	-57	1	1.05 - 1.45	0.1025 ± 0.2
0.0225	1.3475	-55	1	1.05 - 1.45	0.0975 ± 0.2
0.0275	1.3425	-51	1	1.05 - 1.45	0.0925 ± 0.2
0.0325	1.3375	-50	1	1.05 - 1.45	0.0875 ± 0.2
0.0375	1.3325	-49	1	1.05 - 1.45	0.0825 ± 0.2
0.0425	1.3275	-47	1	1.05 - 1.45	0.0775 ± 0.2
0.0475	1.3225	-45	2	1.05 - 1.45	0.0725 ± 0.2
0.0525	1.3175	-42	2	1.05 - 1.45	0.0675 ± 0.2
0.0575	1.3125	-39	2	1.05 - 1.45	0.0625 ± 0.2
0.0625	1.3075	-35	3	1.05 - 1.45	0.0575 ± 0.2
0.0675	1.3025	-30	4	1.05 - 1.45	0.0525 ± 0.2
0.0725	1.2975	-27	4	1.05 - 1.45	0.0475 ± 0.2
0.0775	1.2925	-20	5	1.05 - 1.45	0.0425 ± 0.2
0.0825	1.2875	-14	6	1.05 - 1.45	0.0375 ± 0.2
0.0875	1.2825	-5	8	1.05 - 1.45	0.0325 ± 0.2
0.0975	1.2725	13	15	1.05 - 1.45	0.0225 ± 0.2
0.1075	1.2625	42	35	1.05 - 1.45	0.0125 ± 0.2
0.1675	1.2025	150	50	0.45 - 1.5	0.2275 ± 0.525
0.2075	1.1625	575	125	0.45 - 1.5	0.1875 ± 0.525
0.2325	1.1375	750	100	0.45 - 1.5	0.1625 ± 0.525
0.2575	1.1125	1075	125	0.45 - 1.5	0.1375 ± 0.525
0.2750	1.0950	1750	200	0.45 - 1.5	0.12 ± 0.525
0.3725	0.9975	2152	152	0.45 - 1.5	0.0225 ± 0.525
0.3925	0.9775	2254	97	0.45 - 1.5	0.0025 ± 0.525
0.4675	0.9025	2780	63	0.2 - 0.9	0.3525 ± 0.35
0.4925	0.8775	2528	174	0.2 - 0.9	0.3275 ± 0.35
0.5375	0.8325	2502	140	0.2 - 0.9	0.2825 ± 0.35
0.8500	0.5200	3210	131	< -1.7	> 0.52

Table 6.7 Calculations for sea-level index points from core Sv-CT3-0m

The indicative meanings were converted into sea-level predictions using Equation 8. Only samples from horizons that had been directly dated using one of the three chronological techniques were used to create SLIPs. Full indicative ranges were not available below 67 cm (Table 6.7) and only a minimum PMSE value could be estimated (i.e. subtidal). For this reason only SLIPs younger than 3300 cal yrs BP have been plotted to provide a late Holocene RSL reconstruction (Figure 6.6). SLIPs that are derived from samples that may be suffering from the effects of dissolution have been highlighted using dashed vertical error bars.
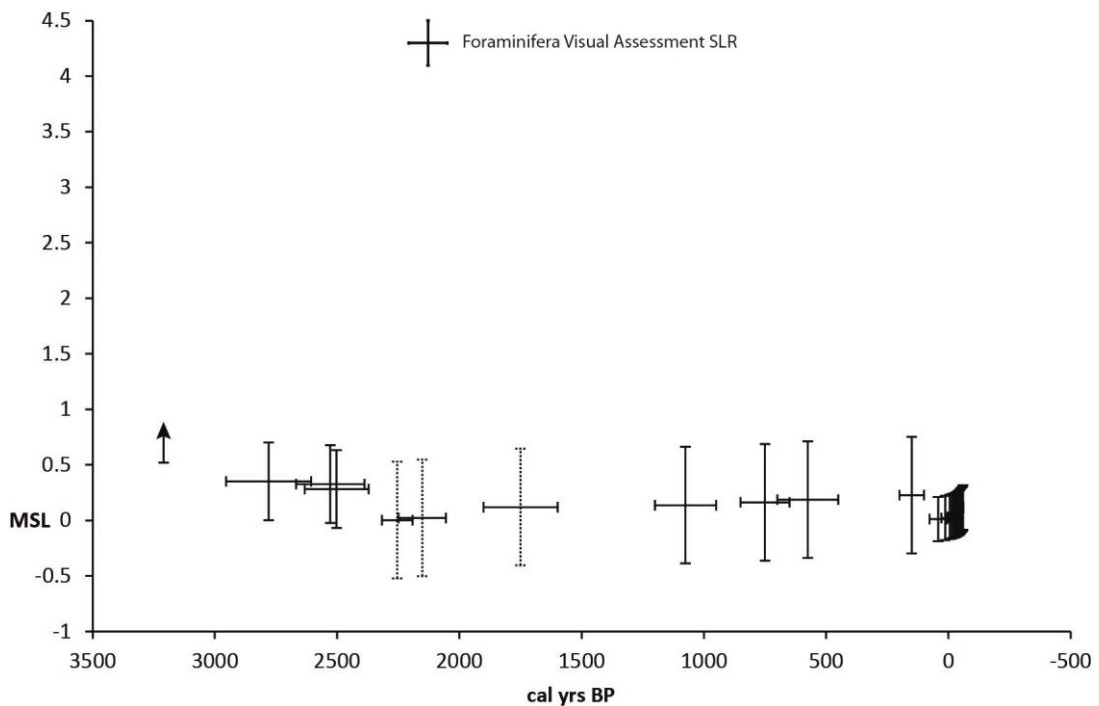
Figure 6.6 The foraminifera qualitative assessment based RSL reconstruction for Svinøyosen with indicative ranges as errors (vertical lines) and chronological uncertainties (horizontal lines)

The visual assessment reconstruction shows a gentle pace of RSL fall throughout the late Holocene. A minimum water depth of ~0.5 m above MSL has been inferred at around 3200 cal yrs BP from the subtidal foraminifera assemblages in core *Sv-CT3-0m*. The qualitative assessment method is vital for extending the RSL reconstruction further back into the Holocene. However, the indicative ranges of the top samples from core *Sv-CT3-0m* can be improved upon by substituting in the better constrained recent testate amoebae reconstruction for the last 100 years or so. For this reason, a final composite RSL curve was produced combining the visual assessment method with the testate amoebae based transfer function from Section 6.1. The testate amoebae based curve covers the time period 12 to -61 cal yrs BP, and the visual assessment curve covers from ~3200 to 13 cal yrs BP (Figure 6.7). This composite curve represents the first attempt at producing a late Holocene RSL reconstruction from the Lofoten – Vesterålen archipelago, using multiple SLIPs from a continuous stratigraphy of sediments.

The reconstruction suggests that late Holocene sea levels may have been falling at a rate of ~ 0.5 mm yr^{-1}. It is hard to derive absolute rates considering the wide vertical ranges implied from some of the SLIPs. The rate of fall appears to be greatest before ~2000 cal yrs BP. The youngest part of the reconstruction largely corresponds with the tide-gauge data as was seen earlier in Section 6.2. The observational data records the current rate of sea-level fall at around -1 mm yr^{-1}.
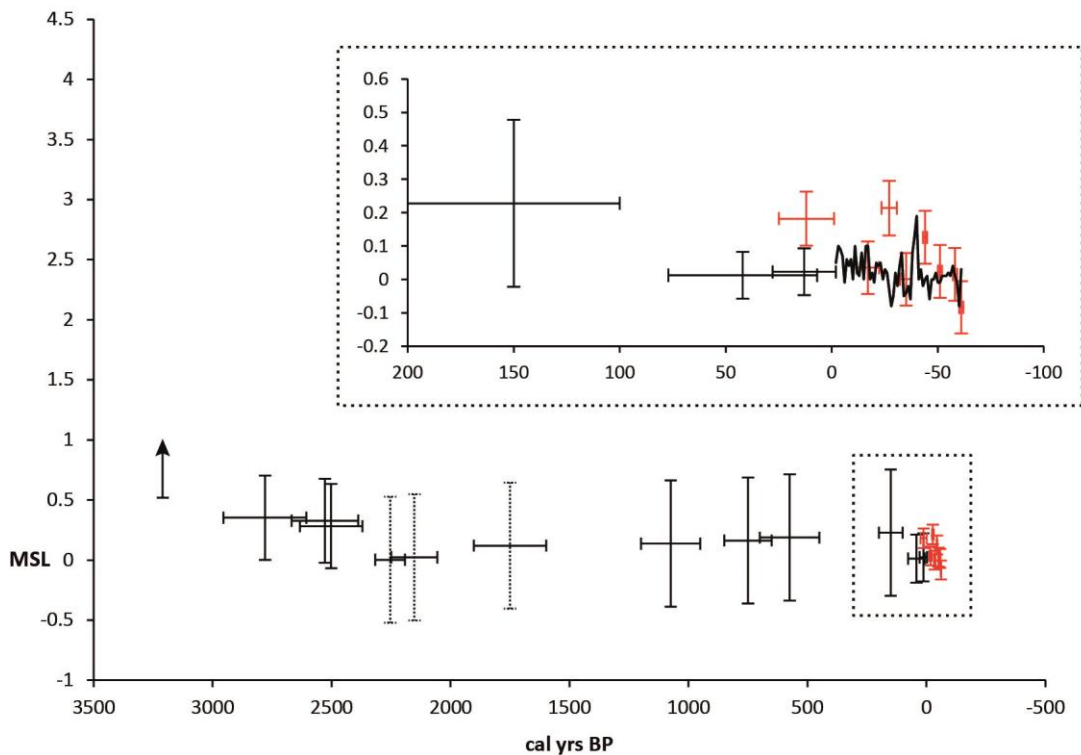
Figure 6.7 The composite late Holocene RSL curve for Svinøyosen. The inset shows the reconstruction for the last ~200 years and distinguishes between the testate amoebae transfer function (red crosses) and the foraminifera based visual assessment (black crosses). The Harstad tide gauge data is shown as a solid black line

6.4 Summary

Presented within this chapter were results from using testate amoebae and foraminifera to reconstruct past RSL histories. Through the use of ordination it was shown that surface assemblage patterns of salt-marsh testate amoebae are intrinsically related to elevation. Elevation can account for over 58% of the variation in surface testate amoebae assemblages. Through the use of regression modelling it was shown that a statistical transfer function based on salt-marsh testate amoebae alone was able to

reconstruct past sea-levels with accuracies of up to ± 8.5 cm. A transfer function based on surface testate amoebae from Svinøyosen was applied to down core fossilised assemblages to reconstruct palaeomarsh-surface elevations for approximately the last 80 years. The resulting RSL curve showed agreement in terms of magnitude and trend with the nearby comparable tide-gauge record from Harstad.

Due to the low presence of testate amoebae within the sediments, foraminifera were used to extend a RSL reconstruction further back into the Holocene. Ordination techniques demonstrated that elevation could account for up to 58% of assemblage variation of surface foraminifera from Svinøyosen and Storosen. Regression modelling of the foraminifera training set was able to predict salt-marsh surface elevations to precisions of up to ±0.27 m. This transfer function was applied to fossilised assemblages from the last 100 years to reconstruct palaeomarsh-surface elevations and relative sea levels. Due to lack of close modern analogues, this transfer function was not applicable to samples older than 42 cal yrs BP. A qualitative assessment method was used to extend the RSL curve further back into the Holocene. The reconstruction used SLIPs that were constrained chronologically by either ^{210}Pb ages, geochemical markers or ^{14}C dates. The resultant RSL curve demonstrated a late Holocene sea-level fall at Svinøyosen at rates approximately equal to -0.5 mm yr^{-1} for the last ~3000 years. Beyond ~3000 cal yrs BP only a minimum sea-level estimate could be predicted. This method was combined with the testate amoebae based RSL curve to provide a late Holocene sea-level reconstruction for this region. The results from this study are compared with existing RSL data in the following chapter.

CHAPTER 7 - Discussion

7.1 Introduction

This thesis has focussed on the analysis and development of using salt-marsh testate amoebae as sea-level indicators. In addition to this, a late Holocene reconstruction for northern Norway has been produced, which represents the first continuous record of recent sea-level change for the region. Developments in the methodologies associated with salt-marsh testate amoebae are discussed below, with particular reference to existing preparation and counting techniques. Caveats associated with the techniques are also presented. The suitability of testate amoebae for sea-level studies is demonstrated and their predictive power is compared with alternative proxies. The foraminifera based reconstruction is compared with existing sea-level studies from northern Norway and its value as a novel piece of work is appraised. Following this, the reconstruction is critically considered and thought is given to the validation attempts, and true errors, associated with the work. Final comments cover potential improvements to this study, future use of testate amoebae as a sea-level proxy, and how and where future RSL studies of Norway should be carried out.

7.2 Salt-marsh testate amoebae

This study represents the first investigation into preparation techniques and count total requirements of salt-marsh testate amoebae for sea-level studies. Peatland studies have often provided the methodologies used in salt-marsh testate amoebae work. Here are discussed the different methods used in the preparation and analysis of this group of microorganisms and their potential as sea-level indicators.

7.2.1 Developments in preparation and analysis: count totals

The question of how many tests to count per ecological sample is an important one for every microfossil proxy. Existing studies have investigated the number of testate amoeba individuals required to represent a given community. The point at which taxon diversity plateaus whilst increasing the count total is often used as an indicator of the required number of tests being reached. Warner (1990) estimated that this plateau was reached at around 60 individuals, Mitchell et al. (2000) and Woodland et al. (1998) both identified a plateau once reaching 100 individuals. Using these studies as a guide, palaeoecological studies could easily justify using a count total of 100 tests to represent sample communities. Depending on the purpose of the research, it may be necessary to increase the count total beyond 100 tests in order to capture subtle yet important changes in community composition or improve percentage accuracies in assemblage counts (Payne & Mitchell 2009).

All existing investigations on optimising count totals stem from peatland research. Sea-level studies using salt-marsh testate amoebae often base their required count total on these results (Gehrels et al. 2006a; Ooms et al. 2012). In other cases (Gehrels et al. 2001; Charman et al. 2002; Ooms et al. 2011) an intuitively derived count total of 150 tests is used. Where the purpose of investigation is based around palaeoenvironmental interpretation and not on detailed, full ecological community identifications, counting over 100 individuals may not be necessary (Payne & Mitchell 2009). Due to the laborious nature of testate amoebae analysis it may be prudent to make time gains by counting 100 individuals per sample instead of, say, 150. The time saved may permit the inclusion of more samples in a transfer function or allow a higher resolution set of fossil counts to be produced.

This research represents the first count total analyses for salt-marsh testate amoebae. In addition to this, the comparative statistics used in the methodology represents a novel way of comparing the effects of differing count totals on community composition. By comparing the community diversities seen at Storosen using the BCI statistics it was clear that there was little statistical difference between assemblages composed of 100 tests or 150 tests. This research independently verifies the use of count totals based on 100 individuals for communities of salt-marsh testate amoebae. The results are in accordance with the published literature based on peatland testate amoebae.

7.2.2 Developments in preparation and analysis: preparation procedures

Almost all salt-marsh testate amoebae studies have employed the use of a water-based soaking method in order to prepare surface samples for analysis (Charman et al. 1998, 2002; Gehrels et al. 2001, 2006a; Ooms et al. 2011). Testate amoebae prepared using more destructive methods, such as those used in palynology, can lead to loss of tests and assemblage bias, although total concentrations may be higher due to more effective sample disaggregation (Hendon and Charman 1997; Payne et al. 2012). A water-based technique will ensure the survival of individual tests, but may be insufficient to disaggregate fibrous salt-marsh peat. This leads to three problems. First, if tests remain attached to conglomerate organic particles they may not pass through the larger sieve. Second, they could be concealed by debris and be missed. Third, due to crowding of clumped sediment particles on the microscope slide, the time required for counting will increase significantly.

Charman et al. (2010) used a weak alkali treatment of 5% KOH in the preparation of testate amoebae that did not lead to the significant loss of tests. In this study, preparation A is largely based on the water soaking method for peat samples outlined in Charman et al. (2000). Preparation B is largely based on the techniques used in Charman et al. (2010) including a mild alkali to aid disaggregation, and preparation C is a development of this method using a smaller upper sieve size to remove larger non-testate particles. Apparently low concentrations of testate amoebae from technique A suggest that not all individuals were counted, possibly because of slides being crowded with organic conglomerate particles and a dense matrix of small inorganic particles. The average length of time required to reach a count total of 100 was approximately 13 hours, and the longest time spent on one sample was 22 hours. In comparison, the

samples prepared using methods B and C took a lot less time to count, the shortest time taken to reach 100 tests being 15 minutes. The high Chao's Sørensen abundance-based similarity index-scores indicate that assemblages produced using the different preparation procedures are actually very similar. Minor dissimilarities between the populations are likely to have been driven by the effects of unseen rare species. So, for the purposes of palaeoenvironmental research, where a full complement of taxa is not required, there are time gains to be made from using a weak alkali treatment with potentially very little loss of information from the destruction of tests.

In this study the testate amoebae samples were stained with rose Bengal in order to differentiate between live and dead tests. A comparison was performed on the two populations (live and dead) following preparation A. No such comparisons were performed following preparations B and C. It was noted that after applying a KOH treatment to the samples there were very few stained testate amoebae tests compared to the equivalent samples from preparation A. This suggests that such a chemical treatment may have led to the bleaching of the rose Bengal stain from live protoplasm. Charman & Hendon (1997) and Booth et al. (2010) suggest staining the sample after the preparation treatment, immediately prior to mounting on a glass slide. This could possibly overcome the issue, providing that the boiling and chemical treatments do not destroy the live protoplasm. Alternatively, Booth et al. (2010) suggest that surface sample counts should include both live and dead populations as both would ultimately end up in the fossil record.

An improved testate amoebae preparation technique

Preparation C was devised for two reasons. First, sieving prior to the alkali treatment in method B may have led to the loss of tests that were encompassed within organic conglomerate particles greater than 300 μm in size. Second, throughout the entire counting process no testate amoebae greater than 160 μm in size were encountered. Therefore, in order to reduce crowding on microscope slides further, a smaller upper mesh sieve of 212 μm was used following the alkali disaggregation. Samples prepared using this method, as a whole, had the shortest count times. However, the use of a sieve smaller than 300 μm is only advised if it is known that there will be no larger taxa present in the samples, checks of the residue retained in the sieve is advisable, yet this may negate time saved using this method. Statistically there was little or no loss of taxa information by applying this preparation method rather than a water-based soaking method.

7.2.3 Salt-marsh testate amoebae distributions

The combined surface datasets from Svinøyosen and Storosen identify some key testate amoebae taxa that appear to inhabit preferentially different areas of the salt-marshes. *Centropyxis* types are common across the marsh and often dominate the assemblages. *C. cassis* type and *C. ecornis* are both common taxa above MHWS, but phase out below this tidal level. Inversely, *D. pristis* type and the taxon named *C. platystoma* morphotype 1 become more relatively abundant below the level of MHWS. The highest sampled areas of the marsh contained a rich diversity of testate amoebae, including numerous taxa of the genus *Euglypha* and *Nebela*. These respective taxa were evident below HAT, however never reached the level of MHWS. The two taxa *T. dentata* and *H.*

ovalis were also key taxa that zoned in accordance with elevation. The clear, elevation dependant, zonation of taxa across the marsh surface identifies testate amoebae as excellent potential sea-level indicators. In addition to this, the surface data presented in this thesis show some remarkable similarities with existing publications of salt-marsh testate amoebae.

To date, salt-marsh surface testate amoebae data are available from three sites within the UK (Charman et al. 1998; Gehrels et al. 2001; Charman et al. 2002), three sites from the North American east coast (Gehrels et al. 2006a), the Scheldt estuary in Belgium (Ooms et al. 2011;Ooms et al. 2012) and one site from the west coast of Iceland (Haynes 2011). The UK datasets identified diverse faunas at the higher elevations of the salt-marshes where several *Difflugia* and *Euglypha* taxa were present. *C. cassis* type and *T. dentata* were both important taxa which occurred lower down the marshes but were not necessarily the most submergent resistant taxa (Gehrels et al. 2001). Dominant taxa at the lowest elevations included *C. platystoma* type, the closest comparable to the low marsh taxon (*C. platystoma* morphotype 1) from this study. The most common lowest marsh taxa associated with the North American datasets were *C. platystoma* type and *D. pristis* type (Gehrels et al. 2006a). The similarities with the Norwegian datasets extend further up the marshes, *C. cassis* type dominated the assemblages with increasing elevation and at the highest sampled elevations numerous *Euglypha* taxa, *T. dentata* and *C. arcelloides* type contributed significantly to the diverse assemblages. The lowest testate amoebae taxa from the Belgium datasets included significant numbers of *D. pristis* type and *Cyphoderia ampulla.* The latter taxon was not encountered in the Norwegian surface data, however was identified as a key low elevation taxon by Charman et al. (2002) in the UK datasets. The Belgian surface assemblages increased

rapidly in diversity with increasing elevation above their lowest testate amoebae zones. Similar taxa to other North Atlantic sites were again shown to have strong relationships with surface elevations (e.g. *T. dentata*). The surface data from Iceland is similar to the zonation shown by salt-marsh testate amoebae described above. *C. ampulla* and *D. pristis* type were common in the lowest samples. *C. cassis* type was highly abundant above these elevations and the highest samples contained diverse assemblages containing *Euglypha* and *Nebela* taxa and significant numbers of *T. dentata.*
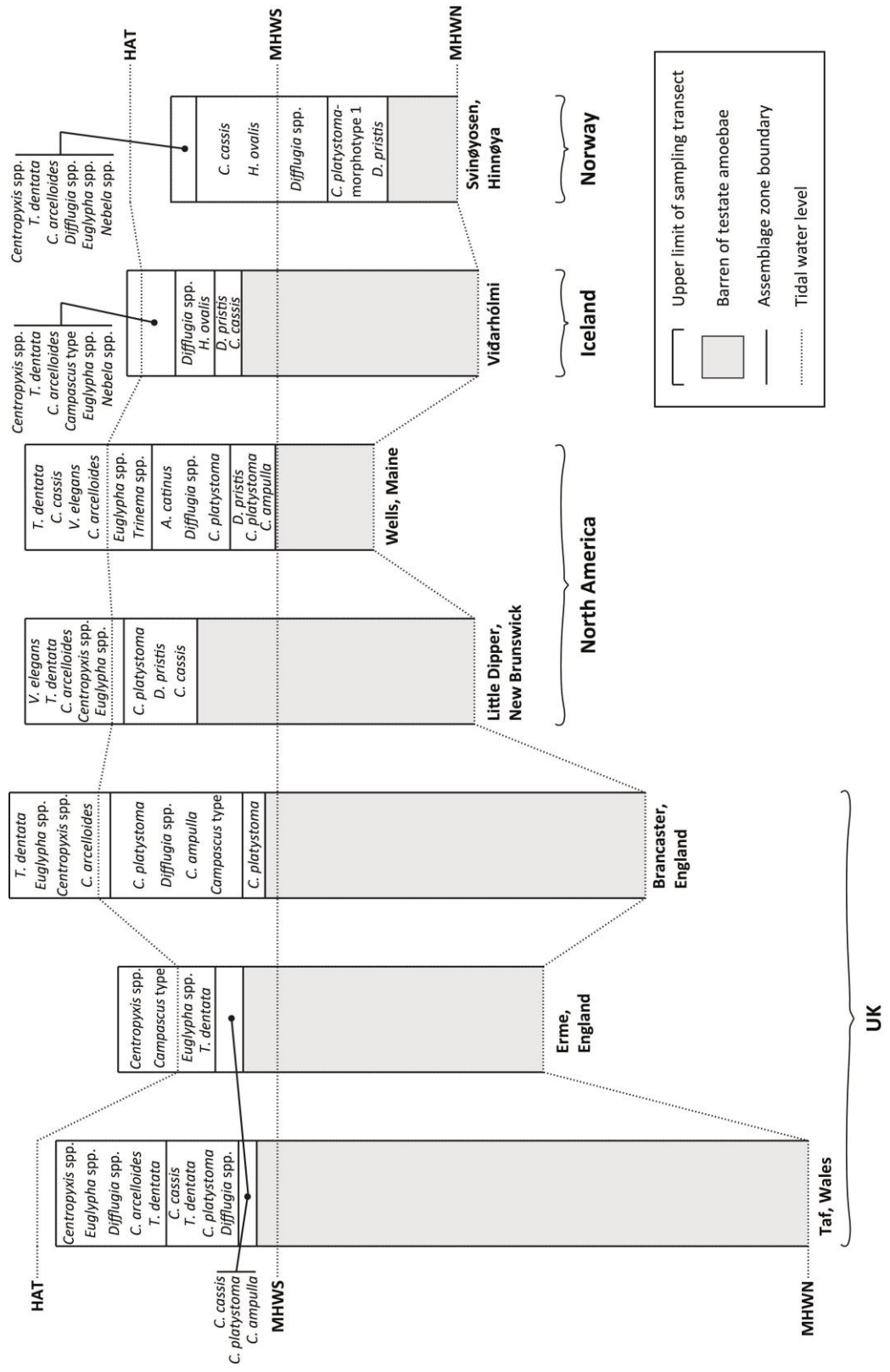
Figure 7.1 The surface sampling ranges and key associated testate amoeba taxa for datasets from the UK, North America, Iceland and Norway alongside relative tidal water levels

The studies from North America, UK, and Iceland record the lower limits of salt-marsh testate amoebae occurring at some point between MHWS and HAT. The Norwegian dataset demonstrates this lower limit occurs at a point between MHWS and MHWN. This significant finding suggests that testate amoebae may be combined more readily in conjunction with foraminifera for palaeoreconstruction purposes. The relationship between this lower limit and the tidal range at each site is presented in Figure 7.1. Importantly zoned and common taxa have also been identified. The different study areas demonstrate similar taxa occurrence and zonation, and even similar lowest habitual elevations relative to tidal range. An unconstrained ordination analysis of the datasets (canonical correspondence analysis) further demonstrates similarities between the surface training sets (Figure 7.2). The majority of the samples from the different sites are situated close together, predominantly ranging along axis 1. The primary separation is seen in the lower samples from Erme, UK, which contain a high number of *C. ampulla*, a taxon which is not always encountered in the other datasets, and in the middle samples from South Hinnøya, Norway, containing significant numbers of *H. ovalis*, which is only also encountered in Iceland. The separation of *C. platystoma* morphotype 1 from *C. platystoma* in this study also contributes to the separation seen in the Norwegian samples in Figure 7.2.

These similarities suggest that a universal training set of surface data may be applicable to fossil data sets from different locations across the North Atlantic. Charman et al. (2010) demonstrated how training sets of surface testate amoebae data from the UK were able to predict known elevations of surface samples from North America, and be used to produce reliable sea-level reconstructions from North American salt-marsh cores. A universal training set applicable to the whole North Atlantic would reduce the

time and costs of salt marsh based sea-level reconstruction work, allowing for higher sampling and spatial resolution study of fossil cores. Additional statistically based comparisons of the existing surface datasets are needed alongside further reconstruction attempts before a universal North Atlantic training set is contemplated.
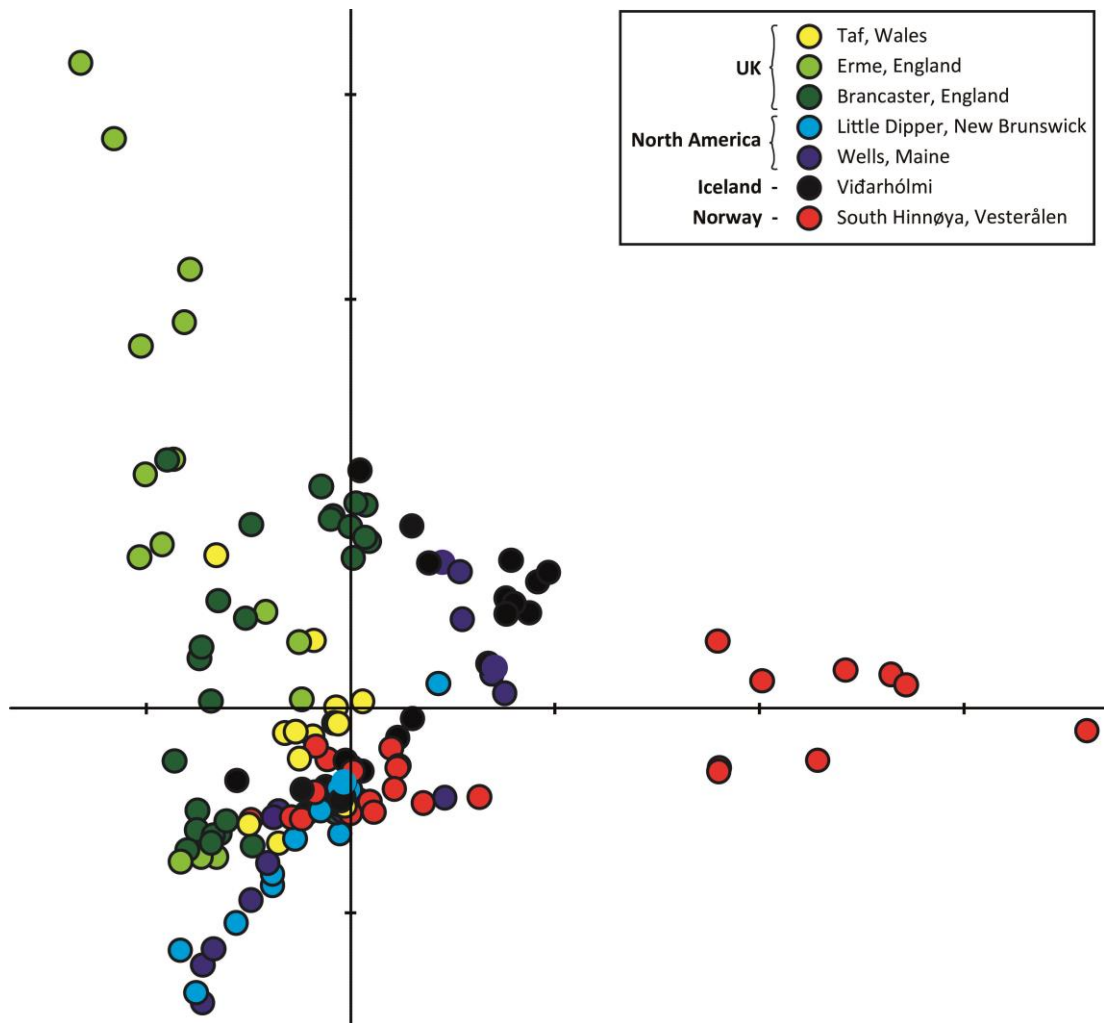
Figure 7.2 Canonical correspondence analysis of the surface samples from the UK, North America, Iceland and Norway

7.2.4 Testate amoebae as sea-level indicators

A number of the testate amoebae studies mentioned above have quantified the predictive power of the surface data sets using transfer functions. Gehrels et al. (2001) demonstrated that testate amoebae were able to predict surface elevations with errors as low as ±0.08 m. These precisions were further improved upon by using a multiproxy approach and incorporating diatom and foraminifera surface data. However, the benefits of using multiple microfossil proxies were deemed disproportionate to the additional time required for the analyses. The North American datasets were capable of similar precisions and could predict elevations to within ±0.07 m (Gehrels et al. 2006a). This study has demonstrated accuracies of ±0.085 m, and the Belgian surface datasets improved on these further (±0.05 m; Ooms et al. 2011). The consistently low errors shown by these studies suggest that testate amoebae may represent a more reliable approach than alternative proxies to reconstructing palaeomarsh-surface elevations from upper salt-marsh facies.

The first sea-level reconstruction using a transfer function based on salt-marsh testate amoebae and applied to fossil assemblages was attempted by Charman et al. (2010). This study was able to obtain reasonable numbers of fossil testate amoebae (>50 tests) down to depths of 19 and 29 cm in two North American salt-marsh cores. The samples represented approximately 100 years of salt-marsh accumulation, and the resultant reconstructions agreed well with nearby tide-gauge records, with good cross-validation precision delivered by the transfer functions (±0.05 and ±0.11 m). This study reports a similar success of producing a recent (~100 year) reconstruction that approximately corresponds with a comparable tide-gauge record in terms of both trend and magnitude. Reconstructions from both studies were hampered by the lack of abundant fossil testate

amoebae below a certain depth. For Norway, this is likely due to the falling relative sea-level trend, producing a regressive sequence. Core sediments from before 1930 AD represent environments too low in the intertidal realm to support populations of testate amoebae. The absence of testate amoebae from the North American cores is less clear and is partially attributed to suboptimal core locations as cores were selected for foraminiferal reconstruction purposes. This raises a question on the preservation potential of fossil testate amoebae. A sea-level indicating proxy with good accuracies is only useful if fossil assemblages can be reliably analysed. In addition to this, salt marsh based sea-level studies must determine their proxy of choice prior to fieldwork as the location of the sediment core in relation to the marsh surface appears paramount (Charman et al. 2010).

A sea-level reconstruction using testate amoebae was also performed by Steffie Haynes (Plymouth University, UK) as part of a Master's thesis (Haynes 2011). The results indicated that the preservation potential of fossil testate amoebae may be more reliable than previously thought. The Iceland study built on the work by Gehrels et al. (2006b) produced a local testate amoebae training set and recovered fossil testate amoebae from between the depths of 45 and 60 cm down core. These samples represented ages between 720 and 340 cal yrs BP and were used to reconstruct sea levels for this period. Comparable reconstructions using diatoms suggested the testate amoebae reconstruction was reliable, and the author noted that the preservation of the tests was good, despite their age. These findings strongly support the notion that the choice of core location is imperative if an extended sea-level reconstruction based on testate amoebae alone is desired. Cores from higher marsh areas will contain more diverse assemblages of testate

amoebae than from middle or lower marsh regions, and are likely to contain longer records of preserved tests.

7.3 Examination of the late Holocene reconstruction

This section critically appraises the late Holocene sea-level reconstruction. Consideration is given to the inclusion of agglutinated and calcareous foraminifera within surface data training sets. Comparisons are made between Norwegian salt-marsh foraminifera, and other comparable data sets from around the globe. Numerous attempts have been made at validating the reconstructions throughout this thesis and comments are made regarding these attempts. This section also includes discussion on the true vertical uncertainties associated with the techniques employed throughout the study and highlights additional sources of error that have not been fully quantified.

7.3.1 Norwegian salt-marsh foraminifera

The notion that salt-marsh foraminifera were useful indicators of sea level was devised from the observation that a variety of agglutinated foraminifera zoned according to a vertical distribution (Scott & Medioli 1980). Since then, the more successful sea-level reconstructions have been developed from transfer functions constructed of a reasonable number of agglutinated surface foraminifera. In Nova Scotia, Gehrels et al. (2005) were able to predict salt-marsh elevations to within ±0.06 m. Their modern surface

foraminifera training set included eight species of agglutinated forms. In New Zealand, Southall et al. (2006) and Gehrels et al. (2008) successfully reconstructed sea-levels using a transfer function with predictions errors of ±0.05 m. Their training set included five agglutinated foraminifera taxa. The reconstruction by Kemp et al. (2009a,b) for North Carolina contained ten agglutinated forms and had errors of ±0.05 m. The recent Tasmania reconstruction (Callard et al. 2012, Gehrels et al. 2012) used six agglutinated forms and had errors of ±0.10 m. Sea-level reconstructions with low prediction errors rely on a reasonable distribution of agglutinated salt-marsh foraminifera which are sensitive to the effects of inundation.

Contemporary agglutinated salt-marsh foraminifera from the Norwegian salt-marshes were restricted to two taxa, *J. macrescens* and *M. fusca*. In one of the marshes (Storosen) it appeared that there was a small band of upper marsh where only *J. macrescens* occurred, and that elevations were too high for the existence of *M. fusca*. Conversely, at Svinøyosen, it appeared that the two taxa inhabited the same elevations of the marsh, albeit in different proportions. The relative abundance of *M. fusca* was consistently around 10 to 20% of the total assemblages, therefore, using a ratio of the two species was not a suitable method of determining surface elevations. The low diversity of agglutinated foraminifera is likely responsible for the large prediction errors associated with both methods of assigning indicative meanings. Below the elevation of vegetation zone 1, the diversity of total foraminifera increased through the introduction of numerous calcareous species. As previously mentioned, despite the abundance and diversity of such species, these are of limited value when constructing training sets as their habitual ranges can be vast in comparison to the indicative ranges of salt-marsh agglutinated foraminifera (Horton et al. 2007; Woodroffe 2009).

7.3.2 Validation efforts

Attempts should always be made at validating sea-level reconstructions in order to strengthen their reliability (Barlow et al. 2013). Both reconstructions from Svinøyosen (testate amoebae based and foraminifera based) underwent validation using independent RSL data, comparisons of measured versus reconstructed core top elevations and analysis of the closeness of modern analogues to fossil samples.

The testate amoebae reconstruction was able to predict trends of falling RSL which matched nearby tide gauge data fairly well. This success can be attributed to the narrow vertical zonation shown by this group of microorganisms. Slight changes in fossil assemblages were correctly identified and assigned appropriate indicative meanings by the transfer function. The recent (~100 year) foraminifera reconstruction was constructed from just two taxa in the fossil record which provided a uniform indicative range for each fossil sample. As the downcore fossil samples became lower relative to MSL (evidently indicating salt-marsh accretion) it therefore appeared that recent RSL had been rising. In reality, the fossil samples represented different elevations along the salt-marsh gradient, but due to the lack of diversity, these subtle changes were not identified. In this instance, the additional testate amoebae taxa would indicate that at these Arctic locations, this would be the proxy of choice over foraminifera for a detailed and accurate RSL reconstruction.

Confidence in reconstructions can be improved upon if the transfer function accurately predicts the elevation of the top core sample to coincide with the surveyed elevation of the core (Barlow et al. 2013). In the case of the testate amoebae reconstruction, the

surveyed elevation of the core top (1.47 ± 0.018 m above MSL) was encompassed within the error margins of the predicted elevation of the top sample (1.55 ± 0.079 m above MSL). Regarding the foraminifera regression modelled reconstruction, the top sample provided a predicted elevation of 1.20 ± 0.262 m above MSL, which encompassed the surveyed elevation of the core top (1.37 ± 0.015 m above MSL). The resulting sea-level reconstruction almost over predicts modern sea-level depths. This is once again likely due to the large indicative range shown by the two salt-marsh species of foraminifera, thereby making the true elevation of a salt-marsh core from Svinøyosen hard to predict accurately with low errors using foraminifera.

An analysis of the resemblance of fossil assemblages to their contemporary counterparts will help determine the reliability of a reconstruction. Fossil samples which contain different communities of microorganisms to the modern samples which are used to construct a transfer function are unlikely to be able to predict palaeomarsh-surface elevations accurately. By establishing a minimum dissimilarity coefficient (minDC) through use of the MAT, similarities between fossil and closest analogue modern samples can be quantified (Simpson 2007). Woodroffe (2009) used a cut off minDC value of > 20th percentile as an indicator of samples with a poor closest modern analogue. The reconstructions from Svinøyosen used a more strict assessment of minDC values in following the methods of Watcham et al. (2013), as outlined in the text. Again, the testate amoebae transfer function performed better than the foraminifera reconstruction and all fossil samples contained good or close fits with their closest modern analogues. Fossil samples from the top 11 cm of the foraminifera reconstruction contained good or close fits with their closest modern analogues. These samples all contained numbers of *J. macrescens* and *M. fusca*. Below this depth all fits were poor.

This may be caused by the dominance of *C.lobatulus* in the modern training set below ~ 0.9 m above MSL. Evidently, using the MAT technique to determine minDC values for fossil samples cannot improve a reconstruction in terms of accuracies, however this validation method does lend some weight towards the credibility of the reconstruction, and perhaps this information should become increasingly included in future salt-marsh sea-level publications.

7.3.3 Compaction

Compaction of salt-marsh sediments can have significant impacts on sea-level reconstructions. In the severest case, lowering of the elevation of subsurface sediments may cause exaggeration of an interpreted RSL rise, or even make a regressive sequence appear transgressive (Mörner 2010). A complication of calculating the compressibility of salt-marsh sediments is the wide range of different grain sizes and organic carbon content encountered across marsh surfaces (Brain et al. 2011). Brain et al. (2012) demonstrated how the effects of compaction, determined primarily through organic productivity and desiccation processes, could have influenced existing sea-level reconstructions. They advise that through monitoring bulk density and organic content through a core, as was performed here, the effects of compaction can be estimated. Where bulk density reaches a constant value in a core and sediments are dominated by sands and silts, compaction is occasionally assumed to be zero (e.g. Gehrels et al. 2012). Brain et al. (2012) suggest that these assumptions may be too easily made, and that other factors, such as the compressibility of underlying layers, ought to be considered.

Compaction was not accounted for in either the testate amoebae based or foraminifera based reconstruction. The former reconstruction was derived from the top 8 cm of core *Sv-CT3-15m* which had a uniform lithology (a semi-elastic salt-marsh peat) and a uniformly low bulk density. It is unlikely, therefore, that this reconstruction has been significantly affected by compaction. The foraminiferal reconstruction from core *Sv-CT3-0m* had a different lithology and bulk density profile to the shorter core. Between 0 and 16 cm the amount of organic carbon varied and bulk density increased steadily with depth down core, suggesting layers between these depths may have undergone compression. Beyond 16 cm the sediments were minerogenic, rich in sand and virtually devoid in organic carbon, and thus less likely to have been compacted. Bird et al. (2004) suggest a correction for compaction based on the assumption that bulk density is intrinsically related to organic carbon and grain size, and is a reasonable proxy for compaction. An uncompacted reference sample with similar grain size and organic carbon properties to compacted samples can be used to resize the width of compacted layers using bulk density as the common variable (Equation 9). This correction was applied to the top 16 cm of core *Sv-CT3-0m* to investigate the potential impacts of sediment compaction. The sample from 1.75 cm depth (bulk density = 0.4374) was used as the reference uncompacted sample as this had similar organic carbon and grain size properties to the samples below.

Equation 9 (Bird et al. 2004):

$$L_{sample} = 0.5 + \left(\frac{\rho_{sample} - \rho_{reference}}{\rho_{sample}} \right)$$

L_{sample} – original vertical length of sample
ρ_{sample} – bulk density of sample
ρ_{sample} – bulk density of reference

The calculation suggests that up to 10.6 cm of compaction may have occurred in in the top of core *Sv-CT3-0m* (Table 7.1). If applied, these compaction corrections would serve to increase sea-level height predictions from ~1900 AD onwards (Table 7.1). In comparison to the tide-gauge data, the recent foraminifera transfer function based sea-level reconstruction already overestimates sea-level heights for the last ~100 years meaning there is little to be gained from including these corrections. The work by Brain et al. (2011, 2012) would suggest the assumptions made by Bird et al. (2004) may be too crude to predict accurately the effects of sediment compaction. Indeed, core *Sv-CT3-0m* represents a short, minerogenic, regressive sequence which is therefore least at risk of compaction. Brain et al. (2012) identify that long (> 1 m), peat rich cores related to transgressive sequences are most at risk of these effects. It is unlikely that 10.6 cm of compaction has taken place over the top 16 cm of core *Sv-CT3-0m*, nevertheless it is important to consider the potential impacts of sediment compaction in these type of sea-level studies.

Depth	True thickness	Compaction	Cumulative compaction
1.75	0.50	0.00	
2.25	0.98	0.48	0.48
2.75	0.80	0.30	0.78
3.25	0.78	0.28	1.06
3.75	0.82	0.32	1.38
4.25	0.84	0.34	1.73
4.75	0.58	0.08	1.81
5.25	0.69	0.19	2.01
5.75	0.58	0.08	2.09
6.25	0.81	0.31	2.40
6.75	0.57	0.07	2.47
7.25	0.92	0.42	2.89
7.75	0.70	0.20	3.09
8.25	0.82	0.32	3.41
8.75	0.73	0.23	3.64
9.25	1.02	0.52	4.17
9.75	0.97	0.47	4.64
10.25	0.94	0.44	5.07
10.75	1.05	0.55	5.62
11.25	0.99	0.49	6.11
11.75	1.04	0.54	6.64
12.25	1.06	0.56	7.20
12.75	1.05	0.55	7.75
13.25	1.13	0.63	8.38
13.75	1.08	0.58	8.96
14.25	0.98	0.48	9.44
14.75	1.14	0.64	10.08
15.25	1.06	0.56	10.64

Table 7.1 Compaction estimates calculated used Bird et al. 2004. All values in cm

7.3.4 Errors

Following the methods used to estimate a composite error term, the total vertical uncertainties associated with the regression modelled foraminifera based sea-level reconstruction came to ± 0.276 m. Total vertical uncertainties for the reconstruction

based on the visual assessment method range from ±0.09 ± 1.05 m depending on the size of the indicative range of the fossil samples. For the case of the testate amoeba reconstruction, total vertical uncertainties came to ±0.10 m.

A number of error factors remain unaccounted for with the above approximation. Although sediment compaction has been estimated, there is an unquantified error term within this calculation. Total core compaction may have been over or underrepresented and no error range has been devised to account for this uncertainty. The survey error associated with the core top elevation has been accounted for. However, vertical survey errors associated with each surface sample have not been taken into consideration as it is likely to be very small. Finally, although an error estimation for the extrapolation of the tidal regime at Svinøyosen has been performed, there is no indication of how the tidal regime of the field site has changed through time. Changing sea levels, climate oscillation patterns, ocean current strengths and changing coastal morphology influence tidal range and it is likely that this has changed at Svinøyosen during the Holocene.

The vertical errors described above account for sea-level height uncertainties. Calibration errors for dates derived from ^{210}Pb and ^{14}C chronologies are given as 2 sigma errors. The uncertainties associated with the geochemical chronology are more subjective. Therefore, attempts were made to incorporate the age error term into the date range of each chronological event. The limitations with this method are understood, yet it was decided that this method provided a reasonable chronology for an otherwise updateable sequence. Only SLIPs derived from a directly dated horizon were included in the sea-level reconstructions. It is possible to produce an age-depth model from the

available dates that could interpolate ages in between these horizons. These methods would have introduced greater uncertainties into the project which are best avoided if possible (Gehrels & Woodworth 2013).

7.4 Holocene sea-level change in north-western Norway

Relative sea-level studies of the Vesterålen – Lofoten region are complicated by the dynamic uplift history of the area since deglaciation. There is a strong uplift gradient running perpendicular to the approximate shoreline direction (e.g. Ekman 1996) which causes significant variability between local RSL curves. The Tapes sea-level maximum produced mid Holocene shoreline limits which could be mapped throughout the archipelago and followed further north into Finnmark (Marthinussen 1962). By connecting locations of similar shoreline limits, isobases for the Tapes maximum could be drawn and used to identify locations of similar and comparable relative sea-level histories (Figure 7.3b; Møller 1987). Subsequent studies of RSL history have naturally been focussed between the 0 and 10 m Tapes isobases in the outer islands of the archipelago (e.g. Andøya and Vastvågøy) where palaeosea-level evidence is more abundant (Figure 7.3c, d, e; Møller 1984, 1986; Vorren & Moe 1986; Balascio et al. 2010). These studies also tend to focus their attention around the early and mid Holocene, specifically at the sea-level minimum prior to the Tapes transgression and at the Tapes itself. Again, this may be due to the evidence available. Svinøyosen sits on the (extrapolated) 17 m isobase line where there is very little published RSL data for comparison.
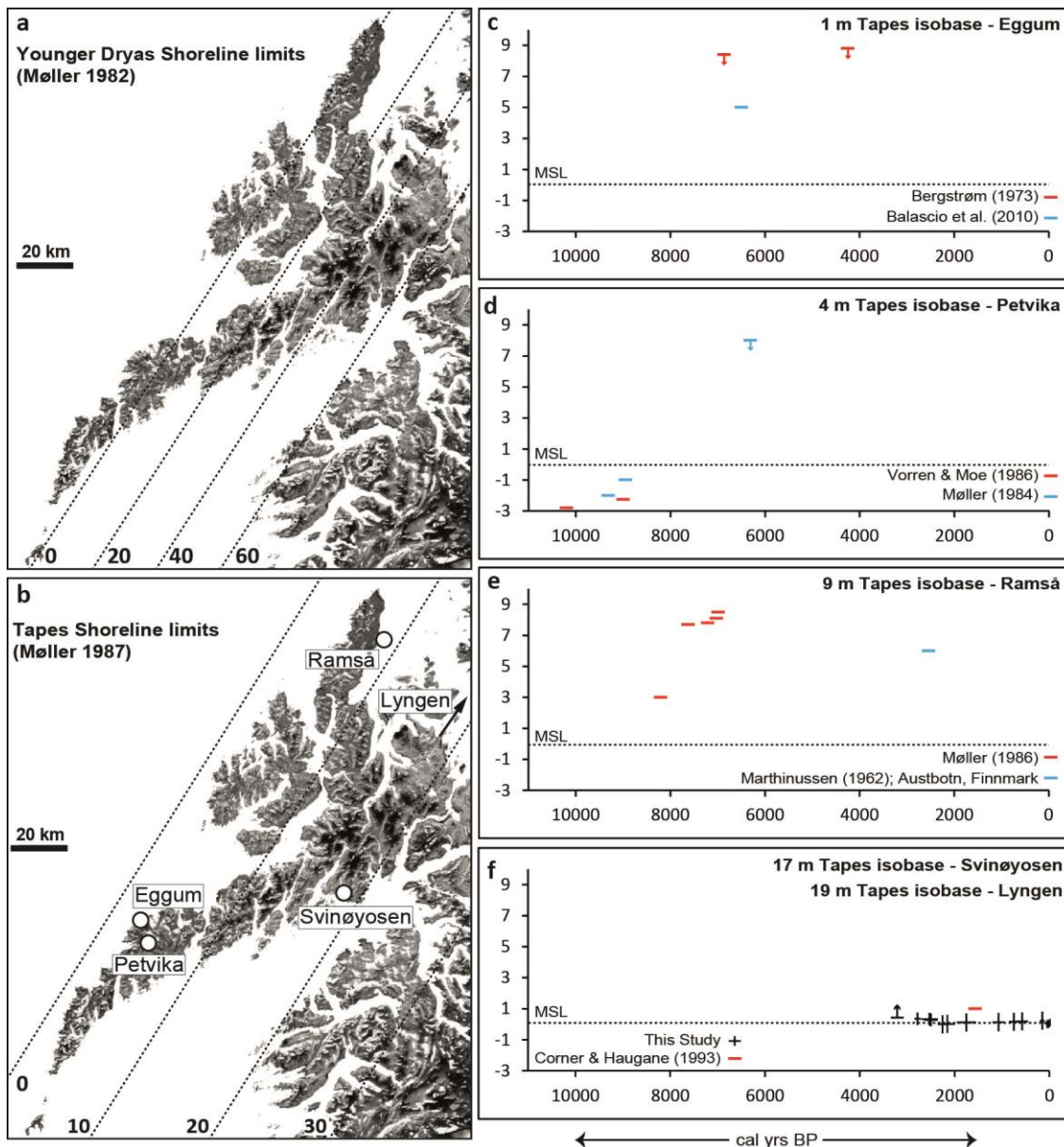
Figure 7.3 Isobase lines of the shoreline limits for the Younger Dryas highstand (a) and the Tapes highstand (b) and published relative sea level index points from sites along different Tapes isobases

Isolation basin studies represent a reliable means of estimating palaeosea levels through the dating of the marine-lacustrine contact that was formed when the basin became isolated from the sea. Corner & Haugane (1993) derived a SLIP using such a method from an isolation basin located on the ~19 m Tapes isobase (Møller 1987) of 1565 ± 185 cal yrs BP. They calculated that MSL at the time was at, or less than, 1 m above

246

present MSL, showing very close agreement with the RSL reconstruction from Svinøyosen (Figure 7.3f). The basin is located in Lyngen, County Troms, and is relatively comparable to our study site as it sits near the same Tapes isobase. The fact that the SLIP sits slightly higher than the Svinøyosen reconstruction may be explained by its location on a greater uplift isobase, thereby having a steeper sea-level history. Alternatively, the Svinøyosen reconstruction may slightly underestimate sea-level depths between ~1000 and 3000 cal yrs BP. Beyond the SLIP from Corner & Haugane (1993) there are very few data available which are directly comparable to the reconstruction.

Marthinussen (1962) produced a Holocene RSL reconstruction for Ramså which is widely referred to in the literature as a reference sea-level curve (Møller 1984, 1986; Vorren & Moe 1986; Balascio et al. 2010). This curve was constructed using data from across north-western Norway and Finnmark. It also provides the only late Holocene SLIPs for the region: two pieces of driftwood found in Finnmark which were assigned indicative elevations in relation to measured shorelines from Marthinussen (1945, 1960), one of which is shown in Figure 7.3e. These SLIPs indicate that relative sea levels on the 9 m Tapes isobase were around 6 m above MSL at ~2000 cal yrs BP. The results from this study and the SLIP from Corner & Haugane (1993) on the 17 and 19 m Tapes isobases suggest Marthinussen (1962) overestimated late Holocene sea-level heights.

The published Holocene sea-level data for northern Norway were collated by Møller (1987) and used to simulate Holocene RSL curves for the entire region (Møller 1989). The geometric simulation was based on the assumption that mapped shoreline elevations were directly and linearly proportional to other raised shorelines. This

allowed the extrapolation of shoreline heights and ages in relation to the Tapes isobases. The model has been updated and is available online (Møller & Holmeslet 2002).

The 500, 1000, 1500, 2000, 2500 and 3000 year shorelines from the model are presented in Figure 7.4. The 17 m Tapes isobase identifies the simulated RSL elevations expected at Svinøyosen at these times. As can be seen, the simulated shoreline history for Svinøyosen disagrees with the RSL reconstruction from this study. As mentioned, there are very few late Holocene sea-level data for this region, and, in addition, the SLIPs used to constrain the model from Møller (1987) often represent highest tide levels, or storm deposits, which are not corrected to mean tidal levels and are therefore not comparable to the mean sea levels that the Svinøyosen reconstruction is in relation to. The shoreline simulation represents raised beaches, which sit above the level of MSL and partially explains the significant difference between the proxy data and the simulation. Other RSL studies from Finnmark have also found that the simulation model can deviate from measured palaeo-RSL elevations by up to 14 m (Romundset et al. 2011). The fact that few studies from northern Norway have been able to constrain accurately the last few thousand years of RSL history means this reconstruction is potentially valuable. In addition, the disagreement with the RSL simulations of Møller (1989) and Møller & Holmeslet (2002) suggests that (i) the methods used for the Svinøyosen reconstruction deserves further consideration in other locations, and that (ii) the new RSL history could be used to help constrain the simulation model, which is widely used in northern Norway for educational purposes.

Further comparisons to existing models are made in Figure 7.4. The RSL data output from Lambeck et al's (1998a) GIA model also shows deviation away from the proxy

data of this study. The sea-level reconstruction implies that the GIA model overestimates sea-level depths for the late Holocene. This may be caused by excessively high rates of land uplift over the last 3000 years. In order to adjust for this some model parameters might be changed. The ice sheet extent may be relocated further in land, or alternatively, the thickness of the ice sheet may be reduced for this region.
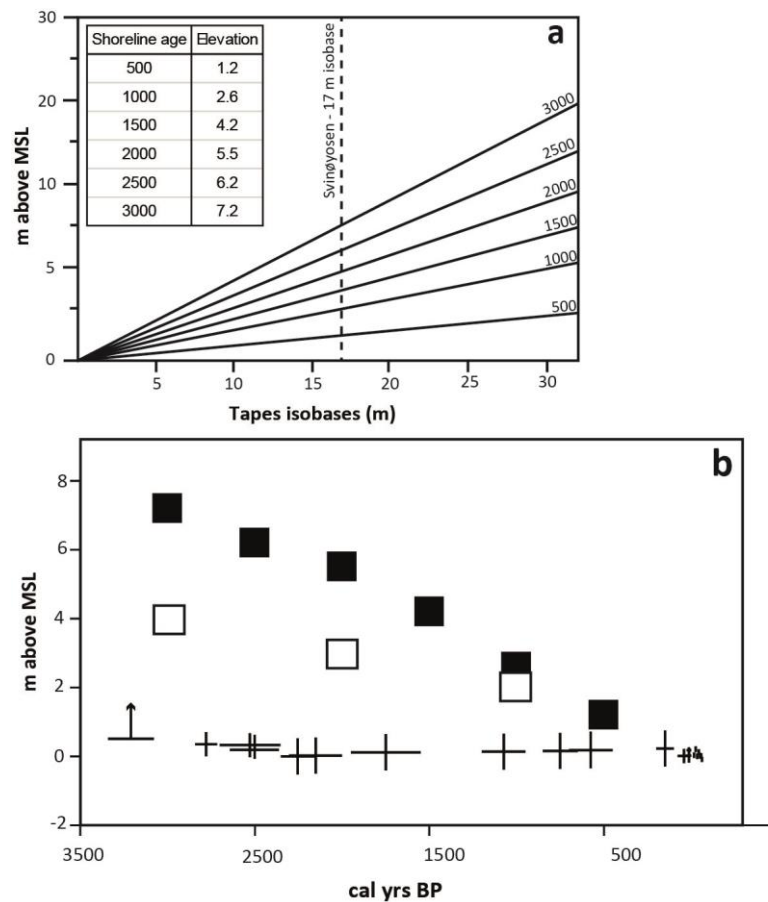
Figure 7.4 Simulated shoreline elevations through the late Holocene for the 17 m Tapes isobase line (a) and comparisons with the Svinøyosen RSL reconstruction (b). Black squares represent the shoreline simulation by Møller(1989) *and Møller & Holmeslet (2002) and the white squares represent the RSL output from the GIA model of Lambeck et al. (1998a)*

7.4.1 Contributions to changing sea levels in Norway

The late Holocene reconstruction from Svinøyosen suggests that the rate of RSL fall may have accelerated in the last 300 to 500 years. The reconstructed rate of fall differs from that recorded by nearby tide-gauge records which demonstrate that modern rates are around -1 mm yr^{-1}. Over the last 3000 years, there has been an approximate rate of sea-level fall of -0.5 mm yr^{-1}. As mentioned, true absolute rates have been hard to distinguish due to the large vertical errors associated with much of the reconstruction. By identifying the different contributions to changing sea levels, we may gain insight into the true nature of late Holocene RSL patterns at Svinøyosen. Recent studies have distinguished oceanic contributions, such as thermo- and halosteric and volumetric changes, from isostatic changes, such as GIA (Henry et al. 2012; Richter et al. 2012). GIA has had a significant influence on Holocene sea-levels in Norway, and a hypothetical reduction in the GIA component may have serious consequences on future sea-level rise at the study location.

The recent (~100 year) RSL reconstructions performed in this study were compared with tide gauges at Harstad and Kabelvåg as these were closely associated with Svinøyosen in terms of their positions relative to uplift isobase lines. Current rates of uplift for these two locations have been calculated using levelling, GPS solutions and tide gauges by Vestøl (2006). The results for Kabelvåg (2.6 mm yr^{-1}) and Harstad (2.7 mm yr^{-1}) seem in good agreement and are preferable to modelled GIA uplift rates using Peltier (2004). Depending on the deglaciation ICE model and mantle viscosity structure used, the GIA results for the Norwegian coastline from Peltier (2004) can vary significantly (e.g. Henry et al. 2012; Richter et al. 2012). In addition, the values given by Vestøl (2006) show reasonable agreement with velocity estimates performed by

Kierulf et al. (2013) using long term (1990s onwards), continuous GPS monitoring throughout Norway.

Uplift rates for this region in Norway have been decelerating throughout the Holocene (Lambeck et al. 1998a) and the rates will reduce below the values presented above. These modern uplift rates are an important contributor to patterns of recent sea-level change in the Lofoten – Vesterålen region. Current RSL trends are ca. -0.75 mm yr^{-1}. If the GIA component is accounted for (alongside the inverted barometer effect – higher air pressures causing sea-surface depression) then current sea-level trends increase to ca. 2 mm yr^{-1} at both Kabelvåg and Harstad (Richter et al. 2012). Mean coastal sea-level trends for the Arctic are estimated at over 2 mm yr^{-1} when GIA and atmospheric pressure changes are accounted for (Henry et al. 2012). The RSL reconstruction from this study suggests the GIA component to RSL may be reducing in comparison to earlier Holocene uplift rates. If the pace of RSL fall has reduced through the last few thousand years, then a neutral trend of RSL may be expected in the future. Modelling of the decelerating GIA component, coupled with IPCC scenario predictions may indicate at when this point will be reached. Rising global sea levels (Church & White 2011), combined with a decreasing GIA uplift component, imply positive RSL trends are a real possibility for this part of Norway.

7.4.2 Uses of a late Holocene sea-level reconstruction: GIA modelling

Well constrained RSL data are important for investigations into, and the modelling of, postglacial GIA (Steffen & Wu 2011). Glacial rebound models are compared against

sea-level reconstructions to ensure that model parameters reasonably predict observed RSL changes. The Fennoscandian GIA model by Lambeck et al. (1998b) is constrained this way. Lambeck et al. (1998a) identify four publications that were used to provide RSL data to help validate their model for north-western Norway. They use Møller (1984) and Vorren & Moe (1986) for the Lofoten region, Hald & Vorren (1983) for near Tromsø and Vorren et al. (1988) for Andøya. All RSL data were stated to derive from isolation basin contacts which are considered reliable sea-level proxies with low associated uncertainties.

Examination of the studies indicates that Møller (1984) and Vorren & Moe (1986) make no reference to SLIPs derived from isolation basins in their work. These two studies provide RSL constraints from the early Holocene to around 5000 cal yrs BP derived from raised shoreline features and from peats located both on- and offshore. The submarine peats indicate minimum relative sea levels for the dated horizons and a transgression maximum is weakly constrained using the dated shorelines. Vorren et al. (1988) make use of two inland lakes to study postglacial environmental change. They derive a single isolation contact at some time between 18500 and 15500 cal yrs BP. No SLIPs are provided from this study for the Holocene. Finally, Hald & Vorren (1983) reconstruct a Holocene shoreline displacement curve largely using the data discussed above from Marthinussen (1962) and a contribution from their own study. Again, no reference is made to any isolation event. Their work derives a single early Holocene RSL minimum from an assumed fluvial deposit sitting above an erosional contact, interpreted as erosion caused by a sea-level regression. The only late Holocene sea-level data identified by the above studies are references made to the two driftwood pieces from Marthinussen (1962).

The RSL data used to constrain the Lambeck et al. (1998b) GIA model for northern Norway, to modern day standards, might be considered imprecise and few in number. As discussed above, the 3000 year RSL history for the area suggests that changes in the active GIA component may have taken place. These changes in GIA uplift rates are not well constrained for the late Holocene and a reassessment of GIA models may be prudent. New sea-level data should always be sought after so that modelled and predicted rates of GIA uplift can be properly constrained. The consideration of past GIA influences on RSL in Norway is an important topic for estimations of future sea-level changes (Simpson et al. 2012).

7.4.3 Uses of a late Holocene sea-level reconstruction: future sea-level changes

Since the publication of the IPCC Fourth Assessment Report (AR4; IPCC, 2007), predicting future sea-level trends has turned up on more government agendas, including Norway's. Simpson et al. (2012) established a framework for estimating future sea-level changes along the Norwegian coastline. Their work followed the original national sea-level prediction report "Havnivåstigning" by the Bjerknes Centre for Climate Research (Vassog et al. 2009). The predictions performed by Simpson et al. (2012) were based on AR4 scenarios and local, instrumental observations of vertical land motion and sea-level movements. GIA was modelled using GPS measurements since 1990 (Kierulf et al. 2013). Sea-level changes were derived from tide-gauge data that (at most) extended back to the early 1880s (Woodworth & Player 2003), and were validated using satellite altimetry from 1992 (Cazenave & Llovel 2010). Estimations of ocean-mass changes were predicted from observed volume changes and surface mass balance changes of glaciers, ice caps and ice sheets using similar methods to the IPCC AR4 predictions

(Slangen et al. 2012). The high end scenario sea-level rise predictions for the 21st century, relative to 2000 AD, for Norway were bound between 70 and 130 cm however they conclude: "We attach no likelihood to any of our projections owing to the lack of understanding of some of the processes that cause sea-level change".

Simpson et al. (2012) demonstrate how through the use of good quality instrumental data, we may be able to prepare coastal zones against future sea-level rise. Yet these predictions are only of limited use as the fundamental components governing sea-level changes are still not entirely understood. Proxy data that extend beyond the longest tide-gauge records are required to identify and describe contributions to 20th century global sea-level change (Douglas 2008). In addition, it is becoming more apparent that instrumental data are still too short in length to determine decadal and multidecadal fluctuations in global sea level, and that predictions based on such data would do well to hindcast and validate their models using palaeosea-level data (Siddall & Milne 2012; Woodroffe & Murray Wallace 2012). In northern Norway the continuous sea-level reconstruction from Svinøyosen offers the opportunity to study recent sea-level changes on timescales beyond local tide-gauge data.

7.5 Improvements and future work

7.5.1 Improvements for the testate amoebae reconstruction

Salt-marsh based sea-level studies using testate amoebae are quite rare in comparison to studies using other available microfossil proxies such as foraminifera and diatoms. The direction of testate amoebae sea-level reconstructions could follow a number of paths. Whether they can be used as a complementary proxy or as a replacement when alternative options fail is yet to be seen. This thesis strongly implies that there is a future for sea-level studies using testate amoebae.

In comparison to other palaeoenvironmental studies, the construction of a transfer function for sea-level purposes using just 29 samples is quite rare. Even Ooms et al. (2012) suggested that their marsh based transfer function model was short on samples; they had used 37. Despite this, the reconstruction produced in this thesis shows similarities with other testate amoebae based models and reconstructions. Whether this suggests that prediction errors are underestimated for this reconstruction or that a large number of samples are not actually required is yet to be seen. Additional surface sampling across Svinøyosen, and from nearby salt marshes would identify whether increased sample numbers improve the model, or introduce greater error terms.

In order to deliver a reasonable sea-level history using fossil testate amoebae, Svinøyosen was revisited in 2011 so that a core from higher up the marsh could be taken. As a result the sea-level reconstruction was extended back to around 1930 AD.

As suggested by Charman et al. (2010), the highest reaches of a salt marsh are the optimal zone to obtain a sediment core for fossil testate amoebae analysis. Perhaps if a new sediment core was to be taken from Svinøyosen then the area at the level of HAT may represent the most suitable elevation. With a falling sea level, presumably fossil sediments would have always been influenced by the tides (assuming a constant palaeotidal regime), and that a core from this location would produce the longest testate amoebae based record available. A sea-level reconstruction that extended back a full 200 or 300 years, and of similar quality to that presented in this thesis, would truly help investigate questions of 19th and 20th century sea-level change.

7.5.2 Salt-marsh testate amoebae work for the future

Following the presentation of Norwegian salt-marsh surface testate amoebae, it was hypothesised that the Arctic climate of northern Norway may have influenced surface assemblages. In comparison to other studies, this effect may be particularly noticeable at the lower elevations of the marsh, where in Norway, taxa diversity was minimal. To investigate this further, a north - south transect of Norwegian salt-marsh testate amoebae would help identify assemblage changes caused by climate, and would also help highlight any regionality shown by this understudied niche of microorganisms.

The extent to which salt-marsh testate amoebae are indeed regional has already been raised in this thesis. It is possible that transfer functions constructed from training sets from across the North Atlantic are applicable to fossil cores derived from different locations (Charman et al. 2010). If a universal training set of North Atlantic testate

amoebae were possible, impacts on future sea-level studies would be considerable. To investigate this further, a statistical analysis of the surface data available (i.e. from North America, UK, Belgium, Iceland and now Norway) may allude to the possibility of a truly universal training set. Comparisons of reconstructions using both local and universal training sets would naturally be imperative.

7.5.3 Improvements for the late Holocene foraminifera reconstruction

The predominant limitations of the late Holocene sea-level reconstruction come from the large vertical uncertainties associated with using low marsh and mud flat intertidal calcareous foraminifera in reconstructions. A possible solution would be to collect surface samples lower into the subtidal realm in an attempt to constrain indicative ranges of different calcareous foraminifera, as per Horton et al. (2007). Vertical errors associated with the subtidal training set from Horton et al. (2007) were around ± 4.5 m. Such large uncertainties on the late Holocene sea-level curve from this thesis would have added little to the reconstruction. The best option to constrain accurately the sea-level history for the field site region would be to identify and core nearby isolation basins from low lying (< 30 m above MSL) topographies. However, despite attempts, the steeply sloping glacial landscape meant that no suitable coastal basins were identified during the 2010 and 2011 field seasons that might have provided suitable isolation contacts. Careful consideration of the purposes of any sea-level reconstruction is paramount. If a Holocene sea-level history is required, then relocation to an isolation basin rich area may be advised. If investigation into late Holocene sea-level accelerations is desired then a location that is less affected by postglacial uplift is more suitable.

7.5.4 Future work for RSL studies of Norway

It is undeniable that RSL reconstructions from higher latitude locations are valuable, but further thought needs to be given to optimal study areas where GIA has less influence on the overriding RSL curve, and where salt-marsh surface microfossils show greater abundance and diversity. It is likely that Arctic salt-marsh conditions have a detrimental impact on the growth patterns of foraminifera. Future Arctic studies might turn to salt-marsh diatoms which have been used in Greenland (Woodroffe & Long 2009) and Alaska (e.g. Hamilton & Shennan 2005a,b; Barlow et al. 2012; Watcham et al. 2013). New RSL reconstruction attempts for Norway might focus efforts towards the south west, between Stavanger and Tregde, where uplift rates are slightly lower (~2 mm yr^{-1}; Kierulf et al. 2013) and current RSL rates are slightly positive.

CHAPTER 8 - Conclusions

8.1 Thesis aims

This thesis contained two overall aims. The first was to produce a late Holocene sea-level record for north-western Norway. There is limited Holocene sea-level data for the Lofoten – Vesterålen archipelago and this project intended to contribute significantly to this dearth by applying established techniques never before used in the region. The second aim was to further establish salt-marsh testate amoebae as a viable sea-level proxy. This proxy is becoming increasingly used, however analytical practises have occasionally been based on inappropriate techniques. This study intended to develop the preparatory and analytical procedures involved with salt-marsh testate amoebae, to suggest a standardise practice, as well to test the suitability of the proxy against observational sea-level records.

8.2 Salt-marsh testate amoebae

8.2.1 Sample preparation and analysis

Surface samples of salt-marsh sediments with surveyed elevations were taken from Svinøyosen and Storosen and used to provide modern assemblage data of testate amoebae. A count total exercise was performed on 11 samples which were each counted for 100 tests, and counting then continued until 150 tests were recorded. The differences seen between the two sets of assemblages were largely driven by the occurrence of rare

species (those making up less than 2 % of the assemblage). By using comparative statistics, it was shown that the assemblage compositions of the datasets were nearly identical and that little is gained from increasing a count total from 100 to 150 tests.

Different preparation techniques were applied to six surface samples from Storosen to investigate the effects different treatments had on assemblage compositions. The first technique (A) used a soaking method with no chemical disaggregant. The samples prepared this way, on average, took the longest to count, possibly due to testate amoebae sized organic and lithic particles crowding the microscope slides and obscuring the tests. The second technique (B) used a chemical disaggregant (5 % KOH) in an attempt to break up the organic conglomerate particles that were common on slides prepared using method A. This treatment took a longer time to prepare and counts of these samples produced the lowest diversity of taxa. It was hypothesised that by sieving prior to the chemical treatment some specimens were being lost within the larger conglomerate particles in the larger sieve. Technique C used a more efficient sieving technique following the chemical treatment, and also used a smaller mesh size for the upper sieve. This method produced the most clear slides to look at and count times for samples prepared this way were lower compared to the other treatments. Following comparative statistics, it was shown that there is very little loss of assemblage information through using techniques B or C despite the possibility that the chemical treatment may lead to the destruction of tests. Preparation method C, which was used as a standardised technique for the remaining testate amoebae analyses (alongside a count total of 100 tests), is described in detail in Table 3.5.

Often the distinction between live and dead modern specimens is required in palaeoenvironmental studies. It was found that samples prepared using technique A contained clearly stained (live) and unstained (dead) specimens, in nearly equal proportions. Samples prepared using techniques B and C contained virtually no live individuals of testate amoebae. It was suggested that removal of the stain may have been caused by the addition of KOH following the staining procedure. A possible solution is to stain the samples following the KOH disaggregation, providing the organic protoplasm of the specimen is not destroyed.

8.2.2 Testate amoebae as sea-level indicators

Surface samples from Svinøyosen and Storosen provided 29 assemblages of modern salt-marsh testate amoebae covering a vertical elevation range of 0.84 m. Assemblage composition changed in relation to changing elevation, and unconstrained cluster analysis identified three different assemblage zones. The lowest zone occupied elevations between MHWN and MHWS tide levels. The middle zone spanned across the level of MHWS, and the highest zone started midway between MHWS and HAT levels. This zonation showed broad agreement with existing modern salt-marsh testate amoebae zonation from the UK, North America, Iceland and Belgium. Through the use of ordination, it was shown that elevation accounted for up to 59 % of species variation within the surface samples from Norway.

The most suitable model identified whilst developing a transfer function for the modern training set was weighted averaging partial least squares with two components and species tolerance downweighting and no data transformation. This model was used to

predict palaeomarsh-surface elevations from assemblages of testate amoebae. Through bootstrapping cross-validation it was shown that the model could predict surface elevations with precisions as low as $\pm$ 0.085 m. The transfer function was applied to fossil assemblages representative of the last ~100 years and used to calculate palaeosea depths. The reconstruction showed a falling relative sea level trend. The individual sea level index points showed close agreement with nearby tide-gauge data, although the overall trend appeared to overestimate rates of relative sea-level fall.

8.2.3 Implications

By adapting existing preparatory techniques for salt-marsh testate amoebae and suggesting a standardised procedure, future studies may be able to make significant time gains during the analytical and counting stages. These improvements may allow studies to analyse a higher number of modern samples or increase the resolution of sediment core investigations.

This study has produced one, of a very few, sea-level reconstruction using salt-marsh testate amoebae. In addition, the transfer function has accurately predicted a falling relative sea-level trend in an area of relatively high isostatic uplift. These successes demonstrate that testate amoebae are a viable sea-level indicating proxy and can be used alongside, or in lieu of, alternative salt-marsh proxies. As previously reported, the location of a salt-marsh sediment core required for fossil analyses is important. A high marsh area, within the realms of the HAT level, may represent the best opportunity of recovering long sequences of fossil testate amoebae.

The additional surface testate amoebae data produced by this study now contributes to a North Atlantic modern training set. Future studies may be able to analyse this distribution of surface data and determine whether samples from different sites contain similar assemblage patterns and therefore test the hypothesis: 'a generic training set of testate amoebae from sites across the North Atlantic can be used to accurately predict past sea-levels using fossil assemblages from salt-marsh sediment cores from different locations about the North Atlantic'.

8.3 Holocene sea-level changes in north-western Norway

Through sedimentological analyses and dating of the lithostratigraphy at Svinøyosen, this project has described a trend of falling relative sea levels during the late Holocene. Mid Holocene age subtidal (~50 m) environments were identified and it seems Svinøyosen became an intertidal environment after around 2500 cal yrs BP. Unconformities were identified in the sediments, implying an event caused redeposition of older, offshore sediments at around 4000 cal yrs BP. Further work is required in order to determine the cause of this erosive events. Continued shallowing took place into the late Holocene and salt-marsh sediments only became established in the last few hundred years.

8.3.1 A late Holocene sea-level reconstruction

Surface foraminifera from Storosen and Svinøyosen were used to develop a local modern training set which spanned a vertical range of 2.02 m. When used to build a transfer function the model was only capable of predicting palaeomarsh-surface elevations to within precisions of ± 0.27 m. This is likely due to the low diversity of agglutinated salt-marsh species and the wide vertical range that low salt-marsh and low intertidal calcareous species exhibit. The transfer function could not be applied to sediments older than ~100 years due to a lack of modern analogues and was therefore replaced by a qualitative assessment method to derive indicative meanings of fossil foraminifera representing the last ~3000 years. The sea-level reconstruction for Svinøyosen shows a late Holocene sea-level fall of approximately 0.5 mm yr^{-1} over the last 3000 years. The most recent part of the reconstruction based on testate amoebae shows good agreement with nearby tide-gauge data although overestimates the rate of RSL fall by approximately 1 mm yr^{-1}. The reconstruction from this study represents an attempt at quantifying sea-level changes in a region of high isostatic uplift and faced some significant challenges. In light of this, some valuable lessons have been learned:

1) Salt-marsh surface foraminifera from northern Norway are short on diversity. Only two species of typical salt-marsh taxa were encountered whereas mid-latitude studies often make use of many more. Only one high marsh species was present and occurred across the entire salt-marsh meaning the indicative range for this taxon was large.

2) Salt-marsh proxy reconstruction errors for sites around the globe are typically between ±0.05 and ±0.20 m, depending on tidal ranges and microfossil choice. Reconstruction errors associated with the foraminifera based transfer function

reconstruction from Svinøyosen are at ±0.27 m from 1930 AD to present. Beyond 1930 AD fossil foraminifera assemblages did not reflect modern salt-marsh assemblages and the transfer function derived reconstruction became unreliable. The qualitative assessment reconstruction presented indicative ranges from ±0.2 to ±0.525 m. The size of these uncertainties meant it was hard to determine true sea-level trends and rates over the last few hundred years.

3) Facies in the core include low marsh and lower tidal environments, which are poor environments from which to obtain indicators of sea-level change. Indeed, in this area of rapidly uplifting coastlines, the reconstructed water depth is greater than the sampled environmental range, therefore limiting the use of transfer functions.

4) The significant influence of GIA caused sea levels to fall throughout the Holocene. This trend was confirmed by the negative rate of modern relative sea-level shown by nearby tide gauge-records. To date, all studies used to identify changes in rates of sea-level movement are from locations where RSL has been rising during the last hundred years. Determining an inflexion signal caused by increased sea-surface height in an area of ongoing RSL fall represents a significant challenge.

8.3.2 Implications

Few late Holocene sea-level data exist for this part of Norway. The reconstruction presented represents a better constrained approximation of late Holocene sea-level than the currently accepted simulated curve and covers a time period that is often neglected in studies, possibly due to the lack of available proxy data. In addition, the

reconstruction can be used to help constrain models of historic GIA which rely heavily on proxy derived Holocene sea-level data.

The reconstruction has been performed in an area of RSL fall where isostatic uplift rates continue to outpace the rise in sea-surface elevation. Studies in regions such as this rarely use salt marshes as sources of proxy data. More commonly, mid latitude salt-marsh studies report recent RSL rise from long sequences of salt-marsh peat. This study therefore encourages the use of these methods in future research of coastal areas still undergoing isostatic uplift.

This study presents the first sea-level reconstructions from Norway based on coastal sediments from a single location. It was made evident that the distribution of salt-marsh foraminifera is less favourable (in terms of sea-level study) at these latitudes in Norway, in comparison to other sites from across the North Atlantic. Further foraminifera research along the Norwegian coastline may have more success, possibly depending on local climate patterns and distance from the centre of land uplift. Alternatively, this project has shown that testate amoebae are a viable alternative when other proxies are less successful, and that this group of microorganisms have a future as sea-level indicators.

APPENDIX I – Foraminifera taxonomy

<u>Order</u> FORAMINIFERIDA (Loeblich & Tappan 1964)

<u>Suborder</u> TEXTULARIINA (Loeblich & Tappan 1964)

    <u>Genus</u> EGGERELLOIDES (Haynes 1973)

        Eggerelloides scaber

            Bulimina scabra (Williamson 1858)

    <u>Genus</u> JADAMMINA (Bartenstein & Brand 1938)

        Jadammina macrescens

            Trochammina inflata (Montagu) var. m*acrescens* (Brady 1870)

    <u>Genus</u> MILIAMMINA (Heron-Allen & Earland 1930)

        Miliammina fusca

            Quinqueloculina fusca (Brady 1870)

    <u>Genus</u> TROCHAMMINA (Parker & Jones 1859)

        Trochammina adaperta

            Trochammina squamata var. *adaperta* (Rhumbler 1938)

<u>Suborder</u> MILIOLINA (Loeblich & Tappan 1964)

    <u>Genus</u> CORNUSPIRA (Schultze 1854)

        Cornuspira involvens

            Operculina invovlens (Reuss 1850)

    <u>Genus</u> MILIOLINELLA (Wiesner 1931)

        Miliolinella subrotunda

            Vermiculum subrotundum (Montagu 1803)

    <u>Genus</u> QUINQUELOCULINA (d'Origney 1826)

        Quinqueloculina bicornis

            Quinqueloculina bicornis (Walker & Jacob 1798)

        Quinqueloculina cliarensis

            Miliolina cliarensis (Heron-Allen & Earland 1930)

        Quinqueloculina dimidiata

            Quinqueloculina dimidiata (Terquem 1876)

        Quinqueloculina lata

            Quinqueloculina lata (Terquem 1876)

        Quinqueloculina oblonga

            Vermiculum oblongum (Montagu 1803)

        Quinqueloculina seminulum

            Serpula seminulum (Linné 1758)

Genus SPIROLOCULINA (d'Orbigny 1826)

Spiroloculina rotunda

Spiroloculina rotundata (d'Orbigny 1826)

Suborder ROTALIINA (Loeblich & Tappan 1964)

Genus AMMONIA (Brünnich 1772)

Ammonia beccarii

Nautilus beccarii (Linné 1758)

Ammonia beccarii var. *batavus* (Murray 1979)

Ammonia beccarii var. *limnetes* (Murray 1979)

Ammonia beccarii var. *tepida* (Murray 1979)

Genus ASTRONONION (Cushman Edwards 1937)

Astrononion gallowayi

Astrononion gallowayi (Loeblich & Tappan 1953)

Genus BOLIVINA (d'Orbrigny 1839)

Bolivina gramen

Bolivina gramen (d'Orbrigny 1839)

Bolivina pseudoplicata

Bolivina pseudoplicata (Heron-Allen & Earland 1930)

Genus BRIZALINA (O. G. Costa 1856)

Brizalina variablis

Textularia variablis (Williamsoni 1858)

Genus BULIMINA (d'Orbigny 1826)

Bulimina marginata

Bulimina marginata (d'Orbigny 1826)

Genus BULIMINELLA (Cushman 1911)

Buliminella elegantissima

Buliminella elegantissima (d'Orbigny 1839)

Genus CASSIDULINA (d'Orbigny 1826)

Cassidulina crassa

Cassidulina crassa (d'Orbigny 1839)

Genus CIBICIDES (de Montfort 1808)

Cibicides lobatulus

Nautilus lobatulus (Walker & Jacob 1798)

Genus ELPHIDIELLA (Cushman 1936)

Elphidiella artica

Polystomella arctica (Parker & Jones 1864)

Genus ELPHIDIUM (de Montfort 1808)

Elphidium clavatum

    Elphidium excavatum clavatum (Cushman 1930)

Elphidium cuvillieri

    Elphidium cuvillieri (Lévy 1966)

Elphidium earlandi

    Elphidium earlandi (Cushman 1936)

Elphidium excavatum

    Polystomella excavata (Terquem 1875)

Elphidium gerthi

    Elphidium gerthi (Van Voorthuysen 1957)

Elphidium incertum

    Polystomella umbilicatula var. *incerta* (Williamson 1858)

Elphidium oceansis

    Polystomella oceansis (d'Orbigny 1826)

Elphidium subarcticum

    Elphidium subarcticum (Cushman 1944)

Elphidium williamsoni

    Elphidium williamsoni (Haynes 1973)

<u>Genus</u> FISSURINA (Reuss 1850)

    Fissurina lucida

        Lagena lucida (Williamson 1848)

    Fissurina marginata

        Lagena marginata (Montagu 1803)

<u>Genus</u> FURSENKOINA (Loeblich Tappan 1961)

    Fursenkoina schreibersiana

        Virgulina schreibersiana (Czjzek 1848)

<u>Genus</u> GAVELINOPSIS (Hofker 1951)

    Gavelinopsis praegeri

        Discorbina praegeri (Heron-Allen & Earland 1913)

<u>Genus</u> HAYNESINA (Banner & Culver 1978)

    Haynesina germanica

        Protelphidium anglicum (Murray 1965)

<u>Genus</u> LARYNGOSIGMA (Loeblich & Tappan 1953)

<u>Genus</u> LAGENA (Walker & Jacob 1798)

    Lagena sulcata

        Serpula (Lagena) sulcata (Walker & Jacob 1798)

<u>Genus</u> MELONIS (de Montfort 1808)

Melonis barleeanus

    Melonis barleeanus (Williamson 1858)

<u>Genus</u> NONION (de Montfort 1808)

Nonion depressulus

    Nautilus depressulus (Walker & Jacob 1798)

<u>Genus</u> OOLINA (d'Orbigny 1839)

Oolina melo

    Oolina melo (d'Orbigny 1839)

<u>Genus</u> PLANORBULINA (d'Orbigny 1826)

Planorbulina mediterranensis

    Planorbulina mediterranensis (d'Orbigny 1826)

<u>Genus</u> PROTELPHIDIUM (Haynes 1956)

Protelphidium orbiculare

    Protelphidium orbiculare (Brady 1881)

<u>Genus</u> ROSALINA (d'Orbigny 1826)

Rosalina anomala

    Rosalina anomala (Terquem 1875)

Rosalina globularis

    Rosalina globularis (d'Orbigny 1826)

Rosalina williamsoni

    Discorbis williamsoni (Chapman & Parr 1932)

<u>Genus</u> SPIRILLINA (Ehrenberg 1843)

Spirillina vivipara

    Spirillina vivipara (Ehrenberg 1843)

<u>Genus</u> STAINFORTHIA (Hofker 1956)

Stainforthia fusiformis

    Bulimina pupoides var. *fusiformis* (Williamson 1848)

<u>Genus</u> TRICHOHYALUS (Loeblich & Tappan 1953)

Trichohyalus bartletti

    Discorbis bartletti (Cushman 1933)

<u>Genus</u> TRIFARINA (Cushman 1923)

Trifarina angulosa

    Uvigerina angulosa (Williamson 1858)

Assulina seminulum
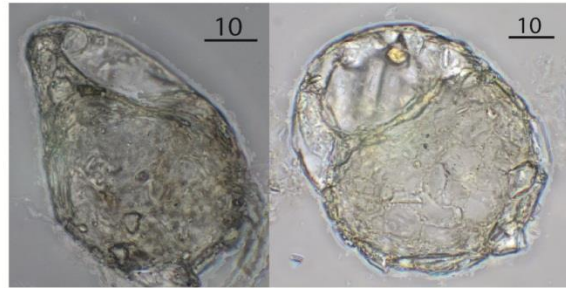
Centropyxis cassis type
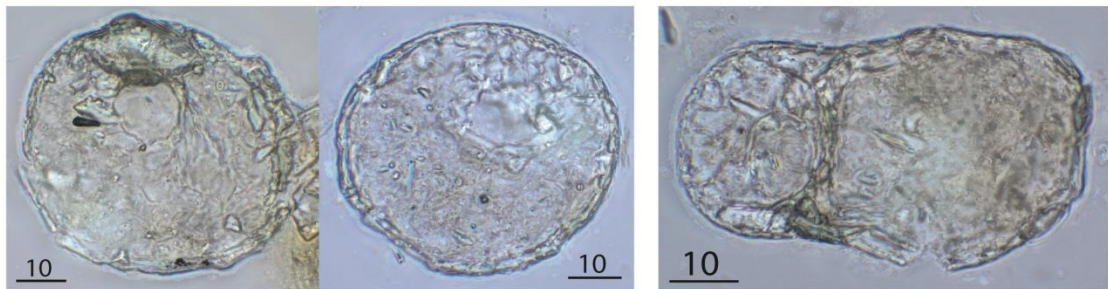
Centropyxis ecornis

Centropyxis platystoma type
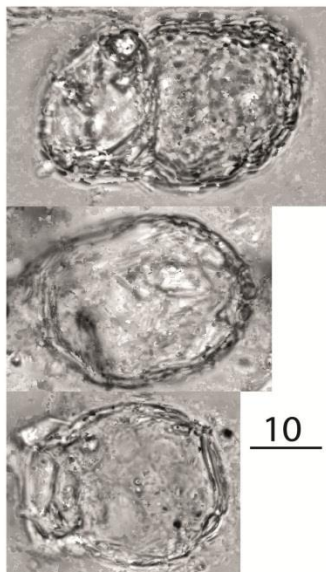
Centropyxis platystoma
morphotype 1

Corythion - Trinema type
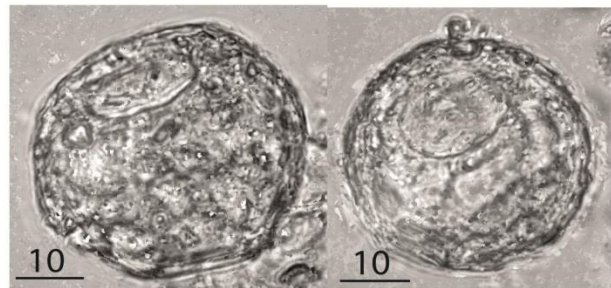
Cyclopyxis arcelloides type
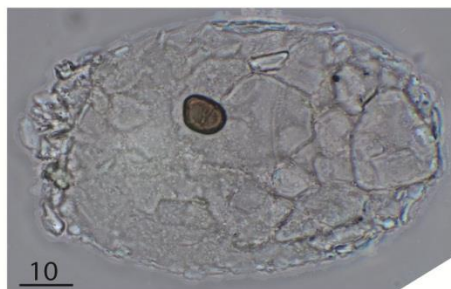
Difflugia lucida type
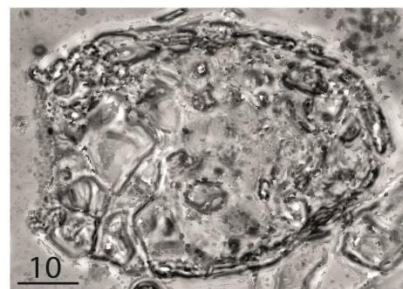
Difflugia pristis type
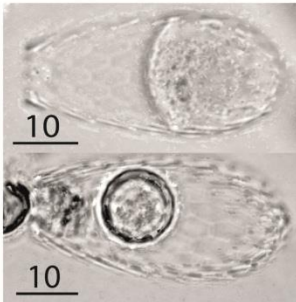
Euglypha rotunda type
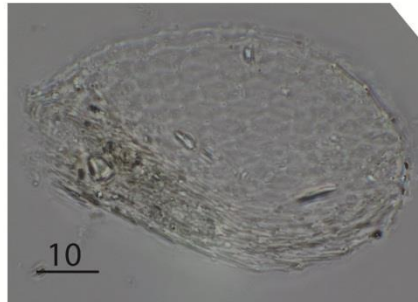
Euglypha tuberculata type
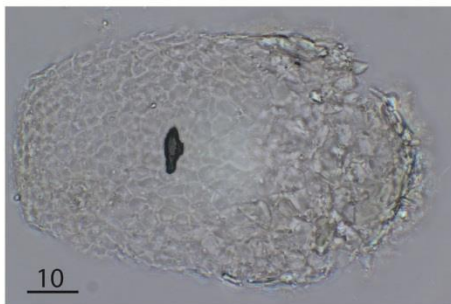
Heleopera petricola

Hyalosphenia ovalis
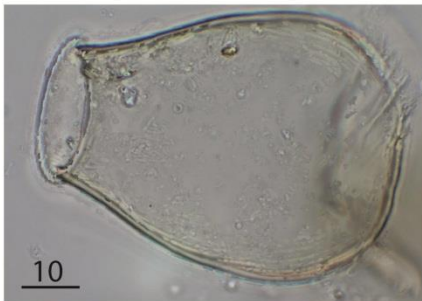
Hyalosphenia papilo

Nebela collaris
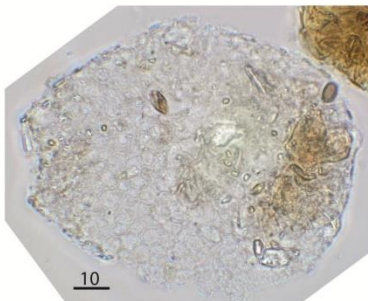
Nebela tincta
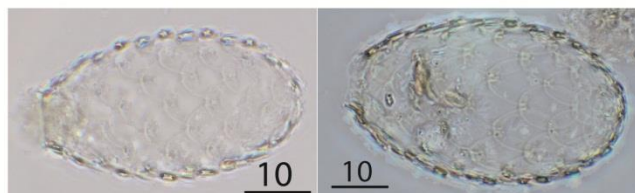
Tracheleuglypha dentata

REFERENCES

Allan, M., Le Roux, G., Sonke, J. E., Piotrowska, N., Streel, M. & Fagel, N. (2013) 'Reconstructing historical atmospheric mercury deposition in Western Europe using: Misten peat bog cores, Belgium'. *Science of the Total Environment*, 442 pp 290-301.

Allen, J. R. L. (1990) 'Constraints on measurement of sea-level movements from salt-marsh accretion rates'. *Journal of the Geological Society*, 147 pp 5-7.

Allen, J. R. L. (2000) 'Morphodynamics of Holocene salt marshes: A review sketch from the Atlantic and Southern North Sea coasts of Europe'. *Quaternary Science Reviews*, 19 (12). pp 1155-1231.

Almås, A.-J. & Hygen, H. O. (2012) 'Impacts of sea level rise towards 2100 on buildings in Norway'. *Building Research and Information*, 40 (3). pp 245-259.

Alve, E. & Murray, J. W. (1999) 'Marginal marine environments of the Skagerrak and Kattegat: A baseline study of living (stained) benthic foraminiferal ecology', *Palaeogeography, Palaeoclimatology, Palaeoecology*, 146 pp 171-193.

Appleby, P. G. (2001) 'Chronostratigraphic techniques in recent sediments'. in Last, W.M. and Smol, J.P. (eds.) *Tracking environmental change using lake sediments. Volume 1: Basin analyis, coring and chronological techniques.* Dordrecht, The Netherlands: Kluwer Academic Publishers.

Ayras, M., Niskavaara, H., Bogatyrev, I., Chekushin, V., Pavlov, V., deCaritat, P., Halleraker, J. H., Finne, T. E., Kashulina, G. & Reimann, C. (1997) 'Regional patterns of heavy metals (Co, Cr, Cu, Fe, Ni, Pb, V and Zn) and sulphur in terrestrial moss samples as indication of airborne pollution in a 188,000 km^2 area in northern Finland, Norway and Russia'. *Journal of Geochemical Exploration*, 58 (2-3). pp 269-281.

Balascio, N. L., Zhang, Z., Bradley, R. S., Perren, B., Dahl, S. O. & Bakke, J. (2011) 'A multi-proxy approach to assessing isolation basin stratigraphy from the Lofoten Islands, Norway'. *Quaternary Research*, 75 (1). pp 288-300.

Ball, D. F. (1964) 'Loss on ignition as an estimate of organic matter and organic carbon in non-calcareous soil'. *Journal of Soil Science*, 15 pp 84-92.

Barlow, N. L. M., Shennan, I. & Long, A. J. (2012) 'Relative sea-level response to Little Ice Age ice mass change in south central Alaska: Reconciling model predictions and geological evidence'. *Earth and Planetary Science Letters*, 315 pp 62-75.

Barlow, N. L. M., Shennan, I., Long, A. J., Gehrels, W. R., Saher, M. H., Woodroffe, S. A. & Hillier, C. (2013) 'Salt marshes as late Holocene tide gauges'. *Global and Planetary Change*, 106 pp 90-110.

Bennet, R. A., Carlsson, T. R., Carlsson, T. M., Chen, R., Davis, J. L., Ekman, M., Elgered, G., Elosegui, P., Hedling, G., Jaldehag, R. T. K., Jarlemark, J. M., Johansson, J. M., Jonsson, B., Kakkuri, J. Koivula, H., Milne, G. A., Mitrovica, J. M., Nilsson, B. I., Ollikainen, M., Paunonen, M., Poutanen, M., Pysklywec, R. N., Ronnang, B. O., Scherneck, H. G., Shapiro, I. I. & Vermeer, M. (1996) 'BIFROST Project: GPS measurements to constrain Geodynamic Processes in Fennoscandia'. *EOS, Trans. AGU,* 77 pp 337-341.

Berg, G. A. & Anthon, H. (1980) *Floraen I Farger.* Oslo: H. Aschehoug & Co.

Bergstrøm, B., Olsen, L. & Sveian, H. (2005) 'The Tromsø-Lyngen glacier readvance (early Younger Dryas) at Hinnøya-Ofotfjorden, northern Norway: A reassessment '. *Norges Geologiske Undersøkelse, Bulletin*, 445 pp 73-88.

Biester, H., Kilian, R., Franzen, C., Woda, C., Mangini, A. & Scholer, H. F. (2002) 'Elevated mercury accumulation in a peat bog of the Magellanic Moorlands, Chile (53 degrees S) - an anthropogenic signal from the Southern Hemisphere'. *Earth and Planetary Science Letters*, 201 (3-4). pp 609-620.

Bindler, R. (2003) 'Estimating the natural background atmospheric deposition rate of mercury utilizing ombrotrophic bogs in southern Sweden'. *Environmental Science & Technology*, 37 (1). pp 40-46.

Bindler, R., Renberg, I., Anderson, N. J., Appleby, P. G., Emteryd, O. & Boyle, J. (2001) 'Pb isotope ratios of lake sediments in West Greenland: inferences on pollution sources'. *Atmospheric Environment*, 35 (27). pp 4675-4685.

Bindler, R., Renberg, I. & Klaminder, J. (2008) 'Bridging the gap between ancient metal pollution and contemporary biogeochemistry'. *Journal of Paleolimnology*, 40 (3). pp 755-770.

Bindoff, N. L., Willebrand, J., Artale, V., Cazenave, A., Gregory, J., Gulev, S., Hanawa, K., Le Quéré, C., Levitus, S., Nojiri, Y., Shum, C. K., Talley, L. D. & Unnikrishnan, A. (2007) 'Observations: Oceanic Climate Change and Sea Level'. in Solomon, S., Qin, D., Manning, M., Chen, Z., Marquis, M., Averyt, K.B., Tignor, M. and Miller, H.L. (eds.) *Climate Change 2007: The Physical Science Basis. Contribution of Working Group I to the Fourth Assessment Report of the Intergovernmental Panel on Climate Change.* Cambridge, United Kingdom and New York, NY, USA: Cambridge University Press, pp 385-432.

Bird, M. I., Fifield, L. K., Chua, S. & Goh, B. (2004) 'Calculating sediment compaction for radiocarbon dating of intertidal sediments'. *Radiocarbon*, 46 (1). pp 421-435.

Birks, H. J. B. (1995) 'Quantitative palaeoenvironmental reconstructions'. in Maddy, D. and Brew, J.S. (eds.) *Statistical modelling of Quaternary Science data.* Cambridge: Quaternary Research Association, pp 161-253.

Birks, H. J. B. (1998) 'Numerical tools in palaeolimnology - Progress, potentialities, and problems'. *Journal of Paleolimnology*, 20 (4). pp 307-332.

Birks, H. J. B. (2010) 'Numerical methods for the analysis of diatom assemblage data'. in Smol, J.P. and Stoermer, E.F. (eds.) *The Diatoms: Applications for the Environmental and Earth Sciences.* 2 edn. Cambridge: Cambridge University Press.

Bondevik, S. J., Mangerud, J., Dawson, S., Dawson, A & Lohne, O. (2005) 'Evidence for three North Sea tsunamis at the Shetland Islands between 8000 and 1500 years ago'. *Quaternary Science Reviews,* 24 pp 1757-1775.

Booth, R. K., Lamentowicz, M. & Charman, D. J. (2010) 'Preparation and analysis of testate amoebae in peatland palaeoenvironmental studies'. *Mires and peat*, 7 pp 1-7.

Booth, R. K. & Sullivan, M. E. (2007) 'Testate amoebae as palaeohydrological proxies in peatlants'. *A workshop focused on testate amoebae identification, ecology and their use in palaeoenvironmental reconstruction*

Boutron, C. F., Candelone, J. P. & Hong, S. M. (1995) 'Greenland snow and ice cores - unique archives of large-scale pollution of the troposphere of the northern-hemisphere by lead and other heavy-metals'. *Science of the Total Environment*, 160-61 pp 233-241.

Brain, M. J., Long, A. J., Petley, D. N., Horton, B. P. & Allison, R. J. (2011) 'Compression behaviour of minerogenic low energy intertidal sediments'. *Sedimentary Geology*, 233 (1-4). pp 28-41.

Brain, M. J., Long, A. J., Woodroffe, S. A., Petley, D. N., Milledge, D. G. & Parnell, A. C. (2012) 'Modelling the effects of sediment compaction on salt marsh reconstructions of recent sea-level rise'. *Earth and Planetary Science Letters*, 345 pp 180-193.

Bray, J. R. & Curtis, J. T. (1957) 'An ordination of the upland forest communities of southern Wisconsin'. *Ecological Monographs*, 27 (4). pp 326-349.

Bush, K. J. (1885) *List of deep-water Mollusca dredged by the United States Fish Commission steamer Fish Hawk in 1880, 1881, and 1882, with their range in depth.,* US Comm Fish Fisher, Part II, Rep COmm 1883, App C, Article 17, 701-727.

Byrne, M. L. & Dionne, J. C. (2002) Typical aspects of cold regions shorelines. in Hewitt, K., Bryne, M. L., English, M. & Young, G. (eds.) *Landscapes of Transition – Landform Assemblages and Transformations in Cold Regions.* Kluwer Academic Publishers, Dordrecht. pp 141-158.

Callard, S. L., Gehrels, W. R., Morrison, B. V. & Grenfell, H. R. (2011) 'Suitability of salt-marsh foraminifera as proxy indicators of sea level in Tasmania'. *Marine Micropaleontology*, 79 (3–4). pp 121-131.

Cambray, R. S., Cawse, P. A., Garland, J. A., Gibson, J. A. B., Johnson, P., Lewis, G. N. J., Newton, D., Salmon, L. & Wade, B. O. (1987) 'Observations on radioactivity from the Chernobyl accident'. *Nuclear Energy-Journal of the British Nuclear Energy Society*, 26 (2). pp 77-101.

Cambray, R. S., Playford, K., Lewis, G. N. J. & Carpenter, C. (1989) *Radioactive fallout in air and rain: results to the end of 1987.* AERE-R 13226. Harwell.

Cazenave, A. & Llovel, W. (2010) 'Contemporary sea level rise'. *Anuual Review of Marine Science*, 2 pp 145-173.

Chao, A., Chazdon, R. L., Colwell, R. K. & Shen, T. J. (2005) 'A new statistical approach for assessing similarity of species composition with incidence and abundance data'. *Ecology Letters*, 8 (2). pp 148-159.

Charman, D. J. (2001) 'Biostratigraphic and palaeoenvironmental applications of testate amoebae'. *Quaternary Science Reviews*, 20 (16-17). pp 1753-1764.

Charman, D. J., Gehrels, W. R., Manning, C. & Sharma, C. (2010) 'Reconstruction of recent sea-level change using testate amoebae'. *Quaternary Research*, 73 (2). pp 208-219.

Charman, D. J., Hendon, D. & Woodland, W. A. (2000) *The identification of testate amoebae (Protozoa: Rhizopoda) in peats. QRA Technical quide No. 9* London: Quaternary Research Association.

Charman, D. J., Roe, H. M. & Gehrels, W. R. (1998) 'The use of testate amoebae in studies of sea-level change: A case study from the Taf Estuary, south Wales, UK'. *Holocene*, 8 (2). pp 209-218.

Charman, D. J., Roe, H. M. & Gehrels, W. R. (2002) 'Modern distribution of saltmarsh testate amoebae: Regional variability of zonation and response to environmental variables'. *Journal of Quaternary Science*, 17 (5-6). pp 387-409.

Charman, D. J. & Warner, B. G. (1992) 'Relationship between testate amoebae (Protozoa:Rhizopoda) and microenvironmental parameters on a forested peatland in northeastern Ontario'. *Canadian Journal of Zoology*, 70 pp 2474-2482.

Chow, T. J. (1965) 'Radiogenic leads of the Canadian and Baltic Shield Regions'. *Symposium on Marine Geochemistry*, 3 pp 169-184.

Church, J. A. & White, N. J. (2011) 'Sea-Level Rise from the Late 19th to the Early 21st Century'. *Surveys in Geophysics*, 32 (4-5). pp 585-602.

Corfu, F. (2004) 'U-Pb age, setting and tectonic significance of the anorthosite-mangerite-charnockite-granite suite, Lofoten-Vesteralen, Norway'. *Journal of Petrology*, 45 (9). pp 1799-1819.

Corner, G. D. & Haugane, E. (1993) 'Marine-lacustrine stratigraphy of raised coastal basins and postglacial sea-level change at Lyngen and Vanna, Troms, northern Norway'. *Norsk Geologisk Tidsskrift*, 73 (3). pp 175-197.

Cundy, A. B., Sprague, D., Hopkinson, L., Maroukian, H., Gaki-Papanastassiou, K., Papanastassiou, D. & Frogley, M. R. (2006) 'Geochemical and stratigraphic indicators of late Holocene coastal evolution in the Gythio area, southern Peloponnese, Greece'. *Marine Geology*, 230 (3-4). pp 161-177.

Devoy, R. J. N., Delaney, C., Carter, R. W. G. & Jennings, S. C. (1996) 'Coastal stratigraphies as indicators of environmental changes upon European Atlantic coasts in the Late Holocene'. *Journal of Coastal Research*, 12 (3). pp 564-588.

Donnelly, J. P., Cleary, P., Newby, P. & Ettinger, R. (2004) 'Coupling instrumental and geological records of sea-level change: Evidence from southern New England of an increase in the rate of sea-level rise in the late 19th century'. *Geophysical Research Letters*, 31 (5).

Douglas, B. C. (2008) 'Concerning evidence for fingerprints of glacial melting'. *Journal of Coastal Research*, 24 pp 218-227.

Ekman, M. (1996) 'A consistent map of the postglacial uplift in Fennoscandia'. *Terra Nova*, 8 pp 158-165.

Fatela, F. & Taborda, R. (2002) 'Confidence limits of species proportions in microfossil assemblages'. *Marine Micropaleontology*, 45 pp 169-174.

Floistad, K. R., Laberg, J. S. & Vorren, T. O. (2009) 'Morphology of younger dryas subglacial and ice-proximal submarine landforms, inner Vestfjorden, northern Norway'. *Boreas*, 38 (3). pp 610-619.

Gehrels, W. R. (1994) 'Determining relative sea-level change from salt-marsh foraminifera and plant zones on the coast of Maine, USA'. *Journal of Coastal Research*, 10 pp 990-1009.

Gehrels, W. R. (1999) 'Middle and late Holocene sea-level changes in eastern Maine reconstructed from foraminiferal saltmarsh stratigraphy and AMS ^{14}C dates on basal peat'. *Quaternary Research*, 52 pp 350-359.

Gehrels, W. R. (2002) 'Intertidal foraminifera as palaeoenvironmental indicators'. in Haslett, S.K. (ed.) *Quaternary Environmental Micropalaeontology.* London/New York: Oxford University Press, 5 5.

Gehrels, W. R., Belknap, D. E. & Kelley, J. T. (1996) 'Integrated high-precision analyses of Holocene relative sea-level changes: lessons from the coast of Maine'. *GSA Bulletin*, 108 (9). pp 1073-1088.

Gehrels, W. R., Belknap, D. F., Black, S. & Newnham, R. M. (2002) 'Rapid sea-level rise in the Gulf of Maine, USA, since AD 1800'. *Holocene*, 12 (4). pp 383-389.

Gehrels, W. R., Callard, S. L., Moss, P. T., Marshall, W. A., Blaauw, M., Hunter, J., Milton, J. A. & Garnett, M. H. (2012) 'Nineteenth and twentieth century sea-level changes in Tasmania and New Zealand'. *Earth and Planetary Science Letters*, 315–316 pp 94-102.

Gehrels, W. R., Hayward, B. W., Newnham, R. M. & Southall, K. E. (2008) 'A 20th century acceleration of sea-level rise in New Zealand'. *Geophysical Research Letters*, 35 (L02717).

Gehrels, W. R., Hendon, D. & Charman, D. J. (2006a) 'Distribution of testate amoebae in salt marshes along the North American East Coast'. *Journal of Foraminiferal Research*, 36 (3). pp 201-214.

Gehrels, W. R., Horton, B. P., Kemp, A. C. & Sivan, D. (2011) 'Two millenia of sea level data: the key to predicting change'. *EOS*, 92 (35). pp 289-296.

Gehrels, W. R., Kirby, J. R., Prokoph, A., Newnham, R. M., Achterberg, E. P., Evans, H., Black, S. & Scot, D. B. (2005) 'Onset of recent rapid sea-level rise in the western Atlantic Ocean'. *Quaternary Science Reviews*, 24 pp 2083-2100.

Gehrels, W. R., Marshall, W. A., Gehrels, M. J., Larsen, G., Kirby, J. R., Eiríksson, J., Heinemeier, J. & Shimmield, T. (2006b) 'Rapid sea-level rise in the North Atlantic Ocean since the first half of the nineteenth century'. *The Holocene*, 16 (7). pp 949-965.

Gehrels, W. R., Roe, H. M. & Charman, D. J. (2001) 'Foraminifera, testate amoebae and diatoms as sea-level indicators in UK saltmarshes: a quantitative multiproxy approach'. *Journal of Quaternary Science*, 16 (3). pp 201-220.

Gehrels, W. R. & Woodworth, P. L. (2013) 'When did modern rates of sea-level rise start?'. *Global and Planetary Change*, 100 pp 263-277.

Gleason, H. A. (1920) 'Some applications of the quadrat method'. *Bulletin, Torry Botanical Club*, 47 pp 21-33.

Goff, J. R. & Chague-Goff, C. (1999) 'A late holocene record of environmental changes from coastal wetlands: Abel Tasman National Park, New Zealand'. *Quaternary International*, 56 pp 39-51.

Green, M. A., Aller, R. C. & Aller, J. Y. (1993) 'Carbonate dissolution and temporal abundances of foraminifera n Long Island Sound Sediments'. *Limnology and Oceanography,* 38 pp 331-345.

Grimm, E. C. (1987) 'CONISS: A Fortran 77 program for stratigraphically constrained cluster analysis by the method of incremental sum of squares'. *Computers and Geosciences*, 13 (1). pp 13-35.

Grimm, E. C. (1992) 'Tilia and Tilia-graph: pollen spreadsheet and graphics programs'. *8th International Palynological Congress*. Aix-en-Provence, France.

Haflidason, H., de Alvaro, M. M., Nygard, A., Sejrup, H. P. & Laberg, J. S. (2007) 'Holocene sedimentary processes in the Andoya Canyon system, north Norway', *Marine Geology,* 246 pp 86-104.

Hald, M. & Vorren, T. O. (1983) 'A shore displacement curve from the Tromsø district, north Norway'. *Norsk Geologisk Tidsskrift*, 63 pp 103-110.

Hamilton, S. & Shennan, I. (2005a) 'Late Holocene great earthquakes and relative sea-level change at Kenai, southern Alaska'. *Journal of Quaternary Science*, 20 (2). pp 95-111.

Hamilton, S. & Shennan, I. (2005b) 'Late Holocene relative sea-level changes and the earthquake deformation cycle around upper Cook Inlet, Alaska'. *Quaternary Science Reviews*, 24 (12-13). pp 1479-1498.

Hansen, B. & Osterhus, S. (2000) 'North Atlantic-Nordic Seas exchanges'. *Progress in Oceanography*, 45 (2). pp 109-208.

Hassan, N. M., Rasmussen, P. E., Dabek-Zlotorrzynska, E., Celo, V. & CHen, H. (2007) 'Analysis of environmental samples using microwave-assissted acid digestion and inductively couple plasma mass spectrometry: maximising total element recoveries'. *Water, Air and Soil Pollution*, 178 pp 323-334.

Haynes, S. (2011) *Salt-marsh testate amoebae as sea-level indicators: Vidarholmi marsh, western Iceland*. Plymouth University.

Hendon, D. & Charman, D. J. (1997) 'The preparation of testate amoebae (Protozoa: Rhizopoda) samples from peat'. *Holocene*, 7 (2). pp 199-205.

Henry, O., Prandi, P., Llovel, W., Cazenave, A., Jevrejeva, S., Stammer, D., Meyssignac, B. & Koldunov, N. (2012) 'Tide gauge-based sea level variations since 1950 along the Norwegian and Russian coasts of the Arctic Ocean: Contribution of the steric and mass components'. *Journal of Geophysical Research-Oceans*, 117

Hill, M. O. & Gauch, H. G. (1980) 'Detrended correspondence-analysis - an improved ordination technique'. *Vegetatio*, 42 (1-3). pp 47-58.

Hjulström, F. (1935) 'Studies of the morphological activity of rivers as illustrated by the river Fyris'. *University of Uppsala Geological Institute Bulletin*, 25 pp 221-557.

Hong, S. M., Candelone, J. P. & Boutron, C. F. (1997) 'Changes in zinc and cadmium concentrations in Greenland ice during the past 7760 years'. *Atmospheric Environment*, 31 (15). pp 2235-2242.

Horton, B. P., Culver, S. J., Hardbattle, M. I. J., Larcombe, P., Milne, G. A., Morigi, C., Whittaker, J. E. & Woodroffe, S. A. (2007) 'Reconstructing holocene sea-level change for the central great barrier reef (Australia) using subtidal foraminifera'. *Journal of Foraminiferal Research*, 37 (4). pp 327-343.

Horton, B. P. & Edwards, R. J. (2005) 'The application of local and regional transfer functions to the reconstruction of Holocene sea levels, North Norfolk, England'. *Holocene*, 15 pp 216-228.

Horton, B. P. & Edwards, R. J. (2006) 'Quantifying Holocene sea-level change using intertidal foraminifera: lessions from the British Isles'. *Cushman Foundation Special Publication*, 40 pp 1-97.

Horton, B. P., Larcombe, P., Woodroffe, S. A., Whittaker, J. E., Wright, M. R. & Wynn, C. (2003) 'Contemporary foraminiferal distributions of a mangrove environment, Great Barrier Reef coastline, Australia: implications for sea-level reconstructions'. *Marine Geology*, 198 pp 225-243.

Horton, B. P. & Murray, J. W. (2007) 'The roles of elevation and salinity as primary controls on living foraminiferal distributions: Cowpen Marsh, Tees Estuary, UK'. *Marine Micropaleontology*, 63 pp 169-186.

Hurrell (2003) NAO index data provuided by the Climate Analysis Section, NCAR, Boulder, USA. Updated regularly. Accessed: 01-01-2012.

Hylander, L. D. & Meili, M. (2003) '500 years of mercury production: global annual inventory by region until 2000 and associated emissions'. *Science of the Total Environment*, 304 (1-3). pp 13-27.

Ishizuka, O., Taylor, R. N., Yuasa, M., Milton, A., Nesbitt, R. W., Uto, K. & Sakamoto, I. (2007) 'Processes controlling along-arc isotopic variation of the south Izu-Bonin arc '. *Geochemistry, Geophysics, Geosystems*, 8 (6).

Jaccard, P. (1908) 'Nouvelles recherches sur la distribution florale'. *Société Vaudoise des Sciences Naturelles. Bulletin.*, 44 pp 223-270.

Jackson, S. T. & Williams, J. W. (2004) 'Modern analogs in Quaternary paleoecology: Here today, gone yesterday, gone tomorrow?'. *Annual Review of Earth and Planetary Sciences*, 32 pp 495-537.

Jiang, S., Liu, X. & Chen, Q. (2011) 'Distribution of total mercury and methylmercury in lake sediments in Arctic Ny-Alesund'. *Chemosphere*, 83 (8). pp 1108-1116.

Johansson, J. M., Davis, J. L., Scherneck, H. G., Milne, G. A., Vermeer, M., Mitrovica, J. X., Bennett, R. A., Jonsson, B., Elgered, G., Elósegui, P., Koivula, H., Poutanen, M., Rönnäng, B. O. & Shapiro, I. I. (2002) 'Continuous GPS measurements of postglacial adjustment in Fennoscandia 1. Geodetic results'. *Journal of Geophysical Research B: Solid Earth*, 107 (8).

Jongman, R. H. G., ter Braak, C. J. F. & van Tongeren, O. F. R. (1995) *Data analysis in community and landscape ecology.* Cambridge University Press, Cambridge.

Juggins, S. (2003) C^2 *User Guide. Software for Ecological and Palaeoecological Data Analysis and Visualisation.* University of Newcastle, Newcastle-upon-Tyne, UK

Keinonen, M. (1992) 'The isotopic compositionof lead in man and the environment in Finland 1966-1987: isotope source of lead as indicators of pollutant sources'. *Science of the Total Environment*, 113 pp 251-268.

Kemp, A. C., Horton, B., Donnelly, J. P., Mann, M. E., Vermeer, M. & Rahmstorf, S. (2011) 'Climate related sea-level variations over the past two millennia'. *Proceedings of the National Academy of Sciences of the United States of America*, 108 (27). pp 11017-11022.

Kemp, A. C., Horton, B. P., Culver, S. J., Corbett, D. R., van de Plassche, O., Gehrels, W. R., Douglas, B. C., Parnell, A. C. (2009a) 'Timing and magnitude of recent accelerated sea-level rise (North Carolina, United States)'. *Geology*, 37 pp 1035-1038.

Kemp, A. C., Horton, B. P., Corbett, D. R., Culver, S. J., Edwards, R. J. & van de Plassche, O. (2009b) 'The relative utility of foraminifera and diatoms for reconstructing late Holocene sea-level change in North Carolina, USA'. *Quaternary Research*, 71 (1). pp 9-21.

Kemp, A. C., Horton, B. P. & Culver, S. J. (2009c) 'Distribution of modern salt-marsh foraminifera in the Albemarle–Pamlico estuarine system of North Carolina, USA: implications for sea-level research'. *Marine Micropaleontology*, 72 pp 222-238.

Kemp, A. C., Horton, B. P., Vann, D. R., Engelhart, S. E., Pre, C. A. G., Vane, C. H., Nikitina, D. & Anisfeld, S. C. (2012) 'Quantitative vertical zonation of salt-marsh foraminifera for reconstructing former sea level, an example from New Jersey, USA'. *Quaternary Science Reviews*, 54 pp 26-39.

Kershaw, K. A. (1976) The vegetation zonation of the East Pen Island salt marshes, Hudson Bay. *Canadian Journal of Botany,* 54 pp 5-13.

Kierulf, H. P., Ouassou, M., Simpson, M. J. R. & Vestol, O. (2013) 'A continuous velocity field for Norway'. *Journal of Geodesy*, 87 (4). pp 337-349.

Klaminder, J., Renberg, I. & Bindler, R. (2003) 'Isotopic trends and background fluxes of atmospheric lead in northern Europe: analyses of three ombotrophic bogs from south Sweden'. *Global Biogeochemical Cycles*, 17 (1).

Koistinen, T., Stephens, M. B., Bogatchev, V., Nordgulen, Ø., Wennerstrøm, M. & Korhonen, J. (2001) *Geological map of the Fennoscandian Shield, scale 1:2 million,* Geological Surveys of Finland, Norway and Sweden and North-West Department of Natural Resources of Russia.

Kuo, C. Y., Shum, C. K., Braun, A., Cheng, K. C. & Yi, Y. (2008) 'Vertical motion determined using satellite altimetry and tide gauges'. *Terrestrial, Atmospheric and Oceanic Sciences*, 19 (1-2). pp 21-35.

Laberg, J. S., Eilertsen, R. S. & Vorren, T. O. (2009) 'The paleo-ice stream in Vestfjorden, north Norway, over the last 35 k.y.: Glacial erosion and sediment yield'. *Geological Society of America Bulletin*, 121 (3-4). pp 434-447.

Laberg, J. S., Vorren, T. O., Mienert, J., Bryn, P. & Lien, R. (2002a) 'The Traenadjupet Slide: a large slope failure affecting the continental margin of Norway 4,000 years ago', *Geo-Marine Letters,* 22 pp 19-24.

Laberg, J. S., Vorren, T. O., Mienert, J., Evans, D., Lindberg, B., Ottesen, D., Kenyon, N. H. & Henriksen, S. (2002b) 'Late Quaternary palaeoenvironment and chronology in the Traenadjupet Slide area offshore Norway', *Marine Geology,188*2 pp 35-60.

 Laberg, J. S. & Vorren, T. O. (2000)) 'The Traenadjupet Slide, offshore Norway – morphology evacuation and triggering mechanisms', *Marine Geology,* 171 pp 95-114.

Lambeck, K., Purcell, A., Zhao, J. & Svensson, N.-O. (2010) 'The Scandinavian Ice Sheet: from MIS 4 to the end of the Last Glacial Maximum'. *Boreas*, 39 (2). pp 410-435.

Lambeck, K., Smither, C. & Ekman, M. (1998a) 'Tests of glacial rebound models for Fennoscandinavia based on instrumented sea- and lake-level records'. *Geophysical Journal International*, 135 pp 375-387.

Lambeck, K., Smither, C. & Johnston, P. (1998b) 'Sea-level change, glacial rebound and mantle viscosity for northern Europe'. *Geophysical Journal International*, 134 pp 102-144.

Langedal, M. & Ottesen, R. T. (1998) 'Airborne pollution in five drainage basins in eastern Finnmark, Norway: An evaluation of overbank sediments as sampling medium for environmental studies and geochemical mapping'. *Water Air and Soil Pollution*, 101 (1-4). pp 377-398.

Legendre, P. & Fortin, M. J. (1989) 'Spatial pattern and ecological analysis'. *Vegetatio*, 80 (2). pp 107-138.

Leorri, E. & Cearreta, A. (2009) 'Recent sea-level changes in the southern Bay of Biscay: transfer function reconstructions from salt-marshes compared with instrumental data'. *Scientia Marina*, 73 (2). pp 287-296.

Leorri, E., Horton, B. P. & Cearreta, A. (2009) 'Development of a foraminifera based transfer function in the Basque marshes, N. Spain: implications for sea-level studies in the Bay of Biscay'. *Marine Geology*, 251 pp 60-74.

Leps, J. & Smilauer, P. (2003) *Multivariate Analysis of Ecological Data Using CANOCO.* Cambridge University Press.

Lidberg, M., Johansson, J. M., Scherneck, H.-G. & Milne, G. A. (2010) 'Recent results based on continuous GPS observations of the GIA process in Fennoscandia from BIFROST'. *Journal of Geodynamics*, 50 (1). pp 8-18.

Lidberg, M., Johansson, J. M., Scherneck, H. G. & Davis, J. L. (2007) 'An improved and extended GPS-derived 3D velocity field of the glacial isostatic adjustment (GIA) in Fennoscandia'. *Journal of Geodesy*, 81 (3). pp 213-230.

Lloyd, J. (2000) 'Combined foraminiferal and thecamoebian environmental reconstruction from an isolation basin in NW Scotland: Implications for sea-level studies'. *Journal of Foraminiferal Research*, 30 (4). pp 294-305.

Loeblich, A. R. & Tappan, H. (1988) *Foraminiferal genera and their classification.* New Yorl: van Nostrand Reinhold Company.

Long, A. J., Innes, J. B., Shennan, I. & Tooley, M. J. (1999) 'Coastal stratigraphy : a case study from Johns River, Washington, USA'. in Jones, A.P., Tucker, M.E. and Hart, J.K. (eds.) *The description and analysis of quaternary stratigraphic field sections; Quaternary Research Association, Technical Guide No 7.* London.

Long, A. J., Waller, M. P. & Stupples, P. (2006) 'Driving mechanisms of coastal change: Peat compaction and the destruction of late Holocene coastal wetlands'. *Marine Geology*, 225 (1-4). pp 63-84.

Long, A. J., Woodroffe, S. A., Milne, G. A., Bryant, C. L. & Wake, L. M. (2010) 'Relative sea level change in west Greenland during the last millennium'. *Quaternary Science Reviews*, 29 pp 367-383.

Longino, J. T., Coddington, J. & Colwell, R. K. (2002) 'The ant fauna of a tropical rain forest: Estimating species richness three different ways'. *Ecology*, 83 (3). pp 689-702.

Lysa, A., Sejrup, H. P. & Aarseth, I. (2004) 'The late glacial-Holocene seismic stratigraphy and sedimentary environment in Ranafjorden, northern Norway'. *Marine Geology*, 211 (1-2). pp 45-78.

Magurran, A. E. (2004) *Measuring Biological Diversity.* Oxford, UK: Blackwell Science Ltd.

Malm, O. & Ormaasen, D. E. (1978) 'Mangerite-charnockite intrusives in the Lofoten-Vesteralen area, North Norway: petrography, chemistry and petrology'. *Norges Geologiske Undersøkelse*, 434 pp 51-73.

Mangerud, J. (1972) 'Radiocarbon dating of marine shells, including a discussion of apparent age of recent shells from Norway'. *Boreas*, 1 pp 143-172.

Mangerud, J. & Gulliksen, S. (1975) 'Apparent radiocarbon ages of recent marine shells from Norway, Spitsbergen and Arctic Canada'. *Quaternary Research*, 5 pp 263-273.

Mariotti, G. & Fagherazzi, S. 'A numerical model for the coupled long-term evolution of salt marshes and tidal flats'. *Journal of Geophysical Research F: Earth Surface*, 115 (1).

Marshall, W. A., Clough, R. & Gehrels, W. R. (2009) 'The isotopic record of atmospheric lead fall-out on an Icelandic salt marsh since AD 50'. *Science of the Total Environment*, 407 (8). pp 2734-2748.

Marthinussen, M. (1945) 'Yngre postglaciale nivaer pa Varangerhalvoya'. *Norges Geologiske Undersøkelse*, 25

Marthinussen, M. (1960) 'Coast and fjord area of Finnmark'. *Norges Geologiske Undersøkelse*, 208 pp 416-429.

Marthinussen, M. (1962) 'C^{14} datings referring to shore lines, transgressions and glacial substages in northern Norway'. *Norges Geologiske Undersøkelse*, 215 pp 37-67.

Martinez-Cortizas, A., Pontevedra-Pombal, X., Garcia-Rodeja, E., Novoa-Munoz, J. C. & Shotyk, W. (1999) 'Mercury in a Spanish peat bog: Archive of climate change and atmospheric metal deposition'. *Science*, 284 (5416). pp 939-942.

Mason, R. P. & Sheu, G. R. (2002) 'Role of the ocean in the global mercury cycle'. *Global Biogeochemical Cycles*, 16 (4).

Massey, A. C., Gehrels, W. R., Charman, D. J. & White, S. V. (2006) 'An intertidal foraminifera-based transfer function for reconstructing Holocene sea-level change in southwest England'. *Journal of Foraminiferal Research*, 36 (3). pp 215-232.

Massey, A. C., Gehrels, W. R., Charman, D. J. & White, S. V. (2008) 'Relative sea-;level change and postglacial isostatic adjustment along the coast of south Devon, United Kingdon'. *Journal of Quaternary Science*, 23 (5). pp 415-433.

McGranahan, G., Balk, D. & Anderson, B. (2007) 'The rising tide: assessing the risks of climate change and human settlements in low elevaton coastal zones'. *Environment and Urbanization*, 19 (1). pp 17-37.

Merilainen, J. J., Kustula, V. & Witick, A. (2011) 'Lead pollution history from 256 BC to AD 2005 inferred from the Pb isotope ratio (Pb-206/Pb-207) in a varve record of Lake Korttajarvi in Finland'. *Journal of Paleolimnology*, 45 (1). pp 1-8.

Merilainen, J. J., Kustula, V., Witick, A., Haltia-Hovi, E. & Saarinen, T. (2010) 'Pollution history from 256 BC to AD 2005 inferred from the accumulation of elements in a varve record of Lake Korttajarvi in Finland'. *Journal of Paleolimnology*, 44 (2). pp 531-545.

Merrill, A. S. & Ropes, J. W. (1969) 'Proceedings of the National Shellfisheries Association'. 59 pp 40-45.

Mills, K., Mackay, A. W., Bradley, R. S. & Finney, B. (2009) 'Diatom and stable isotope records of late Holocene lake ontogeny at Indrepollen, Lofoten, NW Norway: a response to glacio-isostacy and Neoglacial cooling', *Holocene,* 19 pp 261-271.

Milne, G. A., Davis, J. L., Mitrovica, J. X., Scherneck, H.-G., Johansson, J. M., Vermeer, M. & Koivula, H. (2001) 'Space-geodetic constraints on glacial isostatic adjustment in Fennocandia'. *Science*, 291 pp 2381-2385.

Milne, G. A., Mitrovica, J. X., Scherneck, H. G., Davis, J. L., Johansson, J. M., Koivula, H. & Vermeer, M. (2004) 'Continuous GPS measurements of postglacial adjustment in Fennoscandia: 2. Modeling results'. *Journal of Geophysical Research*, 109 pp B02412 02411-02418.

Mimura, N., Nurse, L., McLean, R. F., Agard, J., Briguglio, L., Lefale, P., Payet, R. & Sem, G. (2007) 'Small islands'. in Parry, M.L., Canziani, O.F., Palutikof, J.P., van der Linden, P.J. and Hanson, C.E. (eds.) *Climate Change 2007: Impacts, Adaptation and Vulnerability. Contribution of Working Group II to the Fourth Assessment Report of the Intergovernmental Panel on Climate Change.* Cambridge, UK Cambridge University Press, pp 687-716.

Mitchell, E. A. D., Borcard, D., Buttler, A. J., Grosvernier, P., Gilbert, D. & Gobat, J. M. (2000) 'Horizontal distribution patterns of testate amoebae (Protozoa) in a Sphagnum magellanicum carpet'. *Microbial Ecology*, 39 (4). pp 290-300.

Mitchell, E. A. D., Charman, D. J. & Warner, B. G. (2008) 'Testate amoebae analysis in ecological and paleoecological studies of wetlands: Past, present and future'. *Biodiversity and Conservation*, 17 (9). pp 2115-2137.

Moe, H., Ommundsen, A. & Gjevik, B. (2002) 'A high resolution tidal model for the area around The Lofoten Islands, northern Norway'. *Continental Shelf Research*, 22 (3). pp 485-504.

Møller, J. J. (1982) *Coastal caves, marine limits and ice retreat in Lofoten - Vesteralen, North Norway.*

Møller, J. J. (1984) 'Holocene shoreline displacement at Nappstraumen, Lofoten, North Norway'. *Norsk Geografisk Tidsskrift*, 64 pp 1-5.

Møller, J. J. (1986) 'Holocene transgression maximum about 6000 years BP at Ramsa, Vesteralen, north Norway'. *Norsk Geografisk Tidsskrift*, 40 (2). pp 77-84.

Møller, J. J. (1987) 'Shoreline relation and prehistoric settlement in northern Norway'. *Norsk Geografisk Tidsskrift*, 41 (1). pp 45-60.

Møller, J. J. (1989) 'Geometric simulation and mapping of Holocene relative sea-level changes in northern Norway'. *Journal of Coastal Research*, 5 (3). pp 403-417.

Møller, J. J. & Holmeslet, B. (2002) 'Havets historie i Fennoskandia og NV Russland'. [Online]. Available at: http://geo.phys.uit.no/sealev/ (Accessed: January).

Monna, F., Galop, D., Carozza, L., Tual, M., Beyrie, A., Marembert, F., Chateau, C., Dominik, J. & Grousset, F. (2004) 'Environmental impact of early Basque mining and smelting recorded in a high ash minerogenic peat deposit'. *Science of the Total Environment*, 327 (1-3). pp 197-214.

Morner, N.-A. (2010) 'Some problems in the reconstruction of mean sea level and its changes with time'. *Quaternary International*, 221 (1-2). pp 3-8.

Murray, J. W. (1965) 'Two species of Birtish recent foraminiferida'. *Contributions from the Cushman Foundation for Foraminiferal Research*, 16 (4). pp 148-150.

Murray, J. W. (1971) *An Atlas of British Recent Foraminiferids.* New York: American Elsevier Publishing Company, Inc.

Murray, J. W. (1976) 'Comparative studies of living and dead benthic foraminiferal distributions'. in Hedley, R.H. and Adams, C.G. (eds.) *Foraminifera.* pp 45-109.

Murray, J. W. (1979) *British Nearshore Foraminiferids.* London, New York and San Francisco: Academic Press.

Murray, J. W. (1982) 'Benthic foraminifera: the validity of living, dead, or total assemblages for the interpretation of palaeoecology'. *Journal of Micropalaeontology*, 1 pp 137-140.

Murray, J. W. (1991) *Ecology and Palaeoecology of Benthic Foraminifera.* Longman Scientific & Technical. Essex, England.

Murray, J. W. (2000) 'The enigma of the continued use of total assemblages in ecological studies of benthic foraminifera '. *Journal of Foraminiferal Research*, 30 (3). pp 244-245.

Murray, J. W. (2006) *Ecology and application of benthic foraminifera.* Cambridge University Press. Cambridge.

Murray, J. W. & Bowser, S. S. (2000) 'Mortality, protoplasm decay rate and reliability of staining techniques to recognize 'living' foraminifera: A review'. *Journal of Foraminiferal Research*, 30 pp 66-70.

Nguyen-Viet, H., Gilbert, D., Bernard, N., Mitchell, E. A. D. & Badot, P. M. (2004) 'Relationship between atmospheric pollution characterized by NO2 concentrations and testate amoebae density and diversity'. *Acta Protozoologica*, 43 (3). pp 233-239.

Nicol, D. (1951) 'Recent species of the veneroid pelecypod Arctica'. *Journal of Washington Academy Sciences*, 41 (3). pp 102-106.

Nilsson, Ö. (1992) *Kystflora.* Cappelen.

Nordgulen, Ø., Bargel, T. H., Longva, O., Olesen, O. & Ottesen, D. (2006) *A preliminary study of Lofoten as a potential World Heritage Site based on natural criteria.* Geological Survey of Norway. Available.

Nriagu, J. O. (1989) 'A global assessment of natural sources of atmospheric trace metals'. *Nature*, 338 pp 47-49.

Ooms, M., Beyens, L. & Temmerman, S. (2011) 'Testate amoebae as estuarine water-level indicators: modern distribution and the development of a transfer function from a freshwater tidal marsh (Scheldt estuary, Belgium)'. *Journal of Quaternary Science*, 26 (8). pp 819-828.

Ooms, M., Beyens, L. & Temmerman, S. (2012) 'Testate Amoebae as Proxy for Water Level Changes in a Brackish Tidal Marsh'. *Acta Protozoologica*, 51 (3). pp 271-289.

Palmer, A. J. & Abbott, W. H. (1986) 'Diatoms as indicators of sea level change'. in Van de Plassche, O. (eds.) *Sea Level Research: a manual for the collection and evaluation of data.* Geobooks. Norwich. pp 457-488.

Panagiotaras, D., Papoulis, D., Kontopoulos, N. & Avramidis, P. (2012) 'Geochemical processes and sedimentological characteristics of Holocene lagoon deposits, Alikes Lagoon, Zakynthos Island, western Greece'. *Geological Journal*, 47 (4). pp 372-387.

Payne, R. & Mitchell, E. A. D. (2009) 'How many is enough? Determining optimal count totals for ecological and palaeoecological studies of testate amoebae'. *Journal of Paleolimnology*, 42 (4). pp 483-495.

Payne, R. J., Lamentowicz, M., van der Knaap, W. O., van Leeuwen, J. F. N., Mitchell, E. A. D. & Mazei, Y. (2012) 'Testate amoebae in pollen slides'. *Review of Palaeobotany and Palynology*, 173 pp 68-79.

Peltier, W. R. (2004) 'Global glacial isostasy and the surface of the ice-age Earth: the ICE-5G (VM2) model and GRACE'. *Annual Review of Earth and Planetary Science*, 32 pp 111-149.

Pfeiffer, M. & Mezger, D. (2012) 'Biodiversity Assessment in Incomplete Inventories: Leaf Litter Ant Communities in Several Types of Bornean Rain Forest'. *Plos One*, 7 (7).

Phleger, F. B. & Walton, W. R. (1950) 'Ecology of marsh bay foraminifera, Barnstable, Massachusetts'. *American Journal of Science*, 248 pp 274-294.

Plassen, L. & Vorren, T. O. (2003) 'Sedimentary processes and the environment during deglaciation of a fjord basin in Ullsfjorden, North Norway'. *Norwegian Journal of Geology*, 83 (1). pp 23-36.

Polyak, L., Korsun, S., Febo, L. A., Stanovoy, V., Khusid, T., Hald, M., Paulsen, B. E. & Lubinski, D. J. (2002) 'Benthic foraminiferal assemblages from the southern Kara Sea, a river-influenced Arctic marine environment'. *Journal of Foraminiferal Research*, 32 (3). pp 252-273.

Pontevedra-Pombal, X., Mighall, T. M., Novoa-Munoz, J. C., Peiteado-Varela, E., Rodriguez-Racedo, J., Garcia-Rodeja, E. & Martinez-Cortizas, A. (2013) 'Five thousand years of atmospheric Ni, Zn, As, and Cd deposition recorded in bogs from NW Iberia: prehistoric and historic anthropogenic contributions'. *Journal of Archaeological Science*, 40 (1). pp 764-777.

Prank, M., Sofiev, M., van der Gon, H. A. C. D., Kaasik, M., Ruuskanen, T. M. & Kukkonen, J. (2010) 'A refinement of the emission data for Kola Peninsula based on inverse dispersion modelling'. *Atmospheric Chemistry and Physics*, 10 (22). pp 10849-10865.

Preuss, H. (1979) 'Progress in computer evaluation of sea-level data within the IGCP project no. 61'. *International Symposium on Coastal Evolution in the Quaternary*. Sao-Paulo, Brazil, pp 104-134.

Rabenhorst, M. C. (1988) 'Determination of organic and carbonate carbon in calcareous soils using dry combustion '. *Soil Science Society of America Journal*, 52 (4). pp 965-968.

Reavie, E. D. & Juggins, S. (2011) 'Exploration of sample size and diatom-based indicator performance in three North American phosphorus training sets'. *Aquatic Ecology*, 45 (4). pp 529-538.

Reimann, C., DeCaritat, P., Halleraker, J. H., Finne, T. E., Boyd, R., Jaeger, O., Volden, T., Kashulina, G., Bogatyrev, I., Chekushin, V., Pavlov, V., Ayras, M., Raisanen, M. L. & Niskavaara, H. (1997a) 'Regional atmospheric deposition patterns of Ag, As, Bi, Cd, Hg, Mo, Sb and Tl in a 188,000 km^2 area in the European arctic as displayed by terrestrial moss samples - Long-range atmospheric transport vs local impact'. *Atmospheric Environment*, 31 (23). pp 3887-3901.

Reimann, C., DeCaritat, P., Halleraker, J. H., Volden, T., Ayras, M., Niskavaara, H., Chekushin, V. A. & Pavlov, V. A. (1997b) 'Rainwater composition in eight arctic catchments in northern Europe (Finland, Norway and Russia)'. *Atmospheric Environment*, 31 (2). pp 159-170.

Reimer, P. J., Baillie, M. G. L., Bard, E., Bayliss, A., Beck, J. W., Blackwell, P. G., Ramsey, C. B., Buck, C. E., Burr, G. S., Edwards, R. L., Friedrich, M., Grootes, P. M., Guilderson, T. P., Hajdas, I., Heaton, T. J., Hogg, A. G., Hughen, K. A., Kaiser, K. F., Kromer, B., McCormac, F. G., Manning, S. W., Reimer, R. W., Richards, D. A., Southon, J. R., Talamo, S., Turney, C. S. M., van der Plicht, J. & Weyhenmeyer, C. E. (2009) 'IntCal09 and Marine09 radiocarbon age calibration curves, 0-50,000 years CAL BP'. *Radiocarbon*, 51 (4). pp 1111-1150.

Renberg, I., Bindler, R. & Brannvall, M. L. (2001) 'Using the historical atmospheric lead-deposition record as a chronological marker in sediment deposits in Europe'. *Holocene*, 11 (5). pp 511-516.

Renberg, I., Brannvall, M. L., Bindler, R. & Emteryd, O. (2002) 'Stable lead isotopes and lake sediments - a useful combination for the study of atmospheric lead pollution history'. *Science of the Total Environment*, 292 (1-2). pp 45-54.

Renberg, I., Persson, M. W. & Emteryd, O. (1994) 'Preindustrial atmospheric lead contamination detected in Swedish lake-sediments'. *Nature*, 368 (6469). pp 323-326.

Richter, K., Nilsen, J. E. O. & Drange, H. (2012) 'Contributions to sea level variability along the Norwegian coast for 1960-2010'. *Journal of Geophysical Research-Oceans*, 117

Rigina, O. (1998) 'GIS analysis of surface water chemistry susceptibility and response to the indiustrial air pollution in the Kola Peninsula, northern Russia'. *Water, Air and Soil Pollution*, 105 pp 73-82.

Riveiros, N. V., Babalola, A. O., Boudreau, R. E. A., Patterson, R. T., Roe, H. M. & Doherty, C. (2007) 'Modern distribution of salt marsh foraminifera and thecamoebians in the Seymour-Belize Inlet Complex, British Columbia, Canada'. *Marine Geology*, 242 (1-3). pp 39-63.

Roe, H. M., Charman, D. J. & Gehrels, W. R. (2002) 'Fossil testate amoebae in coastal deposits in the UK: Implications for studies of sea-level change'. *Journal of Quaternary Science*, 17 (5-6). pp 411-429.

Rognerud, S. & Fjeld, E. (2001) 'Trace element contamination of Norwegian lake sediments'. *Ambio*, 30 (1). pp 11-19.

Romundset, A. & Bondevik, S. (2011) 'Propagation of the Storegga tsunami into ice-free lakes along the southern shores of the Barents Sea'. *Journal of Quaternary Science*, 26 (5). pp 457-462.

Romundset, A., Bondevik, S. & Bennike, O. (2011) 'Postglacial uplift and relative sea level changes in Finnmark, northern Norway'. *Quaternary Science Reviews*, 30 (19-20). pp 2398-2421.

Rossman, K. J. R., Chisholm, W., Hong, S. M., Candelone, J. P. & Boutron, C. F. (1997) 'Lead from Carthaginian and Romand Spainish mines isotopically identified in Grennland ice dated from 600 BC to 300 AD'. *Environmental Science and Technology*, 31 pp 3413-3416.

Rowell, D. L. (1994) *Soil Science. Methods and Applications.* Harlow, England: Longman Scientific and Technical.

Scherneck, H. G., Johansson, J. M., Mitrovica, J. X. & Davis, J. L. (1998) 'The BIFROST project: GPS determined 3-D displacement rates in Fennoscandia from 800 days of continuous observations in the SWEPOS network'. *Tectonophysics*, 294 (3-4). pp 305-321.

Scott, D. B., Hasegawa, S., Saito, T., Ito, K. & Collins, E. (1995) 'Marsh foraminifera and vegetation distributions in Nemuro Bay wetland areas, eastern Hokkaido'. *Transactions and Proceedings of the Palaeontological Society of Japan*, 180 pp 282-295.

Scott, D. B. & Martini, I. P. (1982) 'Marsh foraminifera zonations in western James - Hudson Bay'. *Naturaliste Canadienne*, 109 pp 399-414.

Scott, D. B. & Medioli, F. S. (1978) 'Vertical zonations of marsh foraminifera as accurate indicators of former sea-levels'. *Nature*, 272 (5653). pp 528-531.

Scott, D. B. & Medioli, F. S. (1980a) 'Quantitative studies of marsh foraminiferal distributions in Nova Scotia: implications for sea level studies'. *Cushman Foundation for Foraminiferal Research*, Special Publication No. 17

Scott, D. B. & Medioli, F. S. (1982) 'Micropaleontological documentation for early Holocene fall of relative sea level on the Atlantic coast of Nova Scotia'. *Geology*, 10 pp 278-281.

Scott, D. B., Suter, J. R. & Kosters, E. C. (1991) 'Marsh foraminifera and arcellaceans of the lower Mississippi Delta: controls on spatial distributions'. *Micropaleontology*, 37 (4). pp 373-392.

Shennan, I. (2007) 'Sea Level Studies'. in Ellias, S.A. (ed.) *Encyclopedia of Quaternary Sciences.* Oxford, UK: Elsevier.

Shotyk, W., Weiss, D., Appleby, P. G., Cheburkin, A. K., Frei, R., Gloor, M., Kramers, J. D., Reese, S. & Van der Knaap, W. O. (1998) 'History of atmospheric lead deposition since 12,370 C-14 yr BP from a peat bog, Jura Mountains, Switzerland'. *Science*, 281 (5383). pp 1635-1640.

Siddall, M. & Milne, G. A. (2012) 'Understanding sea-level change is impossible without both insights from paleo studies and working across disciplines'. *Earth and Planetary Science Letters*, 315 pp 2-3.

Simpson, G. L. (2007) 'Analogue methods in palaeoecology: Using the analogue package'. *Journal of Statistical Software*, 22 (2). pp 1-29.

Simpson, M., Breili, K., Kierulf, H. P., Lysaker, D., Ouassou, M. & Haug, E. (2012) *Estimates of future sea-level changes for Norway* Available.

Slangen, A. B. A., Katsman, C. A., van de Wal, R. S. W., Vermeersen, L. L. A. & Riva, R. E. M. (2012) 'Towards regional projections of twenty-first century sea-level change based on IPCC SRES scenarios'. *Climate Dynamics*, 38 (5-6). pp 1191-1209.

Southall, K. E., Gehrels, W. R. & Hayward, B. W. (2006) 'Foraminifera in a New Zealand salt marsh and their suitability as sea-level indicators'. *Marine Micropaleontology*, 60 pp 167-179.

Steffen, H., Denker, H. & Müller, J. (2008) 'Glacial isostatic adjustment in Fennoscandia from GRACE data and comparison with geodynamical models'. *Journal of Geodynamics*, 46 pp 155-164.

Steffen, H., Gitlein, O., Denker, H., Müller, J. & Timmen, L. (2009) 'Present rate of uplift in Fennoscandia from GRACE and absolute gravimetry'. *Tectonophysics*, 474 pp 69-77.

Steffen, H. & Wu, P. (2011) 'Glacial isostatic adjustment in Fennoscandia-A review of data and modeling'. *Journal of Geodynamics*, 52 (3-4). pp 169-204.

Stockmarr, J. (1971) 'Tablets with spores used in absolute pollen analysis'. *Pollen et Spores*, 13 pp 615-621.

Stuiver, M. & Reimer, P. J. (1986) 'A computer program for radiocarbon age calibration'. *Proceedings of the 12th International 14C Conference. Radiocarbon*. pp 1022-1030.

Stuiver, M. & Reimer, P. J. (1993) 'Extended 14C data base and revised CALIB 3.0 14C age calibration program'. *Radiocarbon*, 35 (1). pp 215-230.

Sun, L., Yin, X., Liu, X., Zhu, R., Xie, Z. & Wang, Y. (2006) 'A 2000-year record of mercury and ancient civilizations in seal hairs from King George Island, West Antarctica'. *Science of the Total Environment*, 368 (1). pp 236-247.

Svendsen, J. I., Alexanderson, H., Astakhov, V. I., Demidov, I., Dowdeswell, J. A., Funder, S., Gataullin, V., Henriksen, M., Hjort, C., Houmark-Nielsen, M., Hubberten, H. W., Ingolfsson, O., Jakobsson, M., Kjaer, K. H., Larsen, E., Lokrantz, H., Lunkka, J. P., Lysa, A., Mangerud, J., Matiouchkov, A., Murray, A., Moller, P., Niessen, F., Nikolskaya, O., Polyak, L., Saarnisto, M., Siegert, C., Siegert, M. J., Spielhagen, R. F. & Stein, R. (2004) 'Late quaternary ice sheet history of northern Eurasia'. *Quaternary Science Reviews*, 23 (11-13). pp 1229-1271.

Svendsen, J. I. & Mangerud, J. (1987) 'Late Weichselian and Holocene sea-level history for a cross-section of western Norway'. *Journal of Quaternary Science*, 2 pp 113-132.

Telford, R. J. & Birks, H. J. B. (2005) 'The secret assumption of transfer functions: problems with spatial autocorrelation in evaluating model performance'. *Quaternary Science Reviews*, 24 (20-21). pp 2173-2179.

Telford, R. J. & Birks, H. J. B. (2009) 'Evaluation of transfer functions in spatially structured environments'. *Quaternary Science Reviews*, 28 (13-14). pp 1309-1316.

Telford, R. J. & Birks, H. J. B. (2011a) 'A novel method for assessing the statistical significance of quantitative reconstructions inferred from biotic assemblages'. *Quaternary Science Reviews*, 30 (9-10). pp 1272-1278.

Telford, R. J. & Birks, H. J. B. (2011b) 'Effect of uneven sampling along an environmental gradient on transfer-function performance'. *Journal of Paleolimnology*, 46 (1). pp 99-106.

ter Braak, C. J. F. (1985) 'Canonical correspondence analysis a new eigenvector technique for multivariate direct gradient analysis'. *Leemans, R., I. C. Prentice and E. Van Der Maarel.* pp 16-17.

ter Braak, C. J. F. & Prentice, I. C. (1988) 'A theory of gradient analysis '. *Advance in ecological research*, 18 pp 271-317

ter Braak, C. J. F. & Juggins, S. (1993) 'Weighted averaging partial least-squares regression (wa-pls) - an improved method for reconstructing environmental variables from species assemblages'. *Hydrobiologia*, 269 pp 485-502.

Tolonen, K. (1986) 'Rhizopod analysis'. in Berglund, B.E. (ed.) *Handbook of Holocene Palaeoecology and Palaeohydrology.* John Wiley & Sons, pp 645-666.

Tovey, N. K. & Paul, M. A. (2002) 'Modelling self-weight consolidation in Holocene sediments'. *Bulletin of Engineering Geology and the Environment*, 61 (1). pp 21-33.

Troels-Smith, J. (1955) 'Characterization of unconsolidated sediments'. *Danmarks Geologiske Undersogelse*, Series IV 3 pp 38-73.

van de Plassche, O. (2000) 'North Atlantic climate–ocean variations and sea level in Long Island Sound, Connecticut, since 500 cal yr A.D.'. *Quaternary Research*, 53 pp 89-97.

van der Wal, W., Kurtenbach, E., Kusche, J. & Vermeersen, B. (2011) 'Radial and tangential gravity rates from GRACE in areas of glacial isostatic adjustment'. *Geophysical Journal International*, 187 (2). pp 797-812.

Vasskog, K., Drange, H. & Nesje, A. (2009) *Havnivåstigning - Estimater av fremtidig havnivåstigning i norske kystkommuner [Sea Level Rise - Estimations for future sea level rise in Norwegian coastal municipalities].* Available.

Vestøl, O. (2006) 'Determination of postglacial land uplift in fennoscandia from leveling, tide-gauges and continuous GPS stations using least squares collocation'. *Journal of Geodesy*, 80 (5). pp 248-258.

Vorren, K. D. & Moe, D. (1986) 'The early Holocene climate and sea-level changes in Lofoten and Vesteralen, north Norway'. *Norsk Geologisk Tidsskrift*, 66 (2). pp 135-143.

Vorren, T. O. & Plassen, L. (2002) 'Deglaciation and palaeoclimate of the Andfjord-Vagsfjord area, North Norway'. *Boreas*, 31 (2). pp 97-125.

Vorren, T. O., Vorren, K. D., Alm, T., Gulliksen, S. & Lovlie, R. (1988) 'The last deglaciation (20 000 to 11 000 B.P.) on Andoya, northern Norway'. *Boreas*, 17 (1). pp 41-77.

Wahr, J., Wingham, D. & Bentley, C. (2000) 'A method of combining ICESat and GRACE satellite data to constrain Antarctic mass balance'. *Journal of Geophysical Research-Solid Earth*, 105 (B7). pp 16279-16294.

Walton, W. R. (1952) 'Techniques for recognition of living foraminifera'. *Cushman Foundation for Foraminiferal Research Contribution*, 3 pp 56-60.

Warner, B. G. (1990) 'Testate amoebae (Protozoa)'. in Warner, B.G. (ed.) *Methods in Quaternary Ecology.* St John's, Newfoundland: Geoscience Canada, pp 65-74.

Watcham, E. P., Shennan, I. & Barlow, N. L. M. (2013) 'Scale considerations in using diatoms as indicators of sea-level change: lessons from Alaska'. *Journal of Quaternary Science*, 28 (2). pp 165-179.

Whitbaard, R., Dunineveld, G. C. A. & de Wilde, P. A. W. J. (1999) 'Geographical differences in growth rates of *Arctica islandica* (Mollusca: Bivalvia) from the North Sea and adjacent waters'. *Journal of the Marine Biological Association of the United Kingdom*, 79 pp 907-915.

Woodland, W. A., Charman, D. J. & Sims, P. C. (1998) 'Quantitative estimates of water tables and soil moisture in Holocene peatlands from testate amoebae'. *Holocene*, 8 (3). pp 261-273.

Woodroffe, C. D. & Murray-Wallace, C. V. (2012) 'Sea-level rise and coastal change: the past as a guide to the future'. *Quaternary Science Reviews*, 54 pp 4-11.

Woodroffe, S. A. (2009) 'Recognising subtidal foraminiferal assemblages: Implications for quantitative sea-level reconstructions using a foraminifera-based transfer function'. *Journal of Quaternary Science*, 24 (3). pp 215-223.

Woodroffe, S. A. & Long, A. J. (2009) 'Salt marshes as archives of recent relative sea level change in West Greenland'. *Quaternary Science Reviews*, 28 (17-18). pp 1750-1761.

Woodworth, P. L. & Player, R. (2003) 'The permanent service for mean sea level: An update to the 21st century'. *Journal of Coastal Research*, 19 (2). pp 287-295.

Zettler, M. L., Bonsch, R. & Gosselck, F. (2001) 'Distribution, abundance and some population characteristics of the ocean quahog, *Arctica islandica* (Linnaeus, 1767), in the Mecklenburg Bight (Baltic Sea)'. *Jounral of Shellfish Research*, 20 (1). pp 161-169.

Zillen, L., Lenz, C. & Jilbert, T. (2012) 'Stable lead (Pb) isotopes and concentrations - a useful independant dating tool for Blatic Sea sediments'. *Quaternary Geochronology*, 8 pp 41-45.